Neurophysiology of the macaque fronto-parietal magnitude system

Dissertation

zur Erlangung des Grades eines
Doktors der Naturwissenschaften

der Mathematisch-Naturwissenschaftlichen Fakultät
und
der Medizinischen Fakultät
der Eberhard-Karls-Universität Tübingen

vorgelegt von

Pooja Viswanathan

aus Kolkata, Indien

Oktober – 2017

Tag der mündlichen Prüfung:	27. April, 2018
Dekan der Math.-Nat. Fakultät:	Prof. Dr. W. Rosenstiel
Dekan der Medizinischen Fakultät:	Prof. Dr. I. B. Autenrieth
1. Berichterstatter:	Prof. Dr. A. Nieder
2. Berichterstatter:	Prof. Dr. Z. Hafed
3. Berichterstatter:	Prof. Dr. G. Rainer
Prüfungskommission:	Prof. Dr. A. Nieder
	Prof. Dr. Z. Hafed
	Prof. Dr. C. Schwarz
	Prof. Dr. J. Ostwald

Erklärung

Ich erkläre, dass ich die zur Promotion eingereichte Arbeit mit dem Titel:

„Neurophysiology of the macaque fronto-parietal magnitude system“

selbständig verfasst, nur die angegebenen Quellen und Hilfsmittel benutzt und wörtlich oder inhaltlich übernommene Stellen als solche gekennzeichnet habe. Ich versichere an Eides statt, dass diese Angaben wahr sind und dass ich nichts verschwiegen habe. Mir ist bekannt, dass die falsche Abgabe einer Versicherung an Eides statt mit Freiheitsstrafe bis zu drei Jahren oder mit Geldstrafe bestraft wird.

Tübingen, den 25. Oktober, 2017

Pooja Viswanathan

Acknowledgments

This thesis has taken a significant number of years and shaped a significant part of me, which means there are a number of people who have been a part of it whom I must acknowledge and thank.

I owe the most to Andreas Nieder who guided my science and my person through these years. He has been a fantastic mentor, I could not have asked for better. He has always been available, extremely generous with his time and attention, always communicated with admirable balance and improved every bit of text I have produced. If I ever find myself leading a lab, I will take innumerable lessons from Andreas.
I am thankful to all my lab colleagues for discussions during lab meetings and outside of them. A lab is shaped by the people in the lab and it seems like I have been in about three Nieder labs. The first generation of Katharina Merten, Simon Jacob, Anne-Kathrin Eiselt and Maria Moskaleva taught me various things, the different paces of eating with the lab, how the lab functions and how to ask questions in lab meetings. Lena Veit, Torben Ott, Araceli Ramirez-Cardenas, Konstantin Hartmann and Felix Moll were part of many scientific soul-searching conversations. Torben and Simon were the reason I insisted on doing an iontophoresis project in the lab. Lena and Torben have been major culture starters in the lab, we use pieces of their codes, we (forget to) use the LabWiki they helped set up, we take their advice about analyses and we watch Game of Thrones together to this year. Araceli spent many late nights with me in this office, both of us struggling against deadlines and sighing noisily at our computers and then running to the bus stop a few minutes too close. The lab members who now remain, Natalja Gavrilov, Maximilian Stalter, Helen Ditz have been a source of energy, faith, friendship and complete entertainment. After we are all gone, another Nieder lab will seamlessly take shape and hopefully continue fun times at work. Anna Marlina Stein has helped already by taking over my monkeys expertly. Stephanie Westendorff has an easy smile and is a cooperator if there ever was one, bakes like a boss too. Paul Rinnert asks a lot of questions and declares out loud the answers he finds.
Our support staff has been super accommodating of my limited German skills and supported my work in the department. Gabriele Schiffmacher, Bettina Friedrich-Müller, Annette Denzinger, Martin Hoch at the workshop downstairs, the animal caretakers, I thank you. Bettina and Maximilian Kirschhock made great electrodes for me and Sandra Möller trained one of my monkeys at a preliminary stage. Vielen dank!

My time in Tübingen started with the Graduate training centre of neuroscience and they have lent so much support to me over the years. I thank Horst Herbert for his timely advice which led me to join the Nieder lab and the excellent staff Katja Thietges, Tina Lampe, Petya Georgieva and Sandra Fischer for their time and extremely detailed

checklists. You remain indispensable despite those checklists. Jo Ostwald, Ziad Hafed, Uwe Ilg and Cornelius Schwarz have over the years seen many data presentations in the lab, provided valuable feedback and hopefully, asked all the right questions in preparing me to defend my thesis. Eve Marder has said many wise words to me that I cannot help but feel strongly about.

So many of my friends have been role models, science gurus and family away from family that here I start an almost certainly incomplete list of their contributions in my life, and this thesis. Sadashib Ghosh, Pavan Kumar and Megha Sharda, my soulmindmates; Atul Gopal, my first lab coffee mate and coding guide; Ananya Mukherjee, my chaddi buddy; Aditya Murthy and Prof. K.M. Nambiar, my first science mentors; Leslee Lazar taught me far more than he realises and even more helpfully, bookmarked the most essential lessons; Scott Rennie is a great science partner to have and embodies cynicism with an optimistic humanism I did not think possible; my Tübingen family, some of whom may have left Tübingen but took a little bit of mine with them. Dan Arnstein said he had eaten the best mangoes ever, how wrong he was. Thanks for lifting me. Liz "fof" Kiely, Madison Carr, Ceren Battal, thank you for blowing into my life. Thomas and Linda Börner, thanks for housing me and friending me. Marina Fridman, thanks for sharing and competing on caregiving duties with me. Jad Saab brings joy and nice everywhere. Maria Moskaleva has been my rock. Natalja Gavrilov makes all things easy and Galyna Pidpruzhnykova makes all things hilarious and dances around them with ease. Lena and Timo Veit brought much colour into my life. Torben Ott (and Vero) gave me a lot of vodka and even more openness. Felix Moll and Max Stalter helped me manoeuvre many language corners and carried my desk drawer up three flights of stairs without complaint. André Maia Chagas and Samyra Cury Salek, who adopted me, are almost constantly generous beyond measure, and Sudarshan Sekhar my lovely sibling in our odd little family.

And of course, my wonderful unique family is what made me. My mother, Lalitha and sister, Preeti managed to keep me in their (patient) sights across the great geographical distances I put between us. My father, C.V. Viswanathan, who never answered a question straight, became a great personification of scientific data. My family, especially my uncle, Anand and aunts, Ranjani and Shyamala are the wind beneath my wings. Thatha and patti (my grandparents) are the wind beneath theirs.

I am utterly grateful to the animals I have worked with during my time in the lab for enriching it with their idiosyncrasies and all the data. Thank you Louie, Xaver, Schroeder, Ziggy, Yoda and Emil, and a little thanks to one generation of crow chicks (especially little Arya) who convinced me to stick with the non-flying monkeys.

to Ma

Contents

Abstract

In primates, the magnitude system resides in a fronto-parietal network. Single neurons in the monkey prefrontal cortex (PFC) and ventral intraparietal area (VIP) exhibit higher responses to a certain number of stimulus items regardless of their appearance or even sensory modality. Neuroimaging studies in humans show corresponding activation in human fronto-parietal areas during enumeration tasks. However, these areas are also involved in many other executive functions and, thus, the responses of single neurons within the network could be shaped by many factors. Understanding how information about magnitude develops within single neurons in this network was the objective of this thesis.

This thesis includes five studies addressing various aspects of the primate fronto-parietal magnitude system. First, we determined the role of behavioural relevance in shaping neuronal responses to number. Using enumerable coloured stimuli that naïve macaque monkeys discriminated based on their colour rather than number, we examined the selectivity of neuronal responses towards the number of stimuli. We simultaneously recorded single neurons in VIP and PFC. We compared these neurons to those recorded after a period of training for both monkeys, while they discriminated the stimuli based on number. In all the recording sessions, we also mapped the visual receptive fields (RF) of neurons using a passive fixation task. We created RF maps for a large number of spatially-selective neurons in each area and compared the RFs of pairs of neurons recorded at the same electrode tip. We then differentiated the extent of interaction between the RF and number selectivity in both areas.

Neurons in both PFC and VIP were selective for number despite the monkeys being numerically-naïve and number being the behaviourally irrelevant stimulus feature. Post training, neurons in PFC were modulated by behavioural relevance and their selectivity for number became stronger as a result. VIP neurons did not show such an effect. We found that PFC RFs were predominantly contralateral and VIP RFs, foveal. Regardless of RF location and size, we observed heterogeneous and sometimes, inverted RFs in neurons adjacent to each other, more frequently in PFC than in VIP. Lastly, neurons in both PFC and VIP were strongly number-selective even when the number stimuli were shown outside their RFs.

Our results provided valuable insight into the organisation of the magnitude system in primates. The presence of number-selective neuronal responses in numerically-naïve monkeys even when the number of stimuli was behaviourally irrelevant confirmed that our magnitude system processes magnitude spontaneously as a natural category. The strict spatiotopic organisation of RFs characteristic of early visual areas is progressively lower in VIP and PFC. Together, these results point to a hierarchy in the fronto-parietal areas we studied, with PFC located at the apex of the magnitude system and VIP upstream to it.

Part I.
Synopsis

1. Introduction

One of the first attributes we assign to anything has to do with the size or the quantity of it. We use numbers as quantification, ranking, or simply as labels. As early as our birth, we are described by our weight, our size, the date of our birth, the number of intact fingers and toes, our ordinal status in the family. It is hard to imagine human society without such metrics. But for many years, it has been known that animals use quantities to a large extent too, in a variety of contexts. In a foraging decision, it might be valuable to be able to estimate the size of food sources, the distance to the sources. In social situations, it might be valuable to estimate the size or number of the aggressor(s) before planning a response. Much like for humans, it might be important for animals to quantify their brood or offspring in order to identify them and care for them. In this way, we are said to share a primitive non-verbal quantification system with many other living organisms. This thesis describes five studies that support the existence of a mental faculty for estimation of number and describe characteristics of this mental faculty. In the following sections, I will provide a background about the magnitude system, its housing in the primate brain and the motivation for this thesis.

1.1. Behavioural assessment of magnitude

The behaviour of estimating the magnitude of something is multi-faceted and must be characterised in order to understand it and qualify it as such. Humans show recognisable signs of numeracy when they learn to count and enumerate things. This behaviour is guided by verbalising the ordinal relationships between the number of items and learning to deal with the symbolic numerals that stand for a certain discrete quantity (Nieder 2005). However, this ability is very much rooted in culture and language (Nieder 2017). Even more primary is the ability to assess the number or the size of items non-verbally and spontaneously. Animals, preverbal human infants and innumerate adults with the ability of numerical assessment argue for the biological roots of this non-verbal assessment of quantity. This is referred to as the cardinality of a set (**Figure 1)**. Another level of quantity assessment is when an ordinal relationship can be defined between a set of items and then each one can be described in relation to the others such as "first" or "fourth". A third level is used exclusively by humans to label items with a nominal number such as "number seventeen" and can be considered free of quantitative assessment and necessarily dependent on language. The distinction between the different numerical concepts is as much in definition as in representation. There are two systems of

non-verbal assessment. One called the analog magnitude system, processes cardinality as analogous to continuous magnitudes and thus, has no upper limit. The other is called the object tracking system (also known as subitizing) that treats cardinality as discrete items and is most precise for a small number of items (up to 4). Each individual item is assigned a pointer that can be tracked and enumerated implicitly.

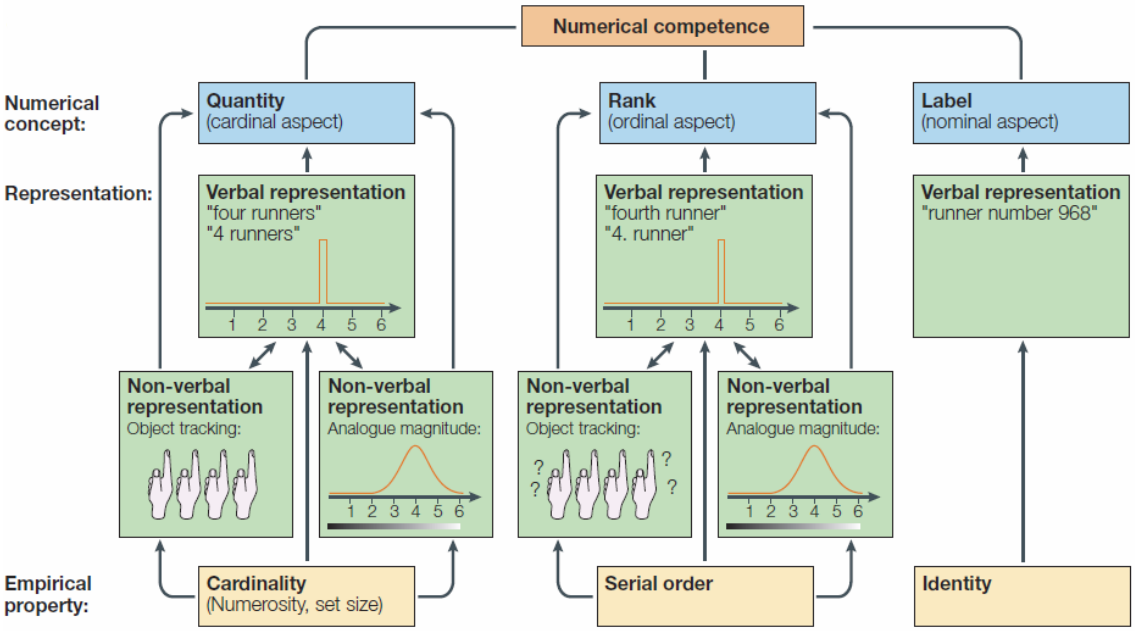

Figure 1: Three numerical concepts Adapted from Nieder (2005). Schematic illustrating the three types of numerical concepts. The non-verbal representations in each case are thought to give rise to the learned verbal representation in spoken/written language. In each case, the non-verbal system is more approximate (or analog) whereas the verbal system is more precise and thus denoted by a digital pulse. A label can only be applied with a verbal representation, requires no cardinal or ordinal system but is useful for precise identification.

Signatures of non-symbolic magnitude system

Based on these representational systems, successful assessment of magnitude can be characterised by certain signatures for example, they follow Weber's law. Weber's law describes that two sensory magnitudes must be at least ΔI apart to be successfully discriminated (just noticeable difference, JND). This difference is described by the product of a constant fraction *(c)* and the stimulus intensity *(I)*. The higher the stimulus intensity *(I)*, the higher the change in intensity *(ΔI)* needs to be for successful discrimination against *I*. All sensory comparisons can thus be scored by calculating a Weber's fraction at each stimulus intensity. An extension on the Weber's law proposed that as the stimulus intensity increases, greater changes in intensity are needed to change the

perceived intensity by a constant amount. This law is called the Fechner's law, and perceived intensity, S can be calculated as the product of a constant (k) and the logarithm of the stimulus intensity, (I). Behavioural discrimination performance of discrete and continuous quantities follows the Weber-Fechner law, such that the higher the quantity, the more difficult the comparisons become (size effect), and the more distant the two quantities, the easier the comparison (distance effect). Together, the Weber-Fechner law explains discrimination behaviour shown by animals and humans, alike (Merten and Nieder 2009).

The first evidence of animals discriminating the cardinality of sets came as early as 1937 from German zoologist, Otto Koehler (Koehler 1937). Recognising possible confounds of such behaviour, he ensured that birds and mammals were not discriminating quantities based on common visual features in dot arrays by changing the dot patterns between comparisons. Since then, a range of animals and birds have demonstrated numerical competence in a variety of contexts (for a detailed review, see Davis and Pérusse (1988)). In the laboratory setting, animals have showed the ability to perform cross-modality comparisons (Church and Meck 1984, Jordan et al. 2005, Nieder 2012) and the ability to generalise ordering to a set of numbers they have not seen before (Brannon and Terrace 1998) quite independently of the co-varying visual features (**Figure 2)**. Animals also generalise discrimination across presentation formats i. e. simultaneous presentation of numerosity against a sequential presentation (Nieder et al. 2006). Importantly, all these behaviours show the characteristic size and distance effects as postulated by the Weber-Fechner law.

Human infants were found to successfully discriminate small quantities. This was considered as evidence for the object tracking system underlying enumeration behaviour in infants. However in later years, human infants were shown to discriminate much higher numerosities and even performed basic operations of addition and subtraction, providing strong evidence for the analog magnitude system (Xu and Spelke 2000, McCrink and Wynn 2004). Infants looked longer at the novel numerosity after familiarisation with a certain numerosity and at the incorrect results of addition or subtraction operations than at the correct result. Human adults without a numerical lexicon show a similar ability to enumerate and discriminate large quantities despite not having precise words for those numbers, adding to evidence for a non-verbal representation of magnitude (Pica et al. 2004, Gordon 2004). In a recent study, performance at numerical comparisons was found to improve with numerical education, resulting in smaller Weber fractions with education in the same Amazonian indigenous group (Piazza et al. 2013). Together, these studies strongly support the existence of an approximate number system (ANS).

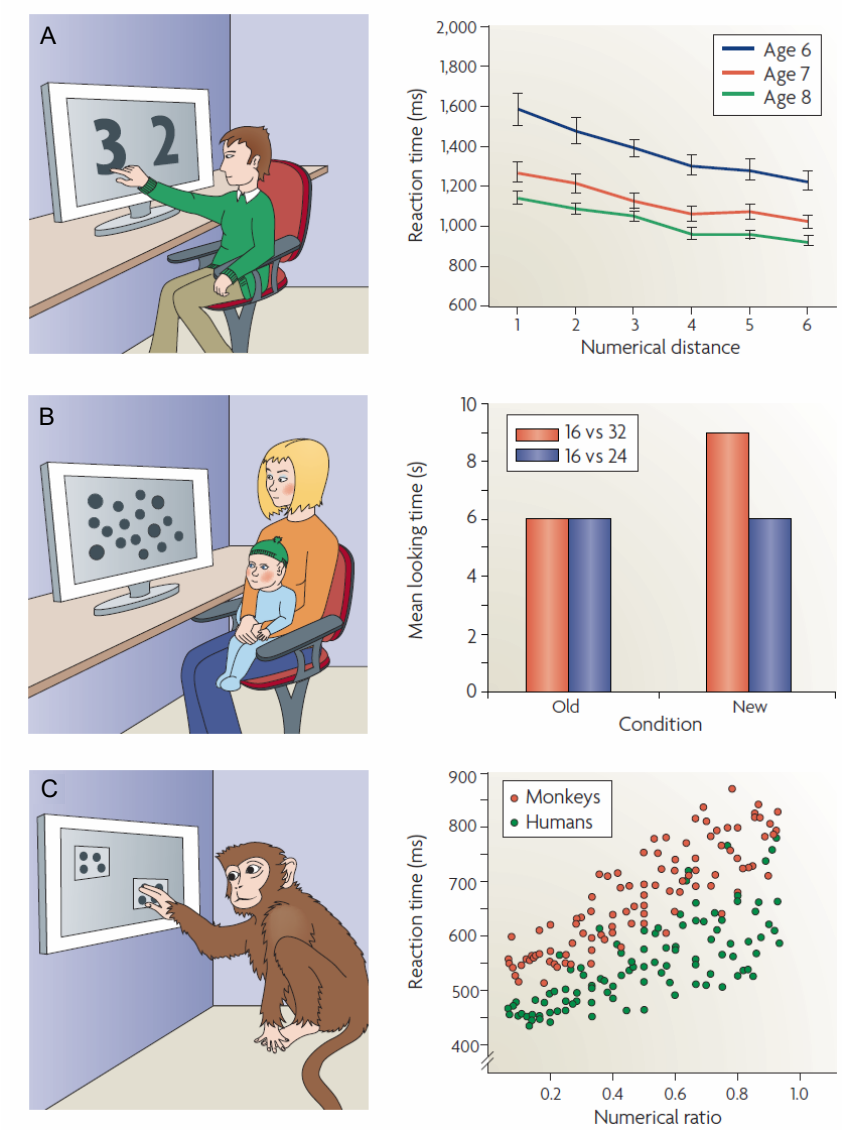

Figure 2: Basic signatures of numerical representation From Ansari (2008). **A.** The distance effect manifests in decreasing reaction time during comparisons with increasing numerical distance between two presented numbers. The effect is seen to decrease with age and mathematical education in humans. The size effect is seen as an increase in reaction time with increasing numbers. **B.** In prelinguistic infants, looking time to new numerosities increases drastically after a period of habituation with the same numerosity presented in a series of displays. This effect scales with the size of numerosity as well as the numerical distance between the old and new numerosity (Xu and Spelke 2000). **C.** Rhesus monkeys learn to order numerosities by touching them in an ordinal sequence. The reaction time in this behaviour also shows the signature effects of distance (here shown as numerical ratio between the numerosities presented on the screen) in a manner similar to those seen in humans.

1.2. Neural substrates of the magnitude system

The quantification system is housed in a fronto-parietal network in primates (**Figure 3)** (Nieder and Dehaene 2009). Evidence for this comes from lesion studies in humans

where damage to parts of the association cortices led to deficits in number processing, called acalculia (Lemer et al. 2003, Ashkenazi et al. 2008). Irregularities in the parieto-frontal network such as reduced cortical thickness in seen in individuals with dyscalculia, a developmental disorder causing disturbances in calculation abilities and the understanding of number (Butterworth et al. 2011). Blood oxygen level dependent (BOLD) activation and electrocorticography (ECoG) signals from the same areas respond to numbers in different formats (Piazza et al. 2007, Cohen Kadosh et al. 2007, Hayashi et al. 2013, Dastjerdi et al. 2013, Daitch et al. 2016). Correspondingly, single neurons within the intraparietal sulcus (IPS), the superior parietal lobule (SPL) and prefrontal cortex (PFC) in macaque monkeys show number-selective activity (Sawamura et al. 2002, Nieder et al. 2002, Nieder and Miller 2004). In a variety of tasks, some involving monkeys discriminating the number of dots in multi-dot arrays or performing a certain number of sequential hand movements, single neurons exhibited selectivity for certain numbers. Pharmacological inactivation of the posterior parietal cortex resulted in monkeys omitting certain actions in the ordinal sequence of movements (Sawamura et al. 2010).

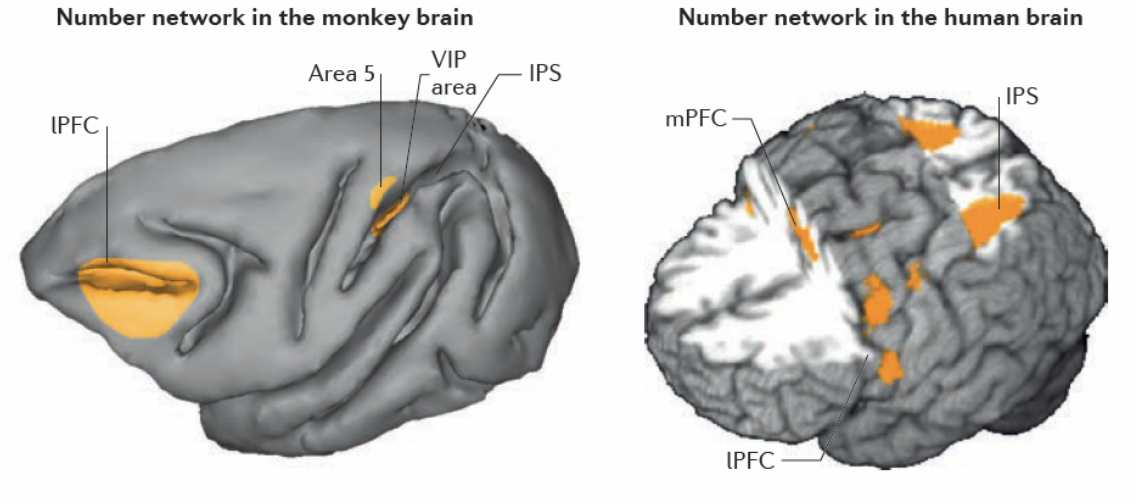

Figure 3: The fronto-parietal magnitude system Adapted from Arsalidou and Taylor (2011), Nieder (2016). A whole brain view of the number network in primates aligned frontolaterally with monkey on the *left* and human on the *right*. Coloured areas indicate activity related to numerosity, proportions, sequential movements, spoken or heard numerals (in the case of humans). The abbreviations are lPFC, lateral prefrontal cortex; VIP, ventral intraparietal area; IPS, intraparietal sulcus; mPFC, medial PFC.

1.2.1. Animal models

As evident from the figure above, the magnitude system seems extremely similar across primates, making rhesus monkeys an ideal animal model to study the approximate number system. The frontal and parietal lobes in primates are both highly associative

and receive multi-modal input, allowing neuronal responses to be more abstract than in early sensory areas. Both primate systems share fundamental tuning properties. For instance, BOLD activity in the human IPS adapts to repeatedly displayed numerosity, and correspondingly less to numerosities close to the adapted numerosities. Thus, a tuning curve formed from the BOLD activity has size and distance effects (Piazza et al. 2004). More recently, a topographic numerosity map has been found using high-field imaging of the SPL in humans involved in an adaptation protocol (Harvey et al. 2013). Mapping of the preferred numerosity for each voxel shows a gradient of preferred numerosity in the area such that neighbouring voxels prefer the same or adjacent numerosities. Over many years, while it has been difficult to find comparable topography in macaque cortex, we have successfully recorded neurons responding selectively to number using various protocols. Interestingly, strikingly similar activity has been found in the functional analog of the PFC in the crow brain as they discriminate the number of items in a dot array (Ditz and Nieder 2015, 2016) despite the absence of layered cortical structures in birds. The nidopallium caudolaterale (NCL) has been proposed as a structure that shares many functional similarities with the primate PFC and the neuronal correlate of the analog magnitude system in birds.

1.2.2. Number neurons

As this thesis primarily deals with single neuron electrophysiology, it is also important to elucidate what number-selective activity looks like in single neurons. Neurons within the fronto-parietal magnitude system in macaque monkeys have been recorded during various behavioural protocols. Neuronal action potentials are collected during ongoing behaviour and those in response to different magnitudes are compared statistically to determine their selectivity (**Figure 4)**. The first number neurons were described in 2002 in two independent studies, one involving a delayed match-to-sample numerosity task and the other involving a sequential hand movement task. The first study reported the presence of number neurons in the PFC, around the principal sulcus (PS) as the monkeys looked at the first dot array that they had to memorise, compare to the following dot arrays and respond to matching number stimuli (Nieder et al. 2002). More than 20 % of PFC neurons showed elevated responses to a certain preferred number and gradually lower responses to the neighbouring numbers regardless of the physical appearance of the stimuli. The neuronal tuning curves to numerosity had the characteristic size and distance effects and matched the monkeys' behavioural performance. The second study recorded neurons from SPL and found 34 % of neurons whose activity correlated with the number of movements the monkeys performed. The monkeys were trained to select a movement and repeat the same movement for five trials before switching without instruction to the other type of movement, thus requiring the monkeys to track how many movements had been performed (Sawamura et al. 2002). They found that neurons

responded selectively to how many movements had been performed which helped the animal track its progress and switch to another movement at the right time accordingly. Following this, Nieder and Miller (2004) recorded neurons in a number of regions in the parietal and temporal cortices and showed that a high proportion of neurons (17 %) in area VIP were also selective for numerosity during a delayed match-to-sample task. In another study most relevant to this thesis, neurons were found to encode the number in a dot array without having any training or doing an active discrimination task in the lateral intraparietal area (LIP) in macaques (Roitman et al. 2007). It is important to note that the monkeys in this case performed a simple delayed saccade task and a dot array simply indicated the "standard" number for each block. In each trial that a non-standard number or a "deviant" was shown to the monkeys, the reward was larger. The monkeys, however, learned to discriminate the numerosity of the dot arrays implicitly and were slower to respond in trials when a deviant number was shown and the expected reward was lower.

1.3. Posterior parietal cortex

As illustrated in the above sections, the primate posterior parietal cortex (PPC) is a node in the magnitude system. The parietal lobe underwent massive expansion in humans showing a higher number of parcellations across cortical areas (Van Essen et al. 2012a,b) presumably to give rise to motor, linguistic and executive functions exclusive to humans. The PPC is the portion of parietal cortex located posterior to the primary somatosensory cortex and has been implicated in movement planning, coordination, attention and spatial processing. In both primates, the divisions of PPC around the intraparietal sulcus (IPS) give rise to the superior and inferior parietal lobule (IPL). The SPL is commonly thought to include Brodmann areas 7 and 5. The IPL in subdivided into the supramarginal gyrus, the temporoparietal junction and the angular gyrus. It roughly corresponds to Brodmann areas 39 and 40. In studies directly comparing the different subdivisions of area 7 for number-selective activity in macaques, area VIP was found to have the highest proportion of such neurons (**Figure 5)**.

Ventral intraparietal area

The area around the IPS is further subdivided into areas based on their location in relation to the sulcus. Area VIP occurs at the fundus of the IPS and single neurons in the area respond to optic flow stimuli (Nieder et al. 2006, Zhang and Britten 2011) which led to the idea that the area participated in heading perception. In contrast to neighbouring area LIP, VIP displays little (Thier and Andersen 1998) to no saccade-related activity (Schaafsma and Duysens 1996), instead responding during smooth pursuit eye movements (Schlack et al. 2003). Neuronal activity in VIP is diverse and multi-modal.

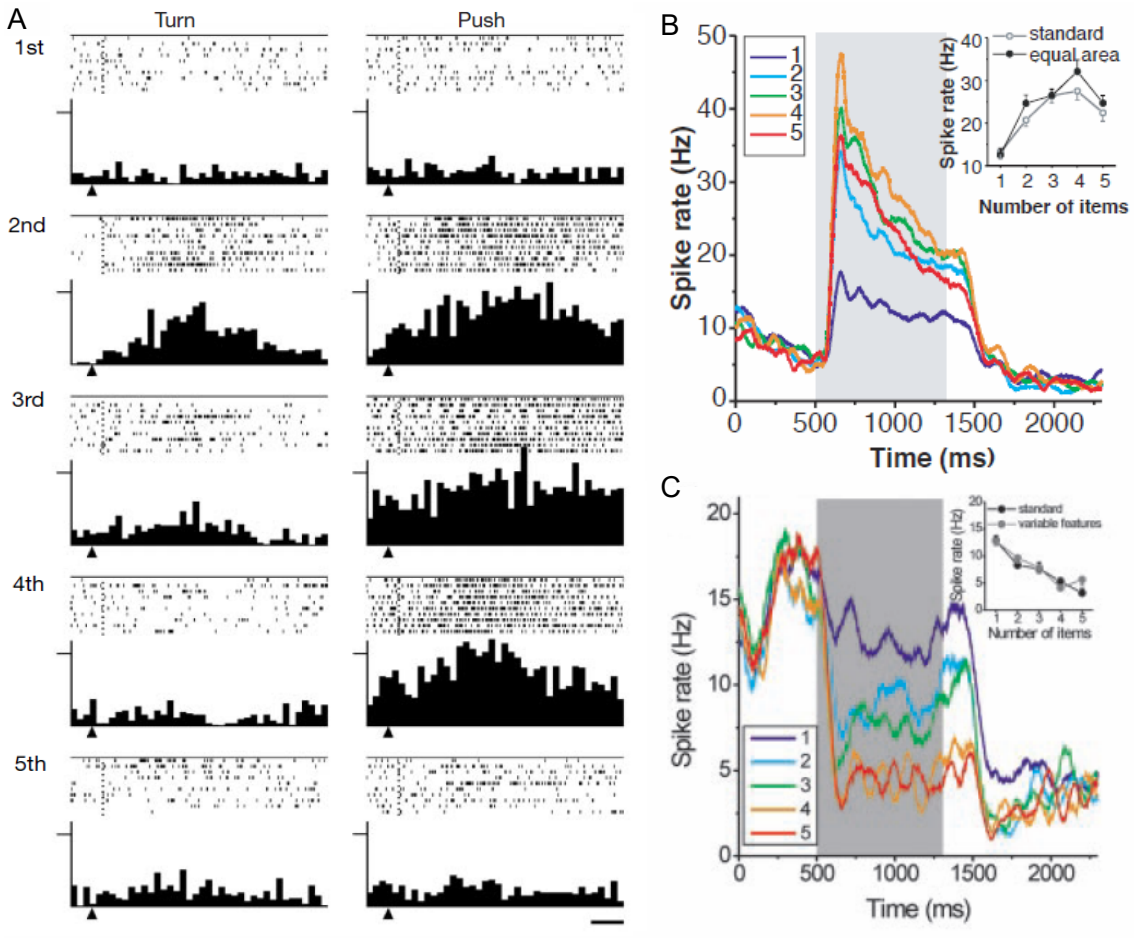

Figure 4: Example number neurons in the fronto-parietal number network Adapted from Sawamura et al. (2002), Nieder et al. (2002), Nieder and Miller (2004) respectively. The first ever number neurons were discovered in the superior parietal lobule, prefrontal cortex and the fundus of the intraparietal sulcus. **A.** A neuron in the SPL showing selective responses to the ordinal position of sequentially performed hand movements. The dot raster shows action potentials across time from the onset of the waiting period in different trials. The peri-event histogram shows the summed activity in 80-ms bins at a scale of 50 discharges per second. **B.** Smoothed spike density functions of an example neuron from the macaque PFC during a delayed match-to-sample numerosity task across different presented numerosities (each coloured line). The inset tuning curve sums the activity during the sample presentation (in the shaded area) in different stimulus formats. In this case, the activity is number-selective irrespective of the summed area of dots. **C.** Similar example neuron from the fundus of the IPS (or area VIP) during the sample presentation that selectively responds to the number one in either the standard format or with variable features.

Single neurons respond to visual (Duhamel et al. 1997), auditory (Schlack et al. 2005), vestibular (Bremmer et al. 2002) and tactile stimuli (Duhamel et al. 1998). Its proposed role has since been advanced to a multi-sensory or sensorimotor integration role (Avillac et al. 2005, 2007). Visual and vestibular responses are shown by the same neurons in some instances such that a neuron that responds to the upper right part of the visual field would also respond to tactile stimuli on the upper right part of the animal's fore-

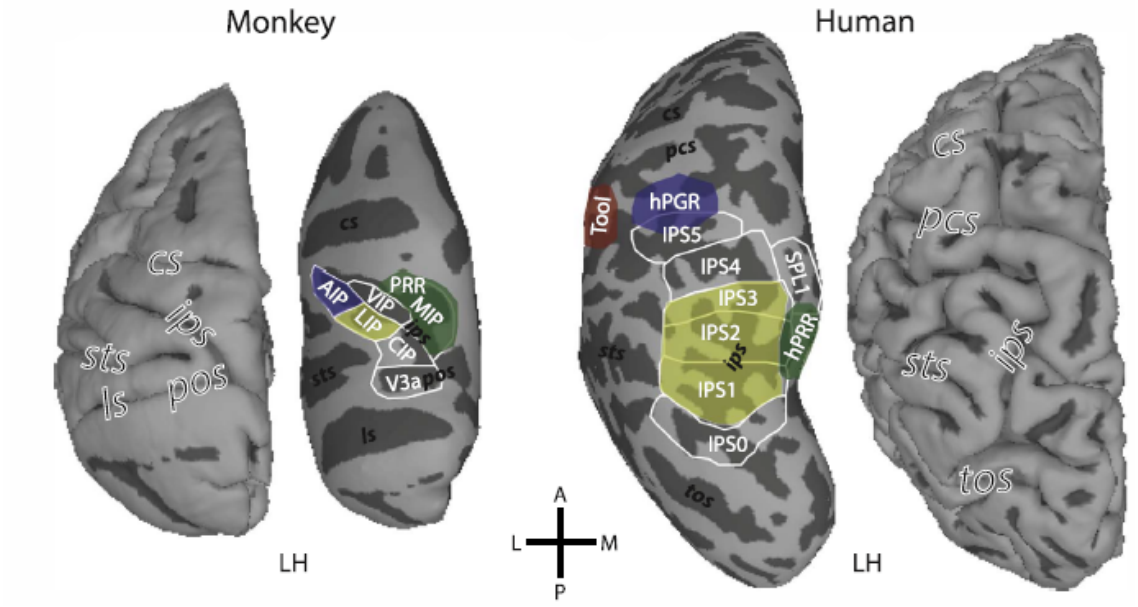

Figure 5: Functional organisation of primate PPC From Kastner et al. (2016). Schematic outline of functional regions with respect to effector responses within monkey (*left*) and human (*right*) parietal cortex. In monkeys, the different areas are anatomically defined along the unfolded IPS, right panel. In humans, the areas are defined topographically in unfolded cortex on the left panel. Saccade-related regions are denoted by yellow, reaching-related regions are indicated by green and grasping-related regions by blue. The human regions are much more dispersed in the parietal cortex than those of the monkey. The red coloured region is a human-specific region showing tool-related responses. Major sulci are labelled: CS, central sulcus; IPS, intraparietal sulcus; STS, superior temporal sulcus; POS, parieto-occipital sulcus; LS, lateral sulcus; TOS, transverse occipital sulcus. The areas marked are: AIP, anterior intraparietal; LIP, lateral intraparietal; VIP, ventral intraparietal; MIP, medial intraparietal; CIP, caudal intraparietal; PRR, parietal reach region; V3a, anterior V3; SPL, superior parietal lobule; hPGR, human parietal grasp region.

head and those closer to the fovea would correspond to touch on the animal's muzzle. Single neurons also encode parts of visual and auditory space similarly. The range of inputs to area provide a clue to its function. VIP receives considerable input from area MSTd which receives both, visual and vestibular information. VIP is also reciprocally connected to parts of the frontal cortex Lewis and Van Essen (2000). In humans, the posterior parietal cortex is much more disperse and the closest homolog of the monkey VIP is believed to be in the anterior-lateral PPC, overlapping with human IPS5. This area also shares response properties with macaque VIP such as selectivity for optic flow, tactile stimuli and stimuli presented within the near space. Magnitude-selective activity appears in regions close to the IPS in comparison tasks during neuroimaging in humans (Cavdaroglu et al. 2015). Many other stimulus features also elicit similar activity during comparison tasks (Cohen Kadosh et al. 2005). With newer and better resolution methods, number-selective activity has been isolated to more anterior and ventral areas like SPL and the parieto-occipital sulcus (POS). The selective expansion of the inferior parietal lobule (IPL) in humans has meant that the IPS occurs much more dorsally (Harvey

et al. 2017).

1.4. Prefrontal cortex

The primate prefrontal cortex is exceptionally well-developed, known to integrate a wide range of information including sensory signals, memory signals and motivational/emotional signals arriving from many other brain areas (Miller and Cohen 2001). The PFC has extensive connections with a large part of cortex, with extensive dendritic trees being one of the earliest defined characteristics of neurons within it. It shares reciprocal connections with other association areas like the parietal cortex (Petrides and Pandya 1984). Distinguishing PFC from other association cortices is its connections with the limbic system (Fuster 2008). It is also known to have an extensive number of local connections (Petrides and Pandya 1999). Single neurons in PFC show persistent activity even after the disappearance of a behavioural cue, possibly as a consequence of the local recurrent connections. This first description of mnemonic activity in the PFC was by Fuster and Alexander (1971) placed PFC firmly in the field of executive function (Fuster 2000).

Cytoarchitectural characteristics allow the PFC to be sub-divided into orbital/medial areas, dorsal/lateral areas and ventral areas. But the cytoarchitecture, together with the connectivity patterns form an updated map of PFC sub-divisions (**Figure 6)**. Of the sub-divisions of PFC, medial and orbital areas exhibit strong connections to the limbic system and are implicated in motivation and emotion-related responses. Within the lateral PFC, monkeys were not earlier believed to contain the Brodmann area 46. However, on functional analysis, area 46 was created in monkey PFC and a segregation of functional roles for the dorsal (9 and 46) and ventral (areas 12, 45 and 47) parts was suggested (Badre and D'Esposito 2009). Ventrolateral PFC is thought to support the maintenance of object-related information while dorsolateral PFC is attributed with more abstract representations and goal-oriented activity. Lesion studies further indicate that dlPFC has much more spatially-selective information while vlPFC has more visual responses (Goldman-Rakic 1988, Constantinidis et al. 2001).

1.5. Connections of VIP and PFC

Both areas we have discussed in detail are jointly implicated in the macaque magnitude system and anatomical tracer studies find them to be reciprocally connected (Lewis and Van Essen 2000). Interestingly, while closely situated LIP receives a lot of input from visual extrastriate areas like V2, V4 and other areas of the ventral visual stream, in addition to dorsal stream input from the middle temporal area (MT), VIP receives almost exclusively dorsal stream input from areas MT and medial superior temporal (MST). LIP and VIP are interconnected, separated by a heavily myelinated section, which has

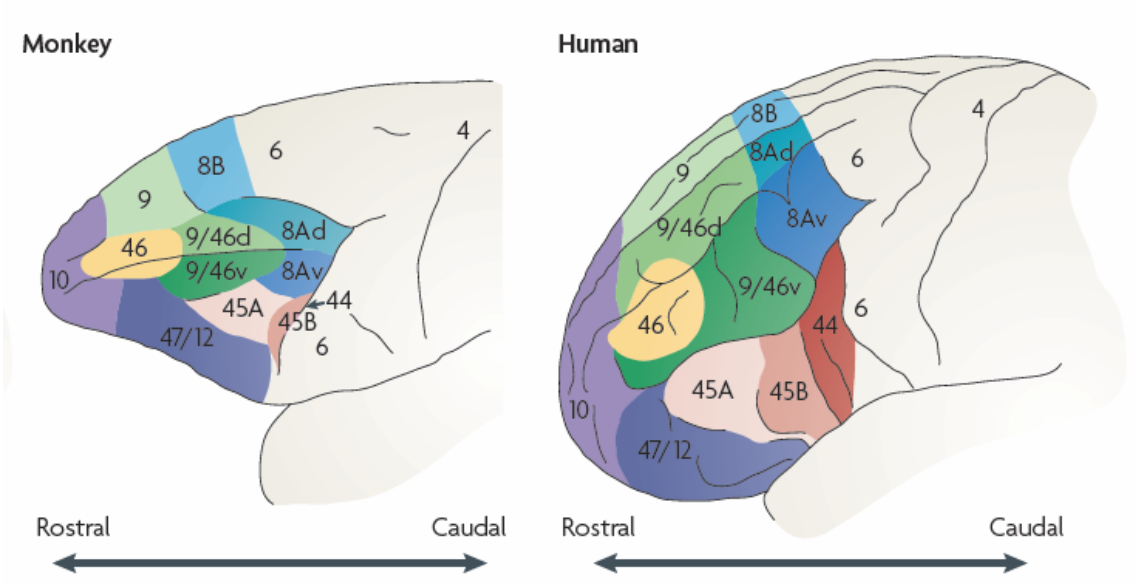

Figure 6: Functional organisation of primate PFC From Badre and D'Esposito (2009). Cytoarchitectonically defined sub-divisions of PFC within monkey (*left*) and human (*right*). The anterior-posterior axis is marked as rostral-caudal. The sub-divisions are labelled according to updates of the Brodmann and Walker maps by Petrides and Pandya (1999), based on the gross characteristics of the cells, the arrangement of cortical layers, distribution of myelination and corticocortical connection patterns. The dorsolateral PFC is said to comprise areas 9 and 46, ventrolateral PFC areas 45A and B, frontal eye fields and supplementary motor areas lie at the lateral and medial parts of area 8, respectively.

been termed as LIPv (Mishkin et al. 1983, Colby et al. 1993). VIP also receives extensive input from somatosensory areas, enabling VIP neurons to be multi-modal, from superior parietal areas and superior temporal cortex (Petrides and Pandya 1984). These range of inputs make VIP an association area and cytoarchitectonically as well as functionally distinct from its parietal neighbours.

Lateral PFC shares these response characteristics and receives information from a variety of modalities. (Petrides and Pandya 1984, Lewis and Van Essen 2000). Reciprocal connections traced with viral tracers between the fundus of macaque IPS and area 46 indicate that these areas of the magnitude system can share numerical information. Simultaneously collected data during numerosity comparison tasks show that VIP neurons precede PFC neurons in processing numerical information (Nieder 2004, Tudusciuc and Nieder 2009). PFC neurons exhibit a higher level of abstraction in responses towards numerosity by responding selectively to the presented number invariantly to the physical features or sensory modality of presentation (Nieder 2004, 2012). Remembered symbolic-like associations are also represented by PFC neurons, but not VIP neurons (Diester and Nieder 2007). Studies of the fronto-parietal association areas within other tasks show that PFC neurons exert top-down control on parietal neurons in processing remembered associations and learned category memberships (Swaminathan and Freed-

man 2012, Crowe et al. 2013). This puts PFC in an ideal position to exercise its hierarchical superiority within the context of non-symbolic magnitudes whereas VIP likely responds to numerosity rather automatically and spontaneously, among other sensory magnitudes.

1.6. Open questions

Box 1. Open questions about the primate magnitude system

1. What is the role of learning in the representation of number in areas VIP and PFC?
2. How are areas VIP and PFC organised?
3. Do the receptive fields of neurons play a role in the representation of number in these areas?

The present state of knowledge about the primate magnitude system leaves a few open questions about the influences on the system and the organisation thereof (**Box 1**) that I will address in this thesis. First, number-selective neurons have only been found in animals that learned to discriminate numerosity. It is not known whether such neurons exist in the absence of learning. If yes, how do their response properties compare to those in experienced animals? Next, we would like to characterise the visual receptive fields of neurons in these areas as a detailed characterisation of RFs is still missing for these areas. Such a characterisation would help us understand how visual information is conveyed to these areas and how these areas might be organised. Lastly, we would like to examine how the RF characteristics affect neuronal responses to number stimuli.

2. Main results

2.1. Statement of contributions

This thesis comprises five publications, which are summarised in the following sections and in **Box 2**. The individual publications and manuscripts can be found in **Part II**.

1. **Viswanathan, P**, Nieder, A. (2013). Neuronal correlates of a visual "sense of number" in primate parietal and prefrontal cortices. *Proc Natl Acad Sci U S A* **110**(27):11187–92.

   I designed the study with A. Nieder. I trained the animals and performed electrophysiological recordings. I analysed the data with A. Nieder. I wrote the paper with A. Nieder.

2. **Viswanathan, P.**, Nieder, A. (2015). Differential impact of behavioral relevance on quantity coding in primate frontal and parietal neurons. *Curr Biol.* **25**(10):1259–69.

   I designed the study with A. Nieder. I performed the experiments. I analysed the data. I wrote the paper with A. Nieder.

3. **Viswanathan, P.**, Nieder, A. (in press). Comparison of visual receptive fields in the dorsolateral prefrontal cortex (dlPFC) and ventral intraparietal area (VIP) in macaques. *Eur. J Neurosci.*

   I designed the study with A. Nieder. I performed the experiments. I analysed the data. I wrote the paper with A. Nieder.

4. **Viswanathan, P.**, Nieder, A. (2017). Visual receptive field heterogeneity and functional connectivity of adjacent neurons in primate fronto-parietal association cortices. *J Neurosci.* **37**(37):8919–8928.

   I designed the study with A. Nieder. I performed the experiments. I analysed the data. I wrote the paper with A. Nieder.

5. **Viswanathan, P.**, Nieder, A. (in preparation). Category tuning for stimuli within and outside receptive fields by primate prefrontal and parietal neurons

   I designed the study with A. Nieder. I performed the experiments. I analysed the data. I wrote the paper with A. Nieder.

2.2. Number sense in prefrontal and parietal areas

Number sense refers to the idea that quantity or magnitude is an essential feature of perception. Humans and animals have the innate ability to perceive the number of items and, thus, our brains have a hard-wired magnitude system. Evidence supporting this idea has come from field studies, infant studies and psychophysical studies. In particular, the prefrontal cortex (PFC) and areas in the posterior parietal cortex (PPC) have been shown to comprise the magnitude system in primates. Single neurons in PFC and PPC encoded the number of items during a task as monkeys discriminated different numbers. It is not known whether these neurons simply reflect learned categories or the behavioural relevance of the stimuli.

We designed a colour discrimination task to examine neuronal responses to number in numerically-naïve monkeys. We used coloured multi-dot arrays as stimuli such that all the dots within a display were uniformly coloured and monkeys matched the colour of sequentially presented arrays by releasing a response bar when a matching stimuli appeared. Every successful colour match was rewarded. We recorded single units in PFC and the ventral intraparietal (VIP) area within the PPC, both known to exhibit number-selective neurons in numerically trained macaques.

We examined each neuron's response to the colour and the number of dots within the stimuli and evaluated them with an ANOVA. We found neurons that responded selectively towards a specific number of dots irrespective of other co-varying visual features. The number-selective responses were also characteristic of tuned neurons recorded from both brain areas in trained monkeys. VIP neurons were, on average, faster at discriminating different numbers than PFC neurons.

These results confirmed that the number of items in a set can be extracted spontaneously by single neurons in the brain in the absence of training and even when the number of items is not behaviourally relevant to the ongoing task. PFC and VIP are part of the fronto-parietal network that possesses the ability to extract magnitudes, and VIP does so about 50ms faster than PFC.

2.3. Behavioural relevance of number in the fronto-parietal network

The identification of prefrontal cortex and posterior parietal cortex as nodes in the primate magnitude system has brought forth questions about how training shapes the neuronal responses towards numerosity. Single neurons in both areas have been known to be modulated by behavioural relevance and experience such that they reflect the arbitrarily-defined but learned category membership of stimuli. We have shown previously that the number of items in a set, however, is spontaneously represented by single neurons in the fronto-parietal network even in monkeys naïve to discriminating them and in the absence of behavioural relevance.

In this study, we compare the neuronal responses in naïve monkeys to those obtained after training them to discriminate the number of items in visual stimuli. Pre-training responses were obtained from monkeys discriminating the colour of coloured multi-dot arrays and post-training responses while the monkeys discriminated the number of items in uniformly black dot arrays. Two types of stimulus arrays were created, one with randomly sized and positioned dots and another to control the total coloured area and density across the different numbers. We recorded single units in the dorsolateral prefrontal cortex and the ventral intraparietal area from the same sites before and after training in both monkeys.

We performed a population analysis to evaluate the trial-by-trial contributions of number and stimulus protocol to the individual neuronal responses. We found that the dependence of neuronal responses on lower visual features decreased in the PFC population with training. We used the same criteria to select number-selective neurons as those in the pre-training phase, using an ANOVA with an alpha of 0.01. The proportion of number-selective neurons in the PFC slightly increased after training from 14 % to 20 % while in VIP, the proportion of number-selective neurons remained similar, from 14 % to 11 %. We calculated two different metrics for number discriminability by the number-selective neurons in both areas and found that in both metrics, PFC neurons

Box 2. Main results of the studies included in my thesis.

1. Number is encoded spontaneously by neurons in PFC and VIP.
   - *A.* Single neurons in PFC and VIP are tuned to number as naïve monkeys perform a colour discrimination task.
   - *B.* VIP neurons discriminate the number of items 50ms before PFC neurons.
   - *C.* After training, as monkeys perform a number discrimination task, PFC neurons encode number more strongly while VIP neurons do not show an enhancement.
   - *D.* Behavioural relevance improves number discriminability in PFC pyramidal neurons.
2. PFC microcircuitry differs markedly from VIP microcircuitry.
   - *A.* PFC neurons have predominantly contra-lateral receptive fields and VIP neurons have foveal receptive fields.
   - *B.* Neurons located close to each other have incongruent or often inverted receptive fields.
   - *C.* Functional connectivity between pyramidal neurons and interneurons was predominantly inhibitory in PFC and excitatory in VIP.
3. Selectivity to number occurs even outside the neurons' RF but PFC and VIP neurons are differentially recruited according to their RFs.

showed significantly improved discrimination of number with training. The variance in firing rates towards the explanatory variable number as well as the differences between firing rates towards the preferred and least preferred number increased in PFC neurons, but not in VIP neurons. In particular, putative pyramidal neurons as determined by their broad spiking waveforms, showed an increased modulation by number during the number discrimination task.

With these results, we showed that numerical information occurred more frequently and strongly in PFC neurons when the monkeys had undergone numerical discrimination training and the number was behaviourally relevant. VIP neurons, on the other hand, spontaneously encoded the number of items regardless of training or relevance. Such coding stability suggests that numerosity, the number of items in a set, is a natural perceptual category. The improvement in PFC coding of number puts PFC in a position to exert top-down control in times of behavioural relevance.

2.4. Visual receptive fields in the fronto-parietal network

The receptive field (RF) of a neuron describes the area of sensory space within which a stimulus can modulate its response. While receptive fields in early sensory areas have simple structures based on the sensory receptors from which they receive information, neurons in higher areas have more complex structures as their inputs vary across modalities and components. Neurons in the posterior parietal area, for instance, respond to stimuli of various modalities and presented in different locations of the visual field if the location is relevant. Prefrontal cortex neurons also respond to stimuli presented across the visual field and show selectivity for the remembered locations of stimuli. However, a broad study of receptive fields in these areas is missing.

We used a moving bar stimulus presented at 80 different locations on the screen as monkeys fixated the centre of the screen to map the receptive fields of individual neurons. This enabled creating high-resolution RF maps for each neuron based on its response to certain stimulus locations during passive fixation, thus, free of effects of attention or behavioural relevance on stimulus positions. We recorded 1186 neurons adjacent to the principal sulcus in the pre-arcuate area and 944 neurons from the fundus of the intraparietal sulcus. We screened the responses of these neurons and tested them for spatially-selective responses, and robust responses during the recording session. We characterised the responses of the significantly selective neurons i. e. 425 PFC and 396 VIP RFs according to the number of maxima, the size and location of their maximum. We measured the eccentricity of the RFs and of those responses that were screen-limited, we calculated the RF sizes. We compared these metrics across both areas. We further examined the metrics across neuronal classes by classifying the neurons based on their extra-cellularly recorded waveforms into putative pyramidal neurons and interneurons with broad and narrow spikes, respectively.

When we compared the proportions of neurons with significant and robust spatial selectivity, we found a higher proportion of such neurons in VIP than in PFC. VIP neurons were also more strongly selective than PFC neurons. Both association areas exhibited a number of non-uniform RFs with multiple local maxima. Of the uniform RFs, some RFs were large and covered 75 % of the screen and others which were more confined to the contralateral, foveal or ipsilateral fields. PFC displayed more contralateral RFs with a slight bias to the lower visual field while VIP displayed many more foveal RFs overlapping with the centre of the screen where the monkeys fixated. Thus, PFC neurons also had more eccentric neurons than VIP. However, of the neurons whose RFs were limited to the screen, those in PFC had smaller RFs than VIP. In this, putative pyramidal neurons had smaller RFs than interneurons within PFC.

Areas within the posterior parietal cortex are often distinguished by their response properties, such that the lateral intraparietal area known for its role in memory guided saccades and decision processes has predominantly eccentric visual RFs while the anterior intraparietal area known for its role in grasping and goal-oriented movements has foveal RFs. The function of these areas is reflected in the location (and size) of their visual RFs. Areas that are involved in the translation or integration of various stimulus components have RFs that lend clues to how they achieve such functions. Our study of visual RFs during passive fixation indicates that such a functional divergence also occurs in PFC and VIP according to their contralateral and foveal biases, respectively.

2.5. Spatiotopy in the fronto-parietal network

Ordered spatial arrangement of inputs about the visual field are common in early visual areas such that adjacent neurons respond to adjacent parts of the visual field. Consequently, receptive fields of adjacent neurons are extremely similar. However, association areas like prefrontal cortex and posterior parietal cortex might be organised differently as they represent the internal state of the animal rather than faithfully represent sensory space. After mapping the receptive fields of individual neuron, we investigated the similarity of neighbouring RFs to understand spatial organisation within these areas.

To do this, we selected neuron pairs where both neurons of the pair exhibited spatial selectivity in the form of RFs during passive fixation and were recorded at the same electrode tip. We quantified the similarity of RFs across each neuron pair by computing a 2D-correlation coefficient that we compared against a distribution of correlations obtained from 1000 shuffles of each map. Comparing the true correlation coefficient with the distribution of shuffled correlations gave us an unbiased estimate of similarity. We classified the neuron pairs as congruent, incongruent or inverted if the true correlation lay above, within, or below the shuffled distribution, respectively. We next compared the proportions of different neuron pairs across the areas. We tested the proportions of similarity for the different neuronal classes: putative interneuron pairs, putative pyramidal

pairs and putative pyramidal-interneuron pairs. We computed the functional connectivity between the neurons using their relative spike timing. Using one of the neurons as trigger for each pair, we calculated the probability of the other neuron (signal) firing against every spike of the trigger within 25 ms.

VIP neuron pairs were found to have predominantly similar RFs in both, horizontal and vertical dimensions. PFC neuron pairs were rather incongruent or inverted. The similarity was distributed across different kinds of neuron pairs. Significant connectivity was found in a small proportion of pairs. Of the functionally connected neuron pairs, PFC pairs shared mostly sharp inhibitory connections while VIP pairs shared broad excitatory connections. Interestingly, the incidence of inhibitory connections between interneuron-pyramidal neuron pairs correlated with the proportions of dissimilar RFs and those of excitatory connections with similar RFs.

With these analyses, we found that neuron pairs in VIP were more similar than those in PFC, suggesting a hierarchy of spatiotopy in these association areas. Both areas showed much more dissimilarity than has been reported for early visual areas. The functional connectivity analysis also showed distinctly different connectivity between neurons across areas. Both metrics differentiate these association areas in aspects of their micro-circuitry and micro-organisation. Such differences naturally raise the question of whether such an organisation plays a role in executive function, especially in their involvement in the magnitude system.

2.6. Number within and without the receptive field

As our representation of the world closely integrates what and where information, information about non-spatial and spatial features of stimuli are often hard to dissociate. In early visual areas, single neurons have smaller RFs and respond to smaller parts of space. In higher areas, RFs of single neurons get larger and neuronal responses integrate more stimulus components or even multiple stimuli. As the organisation of higher areas becomes less spatially organised, the representation of the world gets less veridical and is more subject to internal states, decision processes and relevance. Because studies comparing spatial and non-spatial feature representations often vary both, they do not allow for an independent assessment of both. Since spatiotopy is no longer strictly conserved in higher areas, it is possible that higher association areas respond to stimuli at various positions regardless of their RF. To study this curious aspect of association areas like PFC and VIP, we contrasted single neuron responses to stimuli in a discrimination task against the location of their RFs.

We recorded single neurons from the interconnected areas VIP and PFC during two kinds of discrimination tasks. In separate, interleaved blocks, we mapped the RFs of these neurons using a passive fixation task. These data were then used to compare the recruitment of neurons in discriminating the different categories of stimuli as a

function of their RF. We found three kinds of neurons which responded to discriminative stimuli of colour and number, neurons that showed no significant RFs, neurons whose RFs overlapped with the stimulus location, neurons whose RFs were located elsewhere. We compared the strength of stimulus discriminability across the different classes of neurons in the two areas.

Interestingly, we found significant selectivity for the two kinds discriminative stimuli, colour and number regardless of the presence or location of RF. PFC neurons were more likely to respond to number stimuli if the stimuli were within the RF while VIP neurons responded to stimuli if they were visually responsive, regardless of the location of their RFs. However, number discriminability did not differ across neuron RF classes in either area.

In conclusion, our results allow examination of task recruitment based on the spatial location independently and the ability of association areas to represent stimuli presented outside their RFs show that inputs to these areas may not be as spatially organised as early visual areas. Further analysis will probe into how the RF shapes the responses of neurons, whether different temporal profiles result from stimuli presented within the RF or outside it.

3. Discussion

3.1. Spontaneous representation of number

Our finding of number-selective neurons in areas VIP and PFC as the monkeys discriminated coloured multi-dot displays based on their colour helped clarify many contentious points in the field. Comparing these data directly to those obtained after training as the monkeys discriminated the number of dots in the displays gave us further insight into the magnitude system.

3.1.1. In the absence of training

Studies in many species have indicated that the ability to enumerate up to small quantities is ubiquitous. In the wild, female lions are more likely to defend against three perceived intruders than one, and approached more cautiously in those instances (McComb et al. 1994). Chimpanzees show similar defensive behaviour against groups with more males and approached food at patches where food was more abundant (Wilson et al. 2012). The American coot, a duck-like North American migratory bird, counts its eggs to adjust its own laying behaviour, even discounting parasitic eggs in the process (Lyon 2003). Crows use the number of calls to identify individuals (Thompson 1969). Within laboratory settings, many species are able to use estimates of quantity to guide their behaviour spontaneously: monkeys (Cantlon and Brannon 2007) and insects (Dacke and Srinivasan 2008) and many others with training: fish (Potrich et al. 2015,

Agrillo et al. 2011, Bisazza et al. 2014), amphibians (Uller et al. 2003, Krusche et al. 2010) and birds (Scarf et al. 2011, Ditz and Nieder 2015). Even in humans, prelinguistic infants show the ability of choosing the larger number if the ratio between the options was favourable (Feigenson et al. 2004, Piazza 2010) as do innumerate humans who do not have a formal number system (Gordon 2004, Pica et al. 2004). Such studies have at the very least lifted the cloud on the ability of animals to estimate and use magnitude information although debates about the extent and mechanisms of such behavioural estimations persist. The theories of behavioural estimation of magnitude have been discussed in the **Introduction** but were not directly addressed in this thesis. With our first and second study, however, we were able to examine particular aspects of the neuronal circuitry that might enable such behaviour.

Electrophysiological and neuroimaging studies have pointed to areas in the frontal and parietal cortex in primates as the magnitude system (Nieder et al. 2002, Sawamura et al. 2002, Piazza et al. 2004, 2007, Jacob and Nieder 2009). Numerical processing is selectively impaired by lesions in parietal cortex (Dehaene 1997), distinct from verbal or symbolic deficits. In particular, the prefrontal cortex and areas of the posterior parietal cortex contain neurons that respond selectively to magnitudes in various forms. Since many of these studies are conducted in animals that have undergone extensive behavioural training or humans that are numerate and received mathematical education, it has been difficult to determine to what extent the neuronal correlates of number discrimination are shaped by the behavioural training the animals or humans undergo. As the areas implicated in the magnitude system are higher order areas that house a lot of other executive functions, it is essential to verify that such a magnitude system is not simply a result of the training and the resultant associations (Freedman et al. 2002, Freedman and Assad 2006, Freedman et al. 2006).

A first step in this direction was made when numerical accumulator neurons were found in the lateral intraparietal area of macaque monkeys that were not performing a number discrimination task (Roitman et al. 2007). Monkeys performed a simple delayed saccade task. For each block, a certain number of dots was considered as 'standard' for a reward size and on every trial where a deviant number was displayed, a larger reward was delivered. The monkeys responded more slowly to trials with the 'standard' number and corresponding smaller reward. Reaction times implicitly increased as a function of numerical distance from the 'standard' number for that block. In this case, single neurons responded selectively to the dot display that implicitly indicated the reward size. Our study showed that single neurons in VIP as well as PFC responded to the number of dots in coloured displays as the monkeys were matching the colour of those displays. The monkeys did not learn to discriminate the number of dots, implicitly or explicitly. The presence of number-selective neurons in such an experiment provided evidence for a hard-wired, dedicated neuronal circuitry that encodes visual set size,

even in the absence of corresponding behaviour.

Labelled-line code vs. Summation code

One aspect of the magnitude system has been particularly contentious: the coding mechanism used by selective neurons. Based on computational models and the observation of such coding schemes in other sensory domains, two types of number neurons have been proposed. First, a neuron that sums over many (in the case of numerosity, spatially localised) inputs and responds in a graded, monotonic fashion to number. Such neurons have been reported in LIP (Roitman et al. 2007) and theoretically predicted by theory (Dehaene and Changeux 1993, Verguts and Fias 2004). Second, neurons that respond selectively to one number in a peak-tuned manner and thus function as number detectors on a labelled number line. Such neurons have been reported in VIP and PFC (Nieder et al. 2002, Nieder 2004) and also theoretically predicted (Dehaene and Changeux 1993). These two kinds of number neurons are not necessarily mutually exclusive but can be successive stages of number estimation in a layered computational model and reflect different nodes of the magnitude system. Many models have suggested that the summation model is sufficient for estimation and comparison between different numerosities (Verguts and Fias 2004, Pearson et al. 2010, Stoianov and Zorzi 2012). What follows is the suggestion that the tuned neurons of the labelled-line scheme arise as a result of extensive behavioural training. With our study, we showed tuned neurons are not simply a result of training but present before training. Crucially, our study exploring two essential nodes of the magnitude system before and after discrimination training shows that tuned neurons exist at both stages. Behavioural training also does not register as a sharpening of tuning curves but more as an increase in modulation strength and a decrease in variability (only in PFC).

Distribution of preferred number

Another aspect that follows from the coding scheme is the strength of estimation of various numbers. A labelled-line coding scheme allows us to describe the preferred number for each neuron as the number that elicits the maximal response by the neuron. In other words, it is simply the number towards which the neuron is tuned. In studies reporting such number-tuned neurons, neurons preferring the smallest and largest number of the set are particularly prevalent (Nieder et al. 2002, Nieder 2004). Ruling out the effects of reward expectation towards such a distribution (as trials with the smallest and largest number were usually the easiest and elicited higher reward expectation), we also found such a distribution of preferred numbers despite the monkeys matching the colours of the stimuli and no performance or reward differences across numbers. One

explanation of this is sampling of the neurons that would be tuned to smaller and larger numbers due to a cut-off effect such that neurons that would prefer smaller or larger numbers are sorted as neurons preferring the first and largest numbers of the set.

By those that prescribe to the summation coding scheme, such a distribution of preferred numbers is described as noisy summation coding. As the variability in firing rates increases with increasing numerosities (the size effect), the neurons are increasingly mis-classified as preferring the larger number, resulting in a distribution that has high peaks for the smallest and largest sets, and gradually increasing numbers of neurons preferring the middle numbers. This particular distribution occurs more often in VIP, than in PFC due to greater variability in VIP responses. Whether such a distribution is truly indicative of summation coding or is a feature of labelled-line code is yet to be determined. More importantly, which of these coding schemes is adopted by the brain to extract number information will not be easy to determine as there might be some degeneracy in the magnitude system such that both these coding schemes co-exist.

There has been some recent evidence for a topographic distribution of preferred numbers in the human brain (Harvey et al. 2013). Using high-field functional magnetic resonance imaging, Harvey and colleagues found numerosity selectivity in the superior posterior parietal lobule consistently in all their subjects as they simply judged the colour of the display as white or black. Further, they modelled the response at each recording site with a Gaussian in logarithmic numerosity space, like those used to fit single neuronal responses according to the labeled-line coding scheme. Mapping each recording site's preferred number onto flattened cortical space resulted in a topographic map of gradually increasing numbers along the medio-lateral axis. In another study, they found that the numerosity map overlapped with a map for object size (Harvey et al. 2015) suggesting that the parietal cortex has shared representations for continuous and discrete magnitudes.

3.1.2. In the absence of behavioural relevance

Both the areas we studied as part of the magnitude system are subject to effects of behavioural relevance (Mountcastle et al. 1981, Rainer et al. 1998). In these instances, behavioural relevance facilitated neuronal responses and led to favourable representation of the relevant stimuli compared to the irrelevant stimuli. In other studies, neuronal signals to the same stimuli were shaped by relevance cues that indicate different decision boundaries and consequently, behavioural responses. For instance, responses were dictated by arbitrary category boundaries that had to be learned by trial and error and the neuronal signals gradually separated by the newly learned boundaries (Freedman et al. 2006, Swaminathan and Freedman 2012). In other instances, the stimuli were feature-rich and could be discriminated on the basis of various features that were indicated to the animal (Toth and Assad 2002, Mante et al. 2013) and the neuronal activity reflected

the relevant feature. Thus, relevance-related improvement in number coding could be expected for both VIP and PFC, in addition to learning related improvement. However, we found comparable number coding in VIP before and after training. VIP neurons in our study differentiated between the various numbers whether the number of dots in the stimuli were relevant or not. PFC neurons, on the other hand, showed an improvement in encoding number when number was behaviourally relevant. Seemingly, number is extracted in VIP circuitry without needing a relevance signal from PFC as has been suggested with other visual categories (Swaminathan and Freedman 2012). Perhaps the relevance signal from PFC is only used to shape VIP responses in particularly challenging tasks for instance, a distractor task (Jacob and Nieder 2014) when PFC neurons encode the distractor number intermittently while VIP neurons consistently encode the target.

3.1.3. As evidence for visual "number sense"

Together, our first two studies provide strong evidence for numerosity being a natural category which is stably encoded in the absence of learning or behavioural relevance in the VIP and subject to relevance- and learning-related improvement in the PFC. This adds to the growing consensus from a wide variety of fields for a "number sense". The sense of number refers to a faculty for perceiving the size of visual collections intuitively (Dantzig 1930, Dehaene 1997). Estimates of visual numerosity has been shown to be susceptible to adaptation effects such that seeing a large adapter numerosity induces overestimation of a test numerosity (Burr and Ross 2008, Ross and Burr 2010). This effect is comparable to that seen for many other sensory attributes such as colour, contrast and speed. New evidence suggests that adaptation effects can be seen even across modality (visual-auditory) and across presentation formats (sequential-simultaneous spatial) (Arrighi et al. 2014) suggesting a truly abstract sensory process underlying the estimation of number. These estimates have been shown to be free of other visual co-variates like density or area such that numerosity estimates are truly spontaneous and greatly sensitive (Cicchini et al. 2016). Hierarchical generative computational models show that numerosity detectors can emerge from sensory input purely from top-down connections without the need to classify or discriminate stimuli (Stoianov and Zorzi 2012). In humans, information about number appears earlier than that about other visual co-variates on EEG electrodes over occipito-parietal areas (Park et al. 2016) even as subjects passively viewed dot arrays. Along with the extensive literature in innumerate adults and preverbal infants cited earlier in this section, a spontaneous non-verbal estimation of nonsymbolic numbers is well supported. Improvement of such an ability and an expansion into the symbolic number estimations is seen with mathematical education. In an Amazonian indigene group with a limited numerical lexicon, this improvement is well elucidated by comparing individuals with access to education and those without (Piazza

et al. 2013). Our neuronal data indicates that this improvement must be mediated by the frontal areas in primates.

3.2. Organisation of the fronto-parietal cortices

The second part of this thesis dealt with the micro-organisation of the fronto-parietal areas of the magnitude system to understand how the circuitry might subserve the numerical function of these areas. The visual receptive fields and the organisation of VIP and PFC differ in crucial respects from each other, and from other areas in the brain.

3.2.1. Visual receptive fields

Receptive fields were first described as the region of sensory space within which stimuli can modify a neuron's response (Hubel and Wiesel 1962). Thus, they essentially describe the spatial nature of a neuron's input. Since then, electrophysiology studies have described the RFs of the recorded individual neurons as one of their primary response properties. In association areas, the RFs are less often described with as much detail as in the primary sensory areas. However, RFs provide valuable information about function and the mapping of inputs and connections has helped distinguish essential functional roles that different brain areas play.

Functional parcellation on the basis of RF

The posterior parietal cortex consists of many cytoarchitecturally similar but functionally distinct areas (Mountcastle et al. 1981, Gnadt and Andersen 1988, Blatt et al. 1990, Galletti et al. 1999). While neurons within the posterior parietal areas reflect many cognitive signals, we focus on the sensory nature of their responses for the purpose of this section. Many of these areas receive visual information primarily from the middle temporal (MT) area and parts of PPC receive multi-modal input from other sensory areas proximal to them (Lewis and Van Essen 2000). Parietal areas are interconnected with each other and parts of frontal cortices as determined by tracing anatomical connections (Schwartz and Goldman-Rakic 1984, Petrides and Pandya 1984). Single neurons in VIP respond to visual, auditory, tactile and vestibular information (Bremmer et al. 2002, Avillac et al. 2005, Schlack et al. 2005) crucial for its proposed role in multi-sensory integration (Avillac et al. 2007). We found a foveal bias in VIP visual RFs and the eccentricity of visual and somatic responses in VIP have been shown to strongly correlated (Duhamel et al. 1998). Lateral intraparietal area (LIP) which has been studied extensively for its role in decision-making, is known to have eccentric RFs (Janssen et al. 2008). In particular, LIP neurons are mapped using delayed saccade tasks and show

typical activity that tends to lie on a spectrum of visual to memory signals. Around a saccadic eye movement, LIP RFs show shifts and expansions (Colby et al. 1996, Wang et al. 2016) to accommodate the future position of the eye. This contrasts with receptive fields in the neighbouring anterior intraparietal area (AIP) which tend to be foveal. AIP plays a crucial role in object grasping and inactivation of the area with muscimol results in grasping deficits (Gallese et al. 1994). As grasping of objects with accuracy requires foveation, the foveal nature of neuronal RFs are a clue to their function in the grasping circuitry.

Similarly, areas with the prefrontal cortex are subdivided based on their connection patterns and function (Cavada and Goldman-Rakic 1989, Saleem et al. 2014), however, studies have shown a corresponding pattern in visual RFs. In our study, we mapped a limited number of sites in each monkey as our objective was to return to the same sites at both stages of number training. But in an early study, mapping receptive fields in the prearcuate gyrus using simple light spot, neurons along the principal sulcus (PS) were found to be more eccentric and larger than those along the inferior arcuate sulcus (Suzuki and Azuma 1983). Thus, visual RFs got larger on a posterior-ventral to anterior-dorsal axis while eccentricity varied more strongly on a dorsal-ventral axis.. The pattern of anatomical connections to the PFC suggest a dorso-ventral axis of spatial versus object-based representations (Petrides and Pandya 1984, 1999). A functionally motivated parcellation system suggests that anterior regions engage in more abstract functions while posterior regions in stimulus properties (Badre and D'Esposito 2009) as different deficits are caused by different inactivations or lesions. More recently, RF sizes were found to increase along a posterior-anterior axis supporting older data (Riley et al. 2017) however much less is known about how the RFs relate to function in these areas.

In our study, contrasting RF properties across VIP and PFC certainly helps in relating to the known functional roles of these areas in the magnitude system. VIP neurons in our study had larger RFs covering foveal space which suggests that VIP is in a strong position to integrate signals over a larger area and extract numerical information. It is the ideal area to have local circuits summing over space such that neurons can monotonically encode number. LIP neurons have similarly large RFs in the contralateral field and are known to exhibit largely monotonic responses to number (Roitman et al. 2007). PFC neurons, on the other hand, have much smaller RFs which is perhaps indicative of its role in exercising selective top-down control upon downstream neurons in the circuit or more generally, not spatially integrating information from a large part of the visual field.

3.2.2. Spatiotopy

In early sensory cortices, response properties of neurons are strongly clustered such that neurons close together in the cortex respond similarly to stimulus variables (DeAn-

gelis et al. 1999). The strength of correlated discharge is also known to increase with the degree of similarity in RFs. Among the various stimulus variables, RF location is strongly clustered along with orientation preference (Das and Gilbert 1997). The clustering of similarity occurs along laminar as well as columnar axes in mammals. Columnar organisation is known to give rise to cortical columns as visualised by various clustering methods. However, in association areas such as VIP and PFC, a strict columnar or laminar clustering for space would prove to be too costly in the number of connections required. We found that RF location of nearby neurons (recorded at the same electrode tip) were progressively more dissimilar as we move up in the cortical hierarchy from VIP to PFC. The dissimilarity was also reflected in the connections shared between nearby neurons. VIP neuron pairs shared excitatory connections while PFC neurons shared more inhibitory connections. Response pooling, a well known explanation for clustering, describes the local pooling of inputs and leads to an improvement in the signal-to-noise ratios. Crucially, response pooling seems to occur more strongly in VIP across space than in PFC neurons where response pooling may occur for other stimulus variables, rather than across space. Such a non-canonical circuit would allow for parallel processing of other factors and the recurrence in activity could enable mnemonic activity, thought to be a specialised PFC function.

3.2.3. Interneurons and pyramidal neurons

The two major cell classes in the neocortex are interneurons, typically exhibiting narrow action potentials and pyramidal neurons, with wide action potentials. To our knowledge, only one study has examined differences across parietal neuronal classes (Yokoi and Komatsu 2010) but we did not observe any in our data and will therefore limit this discussion to prefrontal neuronal classes which have been more extensively studied. In our data, we observed some crucial functional and circuit-level differences in PFC neuronal classes. Putative pyramidal neurons in PFC showed a stronger improvement in number coding after training and also had smaller RFs than putative interneurons. Stronger number coding by pyramidal neurons has been reported before (Diester and Nieder 2008) and stronger contributions have been reported for other functions as well. In a study contrasting neuronal responses to spatial positions of remembered objects before and after training, pyramidal neurons showed a sharper improvement in spatial memory than interneurons (Qi et al. 2011). Behavioural relevance also improves direction encoding in PFC pyramidal neurons (Hussar and Pasternak 2009). In many of these instances, pyramidal neurons were sharply and stably tuned while interneurons responded strongly to changes in context. Interneurons with larger RFs can be more flexible and participate in more circuits while pyramidal neurons are more selective to stimulus features and thus, recruited selectively when the stimuli are particularly relevant.

Connections shared between neuronal classes in VIP and PFC further differentiate

the role of these neuronal classes. Interneuron-pyramidal neuron pairs in VIP tended to have similar RFs and shared excitatory connections while those in PFC tended to have dissimilar RFs and shared inhibitory connections. These data point to different VIP and PFC microcircuitry that support different kinds of response pooling. While VIP microcircuitry seems to sum over common spatial inputs, PFC microcircuitry more often inhibits inputs from different parts of visual space. This is a particularly interesting dichotomy that merits further exploration.

3.3. Interaction between number and receptive fields

With this thesis, we thought to probe the interactions between number and space within the magnitude system. Enumerating a spatially dispersed array of items requires integrating over an area of the visual field such that neurons in number-selective cortex can compute the numerosity of the array (see **Labelled-line code vs. Summation code**). We have showed that such neurons occur in VIP and PFC and we have contrasted the types of RFs and the local circuitry of these areas. Few studies have investigated the stimulus discriminability of neurons when the stimulus is presented outside the neuron's RF. Even fewer studies have compared the recruitment of neurons by stimulus presented outside their RF. In a high-field imaging study with humans, preferred numerosity and object size did not correlate with the size or eccentricity of the population RF (Harvey et al. 2015). Association areas of the brain are assumed to overcome default wiring to represent abstract functions that are also non-spatial in nature like reward expectation, value or decision-related factors or choice (Leon and Shadlen 1999, Andersen and Cui 2009). An important caveat of these claims is that the behavioural reports in such tasks tend to be spatial. By separating RF mapping and the discrimination tasks into separate blocks, we were able to look at the RFs independent from the task's demands.

An investigation of LIP responses to stimuli within and outside the RF showed that category-selective responses were found for stimulus outside the RF as well (Freedman and Assad 2009). We found similarly strong number selectivity independent of the stimulus and RF overlap. We found an interesting effect of recruitment in our study. PFC neurons were more likely to be number-selective if the stimulus was presented within their RF i.e. foveal neurons. This raises the possibility that PFC neurons are not as independent of spatial factors as imagined and are much more dependent on foveal VIP neurons for their input about magnitude. This is supported by the finding that PFC direction-selective activity arose earliest in neurons with contralateral fields as are predominant in upstream MT, the prime direction-selective input to PFC (Zaksas and Pasternak 2006, Wimmer et al. 2016).

3.4. Future directions

Several open questions remain and should be addressed in future studies.

1. One of the biggest methodological challenges has been to record the same neuron over a period of time. In understanding the magnitude system, such a study would go a long way in understanding how learning shapes a number-selective neuron's responses over time, especially with natural categories such as number where the category boundaries are naturally occurring but the monkeys discriminate them at varying accuracies, in accordance with the Weber-Fechner law. We believe based on the results in this thesis that number-selective signals would be very stable over time, especially in VIP. It is indeed possible that neuronal tuning curves in PFC would closely match the behavioural tuning curves as behaviour continues to improve (Freedman and Assad 2006).

2. It would also be valuable to understand how context drives the same neurons within the magnitude system. We could achieve this by using different kinds of numerical stimuli and cuing the relevant feature in each trial such that we could study the numerical tuning curves from trials in which number was a relevant feature and those in which number was behaviourally irrelevant. From other studies reporting context-dependent feature representation in prefrontal and parietal areas (Mante et al. 2013, Ibos and Freedman 2014), we would expect that both areas would show effects of context. However, unlike learned categories, we predict that natural categories, of which number is one, would be represented free of context and PFC would specifically exert top-down control of magnitude information on VIP (Crowe et al. 2013).

3. A long-standing question in the field has been whether number selectivity is stable for the number comparison phase. As most studies including those in this thesis involve subjects responding to matching stimuli, the neuronal activity at the initial sample phase and the test phase are not directly comparable (Nieder et al. 2002, Swaminathan and Freedman 2012, Wimmer et al. 2016). We attempt to do this in our next project by designing a task that presents the matching rule after presenting two number stimuli. We can thus record neuronal activity towards the two comparison stimuli and activity reflecting the decision, free of the motor preparation activity as the response can only be prepared *after* the rule is presented. Additionally, we will examine the involvement of the dopaminergic system in the context of this comparison. Studies in our lab have shown that the two kinds of Dopamine receptor families (D1R and D2R) participate in cognitive processes like rule processing and working memory in different ways (Ott et al. 2014, Ott and Nieder 2016).

4. A biologically plausible model that incorporates the spontaneous estimation of number and a relevance-based improvement in tuned responses to number would be welcome in overcoming the methodological constraints of electrophysiology in showing that number selectivity can be independent of visual co-variates. Previous models of the magnitude system have independently established number-tuned responses (Dehaene and Changeux 1993) and the spontaneous generation of number from sensory input (Stoianov and Zorzi 2012).

5. Much more needs to be done to understand how local circuits in the association areas form receptive fields, especially how different neuronal classes interact. This can be done with genetic tools, microstimulation or through microiontophoresis. Iontophoretically blocking GABA-ergic receptors in the inferior temporal cortex enhanced responses to objects presented in the RF centre or even outside the RF. (Wang et al. 2002).

6. Contrasting the responses to number stimuli within and outside the RF of individual neurons would be particularly useful to compare within-neuron effects of variable spatial presentation in number coding (Freedman and Assad 2009).

3.5. Conclusion

Box 3. Main conclusions about the primate magnitude system

1. The number of items is processed as a natural category.
2. The magnitude system operates with a hierarchy; VIP is upstream to PFC.
3. The representation of visual number is independent of visual RFs.

Our studies answer long-standing questions about the magnitude system in primates. We establish that (**Box 3**) number is represented as a natural category by single neurons in VIP and PFC. Not only does VIP lead PFC in extracting the number of items from visual stimuli, but it remains unaffected by training and increased behavioural relevance. PFC, on the other hand, recruits marginally more neurons with higher discriminative ability with behavioural relevance. Next, we examine the organisation principles within these areas and confirm that PFC represents contralateral space while VIP represents our foveal visual space predominantly. VIP boasts a more spatiotopic organisation than PFC such that nearby neurons tend to respond to stimuli within the same space. Local circuits in VIP share excitatory connections while those in PFC share inhibitory connections. Lastly, both areas exhibit strong number tuning even outside neuronal RFs but PFC neurons with foveal RFs are more likely to be number-selective.

Abbreviations

AIP	Anterior intraparietal area
ANOVA	Analysis of variance
BOLD	Blood oxygen level dependent
BS	Broad-spiking neuron
DLPFC	Dorsolateral prefrontal cortex
ECoG	Electrocorticography
FEF	Frontal eye field
FMRI	Functional magnetic resonance imaging
GABA	γ-Aminobutyric acid
IPL	Inferior temporal lobule
IPS	Intraparietal sulcus
ITC	Inferior temporal cortex
JND	Just noticeable difference
LIP	Lateral intraparietal area
MRI	Magnetic resonance imaging
MSTd	Medial superior temporal area
MT	Middle temporal
NCL	Nidopallium caudolaterale
NS	Narrow-spiking neuron
PFC	Prefrontal cortex
PPC	Posterior parietal cortex
RF	Receptive field
SPL	Superior temporal lobule
VIP	Ventral intraparietal area

References

Agrillo, C., Piffer, L. and Bisazza, A. (2011) Number versus continuous quantity in numerosity judgments by fish. *Cognition* **119**, 281–7.

Andersen, R. A. and Cui, H. (2009) Intention, Action Planning, and Decision Making in Parietal-Frontal Circuits. *Neuron* **63**, 568–583.

Ansari, D. (2008) Effects of development and enculturation on number representation in the brain. *Nature reviews. Neuroscience* **9**, 278–91.

Arrighi, R., Togoli, I. and Burr, D. C. (2014) A generalized sense of number. *Proceedings. Biological sciences* **281**, 20141791–20141791.

Arsalidou, M. and Taylor, M. J. (2011) Is 2+2=4? Meta-analyses of brain areas needed for numbers and calculations. *NeuroImage* **54**, 2382–93.

Ashkenazi, S., Henik, A., Ifergane, G. and Shelef, I. (2008) Basic numerical processing in left intraparietal sulcus (IPS) acalculia. *Cortex* **44**, 439–448.

Avillac, M., Ben Hamed, S. and Duhamel, J.-R. (2007) Multisensory integration in the ventral intraparietal area of the macaque monkey. *The Journal of neuroscience : the official journal of the Society for Neuroscience* **27**, 1922–32.

Avillac, M., Denève, S., Olivier, E., Pouget, A. and Duhamel, J.-R. (2005) Reference frames for representing visual and tactile locations in parietal cortex. *Nature neuroscience* **8**, 941–9.

Badre, D. and D'Esposito, M. (2009) Is the rostro-caudal axis of the frontal lobe hierarchical? *Nature reviews. Neuroscience* **10**, 659–69.

Bisazza, A., Tagliapietra, C., Bertolucci, C., Foà, A. and Agrillo, C. (2014) Non-visual numerical discrimination in a blind cavefish (Phreatichthys andruzzii). *The Journal of experimental biology* **217**, 1902–9.

Blatt, G. J., Andersen, R. A. and Stoner, G. R. (1990) Visual receptive field organization and cortico-cortical connections of the lateral intraparietal area (area LIP) in the macaque. *The Journal of comparative neurology* **299**, 421–45.

Brannon, E. M. and Terrace, H. S. (1998) Ordering of the numerosities 1 to 9 by monkeys. *Science (New York, N.Y.)* **282**, 746–9.

Bremmer, F., Klam, F., Duhamel, J.-R., Ben Hamed, S. and Graf, W. (2002) Visual-vestibular interactive responses in the macaque ventral intraparietal area (VIP). *The European journal of neuroscience* **16**, 1569–86.

Burr, D. and Ross, J. (2008) A visual sense of number. *Current biology : CB* **18**, 425–8.

Butterworth, B., Varma, S. and Laurillard, D. (2011) Dyscalculia: From Brain to Education. *Science* **332**, 1049–1053.

Cantlon, J. F. and Brannon, E. M. (2007) How much does number matter to a monkey (Macaca mulatta)? *Journal of experimental psychology. Animal behavior processes* **33**, 32–41.

Cavada, C. and Goldman-Rakic, P. S. (1989) Posterior parietal cortex in rhesus monkey: II. Evidence for segregated corticocortical networks linking sensory and limbic areas with the frontal lobe. *The Journal of comparative neurology* **287**, 422–45.

Cavdaroglu, S., Katz, C. and Knops, A. (2015) Dissociating estimation from comparison and response eliminates parietal involvement in sequential numerosity perception. *NeuroImage* **116**, 135–48.

Church, R. M. and Meck, W. H. (1984) The numerical attribute of stimuli. *Animal cognition* **445464**.

Cicchini, G. M., Anobile, G. and Burr, D. C. (2016) Spontaneous perception of numerosity in humans. *Nature communications* **7**, 12536.

Cohen Kadosh, R., Cohen Kadosh, K., Kaas, A., Henik, A. and Goebel, R. (2007) Notation-dependent and -independent representations of numbers in the parietal lobes. *Neuron* **53**, 307–14.

Cohen Kadosh, R., Henik, A., Rubinsten, O., Mohr, H., Dori, H., Van De Ven, V., Zorzi, M., Hendler, T., Goebel, R. and Linden, D. E. J. (2005) Are numbers special? The comparison systems of the human brain investigated by fMRI. *Neuropsychologia* **43**, 1238–1248.

Colby, C. L., Duhamel, J. R. and Goldberg, M. E. (1993) Ventral intraparietal area of the macaque: anatomic location and visual response properties. *Journal of neurophysiology* **69**, 902–14.

Colby, C. L., Duhamel, J. R. and Goldberg, M. E. (1996) Visual, presaccadic, and cognitive activation of single neurons in monkey lateral intraparietal area. *Journal of neurophysiology* **76**, 2841–2852.

Constantinidis, C., Franowicz, M. N. and Goldman-Rakic, P. S. (2001) The sensory nature of mnemonic representation in the primate prefrontal cortex. *Nature Neuroscience* **4**, 311–6.

Crowe, D. A., Goodwin, S. J., Blackman, R. K., Sakellaridi, S., Sponheim, S. R., MacDonald, A. W. and Chafee, M. V. (2013) Prefrontal neurons transmit signals to parietal neurons that reflect executive control of cognition. *Nature neuroscience* **16**, 1484–91.

Dacke, M. and Srinivasan, M. V. (2008) Evidence for counting in insects. *Animal cognition* **11**, 683–9.

Daitch, A. L., Foster, B. L., Schrouff, J., Rangarajan, V., KaÅŸikçi, I., Gattas, S. and Parvizi, J. (2016) Mapping human temporal and parietal neuronal population activity and functional coupling during mathematical cognition. *Proceedings of the National Academy of Sciences of the United States of America* **113**, E7277–E7286.

Dantzig, T. (1930) *Number: The Language of Science*. New York: The Free Press. URL: `https://books.google.de/books?id=Pg{_}RKtlVlNMC`.

Das, A. and Gilbert, C. D. (1997) Distortions of visuotopic map match orientation singularities in primary visual cortex. *Nature* **387**, 594–8.

Dastjerdi, M., Ozker, M., Foster, B. L., Rangarajan, V. and Parvizi, J. (2013) Numerical processing in the human parietal cortex during experimental and natural conditions. *Nature Communications* **4**, 1–11.

Davis, H. and Pérusse, R. (1988) Numerical competence in animals: Definitional issues, current evidence, and a new research agenda. *Behavioral and brain sciences1* **11**, 561–579.

DeAngelis, G. C., Ghose, G. M., Ohzawa, I. and Freeman, R. D. (1999) Functional micro-organization of primary visual cortex: receptive field analysis of nearby neurons. *The Journal of neuroscience : the official journal of the Society for Neuroscience* **19**, 4046–64.

Dehaene, S. (1997) *The Number Sense*. Oxford University Press. URL: `https://books.google.de/books?id=2zkS7ylIDlsC`.

Dehaene, S. and Changeux, J. P. (1993) Development of elementary numerical abilities: a neuronal model. *Journal of cognitive neuroscience* **5**, 390–407.

Diester, I. and Nieder, A. (2007) Semantic associations between signs and numerical categories in the prefrontal cortex. *PLoS biology* **5**, e294.

Diester, I. and Nieder, A. (2008) Complementary contributions of prefrontal neuron classes in abstract numerical categorization. *The Journal of neuroscience : the official journal of the Society for Neuroscience* **28**, 7737–47.

Ditz, H. M. and Nieder, A. (2015) Neurons selective to the number of visual items in the corvid songbird endbrain. *Proceedings of the National Academy of Sciences of the United States of America* **112**, 7827–32.

Ditz, H. M. and Nieder, A. (2016) Numerosity representations in crows obey the Weber-Fechner law. *Proceedings. Biological sciences* **283**, 20160083.

Duhamel, J. R., Colby, C. L. and Goldberg, M. E. (1998) Ventral intraparietal area of the macaque: congruent visual and somatic response properties. *Journal of neurophysiology* **79**, 126–36.

Duhamel, J.-R. R., Bremmer, F., Ben Hamed, S. and Graf, W. (1997) Spatial invariance of visual receptive fields in parietal cortex neurons. *Nature* **389**, 845–8.

Feigenson, L., Dehaene, S. and Spelke, E. (2004) Core systems of number. *Trends in cognitive sciences* **8**, 307–14.

Freedman, D. J. and Assad, J. A. (2006) Experience-dependent representation of visual categories in parietal cortex. *Nature* **443**, 85–8.

Freedman, D. J. and Assad, J. A. (2009) Distinct encoding of spatial and nonspatial visual information in parietal cortex. *The Journal of neuroscience : the official journal of the Society for Neuroscience* **29**, 5671–80.

Freedman, D. J., Riesenhuber, M., Poggio, T. and Miller, E. K. (2002) Visual categorization and the primate prefrontal cortex: neurophysiology and behavior. *Journal of neurophysiology* **88**, 929–41.

Freedman, D. J., Riesenhuber, M., Poggio, T. and Miller, E. K. (2006) Experience-dependent sharpening of visual shape selectivity in inferior temporal cortex. *Cerebral cortex (New York, N.Y. : 1991)* **16**, 1631–44.

Fuster, J. (2008) *The Prefrontal Cortex*. Elsevier Science. URL: `https://books.google.de/books?id=zuZlvNICdhUC`.

Fuster, J. M. (2000) Executive frontal functions. *Experimental brain research* **133**, 66–70.

Fuster, J. M. and Alexander, G. E. (1971) Neuron activity related to short-term memory. *Science (New York, N.Y.)* **173**, 652–4.

Gallese, V., Murata, A., Kaseda, M., Niki, N. and Sakata, H. (1994) Deficit of hand preshaping after muscimol injection in monkey parietal cortex. *Neuroreport* **5**, 1525–9.

Galletti, C., Fattori, P., Gamberini, M. and Kutz, D. F. (1999) The cortical visual area V6: brain location and visual topography. *The European journal of neuroscience* **11**, 3922–36.

Gnadt, J. W. and Andersen, R. A. (1988) Memory related motor planning activity in posterior parietal cortex of macaque. *Experimental brain research* **70**, 216–20.

Goldman-Rakic, P. S. (1988) Topography of cognition: parallel distributed networks in primate association cortex. *Annual review of neuroscience* **11**, 137–56.

Gordon, P. (2004) Numerical cognition without words: evidence from Amazonia. *Science (New York, N.Y.)* **306**, 496–9.

Harvey, B. M., Ferri, S. and Orban, G. A. (2017) Comparing Parietal Quantity-Processing Mechanisms between Humans and Macaques. *Trends in cognitive sciences* **21**, 779–793.

Harvey, B. M., Fracasso, A., Petridou, N. and Dumoulin, S. O. (2015) Topographic representations of object size and relationships with numerosity reveal generalized quantity processing in human parietal cortex. *Proceedings of the National Academy of Sciences of the United States of America* **112**, 13525–30.

Harvey, B. M., Klein, B. P., Petridou, N. and Dumoulin, S. O. (2013) Topographic representation of numerosity in the human parietal cortex. *Science (New York, N.Y.)* **341**, 1123–6.

Hayashi, M. J., Kanai, R., Tanabe, H. C., Yoshida, Y., Carlson, S., Walsh, V. and Sadato, N. (2013) Interaction of Numerosity and Time in Prefrontal and Parietal Cortex. *Journal of Neuroscience* **33**, 883–893.

Hubel, D. H. and Wiesel, T. N. (1962) Receptive fields, binocular interaction and functional architecture in the cat's visual cortex. *The Journal of physiology* **160**, 106–54.

Hussar, C. R. and Pasternak, T. (2009) Flexibility of sensory representations in prefrontal cortex depends on cell type. *Neuron* **64**, 730–43.

Ibos, G. and Freedman, D. J. (2014) Dynamic integration of task-relevant visual features in posterior parietal cortex. *Neuron* **83**, 1468–80.

Jacob, S. N. and Nieder, A. (2009) Tuning to non-symbolic proportions in the human frontoparietal cortex. *The European journal of neuroscience* **30**, 1432–42.

Jacob, S. N. and Nieder, A. (2014) Complementary roles for primate frontal and parietal cortex in guarding working memory from distractor stimuli. *Neuron* **83**, 226–37.

Janssen, P., Srivastava, S., Ombelet, S. and Orban, G. A. (2008) Coding of shape and position in macaque lateral intraparietal area. *The Journal of neuroscience : the official journal of the Society for Neuroscience* **28**, 6679–6690.

Jordan, K. E., Brannon, E. M., Logothetis, N. K. and Ghazanfar, A. A. (2005) Monkeys match the number of voices they hear to the number of faces they see. *Current biology : CB* **15**, 1034–8.

Kastner, S., Chen, Q., Jeong, S. K. and Mruczek, R. E. B. (2016) A brief comparative review of primate posterior parietal cortex: A novel hypothesis on the human toolmaker. *Neuropsychologia* 0–1.

Koehler, O. (1937) Können Tauben "zählen"? *Zeitschrift für Tierpsychologie* **1**, 39–48.

Krusche, P., Uller, C. and Dicke, U. (2010) Quantity discrimination in salamanders. *Journal of Experimental Biology* **213**, 1822–1828.

Lemer, C., Dehaene, S., Spelke, E. and Cohen, L. (2003) Approximate quantities and exact number words: Dissociable systems. *Neuropsychologia* **41**, 1942–1958.

Leon, M. I. and Shadlen, M. N. (1999) Effect of expected reward magnitude on the response of neurons in the dorsolateral prefrontal cortex of the macaque. *Neuron* **24**, 415–25.

Lewis, J. W. and Van Essen, D. C. (2000) Corticocortical connections of visual, sensorimotor, and multimodal processing areas in the parietal lobe of the macaque monkey. *The Journal of comparative neurology* **428**, 112–37.

Lyon, B. E. (2003) Egg recognition and counting reduce costs of avian conspecific brood parasitism. *Nature* **422**, 495–9.

Mante, V., Sussillo, D., Shenoy, K. V. and Newsome, W. T. (2013) Context-dependent computation by recurrent dynamics in prefrontal cortex. *Nature* **503**, 78–84.

McComb, K., Packer, C. and Pusey, A. (1994) Roaring and numerical assessment in contests between groups of female lions, Panthera leo. *Animal Behaviour* **47**, 379–387.

McCrink, K. and Wynn, K. (2004) Large-number addition and subtraction by 9-month-old infants. *Psychological Science* **15**, 776–781.

Merten, K. and Nieder, A. (2009) Compressed scaling of abstract numerosity representations in adult humans and monkeys. *Journal of cognitive neuroscience* **21**, 333–46.

Miller, E. K. and Cohen, J. D. (2001) An integrative theory of prefrontal cortex function. *Annual review of neuroscience* **24**, 167–202.

Mishkin, M., Ungerleider, L. G. and Macko, K. A. (1983) Object vision and spatial vision: two cortical pathways. *Trends in Neurosciences* **6**, 414–417.

Mountcastle, V. B., Andersen, R. a. and Motter, B. C. (1981) The influence of attentive fixation upon the excitability of the light-sensitive neurons of the posterior parietal cortex. *The Journal of neuroscience : the official journal of the Society for Neuroscience* **1**, 1218–25.

Nieder, A. (2004) The number domain- can we count on parietal cortex? *Neuron* **44**, 407–9.

Nieder, A. (2005) Counting on neurons: the neurobiology of numerical competence. *Nature reviews. Neuroscience* **6**, 177–90.

Nieder, A. (2012) Supramodal numerosity selectivity of neurons in primate prefrontal and posterior parietal cortices. *Proceedings of the National Academy of Sciences of the United States of America* **109**, 11860–5.

Nieder, A. (2016) The neuronal code for number. *Nature reviews. Neuroscience* **17**, 366–82.

Nieder, A. (2017) Number Faculty Is Rooted in Our Biological Heritage. *Trends in cognitive sciences* **21**, 403–404.

Nieder, A. and Dehaene, S. (2009) Representation of number in the brain. *Annual review of neuroscience* **32**, 185–208.

Nieder, A., Diester, I. and Tudusciuc, O. (2006) Temporal and spatial enumeration processes in the primate parietal cortex. *Science (New York, N.Y.)* **313**, 1431–5.

Nieder, A., Freedman, D. J. and Miller, E. K. (2002) Representation of the quantity of visual items in the primate prefrontal cortex. *Science (New York, N.Y.)* **297**, 1708–11.

Nieder, A. and Miller, E. K. (2004) A parieto-frontal network for visual numerical information in the monkey. *Proceedings of the National Academy of Sciences of the United States of America* **101**, 7457–62.

Ott, T., Jacob, S. N. and Nieder, A. (2014) Dopamine receptors differentially enhance rule coding in primate prefrontal cortex neurons. *Neuron* **84**, 1317–28.

Ott, T. and Nieder, A. (2016) Dopamine D2 Receptors Enhance Population Dynamics in Primate Prefrontal Working Memory Circuits. *Cerebral cortex (New York, N.Y. : 1991)* 1–13.

Park, J., DeWind, N. K., Woldorff, M. G. and Brannon, E. M. (2016) Rapid and Direct Encoding of Numerosity in the Visual Stream. *Cerebral cortex (New York, N.Y. : 1991)* **26**, 748–63.

Pearson, J., Roitman, J. D., Brannon, E. M., Platt, M. L. and Raghavachari, S. (2010) A physiologically-inspired model of numerical classification based on graded stimulus coding. *Frontiers in behavioral neuroscience* **4**, 1.

Petrides, M. and Pandya, D. N. (1984) Projections to the frontal cortex from the posterior parietal region in the rhesus monkey. *The Journal of comparative neurology* **228**, 105–16.

Petrides, M. and Pandya, D. N. (1999) Dorsolateral prefrontal cortex: comparative cytoarchitectonic analysis in the human and the macaque brain and corticocortical connection patterns. *The European journal of neuroscience* **11**, 1011–36.

Piazza, M. (2010) Neurocognitive start-up tools for symbolic number representations. *Trends in cognitive sciences* **14**, 542–51.

Piazza, M., Izard, V., Pinel, P., Le Bihan, D. and Dehaene, S. (2004) Tuning curves for approximate numerosity in the human intraparietal sulcus. *Neuron* **44**, 547–55.

Piazza, M., Pica, P., Izard, V., Spelke, E. S. and Dehaene, S. (2013) Education enhances the acuity of the nonverbal approximate number system. *Psychological science* **24**, 1037–43.

Piazza, M., Pinel, P., Le Bihan, D. and Dehaene, S. (2007) A magnitude code common to numerosities and number symbols in human intraparietal cortex. *Neuron* **53**, 293–305.

Pica, P., Lemer, C., Izard, V. and Dehaene, S. (2004) Exact and approximate arithmetic in an Amazonian indigene group. *Science (New York, N.Y.)* **306**, 499–503.

Potrich, D., Sovrano, V. A., Stancher, G. and Vallortigara, G. (2015) Quantity discrimination by zebrafish (Danio rerio). *Journal of comparative psychology (Washington, D.C. : 1983)* **129**, 388–93.

Qi, X.-L., Meyer, T., Stanford, T. R. and Constantinidis, C. (2011) Changes in prefrontal neuronal activity after learning to perform a spatial working memory task. *Cerebral cortex (New York, N.Y. : 1991)* **21**, 2722–32.

Rainer, G., Asaad, W. F. and Miller, E. K. (1998) Selective representation of relevant information by neurons in the primate prefrontal cortex. *Nature* **393**, 577–9.

Riley, M. R., Qi, X.-L. and Constantinidis, C. (2017) Functional specialization of areas along the anterior-posterior axis of the primate prefrontal cortex. *Cerebral cortex (New York, N.Y. : 1991)* **27**, 3683–3697.

Roitman, J. D., Brannon, E. M. and Platt, M. L. (2007) Monotonic coding of numerosity in macaque lateral intraparietal area. *PLoS biology* **5**, e208.

Ross, J. and Burr, D. C. (2010) Vision senses number directly. *Journal of vision* **10**, 10.1–8.

Saleem, K. S., Miller, B. and Price, J. L. (2014) Subdivisions and connectional networks of the lateral prefrontal cortex in the macaque monkey. *The Journal of comparative neurology* **522**, 1641–90.

Sawamura, H., Shima, K. and Tanji, J. (2002) Numerical representation for action in the parietal cortex of the monkey. *Nature* **415**, 918–22.

Sawamura, H., Shima, K. and Tanji, J. (2010) Deficits in Action Selection Based on Numerical Information After Inactivation of the Posterior Parietal Cortex in Monkeys. *Journal of Neurophysiology* **104**, 902–910.

Scarf, D., Hayne, H. and Colombo, M. (2011) Pigeons on par with primates in numerical competence. *Science (New York, N.Y.)* **334**, 1664.

Schaafsma, S. J. and Duysens, J. (1996) Neurons in the ventral intraparietal area of awake macaque monkey closely resemble neurons in the dorsal part of the medial superior temporal area in their responses to optic flow patterns. *Journal of neurophysiology* **76**, 4056–68.

Schlack, A., Hoffmann, K.-P. and Bremmer, F. (2003) Selectivity of macaque ventral intraparietal area (area VIP) for smooth pursuit eye movements. *The Journal of physiology* **551**, 551–61.

Schlack, A., Sterbing-D'Angelo, S. J., Hartung, K., Hoffmann, K.-P. and Bremmer, F. (2005) Multisensory space representations in the macaque ventral intraparietal area. *The Journal of neuroscience : the official journal of the Society for Neuroscience* **25**, 4616–25.

Schwartz, M. L. and Goldman-Rakic, P. S. (1984) Callosal and intrahemispheric connectivity of the prefrontal association cortex in rhesus monkey: relation between intraparietal and principal sulcal cortex. *The Journal of comparative neurology* **226**, 403–20.

Stoianov, I. and Zorzi, M. (2012) Emergence of a 'visual number sense' in hierarchical generative models. *Nature neuroscience* **15**, 194–6.

Suzuki, H. and Azuma, M. (1983) Topographic studies on visual neurons in the dorsolateral prefrontal cortex of the monkey. *Experimental brain research* **53**, 47–58.

Swaminathan, S. K. and Freedman, D. J. (2012) Preferential encoding of visual categories in parietal cortex compared with prefrontal cortex. *Nature neuroscience* **15**, 315–20.

Thier, P. and Andersen, R. A. (1998) Electrical microstimulation distinguishes distinct saccade-related areas in the posterior parietal cortex. *Journal of neurophysiology* **80**, 1713–35.

Thompson, N. S. (1969) Individual identification and temporal patterning in the cawing of common crows. *Communications in Behavioral Biology* **4**, 29–33.

Toth, L. J. and Assad, J. A. (2002) Dynamic coding of behaviourally relevant stimuli in parietal cortex. *Nature* **415**, 165–8.

Tudusciuc, O. and Nieder, A. (2009) Contributions of primate prefrontal and posterior parietal cortices to length and numerosity representation. *Journal of neurophysiology* **101**, 2984–94.

Uller, C., Jaeger, R., Guidry, G. and Martin, C. (2003) Salamanders (Plethodon cinereus) go for more: rudiments of number in an amphibian. *Animal Cognition* **6**, 105–112.

Van Essen, D. C., Glasser, M. F., Dierker, D. L. and Harwell, J. (2012a) Cortical parcellations of the macaque monkey analyzed on surface-based atlases. *Cerebral cortex (New York, N.Y. : 1991)* **22**, 2227–40.

Van Essen, D. C., Glasser, M. F., Dierker, D. L., Harwell, J. and Coalson, T. (2012b) Parcellations and hemispheric asymmetries of human cerebral cortex analyzed on surface-based atlases. *Cerebral cortex (New York, N.Y. : 1991)* **22**, 2241–62.

Verguts, T. and Fias, W. (2004) Representation of number in animals and humans: a neural model. *Journal of cognitive neuroscience* **16**, 1493–504.

Wang, X., Fung, C. C. A., Guan, S., Wu, S., Goldberg, M. E. and Zhang, M. (2016) Perisaccadic Receptive Field Expansion in the Lateral Intraparietal Area. *Neuron* **90**, 400–9.

Wang, Y., Fujita, I., Tamura, H. and Murayama, Y. (2002) Contribution of GABAergic inhibition to receptive field structures of monkey inferior temporal neurons. *Cerebral cortex (New York, N.Y. : 1991)* **12**, 62–74.

Wilson, M. L., Kahlenberg, S. M., Wells, M. and Wrangham, R. W. (2012) Ecological and social factors affect the occurrence and outcomes of intergroup encounters in chimpanzees. *Animal Behaviour* **83**, 277–291.

Wimmer, K., Spinelli, P. and Pasternak, T. (2016) Prefrontal Neurons Represent Motion Signals from Across the Visual Field But for Memory-Guided Comparisons Depend on Neurons Providing These Signals. *The Journal of neuroscience : the official journal of the Society for Neuroscience* **36**, 9351–64.

Xu, F. and Spelke, E. S. (2000) Large number discrimination in 6-month-old infants. *Cognition* **74**, 1–11.

Yokoi, I. and Komatsu, H. (2010) Putative pyramidal neurons and interneurons in the monkey parietal cortex make different contributions to the performance of a visual grouping task. *Journal of neurophysiology* **104**, 1603–11.

Zaksas, D. and Pasternak, T. (2006) Directional signals in the prefrontal cortex and in area MT during a working memory for visual motion task. *The Journal of neuroscience : the official journal of the Society for Neuroscience* **26**, 11726–11742.

Zhang, T. and Britten, K. H. (2011) Parietal area VIP causally influences heading perception during pursuit eye movements. *The Journal of neuroscience : the official journal of the Society for Neuroscience* **31**, 2569–75.

Part II.
Individual studies

Study 1: Number sense in prefrontal and parietal areas

Viswanathan, P, Nieder, A. (2013). Neuronal correlates of a visual "sense of number" in primate parietal and prefrontal cortices. *Proc Natl Acad Sci U S A* **110**(27):11187–92.

Neuronal correlates of a visual "sense of number" in primate parietal and prefrontal cortices

Pooja Viswanathan and Andreas Nieder[1]

Animal Physiology, Institute of Neurobiology, University of Tübingen, 72076 Tübingen, Germany

Edited by Charles Gross, Princeton University, Princeton, NJ, and approved May 21, 2013 (received for review April 30, 2013)

"Sense of number" refers to the classical idea that we perceive the number of items (numerosity) intuitively. However, whether the brain signals numerosity spontaneously, in the absence of learning, remains unknown; therefore, we recorded from neurons in the ventral intraparietal sulcus and the dorsolateral prefrontal cortex of numerically naive monkeys. Neurons in both brain areas responded maximally to a given number of items, showing tuning to a preferred numerosity. Numerosity was encoded earlier in area ventral intraparietal area, suggesting that numerical information is conveyed from the parietal to the frontal lobe. Visual numerosity is thus spontaneously represented as a perceptual category in a dedicated parietofrontal network. This network may form the biological foundation of a spontaneous number sense, allowing primates to intuitively estimate the number of visual items.

association cortices | quantity | single-unit recording

The classical idea of a "sense of number" (1,2) suggests that we and animals are endowed with the faculty to perceive the number of items (i.e., numerosity) intuitively. Numerosity might be a perceptual category provided by hard-wired sensory brain processes, without the need to learn what numerosity refers to. Supporting this hypothesis, numerosity is represented by an approximate nonverbal system that allows wild animals (3,4), prelinguistic infants(5,6), and innumerate humans (7,8) to readily estimate set size. Evidence that the brain is set up to assess visual numerosity spontaneously was recently provided by psychophysical and computational experiments: numerosity—just like color or perceptual categories like faces—in humans is susceptible to adaptation (9,10), and is extracted en passant by computational network models (11).

So far, the neuronal foundations of a perceptual number sense were never tested because all experiments done so far were performed in animals that learned to discriminate numerosity (12–14). Work with behaviorally trained nonhuman primates identified a cortical network with individual neurons in the prefrontal (PFC) and posterior parietal cortex (PPC) selectively responding to the number of items. Such "number neurons" abstractly represent the number of items across space, time, and modalities (15,16,17). Number neurons have also been traced indirectly in the human brain using functional MRI (fMRI) (18,19).

However, because neurons can be trained to represent behaviorally meaningful categories (20,21,22), it has been argued (23) that the presence of previously described number neurons in trained animals might be a product of intense learning, rather than a reflection of a spontaneous number sense. For the same reason, the coding scheme for numerosity has been debated (23): Is the spontaneous neuronal code for numerosity a summation code, as evidenced by monotonic discharges as a function of quantity (14,24), or a labeled-line code as witnessed by numerosity-selective neurons tuned to preferred numerosities analogous to those found in monkeys performing numerical tasks (25,26)? Here, we tested the core idea of the number sense and explored whether numerosity-selective neurons do exist in the brains of numerically naive monkeys (i.e., monkeys that had never been trained to discriminate numerosity).

Results

To ensure that the monkeys paid attention to the stimulus displays (but not to numerosity) during recording, the monkeys were trained to discriminate color in variable dot displays in a delayed match-to-sample task (Fig. 1*A*). Monkeys watched two displays (first sample, then test) separated by a 1-s delay. They were trained to release a bar if the displays contained the same color of dots. Five colors (red, blue, green, yellow, purple) were used. All five colors were presented in displays containing one, two, three, four, or five dots, or numerosities (Fig. 1*B*). Importantly, the number of items in the displays was completely irrelevant to solve the task. All five colors and numerosities were displayed as standard stimuli with variable dot sizes and positions, with control stimuli equating the total area and the average density of all dots across numerosities. All parameters (e.g., colors, numerosities, stimulus protocols, match versus nonmatch trials) were balanced and pseudorandomly presented to the monkeys.

Behavioral Performance. Both animals were proficient in color discrimination and performed well above chance (monkey L: 99.19 ± 0.24%; monkey S: 97.93 ± 0.34%, binomial test, $P < 0.001$) for all color combinations (Fig. 1*C*). To ensure that the monkeys ignored the number of items that covaried with the color of the dots in the sample displays, we tested putative numerosity discrimination by inserting generalization trials of pure numerosity stimuli (only black dots) within the ongoing color discrimination task in two sessions after the end of the recording sessions. With an average numerosity discrimination of 43.8 ± 12.7% (monkey L) and 58.8 ± 12.4% (monkey S), both monkeys performed at chance level (two-tailed binomial test, $P > 0.05$) (Fig. 1*D*). The monkeys were thus exclusively discriminating color; they were ignorant of the numerosity information in the stimuli.

Single-Cell Responses. We recorded single-cell activity from randomly selected neurons in the ventral intraparietal area (VIP) in the fundus of the intraparietal sulcus (IPS) of the PPC and PFC while monkeys performed the color discrimination task (Fig. 1 *A* and *B*). A total of 238 neurons from VIP and 268 neurons from the dorsolateral prefrontal cortex around the principal sulcus were analyzed (Fig. 2*A*). To identify neurons selective to the varying stimulus parameters, we evaluated the average discharge rates of individual neurons during the sample presentation using a three-factor ANOVA, with factors (sample color) × (sample numerosity) × (stimulus protocol) ($P < 0.01$).

Tuning to Visual Numerosity. The behaviorally relevant parameter color significantly modulated neuronal activity in 12% (29/238) of VIP cells and 10% (26/268) of PFC neurons. However, a

Author contributions: P.V. and A.N. designed research; P.V. performed research; A.N. contributed new reagents/analytic tools; P.V. analyzed data; and P.V. and A.N. wrote the paper.

The authors declare no conflict of interest.

This article is a PNAS Direct Submission.

[1]To whom correspondence should be addressed. E-mail: andreas.nieder@uni-tuebingen.de.

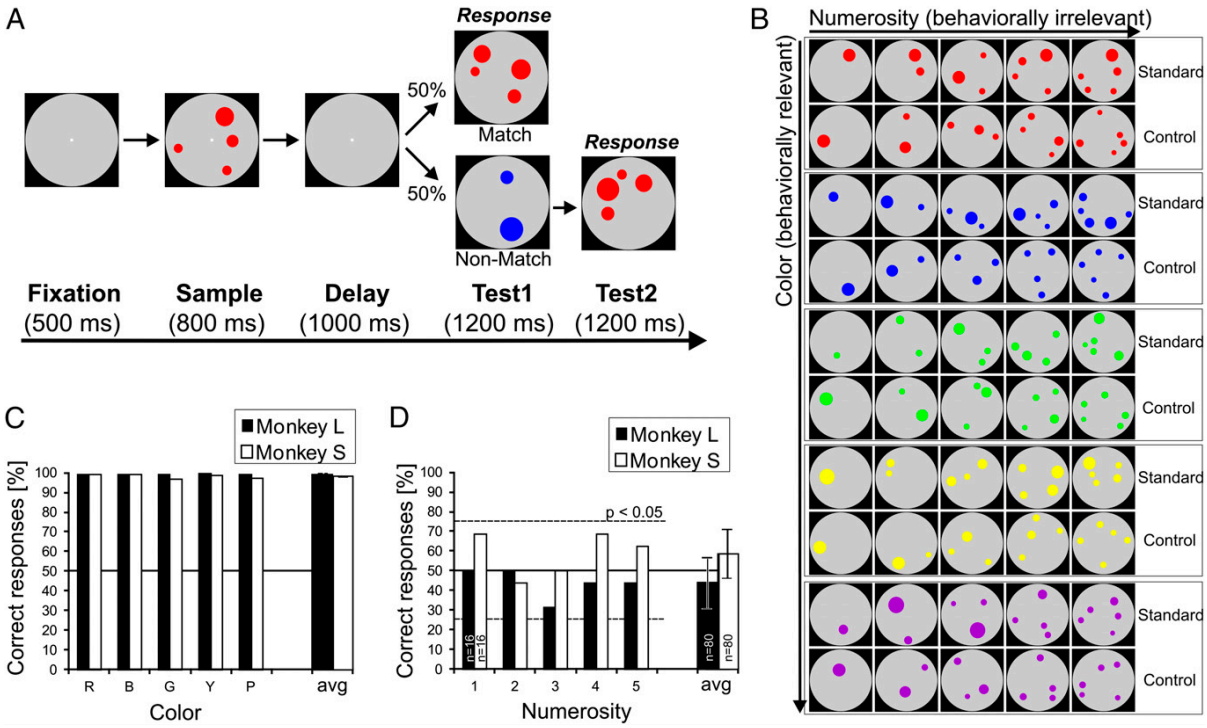

Fig. 1. Task protocol and behavioral performance. (*A*) Delayed match-to-color task. A trial started when the monkey grasped a bar. The monkey had to release the bar if the items in the multidot displays of the sample period and test period were of the same color, and continue holding it if they were not (probability of match/nonmatch condition = 0.5). The sample display contained one to five dots of the same color. (*B*) Example stimulus displays showing the variations of stimulus parameters. Each of the five (behaviorally relevant) colors was shown in five different (behaviorally irrelevant) numerosities, and as standard vs. area and density control stimulus displays, resulting in a three-factorial stimulus design. (*C*) Behavioral color discrimination performance of both monkeys during all recording sessions (50% is chance level). Both monkeys performed equally well and almost perfectly to all five colors (red, blue, green, yellow, purple). Avg, average over all colors. (*D*) Behavioral performance in the generalization tests to numerosity the monkeys were not trained to discriminate (all displays only black dots). Both monkeys showed chance performance to each numerosity and the average (dotted lines indicate binomial threshold at $P = 0.05$), confirming that they did not pay attention to numerosity. Error bars indicate SEM.

similar proportion of neurons spontaneously also encoded the number of items in the dot displays (numerosity) that was behaviorally irrelevant and not discriminated by the animals (Fig. 1*D*). In area VIP, 13% (32/238) of the neurons showed a significant main effect numerosity, and 14% (38/268) in PFC (Fig. 2*B*). Most of these numerosity-selective neurons, i.e., 10% (24/238) of all VIP neurons and 10% (28/268) of all PFC neurons, were not activated by covarying visual parameters but exclusively showed a main effect numerosity (no main effect stimulus protocol or interactions with factor stimulus protocol, $P < 0.01$). Responses of three example numerosity-selective neurons from area VIP and the PFC are depicted in Fig. 2 *C–E* for area VIP, and Fig. 2 *F–H* for PFC. The tuning functions of example VIP neurons showed peak activity for visual numerosity one (Fig. 2*C*), three (Fig. 2*D*), and four (Fig. 2*E*), whereas the PFC neurons had a preferred numerosity of two (Fig. 2*F*), three (Fig. 2*G*), and five (Fig. 2*H*).

Population-tuning functions were calculated by averaging the normalized activity for all neurons that preferred a given numerosity. Similar response profiles were observed for all neurons tuned to numerosities one, two, three, four, and five in area VIP (Fig. 3*A*) and the PFC (Fig. 3*D*). All functions in VIP (Fig. 3*B*) and PFC (Fig. 3*E*) showed a systematic drop off of activity because the number of items in the dot displays varied from the preferred value. To evaluate this across the population of VIP and PFC neurons, we normalized the activity of each numerosity-selective neuron and plotted its activity as a function of distance from its preferred numerosity. A significant decrease of activity from numerical distance one and two was found, even when only considering numerosity-selective VIP neurons tuned to numerosity two, three, and four (paired samples *t* test, two-tailed, all tests $P < 0.05$), indicating peak-tuning functions with systematically falling flanks on both sides of the numerosity tuning curves. Numerosity one was by far the most frequent preferred numerosity in both VIP (Fig. 3*C*) and PFC (Fig. 3*F*). In summary, we find that both VIP and PFC neurons were tuned to preferred numerosities in the absence of numerosity training.

Comparing the Timing of Numerosity Signals in VIP and PFC. We examined the time course of numerosity selectivity in each brain area using a sliding version of the receiver operating characteristic (ROC) applied to the populations of numerosity-selective neurons in the sample epoch (*Materials and Methods*). This selectivity measure revealed that numerosity selectivity appeared with a shorter latency in VIP than PFC following the onset of the sample stimulus (Fig. 4*A*). We quantified the latency of category selectivity for each VIP and PFC neuron by evaluating the time at which the area under the ROC curve (AUROC values) crossed a predefined threshold (3.0 SD above the mean value during the fixation epoch for 20 consecutive 1-ms time bins) in the sample period. Across all neurons for which a latency could be defined with this method (VIP, $n = 23$; PFC, $n = 29$), numerosity selectivity emerged significantly earlier in VIP (median = 71 ms) than in PFC (median = 124 ms) (two-tailed Mann–Whitney *U* test, $P < 0.05$). The observed latency difference between VIP and

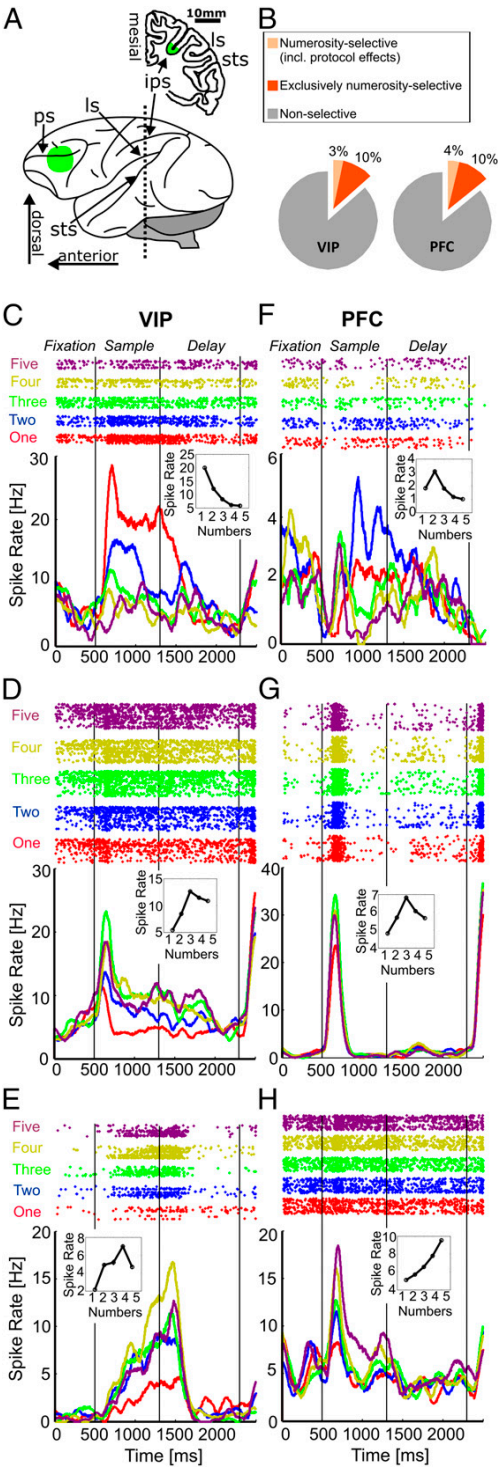

Fig. 2. Recording sites and neural responses to numerosity. (*A*) Lateral view (*Lower*) of the left hemisphere of a monkey brain indicating the topographical relationships of cortical landmarks. Coronal section (*Upper*) at the level of the dotted line in the lateral view reconstructed from a structural MRI scan (Horsley-Clark coordinates 0 mm anterior/posterior). Green regions on the frontal lobe and in the fundus of the IPS mark the recording areas in the PFC and area VIP, respectively. LS, lateral sulcus; PS, principal sulcus; STS, superior temporal sulcus. (*B*) Pie chart depicting the absolute proportions of numerosity-selective neurons found in areas VIP and PFC. (*C*) Responses of an example VIP neuron selective to the numerosity one. (*Upper*) Dot-raster histograms (each dot represents an action potential); (*Lower*) averaged spike density functions (activity averaged and smoothed by a 150-ms Gauss-kernel). The first 500 ms represent the fixation period. Colors of dot histogram and spike density functions correspond to the number of items in the sample displays. (*Inset*) The neuron's tuning function, the discharge rates as a function of the number of items. (*C–E*) Example VIP neurons tuned to numerosities one, three, and four (layout as in *C*). (*F–H*) Example PFC neurons tuned to numerosities two, three, and five (layout as in *C*).

PFC neurons could not be caused by differences in the strength of numerosity selectivity (as measured by AUROC values), which were comparable in both cortical areas (Fig. 4*B*).

Discussion

Our finding of numerosity-selective neurons in numerically naive monkeys supports the idea of a visual number sense, the faculty to perceive visual collections intuitively (1, 2). Because perceived numerosity is susceptible to adaptation just like color, contrast, or speed, Burr and Ross (9,10) recently suggested visual numerosity as a primary sensory attribute. This finding was recently supported by a computational network model in which sensitivity to numerosity spontaneously developed (11). However, because adaptation is not restricted to primary visual attributes, but also observed for high-level visual categories such as faces (27), the category visual numerosity may alternatively be appreciated as a special perceptual category represented spontaneously in a dedicated parietofrontal network. Other complex visual categories are also represented in the primate visual system up to the frontal lobe in a relatively specialized fashion: faces, places, and body parts appear to have dedicated neural substrates for their representation (28,29,30,31). Numerosity may thus be another visual category that is processed hierarchically, not within the ventral visual stream like faces, places, and body parts, but within the dorsal visual stream. Number neurons seem to develop spontaneously and naturally within visual neural structures of the primate brain, probably based on visual input that (unavoidably) contains (among a variety of other visual features) different numbers of objects and events. Such neurons likely provide the neurobiological substrate of the approximate nonverbal system, allowing wild animals (3,4), prelinguistic infants (5,6), and innumerate humans (7,8) to readily estimate set size.

In the absence of a numerosity task, 13% of all neurons in VIP and 14% of all neurons in PFC were numerosity selective. For the VIP, this value is close to the proportion of selective neurons (14% of the neurons) found on average in our previous studies with numerosity-discriminating monkeys (calculated over four different studies (15,32–34). For the PFC, the proportion of numerosity-selective neurons in numerically trained monkeys was about twice as large (around 30% of the neurons). Perhaps PFC representations get "amplified" with numerical training and experience in the sense that a greater number of neurons respond to numerosity if numerosity needs to be processed in a behaviorally relevant way. That such neurons are at all present in naive monkeys may seem at odds with the PFC supporting complex executive functions (35). However, the PFC may be able to exert its cognitive functions precisely because it also has access to sensory information required for goal-directed behavior.

Neurons in area VIP represented their preferred numerosity on average 53 ms earlier than PFC neurons, suggesting that numerosity selectivity evolves along the visual path (see also ref. 32). This suggests that visual numerosity is extracted first in the

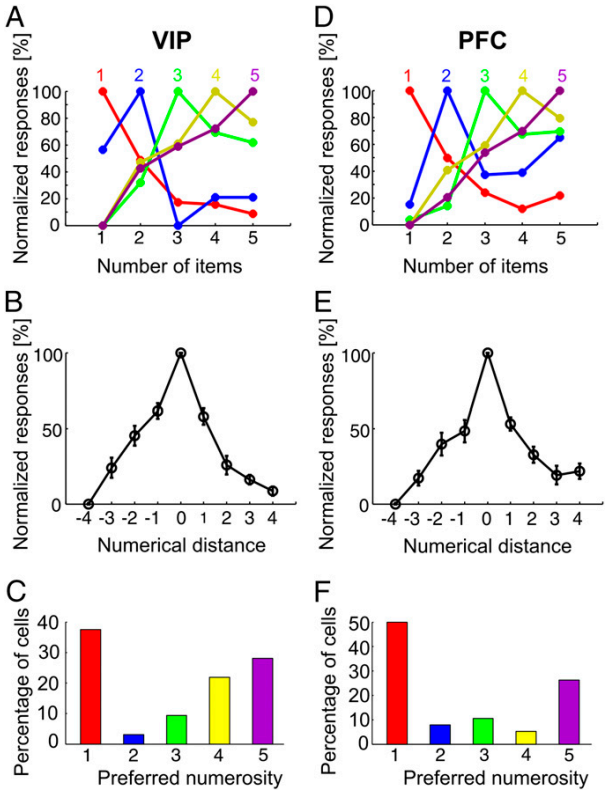

Fig. 3. Normalized response rates of selective neurons as a function of numerical distance. (*A* and *D*) Normalized responses averaged for neurons preferring the same numerosity (color coded) in area VIP (*A*) and in PFC (*D*). (*B* and *E*) Normalized discharge rates of all numerosity-selective cells in (*C*) VIP and (*E*) PFC plotted against the numerical distance from the preferred number of items. Numbers closer to the preferred quantity elicited higher discharge rates. Error bars indicate SEM. (*C* and *F*) Frequency distributions of the preferred numerosities for VIP and PFC, respectively.

termination zone of the dorsal visual pathway of the parietal cortex based on bottom-up process and later conveyed to the functionally connected lateral PFC (36). Even in trained animals, parietal signals of visual numerical categories do not arise as a result of feedback from PFC (22).

The neuronal code for numerosity representations has remained debated since neurons selectively responding to the number of items were discovered (12,13). Neurons in monkeys performing an explicit numerosity task exclusively displayed tuning functions that peak at their respective preferred numerosity (labeled-line code), irrespective of (visual or auditory) numerosity modality (16), spatial or temporal numerosity layout (15), or sensory-motor task demands (12,26). The relevance of tuned neurons' responses for the monkeys' behavioral performance was demonstrated by both error trial analyses (13,16,25) and inactivation of the respective brain areas (26). Contrasting a labeled-line code, an electrophysiological study in which monkeys implicitly discriminated numerosity reported monotonic response functions (summation code) for numerosities in the lateral intraparietal area (LIP) of the parietal lobe (14). Monkeys perform an oculomotor task with numerosity predicting the amount of reward they would receive following a gaze shift. As the authors acknowledge, the monkeys were not numerically naive in this study either (14) because the authors observed significant and consistent effect of numerical values on saccade latency, and thus concluded that the monkeys attended to numerosity.

Roitman and colleagues (23) reasoned that tuning to specific numerosities might be a product of experience and/or task demands because an explicit numerosity task requires monkeys to categorize numerical values. Such a putative learning effect can now be ruled out. In the current study with monkeys that were never trained to discriminate numerosity, both VIP and PFC neurons were still tuned to preferred numerosities. In agreement with influential computational models of number processing (37,38), the labeled-line code is a genuine and spontaneous code for the inherently categorical property number of items of stimuli.

The current data also help to exclude putative nonnumerical factors that were suspected to modulate numerosity-selective neurons during explicit numerosity tasks. It has been argued that the observed overrepresentation of numerosity one in numerosity discriminating monkeys might have been caused by reward expectation (23): because behavioral accuracy was highest when the sample value was 1 (13), monkeys could be more certain of achieving rewards, and this might be reflected in the discharges of neurons preferring numerosity one. Because numerosity one was still overrepresented by the population of neurons in our numerically naive monkeys, this putative nonnumerical factor can be ruled out. Neurons tuned to numerosity one superficially resemble monotonically decreasing units; however, these neurons are too sharply tuned to convey information for numerosities three and higher (Figs. 2*C* and 3 *A* and *D*) and thus cannot be regarded as decreasing summation units. Perhaps numerosity 1 is indeed a special set and thus represented by an abundance of neurons; after all, numerosities are collections of single elements, i.e., multiples of numerosity 1. Interestingly, the special status of

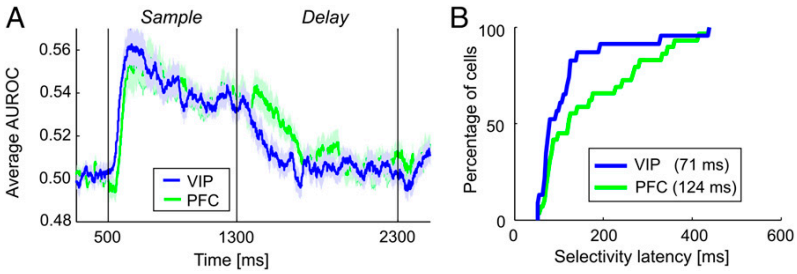

Fig. 4. Time course of VIP and PFC numerosity selectivity. (*A*) The time course of numerosity selectivity across numerosity-selective VIP and PFC populations was determined by a sliding ROC analysis. AUROC values of 0.5 indicate complete indiscriminability of the best and least preferred numerosities; AUROC values larger than 0.5 indicate stronger neuronal activity to the preferred numerosity. (*B*) Cumulative latency distributions across all neurons that showed significant numerosity selectivity after sample onset according to the sliding ROC analysis revealed the fraction of VIP and PFC neurons that had become numerosity selective by each time point. Shading indicates SEM.

one element is omnipresent in the singular-plural dichotomy (or numerosity one vs. all-other-numerosities distinction) found in natural language. Moreover, the singular-plural distinction is suggested to have a nonlinguistic conceptual basis (39,40). Neurons tuned to numerosity five were also abundant, but most likely comprises neurons with larger numerosity preference than our experimentally restricted range from one to five.

Our single-cell data in the naive nonhuman primate are in good agreement with event-related potentials in human infants (41) and human functional imaging data. Using fMRI adaptation, peaked blood oxygenation level dependent activity-tuning profiles were found in bilateral IPS as an indirect measure of neuronal numerosity tuning (18) as well as IPS and PFC (19). Peak-tuned numerosity detectors are also postulated as final stage of numerosity processing by computational models on number processing (37,38). The recently reported summation units (11,14) operating at an intermediate stage of the model hierarchy give rise to numerosity detectors that may constitute a locally restricted precursor mechanism, but current discrepancies between the computational solutions and the biological realizations (monotonically increasing or decreasing functions, or both) need to be reconciled.

Materials and Methods

Behavioral Protocol. Two male rhesus monkeys (*Macaca mulatta*) weighing between 5.5 and 6.3 kg served as subjects for this study. The animals were seated inside primate chairs in a chamber 57 cm away from a 15-inch flat screen monitor (with a resolution of 1,024 × 768 pixels and a refresh rate of 75 Hz). The National Institute of Mental Health Cortex program was used to present the stimuli and monitor behavior. The monkeys' eye gaze was tracked by an infrared eye tracking system (ISCAN).

To ensure that the monkeys paid attention to the stimulus displays (but not to numerosity), the animals were trained to discriminate color in dot displays in a delayed match-to-sample task (Fig. 1*A*). The trial was initiated by the monkeys holding a response bar and fixating within 3.5° of visual angle of a central fixation target throughout the trial. Upon successful fixation for 500 ms, the sample stimulus was shown for 800 ms, followed by a delay period of 1,000 ms without a stimulus. After the delay, a dot display (test 1) was presented, which in 50% of the cases had the same color as the sample (match) and required the monkey to release the response bar to receive a fluid reward. The match display displayed the same color (relevant parameter) and the same numerosity (irrelevant parameter) as the sample stimulus. In the other 50% of the trials, the first test display showed a different color (nonmatch; relevant parameter) as well as a different numerosity (irrelevant parameter); in this case, the monkey had to hold the response bar and wait for the second test that always matched the sample in color to release the bar. Based on this task design, chance performance was 50% correct in the trials.

Stimuli. The visual stimuli were colored dot (diameter range 0.5°–0.9° of visual angle) displays (only one color per stimulus) on a gray background circle (diameter 6° of visual angle). Five colors (red, blue, green, yellow, purple) were chosen for maximum discriminability. All colors were presented in displays containing one, two, three, four, or five dots. This provided a balanced 5 × 5 stimulus design.

Dot patterns were generated using a custom-written MatLab script (MathWorks). These routines enabled the generation of new stimuli sets for each recording session. Moreover, this software provided for the control of parameters of the dot patterns. For the standard stimuli, each stimulus contained a defined set of equally colored dots that appeared at randomized locations within the gray background circle. The diameter of each dot was randomly varied within the given range. To prevent the monkeys from memorizing the visual patterns of the displays, each quantity was tested with many different images per session and the sample and test displays that appeared on each trial were never identical. In addition to the standard stimuli, control stimuli controlling for both the spatial low-level visual features total dot area (total area of all items in a display equated for all stimuli in a trial) and dot density (same mean density of dot patterns for all stimuli in a trial) were used in each session (Fig. 1*B*). All parameters (e.g., colors, numerosities, stimulus protocols, match versus nonmatch trials) were balanced and pseudorandomly presented to the monkeys.

Evaluation of Putative Discrimination Generalization to Numerosity. We also tested whether the monkeys might have learned to discriminate the behaviorally irrelevant stimulus dimension numerosity. For monkey L, blocks (40 trials, eight trials per numerosity, pseudorandomized) of pure numerosity stimuli (only black dots, all other parameters as in the color task) were inserted during the ongoing color discrimination task in two sessions; rewards were delivered after correct numerosity matches. The same procedure was applied for monkey S, except that individual pure numerosity trials were randomly interspersed among ongoing color trails; all trials were rewarded irrespective of response). These tests were done immediately after the end of recording sessions in both monkeys. Percentage of correct performance to each numerosity was tested by a binomial test ($P < 0.05$). The data (Fig. 1*D*) showed that neither monkey was able to discriminate numerosity.

Surgery and Neuronal Recordings. The animals were implanted with a head bolt to allow immobilization of the head during training so that eye movements could be monitored. After the animals reliably discriminated the color of the items in the delayed match-to-sample color task, two recording chambers were implanted over the right lateral prefrontal cortex, centered on the principal sulcus and the right intraparietal sulcus guided by anatomical MRI and stereotaxic measurements. All surgeries were performed under sterile conditions while the monkey was under general anesthesia and received antibiotics and analgesics postprocedure.

Neuronal recordings were made from the two monkeys while they performed the task using arrays of up to eight tungsten microelectrodes attached to screw microdrives in a grid with 1-mm spacing. Neurons were not preselected for any sensory or task-related parameter. To access area VIP, recordings were made exclusively at depths ranging from 9 to 13 mm below the cortical surface and the presence of visual and somatosensory responses was tested qualitatively. Electrophysiological signals were amplified and filtered and waveforms of action potentials sampled at 40 kHz from each channel were stored to disk. Single unit separation was performed offline based on waveform characteristics (Offline Sorter, Plexon Systems). Timestamps of trial events and action potentials were extracted for analysis. Only single units that exhibited a sufficient discharge rate (>1 Hz) during the relevant trial phases and were recorded for at least 30 trials per condition were analyzed. All experimental procedures were in accordance with the guidelines for animal experimentation approved by the Regierungspräsidium Tübingen, Tübingen, Germany.

Behavioral Data Analysis. For the color discrimination task, the percent correct performance for each color in each session was calculated, averaged across all sessions, and statistically verified using a binomial test. To test numerosity discrimination, percent correct performance was derived during the generalization tests and again analyzed with a binomial test for each numerosity.

Neuronal Data Analysis. We analyzed discharge rates during sample presentation in an 800-ms window. By default, the 800-ms windows of the sample phase were shifted by 50 ms after sample onset for area VIP cells and by 100 ms for PFC cells to account for typical response latency of these cells. To determine the selectivity of a neuron, a three-factor ANOVA (criterion $P < 0.01$) using single-trial discharge rates was calculated for each cell in the sample period, with main factors stimulus protocol (standard or control), sample color (red, blue, green, yellow, purple), and sample numerosity (one, two, three, four, five). Each neuron's discharge rates are tested only once; no multiple comparisons are applied. Only neurons with a minimum of 30 stimulus presentations per numerosity were taken into account. To estimate the probability of false positives in our approach (i.e., the probability that a neuron was classified as numerosity selective by chance), we additionally performed a the same three-factor ANOVA (criterion $P < 0.01$) with shuffled data, using recorded single-trial discharge rates that were randomly assigned to the numerical labels (238 VIP cells × 1,000, and 268 PFC cells × 1,000, resulting in 506,000 tests). We found that 1% (5,306/506,000) of the tests with shuffled data resulted in a statistically significant evaluation (at $P < 0.01$), confirming that the reported proportion of numerosity-selective neurons cannot be explained by chance occurrences.

To derive averaged numerosity-tuning functions, the tuning functions of individual neurons were normalized by setting the maximum activity to the most preferred numerosity as 100% and the activity to the least preferred quantity as 0%. Pooling the resulting normalized tuning curves resulted in averaged numerosity-filter functions.

The latency of numerosity selectivity (i.e., not the visual response latency) was calculated using a sliding ROC analysis (42). The true-positive (spike rate for the preferred numerosity) and false-positive rates (spike rate for the least preferred numerosity) were calculated for each neuron to generate the ROC

curve. The AUROC was calculated with a sliding kernel of 50 ms and incremented by 1 ms at each time point. To arrive at baseline and threshold AUC values, the last 200 ms of the fixation period (before sample onset) were used. The threshold for each neuron was defined as the mean AUC during the presample period plus 3 SDs. The numerosity selectivity latency per single neuron was the time point after sample onset where this threshold criterion was exceeded for at least 20 consecutive 1-ms bins.

ACKNOWLEDGMENTS. This work was supported by Deutsche Forschungsgemeinschaft Grant NI 618/2-1 (to A.N.).

1. Danzig T (1930) *Number The Language of Science* (The Free Press, New York).
2. Dehaene S (1997) *The Number Sense* (Oxford Univ Press, Oxford, UK).
3. Wilson ML, Kahlenberg SM, Wells M, Wrangham RW (2012) Ecological and social factors affect the occurrence and outcomes of intergroup encounters in chimpanzees. *Anim Behav* 83:277–291.
4. Cantlon JF, Brannon EM (2007) How much does number matter to a monkey (Macaca mulatta)? *J Exp Psychol Anim Behav Process* 33(1):32–41.
5. Feigenson L, Dehaene S, Spelke E (2004) Core systems of number. *Trends Cogn Sci* 8 (7):307–314.
6. Piazza M (2010) Neurocognitive start-up tools for symbolic number representations. *Trends Cogn Sci* 14(12):542–551.
7. Gordon P (2004) Numerical cognition without words: Evidence from Amazonia. *Science* 306(5695):496–499.
8. Pica P, Lemer C, Izard V, Dehaene S (2004) Exact and approximate arithmetic in an Amazonian indigene group. *Science* 306(5695):499–503.
9. Burr D, Ross J (2008) A visual sense of number. *Curr Biol* 18(6):425–428.
10. Ross J, Burr DC (2010) Vision senses number directly. *J Vis* 10(2):1–8.
11. Stoianov I, Zorzi M (2012) Emergence of a 'visual number sense' in hierarchical generative models. *Nat Neurosci* 15(2):194–196.
12. Sawamura H, Shima K, Tanji J (2002) Numerical representation for action in the parietal cortex of the monkey. *Nature* 415(6874):918–922.
13. Nieder A, Freedman DJ, Miller EK (2002) Representation of the quantity of visual items in the primate prefrontal cortex. *Science* 297(5587):1708–1711.
14. Roitman JD, Brannon EM, Platt ML (2007) Monotonic coding of numerosity in macaque lateral intraparietal area. *PLoS Biol* 5(8):e208.
15. Nieder A, Diester I, Tudusciuc O (2006) Temporal and spatial enumeration processes in the primate parietal cortex. *Science* 313(5792):1431–1435.
16. Nieder A (2012) Supramodal numerosity selectivity of neurons in primate prefrontal and posterior parietal cortices. *Proc Natl Acad Sci USA* 109(29):11860–11865.
17. Nieder A (2013) Coding of abstract quantity by 'number neurons' of the primate brain. *J Comp Physiol A Neuroethol Sens Neural Behav Physiol* 199(1):1–16.
18. Piazza M, Izard V, Pinel P, Le Bihan D, Dehaene S (2004) Tuning curves for approximate numerosity in the human intraparietal sulcus. *Neuron* 44(3):547–555.
19. Jacob SN, Nieder A (2009) Tuning to non-symbolic proportions in the human frontoparietal cortex. *Eur J Neurosci* 30(7):1432–1442.
20. Roy JE, Riesenhuber M, Poggio T, Miller EK (2010) Prefrontal cortex activity during flexible categorization. *J Neurosci* 30(25):8519–8528.
21. Freedman DJ, Assad JA (2006) Experience-dependent representation of visual categories in parietal cortex. *Nature* 443(7107):85–88.
22. Swaminathan SK, Freedman DJ (2012) Preferential encoding of visual categories in parietal cortex compared with prefrontal cortex. *Nat Neurosci* 15(2):315–320.
23. Roitman JD, Brannon EM, Platt ML (2012) Representation of numerosity in posterior parietal cortex. *Front Integr Neurosci* 6:25, 10.3389/fnint.2012.00025.
24. Romo R, Brody CD, Hernández A, Lemus L (1999) Neuronal correlates of parametric working memory in the prefrontal cortex. *Nature* 399(6735):470–473.
25. Nieder A, Merten K (2007) A labeled-line code for small and large numerosities in the monkey prefrontal cortex. *J Neurosci* 27(22):5986–5993.
26. Sawamura H, Shima K, Tanji J (2010) Deficits in action selection based on numerical information after inactivation of the posterior parietal cortex in monkeys. *J Neurophysiol* 104(2):902–910.
27. Webster MA, MacLeod DI (2011) Visual adaptation and face perception. *Philos Trans R Soc Lond B Biol Sci* 366(1571):1702–1725.
28. Tsao DY, Moeller S, Freiwald WA (2008) Comparing face patch systems in macaques and humans. *Proc Natl Acad Sci USA* 105(49):19514–19519.
29. Tsao DY, Schweers N, Moeller S, Freiwald WA (2008) Patches of face-selective cortex in the macaque frontal lobe. *Nat Neurosci* 11(8):877–879.
30. Pinsk MA, et al. (2009) Neural representations of faces and body parts in macaque and human cortex: a comparative FMRI study. *J Neurophysiol* 101(5):2581–2600.
31. Bell AH, et al. (2011) Relationship between functional magnetic resonance imaging-identified regions and neuronal category selectivity. *J Neurosci* 31(34):12229–12240.
32. Nieder A, Miller EK (2004) A parieto-frontal network for visual numerical information in the monkey. *Proc Natl Acad Sci USA* 101(19):7457–7462.
33. Diester I, Nieder A (2007) Semantic associations between signs and numerical categories in the prefrontal cortex. *PLoS Biol* 5(11):e294.
34. Tudusciuc O, Nieder A (2009) Contributions of primate prefrontal and posterior parietal cortices to length and numerosity representation. *J Neurophysiol* 101(6): 2984–2994.
35. Miller EK, Cohen JD (2001) An integrative theory of prefrontal cortex function. *Annu Rev Neurosci* 24:167–202.
36. Chafee MV, Goldman-Rakic PS (2000) Inactivation of parietal and prefrontal cortex reveals interdependence of neural activity during memory-guided saccades. *J Neurophysiol* 83(3):1550–1566.
37. Dehaene S, Changeux JP (1993) Development of elementary numerical abilities: A neural model. *J Cogn Neurosci* 5:390–407.
38. Verguts T, Fias W (2004) Representation of number in animals and humans: A neural model. *J Cogn Neurosci* 16(9):1493–1504.
39. Barner D, Wood J, Hauser M, Carey S (2008) Evidence for a non-linguistic distinction between singular and plural sets in rhesus monkeys. *Cognition* 107(2):603–622.
40. Li P, Ogura T, Barner D, Yang SJ, Carey S (2009) Does the conceptual distinction between singular and plural sets depend on language? *Dev Psychol* 45(6):1644–1653.
41. Izard V, Dehaene-Lambertz G, Dehaene S (2008) Distinct cerebral pathways for object identity and number in human infants. *PLoS Biol* 6(2):e11.
42. Green DM, Swets JA (1966) *Signal Detection Theory and Psychophysics* (John Wiley and Sons, New York).

Study 2: Behavioural relevance of number in the fronto-parietal network

Viswanathan, P., Nieder, A. (2015). Differential impact of behavioral relevance on quantity coding in primate frontal and parietal neurons. *Curr Biol.* **25**(10):1259–69.

Article

Current Biology

Differential Impact of Behavioral Relevance on Quantity Coding in Primate Frontal and Parietal Neurons

Highlights

- Neurons in monkey PFC and VIP were recorded before and after numerosity training
- PFC showed improved responses to numerosity during active discrimination
- VIP neurons continued to respond to numerosity just as before training
- Flexible numerical PFC representations contrast with stable VIP coding

Authors

Pooja Viswanathan, Andreas Nieder

Correspondence

andreas.nieder@uni-tuebingen.de

In Brief

Viswanathan and Nieder describe how the monkey prefrontal cortex shows elevated responses to magnitude categories during active discrimination, whereas the parietal cortex encodes quantity categorically, regardless of behavioral relevance. This indicates that quantity is perceived as a special "natural" category.

Viswanathan & Nieder, 2015, Current Biology *25*, 1259–1269
May 18, 2015 ©2015 Elsevier Ltd All rights reserved
http://dx.doi.org/10.1016/j.cub.2015.03.025

CellPress

Current Biology
Article

Differential Impact of Behavioral Relevance on Quantity Coding in Primate Frontal and Parietal Neurons

Pooja Viswanathan[1] and Andreas Nieder[1,*]
[1]Animal Physiology, Institute of Neurobiology, Auf der Morgenstelle 28, University of Tübingen, 72076 Tübingen, Germany
*Correspondence: andreas.nieder@uni-tuebingen.de
http://dx.doi.org/10.1016/j.cub.2015.03.025

SUMMARY

Prefrontal cortex (PFC) and posterior parietal cortex are key brain areas for magnitude representations. Whether active discrimination of numerosity changes neuronal representations is still not known. We simultaneously recorded from the same recording sites in the PFC and ventral intraparietal area (VIP) before and after monkeys learned to actively discriminate the number of items in a set. Only PFC neurons, and not VIP neurons, exhibited heightened representation of number after numerosity training. Increased responsiveness of PFC was evidenced by enhanced differentiation of numerosity by the population of neurons, as well as increased numerosity encoding by individual selective neurons. None of these effects were observed in the VIP, in which neurons responded invariably to numerosity irrespective of behavioral relevance. This suggests elevated PFC participation during numerical task demands and executive control, whereas VIP encodes quantity as a perceptual category regardless of behavioral relevance.

INTRODUCTION

Assessing the number of elements in a set, its numerosity, requires a high level of sensory abstraction. Studies in behaviorally trained nonhuman primates identified a cortical network in the prefrontal (PFC) and posterior parietal cortex (PPC) with individual neurons selectively responding to the number of items [1, 2]. Such numerosity-selective neurons have also been traced indirectly in the human brain using fMRI [3, 4]. Whereas it was tacitly assumed that neuronal responses to numerosities were shaped by or even caused by extensive behavioral training, neurons in PFC and the intraparietal sulcus have recently been reported to encode numerosity even in monkeys that were never trained to discriminate numerosities [5]. Furthermore, the tuned coding of preferred numerosities in numerically naive monkeys was strikingly similar to that found in experienced animals. Together with psychophysical findings that numerosity representations resemble perceptual categories like color and shape and are susceptible to adaptation [6, 7], the spontaneous presence of numerosity-selective neurons in untrained animals argues for a "sense of number," the faculty to perceive numerosity intuitively [8, 9].

Whereas much has been learned about numerosity coding by neurons in the fronto-parietal cortex, the role of behavioral relevance and learning in the modulation of neuronal selectivity remains unexplored. Both parietal and PFC neurons show increased responses to behaviorally relevant as opposed to irrelevant stimuli [10, 11]. Experience-dependent plasticity is further suggested by observations that visual neurons in prefrontal [12] and parietal [13] visual areas can respond highly selectively to familiar and well-trained visual stimuli. Not only do response properties change, but also the proportion and location of selective neurons change with learning [14]. Moreover, prefrontal and posterior parietal neurons robustly reflect the learned category membership of visual stimuli, and visual selectivity shifts after monkeys were retrained to group the same stimuli into two new categories [13, 15, 16]. Whether abstract representations of quantity experience modifications with behavioral relevance, learning, and familiarity, however, remains elusive.

To address this, we simultaneously recorded from the same recording sites in the PFC and ventral intraparietal area (VIP) while numerically naive monkeys discriminated the color of a set of dots and, after numerosity training, responded to the number of items of equivalent dot collections. We found contrasting neuronal effects for PFC and VIP neurons as a result of learning to discriminate numerosity explicitly. In addition, the observed findings were not predicted by experiments using arbitrary perceptual categories as discriminative stimuli.

RESULTS

We analyzed single-neuron activity from the parietal and prefrontal cortices of two monkeys before and after training on a numerosity-delayed match-to-sample task. Before numerosity training, monkeys matched the color of sequentially presented multi-dot displays (color task; Figure 1A, top). After numerosity training, they matched the number of all black dots in the sequentially presented multi-dot displays (numerosity task; Figure 1A, bottom). The task structure stayed the same for both discrimination protocols: monkeys watched a sample display after a fixed period of visual fixation. The sample was followed by a 1-s memory delay, after which the test display appeared. In the color task, the test1 display matched the sample in color in 50% of the trials (match trials) and did not match in the other 50% of the trials (non-match trials). Importantly, the number of dots also varied systematically in the dot displays but was

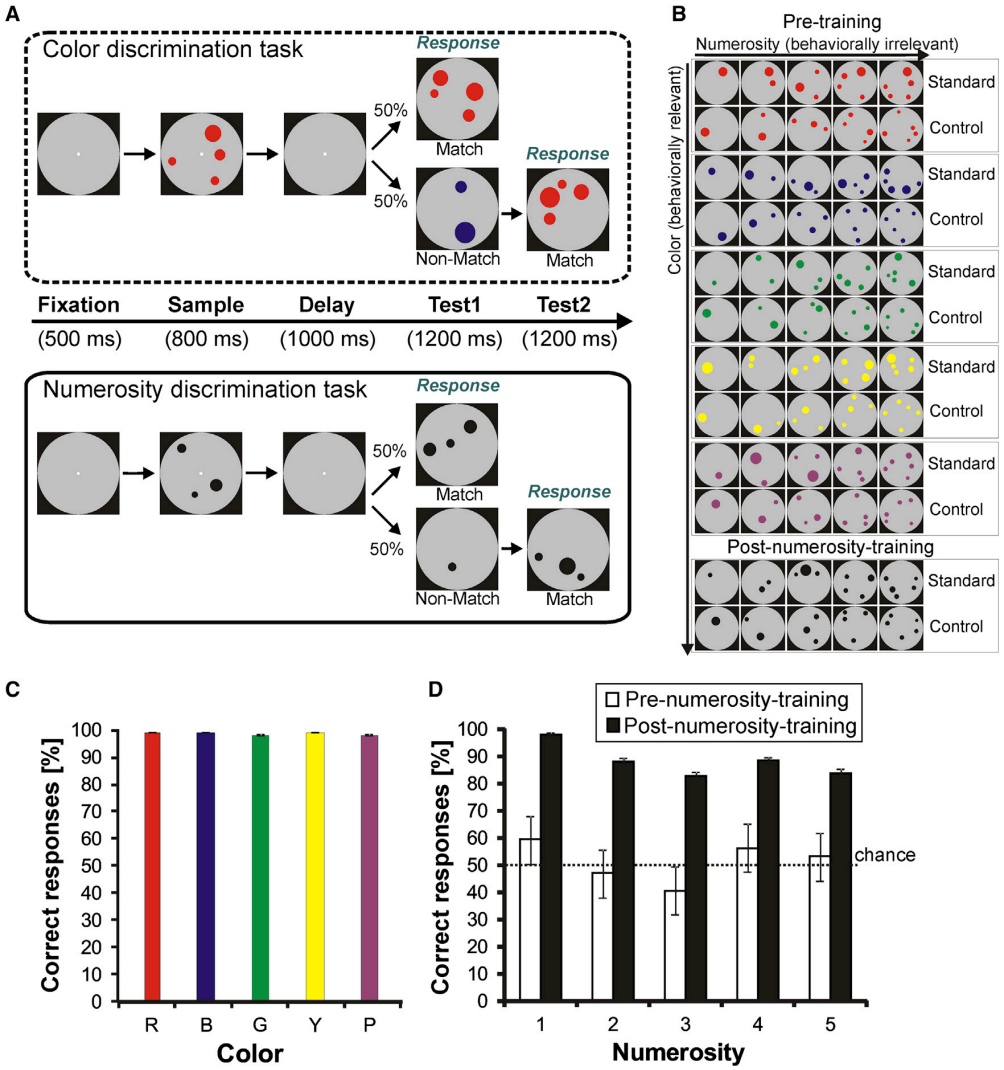

Figure 1. Behavioral Task Design, Example Stimuli, and Behavioral Performance

(A) Task: the delayed match to sample task involved an initial fixation period of 500 ms followed by a sample period where the visual dot arrays were presented. The monkeys were required to remember the sample through the subsequent delay period and respond only to matching test stimuli. If a non-match stimulus followed, they were required to withhold response until the match appeared. The color discrimination task (top panel) was used for all the pre-training data and the numerosity discrimination task (bottom panel) after the monkeys were trained to discriminate numerosity, for the post-training data.

(B) Examples of the dot array stimuli used. For the color-discrimination task, all five colors were tested in all five numerosities and across two stimulus protocols. For the numerosity-discrimination task, only black dot arrays were used in all five numerosities and across two stimulus protocols. The standard stimuli (odd rows) consist of randomly sized and spaced dots. The control stimuli (even rows) are such that the colored area and the dot density are equalized across numerosities.

(C) Behavioral performance on color discrimination task with the various colors as sample, averaged across monkeys, as a percentage of total trials. Error bars denote SEM.

(D) Behavioral performance on the numerosity-discrimination task as tested before and after numerosity training (empty bars denote chance level performance before training; filled bars denote performance after training; dashed horizontal line denotes 50% chance level) for each number as sample numerosity. Error bars denote SEM.

behaviorally irrelevant and was not used by the monkeys (that were not trained to respond to numerosity at that stage) to solve the task. In the numerosity task, the test displays matched the sample with respect to the number of items (50% match trials), whereas the numerosity did not match in the remaining trials (50% non-match trials). In the non-match trials, the non-match test1 item was always followed by a match test2 item. The monkeys had to respond to the matching item (matching

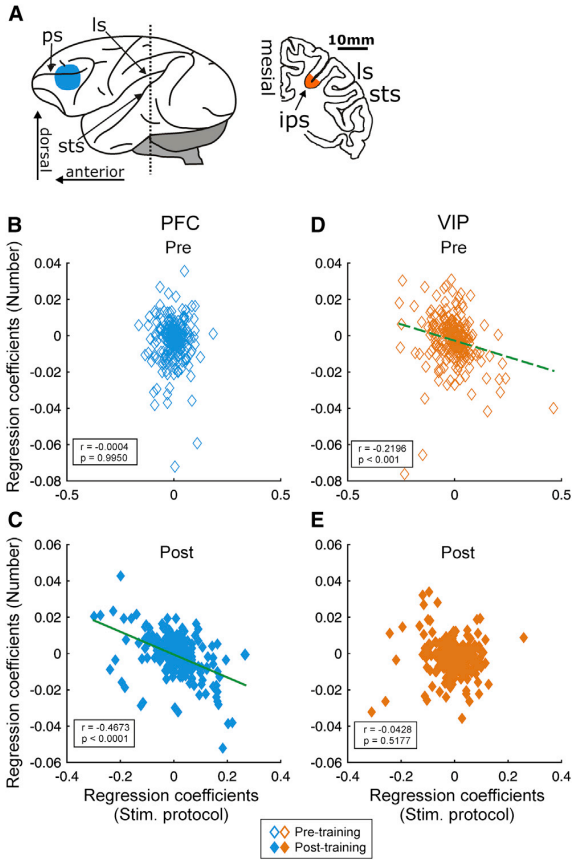

Figure 2. Recording Areas and Neuronal Populations

(A) Schematic diagram of the macaque brain, illustrating the locations where recordings were performed. Abbreviations: AS, arcuate sulcus; IPS, intraparietal sulcus; PS, principal sulcus; STS, superior temporal sulcus.

(B) De-noised regression coefficients for the factor numerosity plotted against those for the factor stimulus protocol for each recorded neuron. The coefficients describe how much of the trial-by-trial firing rate of the neuron is affected by the plotted factors "protocol" and "number". Each dot on the plot denotes a PFC neuron. Correlations between coefficients are shown ($p < 0.05$; Pearson's correlation coefficient, r) and significant correlations are indicated by the regression lines in green.

(C) The same layout as in (B) for the PFC neurons recorded post-training.

(D and E) The same as (B) and (C) for area VIP.

See also Figures S1 and S2.

color—before training; matching number—after training) by releasing a bar that they held throughout the trial. To exclude that the monkeys were responding to low-level visual features that co-varied with numerosity, control stimuli were applied (in 50% of the trials) in addition to the pseudo-randomized standard stimuli. Both in the color task and the numerosity task, the total dot area and density were equated across numerosities in the control stimuli (Figure 1B). All task parameters (match versus non-match, color versus numerosity, and standard versus control stimuli) were balanced and presented pseudo-randomly to the monkeys.

Behavioral Performance before and after Numerosity Training

In the color task, before numerosity training, color discrimination performance (Figure 1C) was well above chance for both monkeys (monkey L: 99.19% ± 0.24%; monkey S: 97.93% ± 0.34%; binomial test; $p < 0.001$) for all color combinations (as reported previously in [5]). We confirmed that none of the monkeys learned to judge numerosity in the color task by confronting the monkeys with colorless black dots. During the color task, numerosity performance tested on two sessions was at chance level for both monkeys (monkey L: 43.8% ± 12.7%; monkey S: 58.8% ± 12.4%; two-tailed binomial test; $p > 0.05$). This suggests that the monkeys were unable to use numerosity as discriminating stimulus feature during the color task.

After single-cell recordings during the color task were completed, the same monkeys were retrained to discriminate numerosity. Color information was eliminated to avoid Stroop-like effects. After approximately 2 months of training (monkey L: 41 sessions; monkey S: 30 sessions), both monkeys reached a high level of numerosity discrimination performance (monkey L: 91.4% ± 0.78%; monkey S: 84.5% ± 0.99%; two-tailed binomial test; $p < 0.001$; same sample numerosities as in the color task; numerical distance between sample and non-match of two or more; Figure 1D). Performance also showed the classical effects reported in earlier studies, such as the numerical distance and size effects [17]. These results collectively show that the monkeys were numerically naive during the color task but numerically competent and able to discriminate the number of items after numerosity training.

Representation of Task Variables in the Neuronal Populations

We recorded single-cell activity from the lateral PFC and the VIP before and after numerosity training, i.e., during the color and the numerosity task, from the same two monkeys (Figure 2A). We targeted the same electrode penetration coordinates and depths in the color and the numerosity task in both individual monkeys. This allowed for recordings from the same recording sites post-numerosity training from where the majority of neurons were sampled before numerosity training.

We applied multi-variable linear regression analysis to the trial-by-trial firing rates of all single neurons [18] to first explore the contributions of the recorded neuronal populations in encoding the behaviorally irrelevant features of number and stimulus protocol during the color task. We then applied the same analysis for the same features, which became behaviorally relevant during the number task. We calculated the weights with which the various stimulus features affected the neuronal activity and used principal-component analysis (PCA) to estimate the most informative (first 12 PCAs) of these weights at each time point within the analysis period. We call these estimated weights "de-noised regression coefficients" of number and stimulus protocol. In particular, we examined the correlations between these de-noised weights of number and stimulus protocol. We compared these correlations in the pre-training and the post-training periods as they reflect how well the neuronal population was able to extract the numerosity of the stimuli from the co-varying lower level visual features to solve the number task.

We compared sample activity of a total of 268 PFC cells recorded during pre-training and 245 cells recorded post-training with the multi-variable linear regression analysis without pre-selecting neurons for any response properties. The weights of the ''number'' or ''protocol'' predictors did not show a significant difference between the pre-training and post-training population (Mann-Whitney U test; $p = 0.08$ and $p = 0.20$, respectively). The regression coefficients (beta values) for the factors ''stimulus protocol'' and ''numerosity'' were not correlated pre-training (Pearson's correlation coefficient; $r < 0.001$; $p = 1.00$; Figure 2B). However, the coefficients were significantly and negatively correlated post-training ($r = -0.4673$; $p < 0.0001$; Figure 2C). The correlations for the population indicate that the neuronal units that are strongly regressed by one of the factors are less or sometimes conversely affected by the other factor. Excluding color as a predictor in the pre-training linear model did not change the main findings. The improvement in the PFC population as evident in the weak negative correlation between the predictors for number and stimulus protocol remained ($r = -0.1355$; $p = 0.03$; Figures S1A and S1B).

In contrast, the comparison of the population of 238 VIP cells pre-training and 231 cells post-training showed the opposite effect when performing the same multi-variable linear regression analysis. The regression coefficients were significantly and negatively correlated pre-training ($r = -0.2196$; $p < 0.001$; Figure 2D) but were no longer correlated post-training ($r = -0.0428$; $p = 0.52$; Figure 2E). The weights of the number or protocol predictors do not show a significant difference between the pre-training and post-training population (Mann-Whitney U test; $p = 0.44$ and $p = 0.26$, respectively). Excluding color as a predictor in the pre-training period only enhanced the negative correlation observed in the VIP population pre-training ($r = -0.6954$; $p < 0.0001$; Figures S1C and S1D).

We used an ANCOVA (at alpha = 0.05) to test the regression lines pre- and post-training for the two areas (green lines, Figure 2). We found that, for both areas, PFC and VIP, the slopes of the regression line were significantly different with active numerical discrimination. For PFC, the slope post-training was significantly higher ($p = 0.0001$), and for VIP, the slope post-training was significantly lower than pre-training ($p = 0.0394$). Additionally, the slope of PFC population post-training was also significantly higher than that of VIP pre-training ($p = 0.0359$).

Proportions of Numerosity-Selective Cells Increased Only in PFC with Behavioral Relevance

To identify individual neurons that were selective to numerosity and presumably maximally contributed to the observed effects found in the population analysis, we performed an ANOVA based on the trial-by-trial firing rates for each neuron separately. For the pre-training data (color task), a three-factor ANOVA with main factors ''sample color'' (five colors), ''sample numerosity'' (numerosity 1–5), and ''stimulus protocol'' (standard versus control stimuli) was calculated (at alpha = 0.01). For the post-training condition (numerosity task), a two-factor ANOVA with main factors ''sample numerosity'' and ''stimulus protocol'' was applied. Numerosity-selective cells were determined to be those cells that displayed a main effect for the factor sample numerosity. In Figure 3, example numerosity-selective neurons and their respective tuning curves from the PFC (Figure 3A) and the VIP (Figure 3B) can be seen.

To confirm that the results from the multi-variable linear regression analysis of the population mainly relied on the contributions of numerosity-selective neurons, we calculated the correlations based solely on the numerosity-selective neurons identified by the ANOVA. In PFC, the coefficients were significantly negatively correlated post-training, but not pre-training (Figures S2A and S2B). In VIP, we found significantly negatively correlated coefficients pre-training, but not post-training (Figures S2C and S2D). For both post-training PFC and pre-training VIP, the magnitude of Pearson's correlation coefficients were higher for the population of numerosity-selective neurons than the entire population of all recorded neurons. This suggests that numerosity-selective neurons contributed significantly to the observed population effects and thus were probably most important to convey numerosity information.

We found evidence that the proportion of numerosity-selective cells in the PFC increased from 14% (38/268) pre-training to 20% (50/245) post-training (chi-square test; $p = 0.06$; Figure 3C; Table S1). The majority of these cells were unaffected by the co-varying lower visual features of the stimuli and thus showed no effect of the stimulus protocol or an interaction of numerosity with stimulus protocol. In the PFC, the proportion of such ''pure'' numerosity-selective cells was 10% pre-training and 13% post-training.

We did not observe a change in the proportion of numerosity-selective neurons in the parietal cortex. Numerosity-selective cells in the VIP were 14% (32/238) pre-training and 11% (26/231) post-training (chi-square test; $p = 0.47$). Pure numerosity proportions, i.e., without effects or interactions of stimulus protocol, were 10% pre-training and 9% post-training (Figure 3D). We report the results of the ANOVAs in detail in Table S1.

Sharpness of Numerosity Tuning Was Unchanged by Relevance

Active discrimination has been shown to change tuning properties of sensory neurons. We therefore investigated whether active numerosity discrimination resulted in an increase in the strength of tuning to numerosity in our selective population. Numerosity-selective cells have displayed tuned responses to the number of items in dot displays [19], in item sequences [20], and across modalities [21]. Such tuning is characterized by a maximal response toward a preferred numerosity with a gradual decrease of activity for numerosities with increasing numerical distance to the preferred numerosity. We also found tuned responses to numerosity in our selective population before and after numerosity training (Figures 4A–4D). The frequencies of preferred numerosities were also similar in both areas pre- and post-training. We compared the tuning sharpness pre-training and post-training in PFC and VIP from population-tuning curves created by normalizing and averaging all individual tuning curves around the preferred numerosity and the graded responses expressed as a factor of numerical distance. The pre-training and post-training population tuning functions for PFC (Figure 4E) and VIP neurons (Figure 4F) were indistinguishable (except for few arbitrary numerical distances; Mann-Whitney U test; $p < 0.05$).

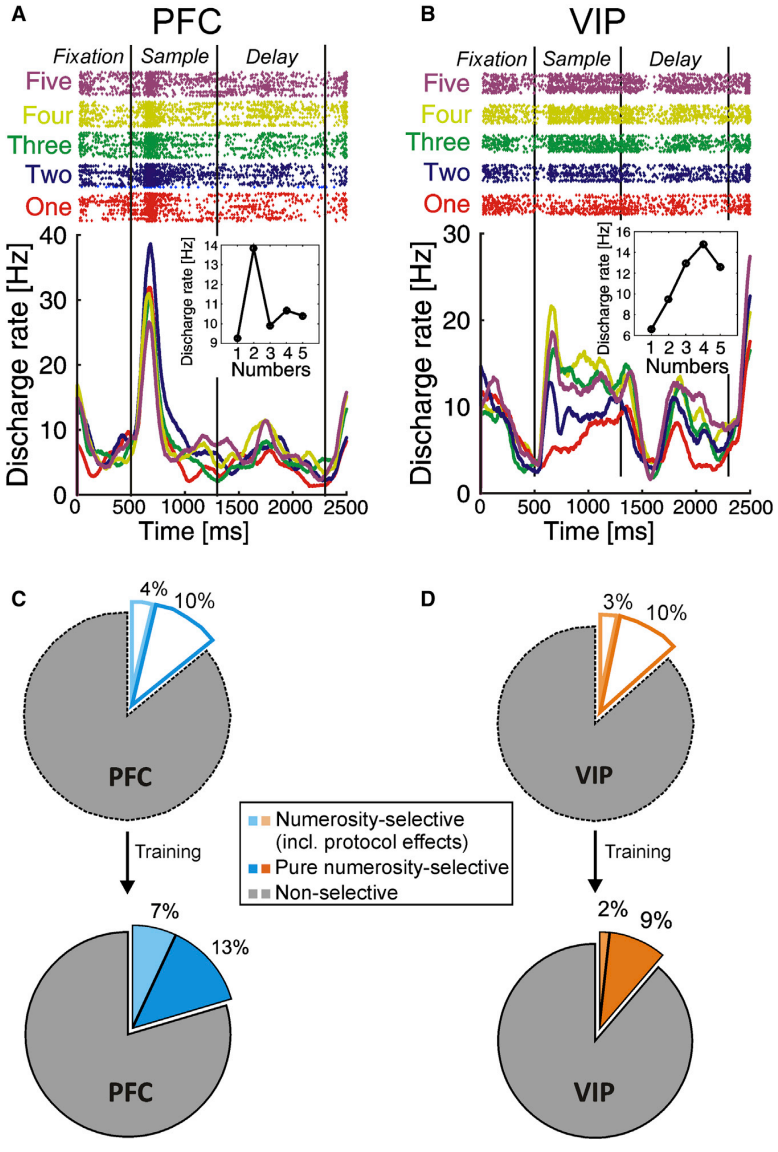

Figure 3. Numerosity-Selective Neurons

(A) An example numerosity-selective cell in PFC. Trials are sorted by sample numerosity (top panel) in the raster plot, and each dot denotes an action potential. Vertical lines mark the various task phases. The discharge is thus averaged across trials to create a peri-stimulus time histogram (bottom panel) for each sample numerosity. The inset shows the numerical tuning function for that neuron by averaging the activity across time and trials.

(B) The same as (A) for an example neuron recorded in VIP.

(C) Pie charts showing the proportions of numerosity-selective neurons among those recorded in the PFC. The dashed contours enclose the proportions found in the PFC pre-training (top), and the solid contours enclose the proportions found post-training (bottom). The colored areas depict the numerosity-selective proportions found with ANOVA. The darker shaded areas depict the "purely" numerosity-selective proportions, and the lighter shaded areas depict the proportions sensitive to stimulus protocol effects, i.e., co-varying low-level visual features of the stimulus.

(D) Same layout as (C) for area VIP.

See also Figure S2 and Table S1.

Explained Variance Measures

Because raw tuning curve measures do not necessarily take the strength of response modulation into account, we also calculated the proportion of explained variance (ω^2 PEV) [22]. It quantifies how much information about the sample numerosity was carried by the discharge rates of the population of numerosity-selective neurons. We used a two-way ANOVA with the factors sample numerosity and stimulus protocol to additionally explore the interaction term between stimulus protocol and numerosity.

The sliding-window analysis in Figure 5A shows that the ω^2 values for PFC neurons increased during the sample period, as expected for selective neurons. Interestingly, however, the ω^2 PEV values were higher during post-training compared to pre-training. This difference was significant when compared in an 800-ms interval covering the entire sample period (median 0.0591 pre-training, n = 38; median 0.0640 post-training, n = 50; Mann-Whitney U test; p = 0.025; Figure 5A, inset). This difference was still present when only the purely numerosity-selective neurons were analyzed (two-tailed Mann-Whitney U test; p = 0.024; n = 28 pre-training and n = 33 post-training). The explained variance for the stimulus protocol and interaction did not show any significant changes (Figure 5A, purple and black functions). The explained variance for the whole population of PFC cells did not change post-training (all cells, median 0.0025 pre-training; median 0.0039 post-training; p = 0.24).

In the VIP, however, the result was different (Figure 5B). The ω^2 PEV for the factor numerosity did not change for pre- compared to post-training (median 0.0577 pre-training, n = 32; median 0.0605 post-training, n = 26; two-tailed Mann-Whitney U test; p = 0.52; Figure 5B, inset). For purely numerosity-selective neurons, there was no difference in ω^2 PEV between pre- and post-training (two-tailed Mann-Whitney U test; p = 0.96; n = 24 pre-training and n = 22 post-training). The explained variance for the stimulus protocol and interaction did not show any significant changes. The explained variance for the whole population of VIP cells did not change

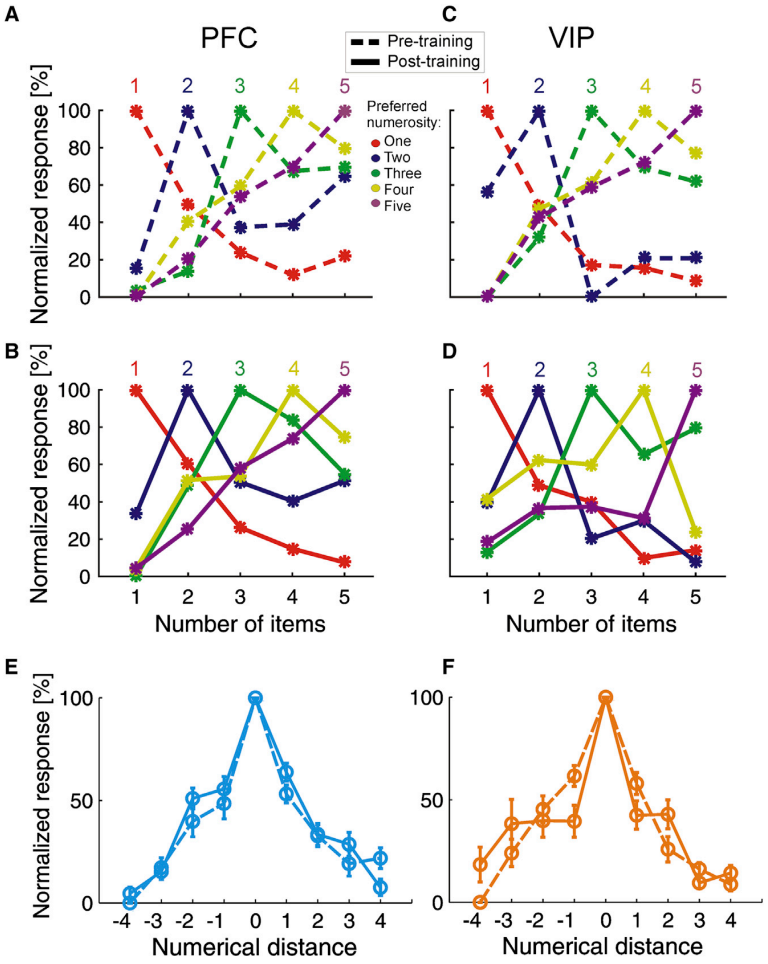

Figure 4. Tuning Curves of Selective Neurons

(A–D) The numerosity-selective neurons are grouped according to the preferred number eliciting the maximal response, indicated here by the different colors. Their responses to the various numerosities are then normalized and plotted here as tuning curves. (A) PFC neurons recorded pre-training (n = 38). (B) PFC neurons recorded post-training (n = 50). (C) VIP neurons pre-training (n = 32). (D) VIP neurons post-training (n = 26).

(E) The neuronal responses to various sample numerosities are normalized (preferred numerosity = 100% and least preferred numerosity = 0%) and centered to the preferred numerosity such that the other sample numerosities are expressed as numerical distance from the preferred numerosity. Dashed lines depict selective cells pre-training and solid lines post-training in the PFC. Error bars denote SEM.

(F) The same as (E) for VIP neurons.

post-training (all cells, median 0.0039 pre-training; median 0.0028 post-training; $p = 0.24$).

Numerosity Discriminability Changes in PFC and VIP

We applied an ROC analysis derived from signal detection theory to quantify the neuronal discriminability for numerosity in the same sample time windows as used for the other analyses. The values of the area under the ROC curve (AUC) could range from 0.5 (no discriminability between most- and least-preferred magnitude value) to 1.0 (perfect discriminability).

In the PFC, the AUC values were significantly higher post-training compared to pre-training (median pre-training = 0.693 to post-training = 0.724; two-tailed Mann-Whitney U test; $p = 0.016$; Figure 6A). This significant improvement in discriminability was also seen for purely numerosity-selective neurons alone (two-tailed Mann-Whitney U test; $p = 0.024$). The AUC value also increased significantly across the whole population of PFC neurons, irrespective of numerosity selectivity (for all recorded PFC cells, median pre-training = 0.586 to median post-training = 0.595; $p < 0.05$). This indicates that numerosity discriminability robustly increased post-training in the PFC for neuronal populations containing numerosity-selective neurons. This improvement did not arise from differences between firing-rate distributions of the two recording periods. We tested the means of distributions (t test; $p > 0.05$) and the shape of the distributions (Kolmogorov-Smirnov test; $p > 0.05$) and found no significant differences between the pre-training and post-training samples. Additionally, this change in the AUC values was stable during the entire recording period (Figure 6C) and did not change over time (regression analysis; $p > 0.1$). For number-selective PFC cells, the AUC calculated for error trials post-training had a median of 0.708 and was not significantly different from those calculated for correct trials ($p = 0.11$). For the whole population of PFC cells, median AUC for error trials was 0.517 and significantly different from those calculated for correct trials ($p < 0.0001$).

The neuronal discriminability in VIP, on the other hand, did not change with training (Figure 6B). The AUC values pre- and post-training were comparable for numerosity-selective neurons (median pre-training = 0.715; post-training = 0.702; two-tailed Mann-Whitney U test; $p = 0.120$) and also for the population of purely numerosity-selective neurons (two-tailed Mann-Whitney U test; $p = 0.286$). Similarly, no difference was detectable for the entire population of all recorded VIP neurons (for all recorded VIP cells, median pre-training = 0.597 to median post-training = 0.598; $p < 0.05$). For number-selective VIP cells, the AUC calculated for error trials post-training had a median of 0.618 and was not significantly different from those calculated for correct trials ($p = 0.06$). For the whole population of VIP cells, median AUC for error trials was 0.515 and significantly different from those calculated for correct trials ($p < 0.001$).

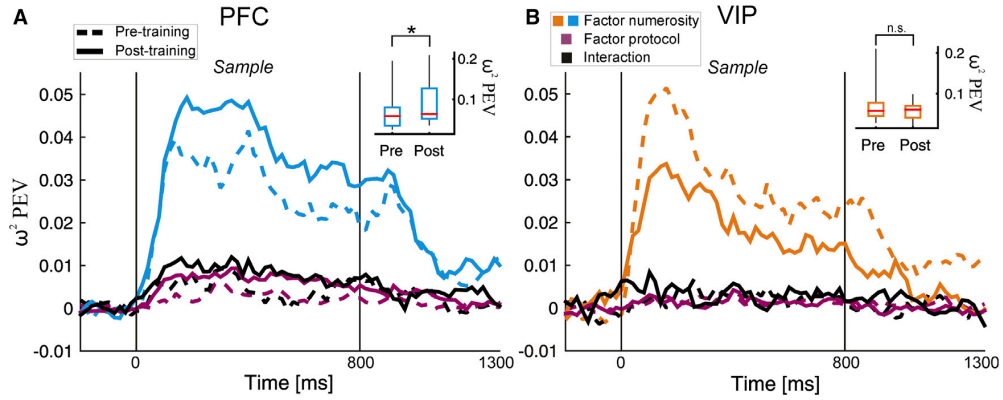

Figure 5. Numerosity Information in Selective Neurons

(A) Proportion explained variance (ω^2 PEV) calculated with a sliding window of 100 ms slid by 20 ms steps for the numerosity-selective cells in PFC. Dashed lines in the plot depict pre-training data, and solid lines depict post-training data. Cyan lines show the ω^2 PEV values for the factor numerosity, purple lines the factor stimulus protocol, and black lines the interaction (numerosity × stimulus protocol). The inset boxplot describes the numerosity ω^2 PEV calculated during the sample period for all the selective neurons. The horizontal red lines indicate the medians within the boxes spanning the 25th–75th percentiles of the data. The whiskers span the 5th–95th percentiles.

(B) The same as (A) for area VIP with orange lines depicting the ω^2 PEV values for the factor numerosity.

Broad Spiking Cells Show Improvement by Numerosity Training in PFC

Finally, we investigated the training effects for the two major cortical cell classes [23–25]. We grouped the recorded neurons based on their extracellularly recorded waveforms into narrow spiking (NS) (23% of all neurons pre-training and 23% post-training), i.e., putative interneurons, and broad spiking (BS) (74% of all neurons pre-training and 73% post-training), i.e., putative pyramidal cells (Figure 7). We calculated an averaged and normalized waveform for each recorded neuron and used a linear classifier to classify the neurons into the two different classes. This method of classification has been used in recent studies to investigate the involvement of different neuronal classes in different aspects of a task [26].

In the PFC (Figure 7A), BS cells showed a slight increase in AUC values (0.693 to 0.718; $p = 0.0505$) post-training. NS cells, however, did not show changes (0.694 to 0.735; $p > 0.1$) with behavioral relevance. In the VIP (Figure 7B), neither cell class showed a corresponding effect (BS cells 0.722 to 0.694; $p = 0.0985$; NS cells 0.705 to 0.708; $p > 0.1$).

DISCUSSION

We hypothesized that active discrimination of numerosity would change response properties of neurons in the PFC and/or VIP, two areas known to be engaged in processing numerical information. We report that only the PFC became more responsive to numerosity during active numerosity discrimination. The regression analysis performed for the entire neuronal population showed that the PFC improved in its ability to differentiate between numerosity and co-varying lower visual parameters. Closely following this finding, numerosity-selective neurons in PFC also became more frequent and more informative about numerosity. This improvement was due mostly to broad-spiking putative pyramidal neurons.

In contrast to the PFC, none of these effects were observed for VIP neurons, even though VIP neurons were also responsive to numerosity. As a population, VIP neurons were not effective in discriminating between numerosity and co-varying lower visual parameters after numerosity training whereas individual numerosity-selective cells maintained their selectivity. Neither the proportion of numerosity-selective cells, nor numerosity discriminability of VIP neurons changed with active discrimination of numerosity. This lack of modulation of quantity categories in the parietal cortex through behavioral relevance stands in contrast to previous findings obtained with arbitrary perceptual categories.

PFC Encodes Behaviorally Relevant Numerical Information

Our population analysis of the task variables and their effect on trial-by-trial firing rates yielded diametrically opposite results in prefrontal and posterior parietal lobe. The post-training emergence of a neuronal PFC population that was differentially influenced by the factors number and stimulus protocol contrasted with the lack of such correlated activity post-training in VIP. As the de-noised regression coefficients describe how much of the trial-by-trial firing rate of the unit depends on the task variables at hand [18], the correlations between the regression coefficients to the different factors are telling of the mixed selectivity experienced by the units [27]. The emergence of this property in PFC during active numerosity discrimination indicates that prefrontal neurons distinguished between the numerosity of the stimuli and the co-varying visual features much more strongly post-training. Thus, our results are indicative of the PFC playing a role in actively discriminating behaviorally relevant numerical categories from the co-varying visual features with decreased behavioral relevance.

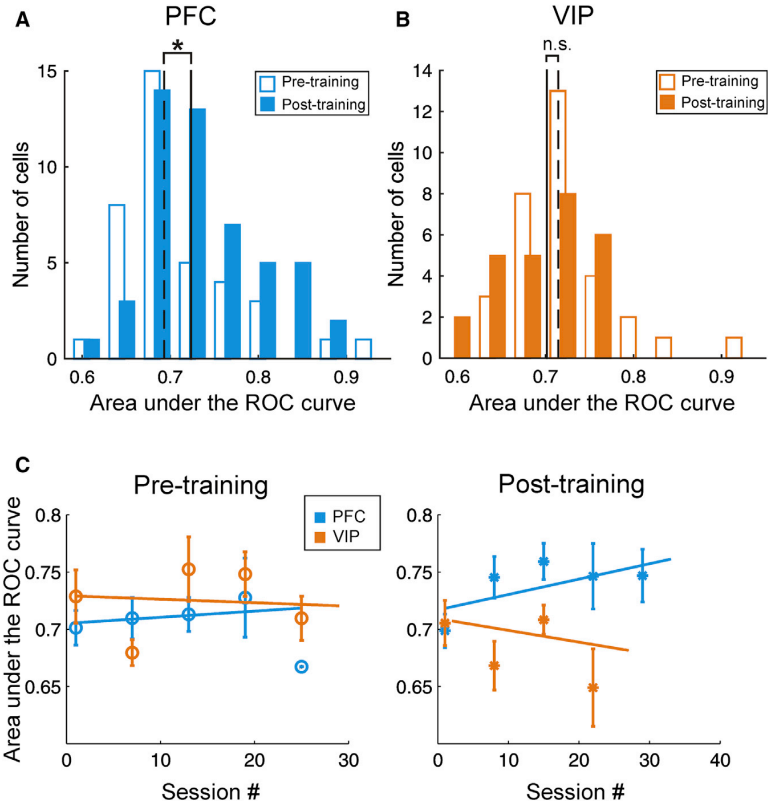

Figure 6. Coding Quality Assessed by Area under the ROC Curve

(A) Histograms showing AUC values in PFC colored by recording periods; empty bars, pre-training; filled bars, post-training. Black vertical lines indicate the median values; dashed lines, pre-training; solid lines, post-training.

(B) The same as (A) for area VIP.

(C) AUC values plotted as a function of days (session numbers) pre-training (left panel) and post-training (right panel). Each data point represents an average across all neurons recorded in a bin of 6 days (pre-training) or 7 days (post-training); cyan data points indicate PFC cells, and orange data points indicate VIP cells. Error bars show SEM. Solid lines represent the linear regression; none of the slopes was significantly different than zero.

This is consistent with the PFC conveying top-down signals to parietal neurons to exert cognitive control during rule-based tasks [16].

Selective Neurons in PFC, but Not VIP, Improve during Active Numerosity Discrimination

After the color-discrimination task, we retrained the monkeys to discriminate numerosity. This introduced numerosity as a behaviorally relevant stimulus feature and increased the monkeys' experience with numerosity. One might expect that these changes also had an impact on the response properties of neurons in such classical association areas like the PFC and the VIP. Experience-dependent sharpening of neuronal selectivity has been described in early (V1) [28] and intermediate (V4) [29, 30] visual cortex. Also in the inferior temporal cortex (area IT), the termination zone of the ventral visual pathway, learning to discriminate among complex objects was found to enhance object selectivity of neurons [31, 32]. Similarly, neurons in the PPC of the dorsal visual pathway have been shown to reflect behavioral relevance [10, 33] and learned arbitrary category membership of visual motion stimuli [13, 34]. In the PFC, behavioral relevance sometimes has dramatic effects on neuronal responses and can even retune cells according to changed boundaries of arbitrary perceptual categories [35]. An increase in proportions of responsive neurons when switching from a passive fixation task to an active working memory task has also been found in PFC [14].

Our data show that learning- and relevance-dependent neuronal plasticity does not hold true for all possible visual stimulus features, particularly in the PPC. After analysis of several neuronal parameters, we could not detect enhancement for numerical categories in VIP. VIP neurons steadily encoded numerosity during both the color- and the numerosity-discrimination tasks but independent of whether numerosity was behaviorally relevant or not. This also suggests that numerosity selectivity in VIP evolves along the visual pathway through a bottom-up process not requiring top-down modulation by the PFC [36]. This is in agreement with the observation that, sometimes even in trained animals, parietal signals of visual categories do not arise as a result of feedback from PFC [34]. Response latency data support this hypothesis because neurons in the intraparietal cortex represent their preferred numerosity on average about 50 ms earlier than PFC neurons, both in numerically naive [5] and numerically trained monkeys [37, 38]. Collectively, this suggests that sensory representations of numerosity are rapidly and automatically encoded in VIP, irrespective of task demands. Of course, this is not to say that VIP neurons cannot be modulated whenever numerical information needs to be processed according to the rules of other cognitive control functions.

In contrast to VIP, active discrimination of set size significantly enhanced the representation of numerosity in PFC. Surprisingly, this enhancement was only modestly based on an increase in the frequency of selective neurons but rather caused by a higher quality of numerosity encoding by a relatively stable set of numerosity-selective neurons. This relevance-induced improvement in numerosity discriminability of PFC neurons was primarily found in BS (putative pyramidal) neurons. This suggests a preferential modulation of BS neurons with active numerosity processing and corresponds with our previous finding that putative pyramidal cells showed a higher degree of numerosity selectivity

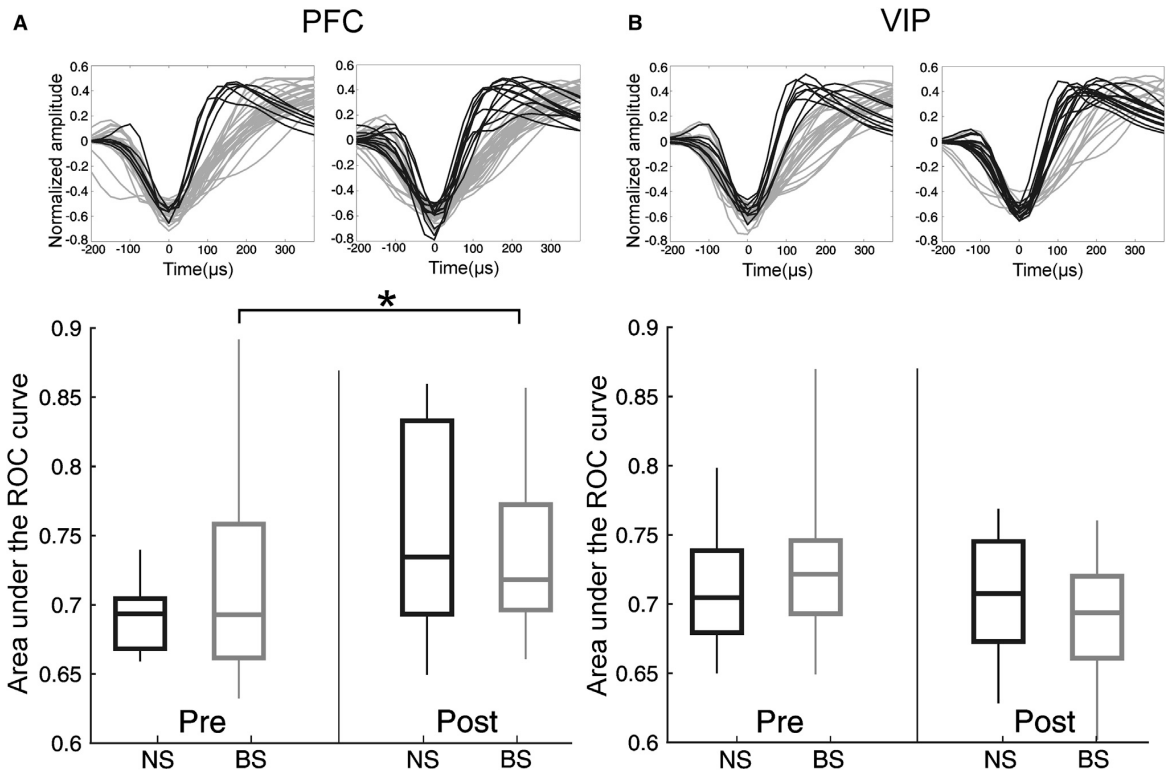

Figure 7. Change in AUC Mediated by Different Neuronal Classes

(A) PFC neurons classified into narrow spiking (NS) (black) and broad spiking (BS) (gray) by their normalized waveforms (top panel) and boxplots depicting the AUC values (bottom panel) for the two cell classes pre-training (left) and post-training (right). The horizontal lines indicate the medians within the boxes spanning the 25th–75th percentiles of the data. The whiskers span the 5th–95th percentiles.

(B) The same as (A) for VIP neurons.

[23]. BS neurons in PFC also seem to contribute to other PFC functions, such as learning to memorize stimuli [14], motion discrimination [26], and decision making [39]. Sensory prefrontal neurons are also differentially affected by dopaminergic modulation [24, 40].

Our results contrast activity changes found in ventral PFC of monkeys before (i.e., during passive fixation) and after training on a spatial working memory task. Qi et al. [14] observed a doubling of the proportion of activated neurons (from 10% to 20%) but also a degradation of the neurons' stimulus selectivity after training. In our study, however, we witnessed only a very moderate increase of the proportion of numerosity-selective neurons but a clear enhancement of the coding quality of such neurons after numerosity training. A possible explanation for this discrepancy may include differences in the discriminative stimulus (numerical versus spatial stimulus feature) but perhaps more importantly differences in the cognitive states the monkeys needed to adopt, because passive fixation (as applied by Qi et al.) demands only little attention and/or arousal compared to an active discrimination task. We, therefore, had the monkeys engaged in equally demanding delayed discrimination tasks pre-training (color discrimination) and post-training (numerosity discrimination) to exclude general internal state differences.

Our data also diverge from results obtained with perceptual category training. Strong categorical representations of stimuli in PFC have been described in monkeys trained to recognize binary category membership of sensory stimuli, such as "up versus down" motion directions [34, 41] or "cats versus dogs" classes [15]. Both in IPS and PFC, such categorical discharges are not present in naive animals but emerge with training to encode behaviorally relevant stimulus groups. Changing category boundaries also causes adaptive changes in PFC neurons [15]. The encoding of numerical categories differed from these findings because numerosity-selective neurons in the IPS and PFC are already present in numerically naive monkeys [5] and they exhibit a stable labeled-line code irrespective of stimulus context (PFC) [42] or training status (current study). We suspect that this coding stability is related to numerosities being "natural" categories, which—unlike arbitrary perceptual categories that necessarily need to be conditioned—possess an inherent meaning with permanent category boundaries. In addition (and unlike VIP), PFC numerosity-selective neurons did experience enhancement of coding quality. We interpret this improved neuronal selectivity as a reflection of increased relevance of numerical categories post-training. This improved selectivity might help the PFC exert top-down influence on downstream

cortical stages and guide executive functions via numerical information.

Quantities as Stable Natural Categories

The current data suggest that numerosity representations in the PFC and VIP rely on a sparse code [43] with dedicated and relatively stable "labeled lines" [44]. Sensory numerosity representations in the parietal lobe seem to be largely independent from task relevance, thus supporting the idea of a visual "number sense," the faculty to perceive visual collections intuitively [8, 9]. Visual numerosity-selective neurons may develop spontaneously and naturally within visual neural structures of the primate brain, prior to learning how to use this information. In agreement with this idea and based on psychophysical findings, Burr and Ross [6] suggested visual numerosity as a sensory attribute that is susceptible to adaptation just like color, contrast, or speed. Perhaps numerosity, like faces [45], constitutes an exceptionally relevant type of information with adaptive value. The numerical category "set size" could therefore emerge as a natural category represented spontaneously in a dedicated parieto-frontal network. Just as face selectivity, numerosity selectivity could potentially be present at birth [46]. In the PFC, however, numerosity selectivity is enhanced during explicit processing of sensory numerical information. This plasticity potentially enables PFC networks to emphasize behavioral relevance of numerosity during executive functions.

EXPERIMENTAL PROCEDURES

All procedures complied with the European Communities Council Directive 2010/63/EC and the German Law for Protection of Animals and were approved by the national authorities, following appropriate ethics review. For detailed methods, please see the Supplemental Experimental Procedures.

SUPPLEMENTAL INFORMATION

Supplemental Information includes Supplemental Experimental Procedures, two figures, and one table and can be found with this article online at http://dx.doi.org/10.1016/j.cub.2015.03.025.

AUTHOR CONTRIBUTIONS

A.N. and P.V. designed the experiments. P.V. performed research and analyzed data. P.V. and A.N. wrote the manuscript.

ACKNOWLEDGMENTS

This work was supported by DFG grant NI 618/2-1 to A.N.

Received: February 3, 2015
Revised: March 2, 2015
Accepted: March 16, 2015
Published: April 23, 2015

REFERENCES

1. Nieder, A. (2013). Coding of abstract quantity by 'number neurons' of the primate brain. J. Comp. Physiol. A Neuroethol. Sens. Neural Behav. Physiol. *199*, 1–16.
2. Ansari, D. (2008). Effects of development and enculturation on number representation in the brain. Nat. Rev. Neurosci. *9*, 278–291.
3. Piazza, M., Izard, V., Pinel, P., Le Bihan, D., and Dehaene, S. (2004). Tuning curves for approximate numerosity in the human intraparietal sulcus. Neuron *44*, 547–555.
4. Eger, E., Michel, V., Thirion, B., Amadon, A., Dehaene, S., and Kleinschmidt, A. (2009). Deciphering cortical number coding from human brain activity patterns. Curr. Biol. *19*, 1608–1615.
5. Viswanathan, P., and Nieder, A. (2013). Neuronal correlates of a visual "sense of number" in primate parietal and prefrontal cortices. Proc. Natl. Acad. Sci. USA *110*, 11187–11192.
6. Burr, D., and Ross, J. (2008). A visual sense of number. Curr. Biol. *18*, 425–428.
7. Arrighi, R., Togoli, I., and Burr, D.C. (2014). A generalized sense of number. Proc. Biol. Sci. *281*, 20141791.
8. Dantzig, T. (1930). Number: The Language of Science. (New York: Free Press).
9. Dehaene, S. (1997). The Number Sense. (Oxford: Oxford University Press).
10. Mountcastle, V.B., Andersen, R.A., and Motter, B.C. (1981). The influence of attentive fixation upon the excitability of the light-sensitive neurons of the posterior parietal cortex. J. Neurosci. *1*, 1218–1225.
11. Rainer, G., Asaad, W.F., and Miller, E.K. (1998). Memory fields of neurons in the primate prefrontal cortex. Proc. Natl. Acad. Sci. USA *95*, 15008–15013.
12. Rainer, G., and Miller, E.K. (2000). Effects of visual experience on the representation of objects in the prefrontal cortex. Neuron *27*, 179–189.
13. Freedman, D.J., and Assad, J.A. (2006). Experience-dependent representation of visual categories in parietal cortex. Nature *443*, 85–88.
14. Qi, X.L., Meyer, T., Stanford, T.R., and Constantinidis, C. (2011). Changes in prefrontal neuronal activity after learning to perform a spatial working memory task. Cereb. Cortex *21*, 2722–2732.
15. Freedman, D.J., Riesenhuber, M., Poggio, T., and Miller, E.K. (2001). Categorical representation of visual stimuli in the primate prefrontal cortex. Science *291*, 312–316.
16. Crowe, D.A., Goodwin, S.J., Blackman, R.K., Sakellaridi, S., Sponheim, S.R., MacDonald, A.W., 3rd, and Chafee, M.V. (2013). Prefrontal neurons transmit signals to parietal neurons that reflect executive control of cognition. Nat. Neurosci. *16*, 1484–1491.
17. Nieder, A., and Miller, E.K. (2003). Coding of cognitive magnitude: compressed scaling of numerical information in the primate prefrontal cortex. Neuron *37*, 149–157.
18. Mante, V., Sussillo, D., Shenoy, K.V., and Newsome, W.T. (2013). Context-dependent computation by recurrent dynamics in prefrontal cortex. Nature *503*, 78–84.
19. Nieder, A., Freedman, D.J., and Miller, E.K. (2002). Representation of the quantity of visual items in the primate prefrontal cortex. Science *297*, 1708–1711.
20. Nieder, A., Diester, I., and Tudusciuc, O. (2006). Temporal and spatial enumeration processes in the primate parietal cortex. Science *313*, 1431–1435.
21. Nieder, A. (2012). Supramodal numerosity selectivity of neurons in primate prefrontal and posterior parietal cortices. Proc. Natl. Acad. Sci. USA *109*, 11860–11865.
22. Siegel, M., Warden, M.R., and Miller, E.K. (2009). Phase-dependent neuronal coding of objects in short-term memory. Proc. Natl. Acad. Sci. USA *106*, 21341–21346.
23. Diester, I., and Nieder, A. (2008). Complementary contributions of prefrontal neuron classes in abstract numerical categorization. J. Neurosci. *28*, 7737–7747.
24. Jacob, S.N., Ott, T., and Nieder, A. (2013). Dopamine regulates two classes of primate prefrontal neurons that represent sensory signals. J. Neurosci. *33*, 13724–13734.
25. Womelsdorf, T., Ardid, S., Everling, S., and Valiante, T.A. (2014). Burst firing synchronizes prefrontal and anterior cingulate cortex during attentional control. Curr. Biol. *24*, 2613–2621.

 ©2015 Elsevier Ltd All rights reserved

26. Hussar, C.R., and Pasternak, T. (2009). Flexibility of sensory representations in prefrontal cortex depends on cell type. Neuron *64*, 730–743.
27. Rigotti, M., Barak, O., Warden, M.R., Wang, X.-J., Daw, N.D., Miller, E.K., and Fusi, S. (2013). The importance of mixed selectivity in complex cognitive tasks. Nature *497*, 585–590.
28. Gilbert, C.D., Li, W., and Piech, V. (2009). Perceptual learning and adult cortical plasticity. J. Physiol. *587*, 2743–2751.
29. Raiguel, S., Vogels, R., Mysore, S.G., and Orban, G.A. (2006). Learning to see the difference specifically alters the most informative V4 neurons. J. Neurosci. *26*, 6589–6602.
30. Yang, T., and Maunsell, J.H.R. (2004). The effect of perceptual learning on neuronal responses in monkey visual area V4. J. Neurosci. *24*, 1617–1626.
31. Freedman, D.J., Riesenhuber, M., Poggio, T., and Miller, E.K. (2006). Experience-dependent sharpening of visual shape selectivity in inferior temporal cortex. Cereb. Cortex *16*, 1631–1644.
32. Kobatake, E., Wang, G., and Tanaka, K. (1998). Effects of shape-discrimination training on the selectivity of inferotemporal cells in adult monkeys. J. Neurophysiol. *80*, 324–330.
33. Toth, L.J., and Assad, J.A. (2002). Dynamic coding of behaviourally relevant stimuli in parietal cortex. Nature *415*, 165–168.
34. Swaminathan, S.K., and Freedman, D.J. (2012). Preferential encoding of visual categories in parietal cortex compared with prefrontal cortex. Nat. Neurosci. *15*, 315–320.
35. Freedman, D.J., Riesenhuber, M., Poggio, T., and Miller, E.K. (2002). Visual categorization and the primate prefrontal cortex: neurophysiology and behavior. J. Neurophysiol. *88*, 929–941.
36. Roitman, J.D., Brannon, E.M., and Platt, M.L. (2007). Monotonic coding of numerosity in macaque lateral intraparietal area. PLoS Biol. *5*, e208.
37. Nieder, A., and Miller, E.K. (2004). A parieto-frontal network for visual numerical information in the monkey. Proc. Natl. Acad. Sci. USA *101*, 7457–7462.
38. Tudusciuc, O., and Nieder, A. (2009). Contributions of primate prefrontal and posterior parietal cortices to length and numerosity representation. J. Neurophysiol. *101*, 2984–2994.
39. Ding, L., and Gold, J.I. (2012). Neural correlates of perceptual decision making before, during, and after decision commitment in monkey frontal eye field. Cereb. Cortex *22*, 1052–1067.
40. Ott, T., Jacob, S.N., and Nieder, A. (2014). Dopamine receptors differentially enhance rule coding in primate prefrontal cortex neurons. Neuron *84*, 1317–1328.
41. Mendoza-Halliday, D., Torres, S., and Martinez-Trujillo, J.C. (2014). Sharp emergence of feature-selective sustained activity along the dorsal visual pathway. Nat. Neurosci. *17*, 1255–1262.
42. Moskaleva, M., and Nieder, A. (2014). Stable numerosity representations irrespective of magnitude context in macaque prefrontal cortex. Eur. J. Neurosci. *39*, 866–874.
43. Olshausen, B.A., and Field, D.J. (2004). Sparse coding of sensory inputs. Curr. Opin. Neurobiol. *14*, 481–487.
44. Nieder, A., and Merten, K. (2007). A labeled-line code for small and large numerosities in the monkey prefrontal cortex. J. Neurosci. *27*, 5986–5993.
45. Moeller, S., Freiwald, W.A., and Tsao, D.Y. (2008). Patches with links: a unified system for processing faces in the macaque temporal lobe. Science *320*, 1355–1359.
46. Rodman, H.R., Skelly, J.P., and Gross, C.G. (1991). Stimulus selectivity and state dependence of activity in inferior temporal cortex of infant monkeys. Proc. Natl. Acad. Sci. USA *88*, 7572–7575.

Current Biology

Supplemental Information

Differential Impact of Behavioral Relevance on Quantity Coding in Primate Frontal and Parietal Neurons

Pooja Viswanathan and Andreas Nieder

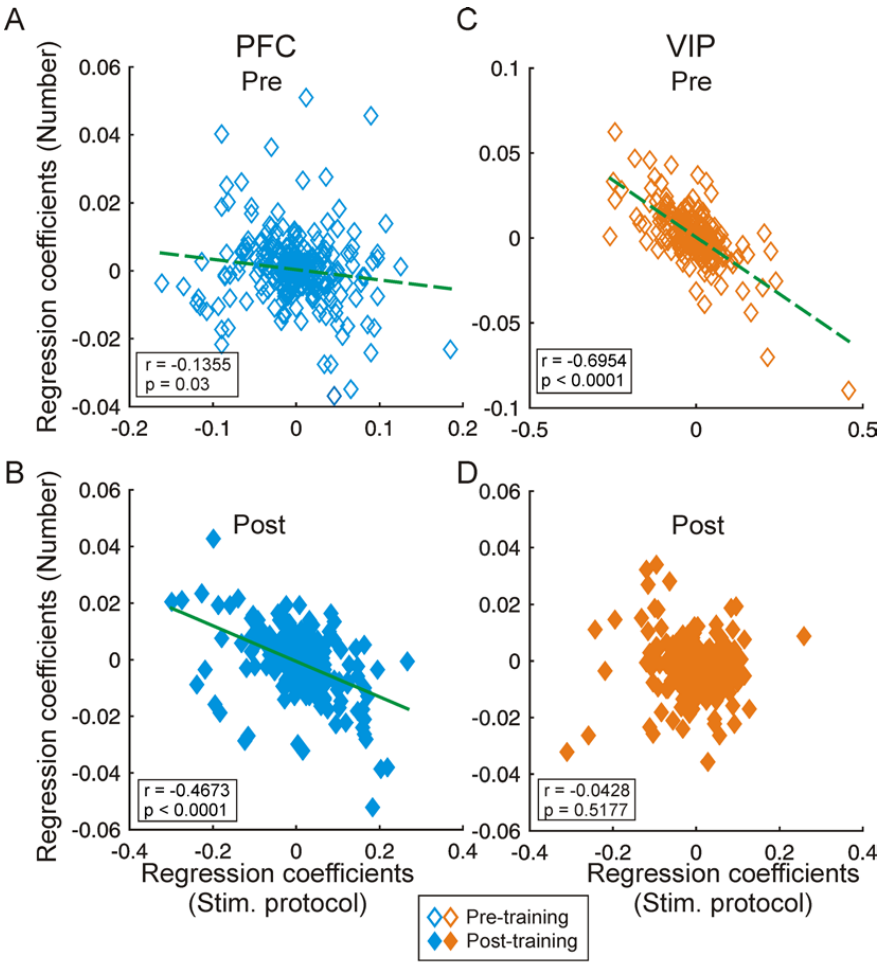

FIGURE S1, related to Figure 2 (A) De-noised regression coefficients during the pre-training period calculated without the color predictor for the factor numerosity plotted against those for the factor stimulus protocol for each recorded neuron. Each dot on the plot denotes a PFC neuron. Correlations between coefficients are shown ($p < 0.05$, Pearson's correlation coefficient, r) with significant correlations indicated by the green lines. **(B)** The same data as in A for the PFC neurons recorded post-training. **(C)** and **(D)** The same as (A) and (B) for area VIP neurons.

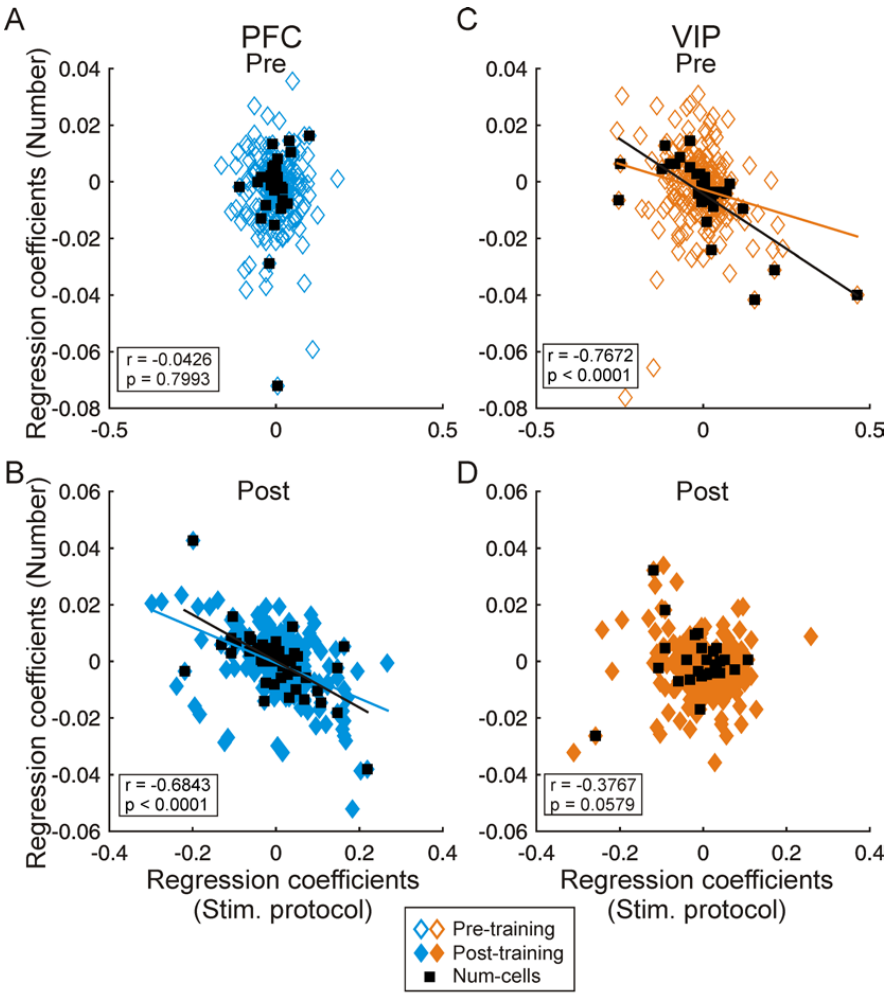

FIGURE S2, related to Figures 2 and 3 (A) De-noised regression coefficients for the factor numerosity plotted against those for the factor stimulus protocol for each recorded neuron. Each dot on the plot denotes a PFC neuron. The numerosity-selective cells found in ANOVA are plotted as black squares and the correlation coefficients calculated for only the selective cells (shown in black) are shown ($p < 0.05$, Pearson's correlation coefficient, r). The regression lines denote the regression calculated for the entire population (same color as dots) and the numerosity-selective cells (in black). **(B)** The same data as in A for the PFC neurons recorded post-training. **(C)** and **(D)** The same as (A) and (B) for area VIP neurons.

Table S1. related to **Figure 3**

ANOVA results summarized in the table to report the percentage of cells with the various main effects in both recording periods. The absolute number of cells are indicated in brackets.

	PFC		**VIP**	
Main effects	**Pre (n = 268)**	**Post (n = 245)**	**Pre (n = 238)**	**Post (n = 231)**
Color	10% (26)	-	12% (29)	-
Stimulus Protocol	4% (10)	8% (19)	5% (12)	6% (13)
'Pure' protocol	2% (5)	2% (4)	3% (8)	5% (11)
Numerosity (with interactions)	14% (38)	20% (50)	13% (32)	11% (26)
'Pure' numerosity	10% (28)	13% (33)	10% (24)	10% (22)

SUPPLEMENTAL EXPERIMENTAL PROCEDURES

Experimental setup

Two male rhesus monkeys (Macaca mulatta) weighing between 5.5 to 6.3 kg served as subjects for this study. The animals were seated inside primate chairs in a chamber 57 cm away from a 15" flat screen monitor (with a resolution of 1,024 by 768 pixels and a refresh rate of 75 Hz). The NIMH Cortex program was used to present the stimuli and monitor ongoing behavior. The monkeys' eye gaze was tracked by an Infrared eye tracking system (ISCAN, Cambridge, MA). All data analysis was performed using the MATLAB computational environment (Mathworks).

Behavioral task

The basic task design stayed the same for both recording phases: pre and post training. The monkeys performed a delayed match-to-sample task (**Figure 1A**) with different matching rules for the two phases. We compared coding in monkeys that were actively engaged in discrimination tasks both pre and post numerosity training (rather than comparing passive fixation versus numerosity discrimination) in order to have the monkeys in similar attentive states while comparing active neurons in cognitive brain areas, and to have the monkeys pay attention to the dot stimuli. The trial was initiated by the monkeys holding a response bar and fixating within 3.5° of visual angle of a central fixation target throughout the trial. Upon successful fixation for 500 ms, the sample stimulus was shown for 800 ms, followed by a delay period of 1000 ms without a stimulus. After the delay, a dot display (test1) was presented which in 50 % of the trials (match) had the same color (pre-training)/number (post-training) as the sample and required the monkey to release the response bar to receive a fluid reward. In the other 50 % of the trials (non-match), the first test display showed a different color (pre-training)/number (post-training); in this case the monkey had to hold the response

bar and wait for the second test (test2) that always matched the sample in color/number to release the bar. Based on this task design, chance performance was 50 % correct trials.

Stimuli and matching rule in Pre-training color phase

The visual stimuli were colored dot (diameter range from 0.5° to 0.9° of visual angle) displays (only one color per stimulus) on a gray background circle (diameter - 6° of visual angle). Five colors (red, blue, green, yellow, purple) were chosen for maximum discriminability. The luminance values of the dot colors were Red = 0.63 cd/m^2, Blue = 0.37 cd/m^2, Green = 1.63 cd/m^2, Yellow = 4.12 cd/m^2, Purple = 1.75 cd/m^2. All colors were presented in displays containing either one, two, three, four or five dots. These dot patterns were generated using a custom-written MatLab script (The Mathworks, Natick, MA). These routines enabled generation of new stimulus sets for each recording session. Moreover, this software provided for the control of visual parameters of the dot-patterns. For the standard stimuli, each stimulus contained a defined set of colored dots that appeared at randomized locations within the gray background circle. The diameter of each dot was randomly varied within a given range. To prevent the monkeys from memorizing the visual patterns of the displays, each quantity was tested with many different images per session and the sample and test displays that appeared on each trial were never identical. In addition to the standard stimuli, control stimuli controlling for the spatial low-level visual features, 'total dot area' (total area of all items in a display equated for all stimuli in a trial) and 'dot density' (same mean density of dot patterns for all stimuli in a trial) were employed in each session (**Figure 1B**). The matching rule in the pre-training phase was color and the monkeys were required to match the color of the sample stimulus to the test stimuli presented. During training (before recording began), both numerically congruent and numerically incongruent stimuli were used as non-match stimuli. The numerically incongruent trials were removed for recording to end up with a viable number of conditions with many trial repetitions for stable statistical analyses and to have a

consistent trial layout with the post-training phase. All parameters (colors, numerosities, stimulus protocols, match versus non-match trials, etc.) were balanced and pseudo-randomly presented to the monkeys.

Stimuli and matching rule in Post-training numerosity phase

We trained the same monkeys to discriminate numerosity in a delayed match-to-sample design. The visual stimuli were similar to those used in the pre-training phase except for one crucial difference: the dots were uniformly black in color. Luminance levels of the dots changed slightly from pre to post-training due to removal of color. The luminance of the black we used for the dots was 0.19 cd/m^2.The matching rule in the post-training phase was numerosity and the monkeys were required to match the number of dots in the sample stimulus to those in the test stimuli presented. Color was not returned to the post-training protocol to avoid Stroop-like effects. All parameters (numerosities, stimulus protocols, match versus non-match trials, etc.) were balanced and pseudo-randomly presented to the monkeys.

Evaluation of putative numerosity discrimination prior to training

We also tested whether the monkeys might have learned to discriminate the behaviorally-irrelevant stimulus dimension 'numerosity' in the pre-training phase. For monkey L, blocks (40 trials, 8 trials per numerosity, pseudo-randomized) of pure numerosity stimuli (only black dots, all other parameters as in the color task) were inserted during the ongoing color discrimination task in two sessions; rewards were delivered following correct numerosity matches. The same procedure was applied for monkey S, except that individual pure numerosity trials were randomly interspersed among ongoing color trials; all trials were rewarded irrespective of response. These tests were done immediately after the end of the pre-training recording sessions in both monkeys. Percentage correct performance to each

numerosity was tested by a binomial test ($p < 0.05$). The data (**Figure 1D, empty bars**) showed that neither monkey was able to discriminate numerosity.

Surgery and neuronal recordings

The animals were implanted with a head bolt to allow immobilization of the head during training so that eye movements could be monitored. After the animals reliably discriminated the color of the items in the delayed match-to-sample color task, two recording chambers were implanted over the right lateral prefrontal cortex, centered on the principal sulcus and the right intraparietal sulcus guided by anatomical MRI and strereotaxic measurements. All surgeries were performed under sterile conditions while the monkeys were under general anesthesia and the monkeys received antibiotics and analgesics post-procedure.

Neuronal recordings were made from the two monkeys while they performed the task using arrays of up to eight tungsten micro-electrodes attached to screw micro-drives in a grid with 1 mm spacing. Neurons were not pre-selected for any sensory or task-related parameter. To access area VIP, recordings were made exclusively at depths ranging from 9 to 13 mm below the cortical surface and the presence of visual and somatosensory responses was tested qualitatively. Electrophysiological signals were amplified and filtered and waveforms of action potentials sampled at 40 kHz from each channel were stored to disk. Single unit separation was performed offline based on waveform characteristics (Offline Sorter, Plexon Systems). Timestamps of trial events and action potentials were extracted for analysis. Only single units that exhibited a sufficient discharge rate (> 1 Hz) during the relevant trial phases and were recorded for at least 30 trials per condition were analyzed. All experimental procedures were in accordance with the guidelines for animal experimentation approved by the Regierungspräsidium Tübingen, Germany.

Behavioral data analysis

For the color discrimination task, the percent correct performance for each color in each session was calculated, averaged across all sessions, and statistically verified using a binomial test. To test numerosity discrimination, percent correct performance was calculated for each sample numerosity and again analyzed with a binomial test.

Population analysis

We used multivariate linear regression to be able to look at the whole population and to determine how the various task variables affect trial-by-trial responses of each cell. To do this, we followed a method described by Mante et al, 2013 [1]. We computed the firing rates in the 800 ms sample period in a 50 ms sliding window moved in 50 ms steps, offset by 50 ms for parietal units and 100 ms for prefrontal units, for all correct trials. The firing rates of all the cells were z-scored by subtracting the mean response from the firing rate for each window and in each trial and then dividing by the standard deviation. The z-scored firing rates *(r)* can be represented as a linear combination of the task variables for every neuron *(n)* at time *(t)* for any trial *(x)* can be described as follows:

Pre-training –

$$r_{n,t}(x) = \beta_{n,t}(1)protocol(x) + \beta_{n,t}(2)color(x) + \beta_{n,t}(3)number(x) + \beta_{n,t}(4)$$

Post-training –

$$r_{n,t}(x) = \beta_{n,t}(1)protocol(x) + \beta_{n,t}(2)number(x) + \beta_{n,t}(3)$$

where x takes the identifier of every trial variable for that trial. For the color and number variables, *color (x)* and *number (x)* take a value between 1 and 5 indicating the preference of the neuron (1 to the trial with the most preferred color or number and 5 to that with the least preferred color or number). The stimulus protocol was denoted by the values 1 or 2. The preferences were determined by comparing the average firing rate for the entire sample period calculated across all trials. Thus, we have for each neuron, a matrix $\boldsymbol{X_n}$ with the columns

corresponding to the trial-by-trial values of the task variables, the last column containing ones. We additionally calculated a model for the pre-training phase without the color predictor.

The regression coefficients β calculated in this fashion, describe how much the trial-by-trial firing rate of neuron *(n)* at a given time *(t)* during the trial depends on the corresponding task variables *(v)*:

$$\beta_{n,t} = \left[\left(X\right]_n X_n^T\right)^{-1} X_n r_{n,t}$$

where $\boldsymbol{\beta}_{n,t}$ is a vector describing the regression coefficient for each task variable of length N_{coef}, $\boldsymbol{X}$ is the matrix with trial by trial values of each task variable for that trial ($N_{coef} \times N_{trial}$) and the corresponding trial-by-trial firing rates contained in r.

We further de-noised the population regression coefficients using principal component analysis (PCA) and used it to compare our populations on only the first 12 principal components (PCs). To do this, we first obtained a de-noising matrix $\boldsymbol{D}$ of size $N_{unit} \times N_{unit}$ from the data matrix consisting of smoothed, z-scored population vectors in response to the various combinations of task variables in time:

$$D = \sum_{a=1}^{N_{pca}} v_a v_a^T$$

where vector v_a describes the PCs of the data and $\boldsymbol{D}$ combines the contribution of the first 12 PCs.

We then de-noised each vector of β by projecting it into the subspace spanned by the first $N_{pca} = 12$ principal components and removing the components lying outside this subspace:

$$\beta_{v,t}^{pca} = D\beta_{v,t}$$

where β_{pca} is a set of vectors for each task variable v and each time t of length N_{unit}. We can, thus, plot these de-noised regression coefficients for the task variables influencing pre-training and post-training data in our populations. In particular, we tested the correlations between the de-noised regression coefficients of stimulus protocol against numerosity to see if the same neurons are influenced by the factors tested.

Neuronal data analysis

To examine the neuronal selectivity for numerosity before and after training, we analyzed discharge rates during sample numerosity presentation in an 800 ms window. By default, the 800 ms windows of the sample phase were offset by 50 ms for area VIP cells and by 100 ms for PFC cells to account for typical response latency of these cells. The selectivity of a neuron for a feature of the sample stimulus, a multiple factor ANOVA (criterion $p < 0.01$; interaction model) was calculated using single-trial discharge rates for each cell in the analysis window. Only correct trials were used in all neuronal analyses. The main factors pre-training were 'stimulus protocol' (standard or control), 'sample color' (red, blue, green, yellow, purple) and 'sample numerosity' (one, two, three, four, five). The main factors post-training were simply 'stimulus protocol' and 'sample numerosity'. Each neuron's discharge rates were tested only once, no multiple comparisons were applied. Only neurons with a minimum of 30 stimulus presentations per numerosity were taken into account. The neurons' tuning functions were obtained by simply plotting the trial-averaged firing rates against the numerosity. To derive averaged numerosity tuning functions, those of individual neurons were normalized by setting the maximum activity to the most preferred numerosity as 100% and the activity to the least preferred quantity as 0% and pooling those individual tuning curves for each sample numerosity. Normalized-to-baseline firing rates for the numerosity-selective cells were obtained by subtracting the average firing rate during 300 ms of the fixation period from the firing rate during the sample phase and dividing by the standard deviation during the fixation period.

To quantify the effects of the varying stimuli on the neuronal firing rates, we calculated a ω^2 PEV measure. This measure is derived from an ANOVA and reflects how much of the variance in a neuron's firing rate can be explained by the various factors in a stimulus set. In our case, we derived this from a two-way ANOVA with the factors sample numerosity and stimulus protocol. We calculated the ω^2 PEV over the entire sample period as well as in 100 ms windows moved in steps of 20 ms over the sample period (**Figure 5**).

We also calculated a receiver operating characteristic (ROC) curve [2] to evaluate the stimulus discriminability by the numerosity-selective cells. The true positive rate (firing rate in response to the preferred numerosity) and false positive rate (firing rate in response to the least preferred numerosity) were calculated for each neuron to generate the ROC curve. The area under the ROC curve was then calculated for each neuron to arrive at the AUC values. An AUC value of 0.5 describes no discrimination and a value of 1 describes perfect discrimination. The area under the ROC curve represents the probability that an ideal observer can discriminate between the two distributions based on the trial-by-trial firing rate.

Waveform analysis

We also categorized the recorded single units into narrow-spiking (NS) and broad-spiking (BS) neurons based on their waveforms. For each single unit, we saved the template waveform using Plexon Offline Sorter. We included only the cells with a crest followed by a trough after reaching the threshold voltage i.e. cells with a trough that occurred within 200-400 μs of reaching threshold and did not have a crest within 300 μs of reaching the threshold. We normalized the waveforms to the difference between the maximum amplitude and the minimum amplitude and aligned them to their troughs. We then entered the waveforms through a linear classifier (k-means; k = 2, squared Euclidean distance) to cluster the cells into two categories: narrow-spiking (NS) and broad-spiking (BS) such that the units with smaller

mean widths constituted the narrow-spiking cluster and those with larger mean widths constituted the broad-spiking cluster.

SUPPLEMENTAL REFERENCES

S1. Mante, V., Sussillo, D., Shenoy, K. V, and Newsome, W. T. (2013). Context-dependent computation by recurrent dynamics in prefrontal cortex. Nature *503*, 78–84.

S2. Green, D. M., and Swets, J. A. (1966). Signal Detection Theory and Psychophysics (New York: John Wiley and Sons)

Study 3: Visual receptive fields in the fronto-parietal network

Viswanathan, P., Nieder, A. (under review). Comparison of visual receptive fields in the dorsolateral prefrontal cortex (dlPFC) and ventral intraparietal area (VIP) in macaques.

DR. ANDREAS NIEDER (Orcid ID : 0000-0001-6381-0375)

Accepted Article

Article type : Research Report

Reviewers: Christos Constantinidis, Wake Forest University School of Medicine, USA

Maria Medalla, Boston University, USA

Comparison of visual receptive fields in the dorsolateral prefrontal cortex (dlPFC) and ventral intraparietal area (VIP) in macaques

Pooja Viswanathan & Andreas Nieder*

Animal Physiology, Institute of Neurobiology, Auf der Morgenstelle 28, University of Tübingen, 72076 Tübingen, Germany

Running title: Receptive fields in dlPFC and VIP

Keywords: RF, association cortex, primate, single-unit recording

* To whom correspondence should be addressed:
E-mail: andreas.nieder@uni-tuebingen.de

ABSTRACT

The concept of receptive field (RF) describes the responsiveness of neurons to sensory space. Neurons in the primate association cortices have long been known to be spatially selective but a detailed characterization and direct comparison of RFs between frontal and parietal association cortices is missing. We sampled the RFs of a large number of neurons from two interconnected areas of the frontal and parietal lobes, the dorsolateral prefrontal cortex (dlPFC) and ventral intraparietal area (VIP), of rhesus monkeys by systematically presenting a moving bar during passive fixation. We found that more than half of neurons in both areas

This article has been accepted for publication and undergone full peer review but has not been through the copyediting, typesetting, pagination and proofreading process, which may lead to differences between this version and the Version of Record. Please cite this article as doi: 10.1111/ejn.13740

This article is protected by copyright. All rights reserved.

Accepted Article

showed spatial selectivity. Single neurons in both areas could be assigned to five classes according to the spatial response patterns: few non-uniform RFs with multiple discrete response maxima could be dissociated from the vast majority of uniform RFs showing a single maximum; the latter were further classified into full-field, and confined foveal, contralateral and ipsilateral RFs. Neurons in dlPFC showed a preference for the contralateral visual space and collectively encoded the contralateral visual hemi-field. In contrast, VIP neurons preferred central locations, predominantly covering the foveal visual space. Putative pyramidal cells with broad spiking waveforms in PFC had smaller RFs than putative interneurons showing narrow spiking waveforms, but distributed similarly across the visual field. In VIP, however, both putative pyramidal cells and interneurons had similar RFs at similar eccentricities. We provide a first, thorough characterisation of visual RFs in two reciprocally connected areas of a fronto-parietal cortical network.

INTRODUCTION

The region of sensory space within which a stimulus can modulate a neuron's response circumscribes the receptive field (RF) of that neuron (Hubel & Wiesel, 1962). For neurons in primary sensory areas, this region is described quite simply by the sensory receptors that relay information to it. Higher association areas that receive information from lower areas are able to integrate information across various stimulus components and can, thus, display a range of complexity in their RFs (Blatt *et al*., 1990; Avillac *et al*., 2005). However, neurons in higher association cortices, such as areas in the dorsolateral prefrontal cortex (dlPFC) and in the posterior parietal cortex (PPC), are not often characterised by their receptive field structure as they are in primary sensory cortices (Alonso, 2002; Solomon *et al*., 2002; Swadlow & Gusev, 2002; Yoshor *et al*., 2007; Veit *et al*., 2014). Most studies map either

This article is protected by copyright. All rights reserved.

dlPFC or PPC RFs coarsely and in isolation from one another to aid presentation of stimuli that require active discrimination or subsequent comparison.

Ventral intraparietal area (VIP) of the PPC is located in the fundus of the intraparietal sulcus (IPS) (Colby *et al*., 1993). It receives visual information primarily from the middle temporal (MT) area and dense multi-modal input from its surrounding areas (Lewis & Van Essen, 2000). Consequently, VIP neurons respond to visual, auditory, tactile and vestibular information (Bremmer *et al*., 2002; Avillac *et al*., 2005; Schlack *et al*., 2005). Single neurons in VIP have a sophisticated multi-modal representation of objects in space using different reference frames (Avillac *et al*., 2007; Zhang & Britten, 2011). During steady fixation, these reference frames converge allowing for different sensory modalities to be represented in a single frame. During movement, these reference frames are sometimes found to shift from eye-centred (Chen *et al*., 2014) to head-centred representations (Duhamel *et al*., 1997), possibly enabling spatial transformations during movement (Bremmer, 2011).

Neurons in the dlPFC exhibit visual RFs (Mikami *et al*., 1982; Suzuki & Azuma, 1983) and also show multi-sensory responses (Suzuki, 1985; Romo *et al*., 1999; Sugihara *et al*., 2006; Nieder, 2012; Wang *et al*., 2015). Even the hallmark feature of prefrontal neurons: working memory (Fuster & Alexander, 1971; Fuster & Bauer, 1974), has a spatial component. Neurons have been described as having "memory fields" (Funahashi & Bruce, 1989) which circumscribe the area of increased delay period activity of a certain neuron to a preferred object when it is presented in a specific part of the visual field (Rainer *et al*., 1998a). Thus, while retaining the representation of an object, they additionally retain its location.

This article is protected by copyright. All rights reserved.

Accepted Article

Accepted Article

Examining RFs in both PFC and PPC together is motivated by the finding that areas of the PPC and dlPFC are anatomically and functionally connected (Schwartz & Goldman-Rakic, 1984; Pandya & Yeterian, 1991; Lewis & Van Essen, 2000). For example, temporary inactivation of one region changes the response properties of neurons in the other (Quintana & Fuster, 1999; Chafee & Goldman-Rakic, 2000). This suggests a close functional interdependence between the two regions that form association networks. In order to learn about their respective contributions, neurons in the dlPFC and intraparietal sulcus (IPS) have been studied together as part of a fronto-parietal network (Buschman & Miller, 2007; Swaminathan & Freedman, 2012; Crowe *et al*., 2013). The fronto-parietal network involving the dlPFC and the ventral intraparietal area (VIP) and is specifically implicated in the magnitude system in primates (Nieder & Miller, 2004; Tudusciuc & Nieder, 2009; Vallentin *et al*., 2012; Viswanathan & Nieder, 2013, 2015; Nieder, 2016). However, surprisingly little is known about the RFs in these areas, how they compare to the visual cortex, and how they compare with each other. We have recently found that the spatiotopic organisation of early visual cortices is no longer retained in these higher association areas (Viswanathan & Nieder, 2017), thus, motivating the question whether the RFs in these association areas display much non-uniformity.

Here, we investigate the spatial selectivity of neurons in the dlPFC and VIP with a moving bar stimulus shown at different locations on the screen while the monkeys passively fixate a central fixation spot. We found that a large number of neurons selectively responded to the object at various positions of the screen and we created receptive field maps for these neurons. We characterise the different types of receptive fields in the respective brain areas based on their structure, location and size and the different the types of neurons based on their extracellular

This article is protected by copyright. All rights reserved.

waveforms. These results provide the first and largest detailed characterisation of PFC receptive fields, in direct comparison with VIP receptive fields acquired simultaneously.

Accepted Article

MATERIALS AND METHODS

Subjects and experimental setup

Two male rhesus monkeys (*Macaca mulatta*) weighing between 5.5 and 6.3 kg were used for this experiment. All experimental procedures were in accordance with the guidelines for animal experimentation approved by the national authority, the Regierungspräsidium Tübingen, Germany. The monkeys were socially housed, in groups of 2 to 4. During experiments, the monkeys sat in primate chairs within experimental chambers and received fluid rewards. The monkeys were positioned 57 cm from a 15″ flat screen monitor with a resolution of 1024 by 768 pixels and a refresh rate of 75 Hz. We used the NIMH Cortex program to present the stimuli, monitor the behaviour and collect behavioural data. Cortex communicated with an infrared tracking system (ISCAN, Cambridge, MA) to monitor the monkeys' eyes and collect eye-tracking data. All data analysis was performed using custom-written scripts in the MATLAB computational environment (Mathworks).

Surgery and electrophysiological recordings

First, the monkeys were implanted with a head bolt to allow monitoring of eye movements during the task. After training on the behavioural tasks, we implanted recording chambers over the right dorsolateral prefrontal cortex, centred on the principal sulcus, and the right intraparietal sulcus guided by anatomical MRI and stereotaxic measurements (**Fig. 1A** and **Fig. 3**). The surgical procedures were performed under sterile conditions. Anaesthesia was induced by ketamine hydrochloride (10 mg/kg) and xylazine (5 mg/kg). For maintenance of

This article is protected by copyright. All rights reserved.

anaesthesia, we used nitrous oxide and isoflurane, monitoring the levels and vital signs during the procedure. The monkeys received post-surgical analgesics and antibiotics. The recording chambers were sealed with sterile caps and cleaned regularly with antiseptic washes.

For the recordings, we used arrays of eight glass-coated tungsten microelectrodes (Alpha Omega Ltd., Israel) attached to screw micro-drives in a grid with 1 mm spacing. For PFC recordings, we recorded from neurons as soon as we entered cortex (**Fig. 3A** and **B**). For VIP recordings, we lowered the electrodes to depths of 9 to 14 mm from the cortical surface (**Fig. 3C** and **D**). The electrophysiological signals were amplified, filtered and waveforms of the actions potentials sampled at 40 kHz from each electrode were stored (Plexon Systems, USA). Single units were sorted offline based on waveform characteristics (Offline Sorter, Plexon Systems). In all, we recorded 1186 PFC neurons and 944 VIP neurons.

Behavioural task

During the receptive field measurements, the monkeys performed a passive fixation task. They were rewarded for maintaining fixation on a central white square (0.10° x 0.10° of visual angle or dva) while a grey moving bar (3° x 0.20°) appeared on the screen at five successive positions on the screen (**Fig. 1B**) in each trial. The positions were selected pseudo randomly from a 10 (horizontal) x 8 (vertical) grid of positions. The moving bar covered each position for 1000 ms divided between 2 orientations and 2 directions of movement. First, the bar was oriented vertically moving left to right (0° for 250 ms), right to left (180° for 250 ms), then oriented horizontally moving up (90° for 250 ms), moving down (270° for 250 ms). The bar moved at a constant speed of 8° per second and covered a distance of 2° per sweep. The grid of locations thus covered the entire screen i.e. 30.5° x 23° of central vision. The monkeys were rewarded for successfully fixating the whole trial. Receptive field

This article is protected by copyright. All rights reserved.

Accepted Article

measurement blocks were interleaved with delayed match-to-sample task blocks (Viswanathan & Nieder, 2013, 2015). Each recording session could yield up to 4 RF mapping blocks.

Spatial selectivity

Of the neurons we recorded, many of them responded to the spatial position of the moving bar even as the monkeys fixated the central fixation spot. To ascertain their receptive fields, we first tested the neurons for spatially-selective responses. We analysed the responses of all the neurons in the 1000 ms period that each position was tested. To account for well-known differences in response latencies in these two areas (Nieder & Miller, 2004; Viswanathan & Nieder, 2013), we delayed the onset of the analysis window for VIP neurons by 50 ms and for PFC neurons by 100 ms. We calculated a 3-way ANOVA on firing rates calculated in a 250 ms period corresponding to the duration of a single bar sweep, with position, movement direction and orientation of the bar as factors (Rainer *et al*., 1998a; Romero & Janssen, 2016). The movement direction was applied as a nested variable of orientation. We down-sampled the screen into 5 zones (top left, top right, bottom left, bottom right and centre) to limit the levels of the variable position to 5, comparable to 4 directions and 2 orientations. We tested every neuron with a minimum of 2 trials per location (859 PFC neurons and 693 VIP neurons) and evaluated the ANOVA results with an alpha of 0.05.

We created raw RF maps for every neuron with $P < 0.05$ by averaging the responses for each position over the 1000 ms period. To view responses at a higher resolution, we linearly interpolated the raw RF maps by 3-fold in both spatial dimensions, and smoothed them with a 2D Gaussian kernel of 2 dva. We conducted a further cross-validation using these maps to confirm robust spatial selectivity. We created two separate RF maps for each neuron; one from the first half of RF trials and another from the second half of trials. We calculated a 2D

This article is protected by copyright. All rights reserved.

Accepted Article

cross-correlation between the two maps created for each neuron and compared this against a distribution of 2D cross-correlations calculated from 1000 shuffles of each half map.

$$r = \frac{\sum_h \sum_v (Half1 - \overline{Half1})(Half2 - \overline{Half2})}{\sqrt{(\sum_h \sum_v (Half1 - \overline{Half1})^2)(\sum_h \sum_v (Half2 - \overline{Half2})^2)}}$$

where *Half1* is the map created from the first half of trials and *Half2* is the map created from the second half of trials. The means of the maps are subtracted before summing them over the horizontal, *h* and vertical, *v* dimensions. Only if the true correlation across halves of trials lay above the 95th percentile of the distribution of surrogate correlations (one-tailed, $P < 0.05$), we accepted the neuron and its RF map into further analysis.

Strength of spatial selectivity

Using these spatially selective neurons, we created average maps for each area. We also created normalised maps for each neuron by dividing the RF map by the maximum of each map. We then averaged the normalised maps of all PFC neurons and all VIP neurons (Rainer *et al*., 1998a) to quantify the strength of spatial modulation in each area.

We calculated an omega-squared (ϖ^2) value for each neuron. This estimates how much of the variance in the trial-by-trial firing rates could be explained by the position of the bar stimuli on the screen. It is derived from a one-way ANOVA with the factor position over the entire 1000 ms of stimulation at each position.

A selectivity index (SI) helped to compare the response of each neuron within its RF and outside its RF and was calculated using:

$$SI = (FRmax\text{-}FRmin)/(FRmax + FRmin)$$

where *FRmax* is the maximum firing rate of the neuron and *FRmin* is the minimum firing rate of the neuron. The SI can have values between 0 and 1. Values close to 1 indicate high spatial selectivity and very low responses to areas outside the RF.

This article is protected by copyright. All rights reserved.

Accepted Article

Accepted Article

Characterisation of receptive fields

We found 5 possible classes of receptive fields which could be separated based on the uniformity, size and location of responses. To separate them in an unbiased manner, we normalised each map to the maximum across positions for that neuron. Some neurons showed multiple local maxima of more than 9° and we characterised these as non-uniform (threshold = 98% of maximum). For the remaining neurons, the receptive field could simply be described as the contiguous area that activated the neuron to more than half of its maximal response (Rainer *et al*., 1998a; Romero & Janssen, 2016). However, a subset of these neurons had receptive fields that spanned more than 75% of the screen showing very small local minima. We considered these neurons to be full-field neurons. We classified the remaining neurons with confined fields according to where their maxima lay on the horizontal axis of the visual field, contralateral visual field, foveal or ipsilateral visual field. We confirmed that classifying them according to the centre of mass i.e. the geometric centre weighted by the activity, yielded quantitatively similar results as classifying them using the location of the maxima.

To reliably calculate RF eccentricities, we limited our analysis to neurons whose receptive fields were uniform, but not full-field. We calculated the Euclidian distance of the RF maxima from the central fixation point as the RF eccentricity. Calculating the Euclidian distance between the centre of mass of the RF and the fixation point yielded similar results. Our calculation of RF sizes further took into account that not all RFs were within the screen. Some neurons seemed to have RFs that began at the edges of the screen and possibly extended to visual space outside it. So, we limited our calculation of RF sizes to neurons with screen-limited RFs. We did not fit a shape to the receptive field to allow for complex, non-Gaussian shapes as can be expected from such associative areas. The RF of the neuron was

This article is protected by copyright. All rights reserved.

the area of the map that displayed activity > 0.5 of maximal response. The RF size was thus the square root of the total degrees of visual angle it spanned.

We use the Kolmogorov-Smirnov test to compare the distributions of RF eccentricity and size. We use the non-parametric Mann-Whitney U test to compare the central tendencies (the medians) of RF eccentricity and size across areas and judged the results with an alpha of 0.5. All tests, unless specified, are two-tailed.

Receptive fields of neuronal classes

We classified the recorded single units into putatively interneuron (narrow-spiking, NS) and pyramidal (broad-spiking, BS) neuronal classes based on their extracellular waveforms (Diester & Nieder, 2008; Viswanathan & Nieder, 2015). We saved the template waveforms for each single unit but only classified those that had a classic downward deflection upon reaching threshold followed by an upward peak (1951/2130 neurons). The troughs occurred between 200 to 400 μs and the crests only after 300 μs. We normalised the waveforms to the difference between the maximum amplitude and the minimum amplitude and aligned them to their troughs. We then entered the waveforms through a linear classifier (k-means*;* $k = 2$, squared Euclidian distance) to cluster the cells into two categories: narrow-spiking (NS) and broad-spiking (BS) such that on average, the units with smaller widths constituted the narrow-spiking cluster (537 neurons) and those with the larger widths constituted the broad-spiking cluster (1414 neurons) (**Fig. 8A** and **B**).

This article is protected by copyright. All rights reserved.

Accepted Article

Accepted Article

RESULTS

Single neurons in PFC and VIP exhibit visual RFs

We simultaneously recorded single-cell activity in the dorsolateral prefrontal cortex (dlPFC) around the principal sulcus (PS) and in the ventral intraparietal area (VIP) in depths of the intraparietal sulcus (IPS). The recordings were made in the right hemisphere of two monkeys performing a simple passive fixation task (**Fig. 1A**). While the monkeys fixated a central fixation target, a moving bar was presented at various locations of the screen (**Fig. 1B**). In response to this simple stimulus, many dlPFC and VIP neurons fired action potentials when the stimulus was at certain positions in the visual field. We collected firing rates for each of the 80 positions investigated over multiple trials (**Fig. 1C** and **F**). Activity was then averaged across trials (**Fig. 1D** and **G)** to create receptive field (RF) maps (**Fig. 1E** and **H**) for every spatially-selective neuron. **Figure 1C-E** displays a dlPFC neuron with selective increases in firing rates whenever the bar was presented to the left of the fixation target, i.e. this neuron had a large RF in the contralateral visual hemi-field because all recordings were made from the right hemisphere. In contrast, a representative VIP neuron (**Fig. 1F-H**) only responded to bars in a very confined visual region about 5 deg below and 2 deg right from the fixation target, or visual fovea, respectively. This resulted in a small and strongly spatially selective RF in this VIP neuron.

We statistically tested neuronal selectivity to the moving bar by calculating a 3-way ANOVA with “position”, “movement direction” and “orientation” as main factors. The highest proportion of neurons was selective to bar position than the other main factors ($P < 0.05$). In the dlPFC, 64% (545/859) of the neurons showed a stimulus position effect. In VIP, 69% (480/693) of all neurons were spatially-tuned. Neurons in both areas were also tuned to the movement direction and orientation of the bar. In dlPFC, 39% (332/859) and 44% (374/859)

This article is protected by copyright. All rights reserved.

Accepted Article

neurons were selective for direction and orientation, respectively. In VIP, 46% (317/693) and 44% (307/693) of neurons were selectively tuned to the direction and orientation. We cross-validated the RFs of spatially-tuned neurons to ensure that their responses were robust and stable in time (Viswanathan & Nieder, 2017). To that aim, we created two separate RF maps for every neuron from half the trials each and calculated the 2D correlation coefficient between them. We compared the neuron's true correlation coefficient against a distribution of coefficients obtained from correlating shuffled surrogates (one-tailed, $P < 0.05$). Half of the dlPFC neurons (50%, 425/859) passed both the ANOVA test and the 2D correlation-criterion and henceforth constituted the population of dlPFC neurons with a visual RFs (**Fig. 2A**). The same criterion applied to the VIP resulted in 57% (396/693) of VIP neurons showing a robust visual RF (**Fig. 2B**). Only these neurons and their RFs were used in further analyses. The proportion of neurons showing visual RFs was higher in VIP compared to dlPFC ($\chi^2 = 9.05$, $P = 0.003$).

To find out whether the population of neurons in PFC and VIP cover the visual field evenly or rather show spatial preferences, we examined the distribution of the RFs across the visual fields. We found that most PFC neurons had their RF maxima in the visual hemi-field contralateral to the recorded hemisphere, i.e. covered predominantly the left visual hemi-field for recording sites in the right hemisphere. (**Fig. 2C**). The largest number of neurons (n = 132) in PFC had their RFs between -10˚ and -17˚ on the horizontal axis. In VIP, on the other hand, most neurons had their RFs clustered around the fovea with a bias towards the contralateral hemi-field (**Fig. 2D**). The neurons (n = 154) were maximally clustered between -3˚ and -10˚ on the horizontal axis.

We reconstructed the recording sites and examined the topographic layout of RFs (**Fig. 3**). In PFC, our recordings sites mostly spanned the dorsal and ventral parts of the prearcuate gyrus

This article is protected by copyright. All rights reserved.

Accepted Article

in both monkeys (**Fig. 3A** and **B**). We normalised each RF map to its maximum and averaged all such maps obtained at each recording site. We did not observe a topographic difference in the kinds of RFs. In the VIP, our recordings were in the depth of the intraparietal sulcus, starting at 9mm from the cortical surface and exploring up to 14mm into the banks of the IPS in both monkeys (**Fig. 3C** and **D**). The averaged maps at each site again show no topographic organisation.

In order to visualize how the entire population of neurons in the respective brain areas would encode the visual space as a whole, we created average RF maps. First, we constructed such maps by averaging the absolute firing rates of individual neurons, which emphasized the contribution of the neurons with strong spatial firing rate modulation. The population of dlPFC neurons responded more strongly to the contralateral visual hemisphere with an emphasis on the lower quadrant (**Fig. 4A**). In contrast, VIP neurons displayed strongest responses around the central fixation area with a bias towards the contralateral hemi-field (**Fig. 4B**).

The average RF maps might be dominated by neurons with particularly high firing rates. In fact, VIP neurons displayed on average higher firing rates than dlPFC neurons ($mean_{PFC}$ = 5.1Hz, $mean_{VIP}$ = 6.8Hz; Mann-Whitney U test, Z = -2.8, P = 0.005). To weigh the contribution of individual neurons equally and irrespectively of their absolute firing rates, we constructed normalized average RF maps for dlPFC and VIP by normalizing the response of each neuron relative to its maximum activity. After normalization, the population RF map in VIP still shows a predominantly foveal focus with a bias towards the contralateral hemi-field (**Fig. 4D**). In the PFC, however, the representation of visual space (based on spatial activity modulation) became much more evenly distributed across the entire visual field, with a mild over-representation of the contralateral hemi-field (**Fig. 4C**). We quantified the

This article is protected by copyright. All rights reserved.

Accepted Article

strength of spatial modulation in the population of selective neurons by calculating the ϖ^2 value. The measure describes how much of the variance in the firing rate of a neuron was explained by the explanatory variable, stimulus location. On average, 9% of the variance in PFC neuronal activity was explained by the spatial position while as much as 11% of the variance in VIP neuronal activity was explained by bar location. This difference in ϖ^2 was highly significant (Mann-Whitney U test, $Z = -4.2$, $P < 0.0001$). A comparison of modulation of firing rates by the RF showed that VIP neurons had slightly higher selectivity indices than PFC neurons ($median_{PFC} = 0.889$, $median_{VIP} = 0.894$; Mann-Whitney U test, $Z = -2.16$, $P = 0.03$).

Classes of receptive fields

The detailed RF maps we created helped to characterise the selective responses of the neurons and examine the structures of RFs. The RFs could be assigned to five classes (Romero & Janssen, 2016) in both dlPFC and VIP (**Fig. 5**). We found 44 dlPFC and 38 VIP neurons that had multiple discrete maxima and classified them as non-uniform RFs (**Fig. 5A** and **B**). The rest of the neurons could be described as uniform RFs. However, a small proportion of neurons, 23 PFC neurons and 34 VIP neurons, respectively, showed full-field activity with the RF covering more than 75 % of the visual field on the screen (**Fig. 5C** and **D**). The frequencies of these classes of RFs were indistinguishable between areas ($\chi^2 = 2.39$, $P = 0.12$). The rest of the neurons had uniform, confined receptive fields located either in the contralateral (i.e. left) visual field (**Fig. 5E and F**), foveally (central) (**Fig. 5G and H**) or in the ipsilateral (i.e. right) visual field (**Fig. 5I and J**). The frequency counts of the various types of RFs are shown in **Figures 6A** and **B** for areas dlPFC and VIP, respectively. Note that dlPFC exhibited a much higher frequency of contralateral RFs than VIP ($\chi^2 = 17.22$, $P < 0.0001$) In contrast, VIP contained a higher number of neurons with foveal RFs (χ^2

This article is protected by copyright. All rights reserved.

= 21.17, $P < 0.0001$). The frequency of ipsilateral RFs between the two areas, however, were indistinguishable ($\chi^2 = 0.92$, $P = 0.34$).

Receptive field eccentricity and size

A characteristic aspect of receptive fields is their eccentricity from the fovea, measured as the Euclidean distance between the RF maxima and the centre. When we estimated this for the neurons with uniform, confined RFs, we found uniformly-distributed RF-eccentricities covering the entire monitor space between 0.1° and 18° (**Fig. 7A** and **B**). With a median RF-eccentricity of 12°, neurons in dlPFC exhibited more eccentric RFs than VIP neurons with a median of 9.6° (Mann-Whitney U test, $Z = 3.49$, $P < 0.001$).

We measured the receptive field sizes of the neurons whose RFs were confined. Non-uniform or uniform full-field RFs were therefore excluded. Further, 80% (286/358) PFC neurons and 74% (241/324) VIP neurons had RFs that were confined but extended beyond the borders of our measurement. We excluded such neurons to limit our calculation of RF sizes to neurons whose fields were limited to the screen. The RF size of such screen-limited neurons was the square root of the area with half-max activity. For both dlPFC and VIP, this yielded RF sizes between 3.7° and 13.8° (**Fig. 7C** and **D**). The distributions of RF sizes, however, were significantly different in the two areas (Kolmogorov-Smirnov test for unequal cdfs = 0.29, $P = 0.003$), with larger RF sizes in VIP than those in dlPFC (medianPFC = 6.3°, medianVIP = 7.5°; two-sided Mann-Whitney test, $Z = -3.18$, $P = 0.002$).

Receptive fields properties by neuron types

As different neuronal subtypes might well exhibit characteristically different receptive fields, we sorted the recorded neurons into putatively pyramidal (broad-spiking, BS) and

This article is protected by copyright. All rights reserved.

Accepted Article

interneuron (narrow-spiking, NS) classes based on their waveform widths (**Fig. 8A** and **B**) (Swadlow & Weyand, 1987; Constantinidis & Goldman-Rakic, 2002; Diester & Nieder, 2008; Viswanathan & Nieder, 2015, 2017).

In terms of RF eccentricity, both BS neurons and NS neurons in dlPFC displayed similar eccentricities (**Fig. 8C**). Median BS neurons had fields located 11.9° from the centre and median NS neurons at 12.4° (Mann-Whitney U test, $Z = 0.58$, $P = 0.56$). This was also the case for VIP eccentricities (**Fig. 8D**). BS neurons had a median eccentricity of 11.2° and NS neurons, 9.1° (Mann-Whitney U test, $Z = 0.86$, $P = 0.39$).

When comparing sizes of screen-limited RFs within dlPFC, we found that BS neurons displayed smaller RFs than NS neurons (**Fig. 8E**). BS neurons had receptive fields of a median 6.1° and NS neurons, 8.7° (Mann-Whitney U test, $Z = -2.33$, $P = 0.02$). In VIP, however, we found no significant differences between the two neuronal classes in field size (**Fig. 8F**) Both BS neurons and NS neurons had a median RF size between 7.2° and 8.3° (Mann-Whitney U test, $Z = -1.81$, $P = 0.07$).

DISCUSSION

While monkeys fixated passively, we found that more than half of the recorded dlPFC and VIP neurons responded selectively to a moving bar presented at various locations of the screen. VIP neurons displayed larger RFs that were more foveally located than PFC receptive fields, which were more contralateral. Additionally, VIP neurons were more strongly modulated by position than PFC neurons. Finally, putative inhibitory neurons in PFC displayed larger RFs than excitatory neurons but across the same eccentricities while no such difference was seen across VIP neuronal classes.

This article is protected by copyright. All rights reserved.

Accepted Article

Accepted Article

Visual RFs in dlPFC and VIP during passive fixation

Our study represents the most detailed characterisation of receptive fields in dorsolateral prefrontal cortex (dlPFC) and VIP, not only in the number of neurons sampled, but also in the resolution of mapping, i.e., 80 positions across 30.5° (horizontal) x 23° (vertical) of the visual field. As a result, a majority of cells in dlPFC and VIP could be activated to construct high resolution spatial RF maps. Bar stimuli with a higher range of sizes, speeds and directions (Schaafsma & Duysens, 1996; Bremmer *et al*., 2002; Gabel *et al*., 2002) might have activated even more neurons. Moreover, probabilistic mapping has been proposed as an efficient method to assess the spatio-temporal structures of frontal eye field (FEF) receptive fields (Mayo *et al*., 2015, 2016).

One of the prime problems in RF mappings therefore, is that of the optimal stimulus to be used. This is a relatively simple issue for early visual areas, but a graver problem higher up the processing hierarchy. After all, neurons in the association cortices process higher-order information pertinent to all sorts of cognitive processing. The dlPFC, in particular, is a high-level area that is operating at the apex of the cortical hierarchy and is renowned for encoding highly cognitive parameters, such as perceptual categories (Freedman & Assad, 2016), numerical quantities (Nieder *et al*., 2002; Nieder, 2012; Viswanathan & Nieder, 2013; Ramirez-Cardenas *et al*., 2016), rules (Bongard & Nieder, 2010; Eiselt & Nieder, 2013; Ott *et al*., 2014), reward contingencies (Kennerley & Wallis, 2009; Asaad & Eskandar, 2011), and other behavioural principles. But also VIP neurons operating slightly more upstream of the cortical hierarchy are well known to represent almost equally abstract concepts (Tudusciuc & Nieder, 2009; Nieder, 2012; Jacob & Nieder, 2014). Since both VIP and dlPFC require sensory input, tuning to simple stimuli must emerge due to visual input from upstream visual areas where neurons respond to basic features. Despite the anatomical and functional distance

This article is protected by copyright. All rights reserved.

of VIP and dlPFC from the early visual areas, it is surprising to find confined visual responses to basic visual parameters in these association cortices. As visual RFs in the association cortices are indicative of default anatomical wiring, this default wiring might be useful for multi-modal integration and the mapping of different reference frames onto a circuit.

In the case of dlPFC, early studies reported confined visual responses (Mikami *et al*., 1982; Suzuki & Azuma, 1983). Neurons around the principal sulcus were responsive to a moving slit/dot presented foveally or para-foveally. The visual receptive fields in dlPFC thus recorded, were found to be largely contralateral and in strong agreement with our data though less was reported about their spatial structure than the latency of their responses. Neurons rostral to the inferior arcuate sulcus were said to have small, foveal RFs and those in the anterior and posterior parts of the prearcuate area had large RFs at greater eccentricities (Suzuki & Azuma, 1983; Riley *et al*., 2016). We did not find such a reliable layout of dlPFC RFs based on our small number of recording sites.

Much more is known about the receptive fields in VIP, which is part of the cluster of IPS areas that constitute the termination zone of the dorsal, parietal visual stream (Mishkin *et al*., 1983). For instance, RFs of many VIP neurons are not only visual, but multi-modal (Bremmer *et al*., 2002; Schlack *et al*., 2005), and show shifts according to different frames of reference (Chen *et al*., 2011, 2014). Still, the size and eccentricity of these fields within a retinotopic frame were unknown. These features of the receptive field are important as clues to function. For instance, lateral intraparietal area (LIP) receptive fields, on average, fall a bit eccentric from the fovea at about 5° (Janssen *et al*., 2008) while posterior anterior intraparietal area (pAIP) receptive fields are frequently foveal (Romero & Janssen, 2016). It

This article is protected by copyright. All rights reserved.

Accepted Article

has been proposed that this difference reflects the role of LIP in saccade movements and of pAIP in grasping as objects are often foveated before successful grasping (Blatt *et al*., 1990; Ben Hamed *et al*., 2001). VIP receptive fields in our study are much more reminiscent of AIP RFs than those of LIP in their spans and possibly reflect the role of VIP in multi-sensory integration and transformations (Bremmer *et al*., 2002; Schlack *et al*., 2005; Zhang & Britten, 2011).

From passive to active vision

The dlPFC and VIP are part of the frontal and parietal association cortices, respectively. As such, they show non-canonical circuit properties characteristic of the association cortices (Goldman-Rakic, 1988). Non-canonical circuits enable parallel and re-entrant processing required for persistent activity shown by PFC and PPC neurons during temporal delays in cognitive task. Because of this functionality, neurons in the association cortices are expected to be released from the rigid topographic layout found in early sensory areas (Galletti *et al*., 1999). Indeed, we have recently demonstrated that neurons in dlPFC and VIP show progressively lower spatiotopy than has been reported for neurons in early visual cortices (Viswanathan & Nieder, 2017), dlPFC much less than VIP. Pairs of neurons recorded at the same electrode tip often had dissimilar or inverted RFs, contrary to the more than 80% spatial similarity seen in neighbouring RFs in early visual cortices (Das & Gilbert, 1997; DeAngelis *et al*., 1999).

Unlike neurons in early visual areas that have to provide a veridical representation of the outside world, neurons in the association cortices are more related to the internal state of an animal. Therefore, spatial visual representations may become modulated or changed by cognitive factors, such as spatial attention or the grouping of objects into behaviourally

This article is protected by copyright. All rights reserved.

Accepted Article

meaningful categories. Indeed, they have been found to shift sometimes dramatically with behavioural relevance in active tasks (Freedman & Assad, 2006; Viswanathan & Nieder, 2015). When active tasks involve the discrimination of spatial features, PFC neurons encode the location of an object along with its identity during a matching task (Funahashi & Bruce, 1989; Rainer *et al*., 1998a), or differentially encode the location of an object based on the ongoing task (Asaad *et al*., 2000). PFC neurons also shift the response field with attention and filter out spatial locations that are unattended (Everling *et al*., 2002) or non-target (Rainer *et al*., 1998b). We know that even working memory activity in PFC is shaped by the identity of the object as by the location of the object (Rainer *et al*., 1998a; Kennerley & Wallis, 2009)

Areas in the parietal cortex have been mapped in tasks involving saccades (Dunn & Colby, 2010) in order to ensure strong neuronal responses at the visual location being tested (Colby *et al*., 1996). VIP neurons also exhibit strong modulation by attentional signals (Cook & Maunsell, 2002). It may therefore be expected that visual RFs in the association cortex shift and change with cognitive demands (Ben Hamed *et al*., 2002; Womelsdorf *et al*., 2008). Further research would be required to show the potential flexibility of these maps during active spatial discrimination, or whether the receptive field structures and locations play a role when the animals are involved in a non-spatial task (Freedman & Assad, 2009; Ibos & Freedman, 2016). An ongoing task might recruit spatially selective neurons in non-spatial events. Since we find VIP neurons to be more strongly modulated by space than PFC neurons, we predict that VIP neurons would be weakly recruited when stimuli are presented outside of their RFs, whereas PFC neurons would be more independent from their passive, default RFs.

This article is protected by copyright. All rights reserved.

Accepted Article

Accepted Article

Pyramidal neurons and interneurons

Pyramidal neurons and interneurons, the two major cell classes in the neocortex, sculpt neuronal response properties in different contexts. We have observed that putative pyramidal neurons in PFC showed increased modulation by the behaviourally relevant numerosity stimuli than interneurons (Viswanathan & Nieder, 2015). Several other studies suggest differential participation of prefrontal pyramidal neurons and interneurons in behavioural relevance (Hussar & Pasternak, 2009), in working memory (Hussar & Pasternak, 2012) and in learned numerosity representations (Diester & Nieder, 2008). Putative pyramidal neurons exhibit sharper tuning and stable representations of features while interneurons facilitate flexibility by responding strongly to changes in context or task demands. These differences, together with the observed difference in RF sizes indicate that these neuronal classes are set up for differential recruitment by their circuitry. Our finding of larger RFs in PFC interneurons might enable them to participate more flexibly in active tasks whereas smaller RFs in pyramidal neurons allow them to sharply distinguish stimulus features. This is supported by the finding that putative pyramidal neurons in area LIP were selective to fine features of the stimuli whereas interneurons responded strongly to target stimuli and were not as selective for the finer stimulus features (Yokoi & Komatsu, 2010). Differential targeting by different interneuron subtypes shaped persistent activity in PFC pyramidal neurons and lends weight to the idea of distributed roles in spatial tuning (Wang *et al*., 2004). Spatial tuning in dlPFC is significantly impaired with iontophoretic disinhibition (Rao *et al*., 2000). PFC interneurons, while similarly tuned (to similar eccentricities) as pyramidal neurons during sensory and delay phases shifted their tuning in response phases to opposite directions, exhibiting greater flexibility than pyramidal neurons (Rao *et al*., 1999). VIP neurons, whose RFs do not show a difference in sizes or eccentricities for the two neuronal classes, might share their task loads more equitably.

This article is protected by copyright. All rights reserved.

Accepted Article

Understanding how different neuronal classes participate in such circuitry and how they represent visual space are important steps in understanding how our visual space might be represented in cortical circuits. Together with our recent results about the non-canonical arrangement about RFs in association cortices, we suggest that RFs of sensory neurons may play very different roles according to where in the processing streams they lie.

ACKNOWLEDGMENTS:

This work was supported by DFG grant NI 618/2-1 to A.N.

The authors declare no competing financial interests.

LIST OF ABBREVIATIONS:

ANOVA – Analysis of variance
AIP – Anterior intraparietal area; pAIP – posterior Anterior Intraparietal area
BS – Broad-spiking neurons
cdf – Cumulative distribution function
FEF – Frontal eye field
IPS – Intraparietal sulcus
LIP – Lateral intraparietal area
LS – Lateral sulcus
MRI – Magnetic Resonance Imaging
MT – Middle Temporal area
NS – Narrow-spiking neurons
PFC – Prefrontal cortex; dlPFC – dorsolateral prefrontal cortex
PPC – Posterior parietal cortex
PS – Principal sulcus
RF – Receptive field
STS – Superior temporal sulcus
VIP – Ventral intraparietal area
ϖ^2 – omega-squared (measure of effect size)

This article is protected by copyright. All rights reserved.

Accepted Article

AUTHOR CONTRIBUTIONS:

P.V. and A.N. designed research; P.V. performed research; P.V. and A.N. wrote the paper.

DATA ACCESSIBILITY:

All primary data generated in this study will be available upon request.

REFERENCES:

Alonso, J.-M. (2002) Neural connections and receptive field properties in the primary visual cortex. *Neuroscientist*, **8**, 443–456.

Asaad, W.F. & Eskandar, E.N. (2011) Encoding of both positive and negative reward prediction errors by neurons of the primate lateral prefrontal cortex and caudate nucleus. *J. Neurosci.*, **31**, 17772–17787.

Asaad, W.F., Rainer, G., & Miller, E.K. (2000) Task-specific neural activity in the primate prefrontal cortex. *J. Neurophysiol.*, **84**, 451–459.

Avillac, M., Ben Hamed, S., & Duhamel, J.-R. (2007) Multisensory Integration in the Ventral Intraparietal Area of the Macaque Monkey. *J. Neurosci.*, **27**, 1922–1932.

Avillac, M., Denève, S., Olivier, E., Pouget, A., & Duhamel, J.-R. (2005) Reference frames for representing visual and tactile locations in parietal cortex. *Nat. Neurosci.*, **8**, 941–949.

Ben Hamed, S., Duhamel, J.-R., Bremmer, F., & Graf, W. (2002) Visual receptive field modulation in the lateral intraparietal area during attentive fixation and free gaze. *Cereb. Cortex*, **12**, 234–245.

Ben Hamed, S., Duhamel, J.R., Bremmer, F., & Graf, W. (2001) Representation of the visual field in the lateral intraparietal area of macaque monkeys: a quantitative receptive field analysis. *Exp. brain Res.*, **140**, 127–144.

Blatt, G.J., Andersen, R.A., & Stoner, G.R. (1990) Visual receptive field organization and cortico-cortical connections of the lateral intraparietal area (area LIP) in the macaque. *J. Comp. Neurol.*, **299**, 421–445.

This article is protected by copyright. All rights reserved.

Accepted Article

Bongard, S. & Nieder, A. (2010) Basic mathematical rules are encoded by primate prefrontal cortex neurons. *Proc. Natl. Acad. Sci. U. S. A.*, **107**, 2277–2282.

Bremmer, F. (2011) Multisensory space: from eye-movements to self-motion. *J. Physiol.*, **589**, 815–823.

Bremmer, F., Klam, F., Duhamel, J.-R., Ben Hamed, S., & Graf, W. (2002) Visual-vestibular interactive responses in the macaque ventral intraparietal area (VIP). *Eur. J. Neurosci.*, **16**, 1569–1586.

Buschman, T.J. & Miller, E.K. (2007) Top-down versus bottom-up control of attention in the prefrontal and posterior parietal cortices. *Science*, **315**, 1860–1862.

Chafee, M. V & Goldman-Rakic, P.S. (2000) Inactivation of parietal and prefrontal cortex reveals interdependence of neural activity during memory-guided saccades. *J. Neurophysiol.*, **83**, 1550–1566.

Chen, A., DeAngelis, G.C., & Angelaki, D.E. (2011) A comparison of vestibular spatiotemporal tuning in macaque parietoinsular vestibular cortex, ventral intraparietal area, and medial superior temporal area. *J. Neurosci.*, **31**, 3082–3094.

Chen, X., DeAngelis, G.C., & Angelaki, D.E. (2014) Eye-centered visual receptive fields in the ventral intraparietal area. *J. Neurophysiol.*, **112**, 353–361.

Colby, C.L., Duhamel, J.R., & Goldberg, M.E. (1993) Ventral intraparietal area of the macaque: anatomic location and visual response properties. *J. Neurophysiol.*, **69**, 902–914.

Colby, C.L., Duhamel, J.R., & Goldberg, M.E. (1996) Visual, presaccadic, and cognitive activation of single neurons in monkey lateral intraparietal area. *J. Neurophysiol.*, **76**, 2841–2852.

Constantinidis, C. & Goldman-Rakic, P.S. (2002) Correlated discharges among putative pyramidal neurons and interneurons in the primate prefrontal cortex. *J. Neurophysiol.*, **88**, 3487–3497.

Cook, E.P. & Maunsell, J.H.R. (2002) Attentional modulation of behavioral performance and neuronal responses in middle temporal and ventral intraparietal areas of macaque monkey. *J. Neurosci.*, **22**, 1994–2004.

Crowe, D.A., Goodwin, S.J., Blackman, R.K., Sakellaridi, S., Sponheim, S.R., MacDonald, A.W., & Chafee, M. V (2013) Prefrontal neurons transmit signals to parietal neurons that reflect executive control of cognition. *Nat. Neurosci.*, **16**, 1484–1491.

This article is protected by copyright. All rights reserved.

Accepted Article

Das, A. & Gilbert, C.D. (1997) Distortions of visuotopic map match orientation singularities in primary visual cortex. *Nature*, **387**, 594–598.

DeAngelis, G.C., Ghose, G.M., Ohzawa, I., & Freeman, R.D. (1999) Functional micro-organization of primary visual cortex: receptive field analysis of nearby neurons. *J. Neurosci.*, **19**, 4046–4064.

Diester, I. & Nieder, A. (2008) Complementary contributions of prefrontal neuron classes in abstract numerical categorization. *J. Neurosci.*, **28**, 7737–7747.

Duhamel, J.-R.R., Bremmer, F., Ben Hamed, S., & Graf, W. (1997) Spatial invariance of visual receptive fields in parietal cortex neurons. *Nature*, **389**, 845–848.

Dunn, C.A. & Colby, C.L. (2010) Representation of the ipsilateral visual field by neurons in the macaque lateral intraparietal cortex depends on the forebrain commissures. *J. Neurophysiol.*, **104**, 2624–2633.

Eiselt, A.-K. & Nieder, A. (2013) Representation of abstract quantitative rules applied to spatial and numerical magnitudes in primate prefrontal cortex. *J. Neurosci.*, **33**, 7526–7534.

Everling, S., Tinsley, C.J., Gaffan, D., & Duncan, J. (2002) Filtering of neural signals by focused attention in the monkey prefrontal cortex. *Nat.Neurosci.*, **5**, 671–676.

Freedman, D.J. & Assad, J.A. (2006) Experience-dependent representation of visual categories in parietal cortex. *Nature*, **443**, 85–88.

Freedman, D.J. & Assad, J.A. (2009) Distinct encoding of spatial and nonspatial visual information in parietal cortex. *J. Neurosci.*, **29**, 5671–5680.

Freedman, D.J. & Assad, J.A. (2016) Neuronal Mechanisms of Visual Categorization: An Abstract View on Decision Making. *Annu. Rev. Neurosci.*, **39**, 129–147.

Funahashi, S. & Bruce, C.J. (1989) Mnemonic coding of visual space in the monkey ' s dorsolateral prefrontal cortex. *J. Neurophysiol.*, **61**, 331–349.

Fuster, J.M. & Alexander, G.E. (1971) Neuron activity related to short-term memory. *Science*, **173**, 652–654.

Fuster, J.M. & Bauer, R.H. (1974) Visual short-term memory deficit from hypothermia of frontal cortex. *Brain Res.*, **81**, 393–400.

This article is protected by copyright. All rights reserved.

Accepted Article

Gabel, S.F., Misslisch, H., Schaafsma, S.J., & Duysens, J. (2002) Temporal properties of optic flow responses in the ventral intraparietal area. *Vis. Neurosci.*, **19**, 381–388.

Galletti, C., Fattori, P., Gamberini, M., & Kutz, D.F. (1999) The cortical visual area V6: brain location and visual topography. *Eur. J. Neurosci.*, **11**, 3922–3936.

Goldman-Rakic, P.S. (1988) Topography of cognition: parallel distributed networks in primate association cortex. *Annu. Rev. Neurosci.*, **11**, 137–156.

Hubel, D.H. & Wiesel, T.N. (1962) Receptive fields, binocular interaction and functional architecture in the cat's visual cortex. *J. Physiol.*, **160**, 106–154.

Hussar, C.R. & Pasternak, T. (2009) Flexibility of sensory representations in prefrontal cortex depends on cell type. *Neuron*, **64**, 730–743.

Hussar, C.R. & Pasternak, T. (2012) Memory-guided sensory comparisons in the prefrontal cortex: contribution of putative pyramidal cells and interneurons. *J. Neurosci.*, **32**, 2747–2761.

Ibos, G. & Freedman, D.J. (2016) Interaction between Spatial and Feature Attention in Posterior Parietal Cortex. *Neuron*, **91**, 931–943.

Jacob, S.N., & Nieder, A. (2014) Complementary roles for primate frontal and parietal cortex in guarding working memory from distractor stimuli. *Neuron* **83**, 226-37.

Janssen, P., Srivastava, S., Ombelet, S., & Orban, G.A. (2008) Coding of shape and position in macaque lateral intraparietal area. *J. Neurosci.*, **28**, 6679–6690.

Kennerley, S.W. & Wallis, J.D. (2009) Encoding of reward and space during a working memory task in the orbitofrontal cortex and anterior cingulate sulcus. *J. Neurophysiol.*, **102**, 3352–3364.

Lewis, J.W. & Van Essen, D.C. (2000) Corticocortical connections of visual, sensorimotor, and multimodal processing areas in the parietal lobe of the macaque monkey. *J. Comp. Neurol.*, **428**, 112–137.

Mayo, J.P., DiTomasso, A.R., Sommer, M.A., & Smith, M.A. (2015) Dynamics of visual receptive fields in the macaque frontal eye field. *J. Neurophysiol.*, **114**, 3201–3210.

Mayo, J.P., Morrison, R.M., & Smith, M.A. (2016) A Probabilistic Approach to Receptive Field Mapping in the

This article is protected by copyright. All rights reserved.

Frontal Eye Fields. *Front. Syst. Neurosci.*, **10**, 25.

Mikami, A., Ito, S., & Kubota, K. (1982) Visual response properties of dorsolateral prefrontal neurons during visual fixation task. *J. Neurophysiol.*, **47**, 593–605.

Mishkin, M., Ungerleider, L.G., & Macko, K.A. (1983) Object vision and spatial vision: two cortical pathways. *Trends Neurosci.*, **6**, 414–417.

Nieder, A. (2012) Supramodal numerosity selectivity of neurons in primate prefrontal and posterior parietal cortices. *Proc. Natl. Acad. Sci. U. S. A.*, **109**, 11860–11865.

Nieder, A. (2016) The neuronal code for number. *Nat. Rev. Neurosci.*, **17**, 366–382.

Nieder, A., Freedman, D.J., & Miller, E.K. (2002) Representation of the quantity of visual items in the primate prefrontal cortex. *Science*, **297**, 1708–1711.

Nieder, A. & Miller, E.K. (2004) A parieto-frontal network for visual numerical information in the monkey. *Proc. Natl. Acad. Sci. U. S. A.*, **101**, 7457–7462.

Ott, T., Jacob, S.N., & Nieder, A. (2014) Dopamine receptors differentially enhance rule coding in primate prefrontal cortex neurons. *Neuron*, **84**, 1317–1328.

Pandya, D.N. & Yeterian, E.H. (1991) Chapter 4 Prefrontal cortex in relation to other cortical areas in rhesus monkey: Architecture and connections. pp. 63–94.

Quintana, J. & Fuster, J.M. (1999) From perception to action: temporal integrative functions of prefrontal and parietal neurons. *Cereb. Cortex*, **9**, 213–221.

Rainer, G., Asaad, W.F., & Miller, E.K. (1998a) Memory fields of neurons in the primate prefrontal cortex. *Proc. Natl. Acad. Sci. U. S. A.*, **95**, 15008–15013.

Rainer, G., Asaad, W.F., & Miller, E.K. (1998b) Selective representation of relevant information by neurons in the primate prefrontal cortex. *Nature*, **393**, 577–579.

Ramirez-Cardenas, A., Moskaleva, M., & Nieder, A. (2016) Neuronal Representation of Numerosity Zero in the Primate Parieto-Frontal Number Network. *Curr Biol*. **26**, 1285-94.

Rao, S.G., Williams, G. V, & Goldman-Rakic, P.S. (1999) Isodirectional tuning of adjacent interneurons and

This article is protected by copyright. All rights reserved.

Accepted Article

Accepted Article

pyramidal cells during working memory: evidence for microcolumnar organization in PFC. *J. Neurophysiol.*, **81**, 1903–1916.

Rao, S.G., Williams, G. V, & Goldman-Rakic, P.S. (2000) Destruction and creation of spatial tuning by disinhibition: GABA(A) blockade of prefrontal cortical neurons engaged by working memory. *J. Neurosci.*, **20**, 485–494.

Riley, M.R., Qi, X.-L., & Constantinidis, C. (2016) Functional specialization of areas along the anterior-posterior axis of the primate prefrontal cortex. *Cereb. Cortex*, 1–15.

Romero, M.C. & Janssen, P. (2016) Receptive field properties of neurons in the macaque anterior intraparietal area. *J. Neurophysiol.*, **115**, 1542–1555.

Romo, R., Brody, C.D., Hernández, A., & Lemus, L. (1999) Neuronal correlates of parametric working memory in the prefrontal cortex. *Nature*, **399**, 470–473.

Schaafsma, S.J. & Duysens, J. (1996) Neurons in the ventral intraparietal area of awake macaque monkey closely resemble neurons in the dorsal part of the medial superior temporal area in their responses to optic flow patterns. *J. Neurophysiol.*, **76**, 4056–4068.

Schlack, A., Sterbing-D'Angelo, S.J., Hartung, K., Hoffmann, K.-P., & Bremmer, F. (2005) Multisensory space representations in the macaque ventral intraparietal area. *J. Neurosci.*, **25**, 4616–4625.

Schwartz, M.L. & Goldman-Rakic, P.S. (1984) Callosal and intrahemispheric connectivity of the prefrontal association cortex in rhesus monkey: Relation between intraparietal and principal sulcal cortex. *J. Comp. Neurol.*, **226**, 403–420.

Solomon, S.G., White, A.J.R., & Martin, P.R. (2002) Extraclassical receptive field properties of parvocellular, magnocellular, and koniocellular cells in the primate lateral geniculate nucleus. *J. Neurosci.*, **22**, 338–349.

Sugihara, T., Diltz, M.D., Averbeck, B.B., & Romanski, L.M. (2006) Integration of auditory and visual communication information in the primate ventrolateral prefrontal cortex. *J. Neurosci.*, **26**, 11138–11147.

Suzuki, H. (1985) Distribution and organization of visual and auditory neurons in the monkey prefrontal cortex. *Vision Res.*, **25**, 465–469.

Suzuki, H. & Azuma, M. (1983) Topographic studies on visual neurons in the dorsolateral prefrontal cortex of

This article is protected by copyright. All rights reserved.

the monkey. *Exp. brain Res.*, **53**, 47–58.

Swadlow, H.A. & Gusev, A.G. (2002) Receptive-field construction in cortical inhibitory interneurons. *Nat. Neurosci.*, **5**, 403–404.

Swadlow, H.A. & Weyand, T.G. (1987) Corticogeniculate neurons, corticotectal neurons, and suspected interneurons in visual cortex of awake rabbits: receptive-field properties, axonal properties, and effects of EEG arousal. *J. Neurophysiol.*, **57**, 977–1001.

Swaminathan, S.K. & Freedman, D.J. (2012) Preferential encoding of visual categories in parietal cortex compared with prefrontal cortex. *Nat. Neurosci.*, **15**, 315–320.

Tudusciuc, O. & Nieder, A. (2009) Contributions of primate prefrontal and posterior parietal cortices to length and numerosity representation. *J. Neurophysiol.*, **101**, 2984–2994.

Vallentin, D., Bongard, S., & Nieder, A. (2012) Numerical rule coding in the prefrontal, premotor, and posterior parietal cortices of macaques. *J. Neurosci.*, **32**, 6621–6630.

Veit, J., Bhattacharyya, A., Kretz, R., & Rainer, G. (2014) On the relation between receptive field structure and stimulus selectivity in the tree shrew primary visual cortex. *Cereb. Cortex*, **24**, 2761–2771.

Viswanathan, P. & Nieder, A. (2013) Neuronal correlates of a visual "sense of number" in primate parietal and prefrontal cortices. *Proc. Natl. Acad. Sci. U. S. A.*, **110**, 11187–11192.

Viswanathan, P. & Nieder, A. (2015) Differential impact of behavioral relevance on quantity coding in primate frontal and parietal neurons. *Curr. Biol.*, **25**, 1259–1269.

Viswanathan, P. & Nieder, A. (2017) Visual receptive field heterogeneity and functional connectivity of adjacent neurons in primate fronto-parietal association cortices. *J. Neurosci.*, **37**, 8919–8928.

Wang, L., Li, X., Hsiao, S.S., Lenz, F.A., Bodner, M., Zhou, Y.-D., & Fuster, J.M. (2015) Differential roles of delay-period neural activity in the monkey dorsolateral prefrontal cortex in visual-haptic crossmodal working memory. *Proc. Natl. Acad. Sci. U. S. A.*, **112**, E214-9.

Wang, X.-J., Tegnér, J., Constantinidis, C., & Goldman-Rakic, P.S. (2004) Division of labor among distinct subtypes of inhibitory neurons in a cortical microcircuit of working memory. *Proc. Natl. Acad. Sci. U. S. A.*, **101**, 1368–1373.

This article is protected by copyright. All rights reserved.

Accepted Article

Womelsdorf, T., Anton-Erxleben, K., & Treue, S. (2008) Receptive field shift and shrinkage in macaque middle temporal area through attentional gain modulation. *J. Neurosci.*, **28**, 8934–8944.

Yokoi, I. & Komatsu, H. (2010) Putative pyramidal neurons and interneurons in the monkey parietal cortex make different contributions to the performance of a visual grouping task. *J. Neurophysiol.*, **104**, 1603–1611.

Yoshor, D., Bosking, W.H., Ghose, G.M., & Maunsell, J.H.R. (2007) Receptive fields in human visual cortex mapped with surface electrodes. *Cereb. Cortex*, **17**, 2293–2302.

Zhang, T. & Britten, K.H. (2011) Parietal area VIP causally influences heading perception during pursuit eye movements. *J. Neurosci.*, **31**, 2569–2575.

FIGURE LEGENDS

FIG. 1. Receptive field mapping. (**A**) Positions of recording sites in the dorsolateral prefrontal cortex (dlPFC, cyan) shown in the lateral view of a rhesus monkey brain and the ventral intraparietal area (VIP, orange) in the depth of the intraparietal sulcus (IPS) depicted in a coronal section of the sulcus. LS, lateral sulcus; PS, principal sulcus; STS, superior temporal sulcus. (**B**) The receptive field mapping task began with a short fixation period of 100 ms. Following this, a moving bar was shown in five successive positions on the screen while the monkeys continued to fixate centrally. The screen was divided into 80 locations sampled over multiple trials. Each trial of successful fixation was positively reinforced. (**C**) The trial-by-trial activity of an example PFC neuron is shown as a raster plot. Each subplot has trials plotted against time during the 1000 ms of stimulus presentation at that location of the screen. Each individual line shows an action potential fired by the neuron. (**D**) The trial-averaged activity of the same neuron is shown for every location, the average discharge rate against time. (**E**) Next, the activity at each location is averaged in time to create a raw RF map. The raw RF map is then linearly interpolated in both dimensions and smoothed with a

This article is protected by copyright. All rights reserved.

Accepted Article

2D Gaussian to create a high resolution RF map. The discharge rate is indicated by the warmth of the colour. (**F**) Dot raster plot for an example VIP neuron. (**G**) Peri-stimulus time histogram (PSTH) of the same neuron for every stimulus location. (**H**) High-resolution RF map for the VIP neuron.

FIG. 2. Spatially-selective population and the spatial distribution of RFs. (**A**) Proportion of PFC neurons that exhibit a spatial RF; 49% of 859 neurons against the non-selective population depicted in grey. (**B**) Proportion of VIP neurons that exhibit a spatial RF; 57% of 693 neurons against the non-selective population. (**C**) Distribution of the location of PFC RF maxima across the screen. The size of the circle reflects the number of neurons with their maxima at that location. (**D**) the same as **C** for VIP neurons. PFC shows a contralateral bias.

FIG. 3. Recording sites in the dlPFC and VIP. (**A**) RF maps from the individual recording sites around the principal sulcus of monkey L. All the RFs recorded at each site are normalised individually and then averaged. AS, arcuate sulcus; sAS, superior arcuate sulcus; iAS, inferior arcuate sulcus; PS, principal sulcus. (**B**) Averaged RF maps from the individual recording sites in monkey S. (**C**) Recording sites in area VIP of monkey L on the banks of the intraparietal sulcus, labelled and numbered, *left panel*. IPS, intraparietal sulcus; CS, central sulcus. RF maps from each site and at the indicated depth from the cortical surface, *right panel*. (**D**) same as **C** for recording sites in monkey S.

FIG. 4. Average RF maps. (**A**) Average of all 425 PFC RF maps as a heat map. The average firing rate is shown in the colour bar below. (**B**) Average of all 396 VIP RF maps. (**C**) Average of all PFC maps normalised individually to their maxima. The normalised firing rate

This article is protected by copyright. All rights reserved.

Accepted Article

is shown in the colour bar below. (**D**) the same as **C** for all VIP RFs. VIP neurons show higher spatial modulation.

FIG. 5. Characterisation of RF types. Examples of receptive field types from PFC (left column) and VIP (right column), presented as RF maps with the colours indicating individual firing rates. (**A** and **B**) Non-uniform receptive field showing >1 discrete locations with maximal response. (**C - J**) Uniform receptive fields consisting of sub-types. (**C** and **D**) Full-field responses with more than 75% of locations with > half-max responses. (**E - J**) Uniform, confined responses. (**E** and **F**) Contralateral receptive fields with the RF maxima situated on the contralateral third of the screen. (**G** and **H**) Foveal receptive fields covering the central portion of the screen. (**I** and **J**) Ipsilateral receptive fields with the maxima situated ipsilaterally.

FIG. 6. Frequencies of different RF types. (**A**) Percentage of neurons that exhibit various types of receptive fields in PFC, (**B**) and VIP. The number of neurons in each case is indicated above the bar. The contralateral, foveal and ipsilateral RFs constitute the uniform, confined population. PFC contains more contralateral RFs than VIP and VIP more foveal RFs.

FIG. 7. Receptive field properties of confined RFs (**A**) Probability histograms of eccentricity measured in degrees of visual angle from the centre, for uniform, confined RFs in PFC, (**B**) and VIP. Vertical grey lines mark the medians of the distributions. (**C**) Histogram of PFC receptive field sizes, in dva, of neurons whose fields were uniform, confined and did not touch the borders of the screen (screen-limited). These could, thus, be reliably measured in our experiment. (**D**) the same as **C** for VIP neurons.

This article is protected by copyright. All rights reserved.

Accepted Article

Accepted Article

FIG. 8. Receptive field properties by neuron class (**A**) Classification of neuronal classes by waveforms; 50 randomly chosen narrow-spiking (NS) neurons are shown in grey, and broad-spiking (BS) neurons in black. The waveforms are normalised and aligned to their troughs. (**B**) Histogram of spike widths for all NS and BS neurons with the means of both classes plotted as black vertical lines. (**C**) Probability histograms of RF eccentricity by neuron class in PFC, (**D**) in VIP. The vertical lines mark the medians of the respective distributions. (**E**) Probability histograms of RF sizes by neuron class in PFC, (**F**) and VIP. Dotted vertical lines mark the medians of the RF sizes. PFC BS neurons had smaller RFs than NS neurons (Mann-Whitney U test, $P = 0.02$).

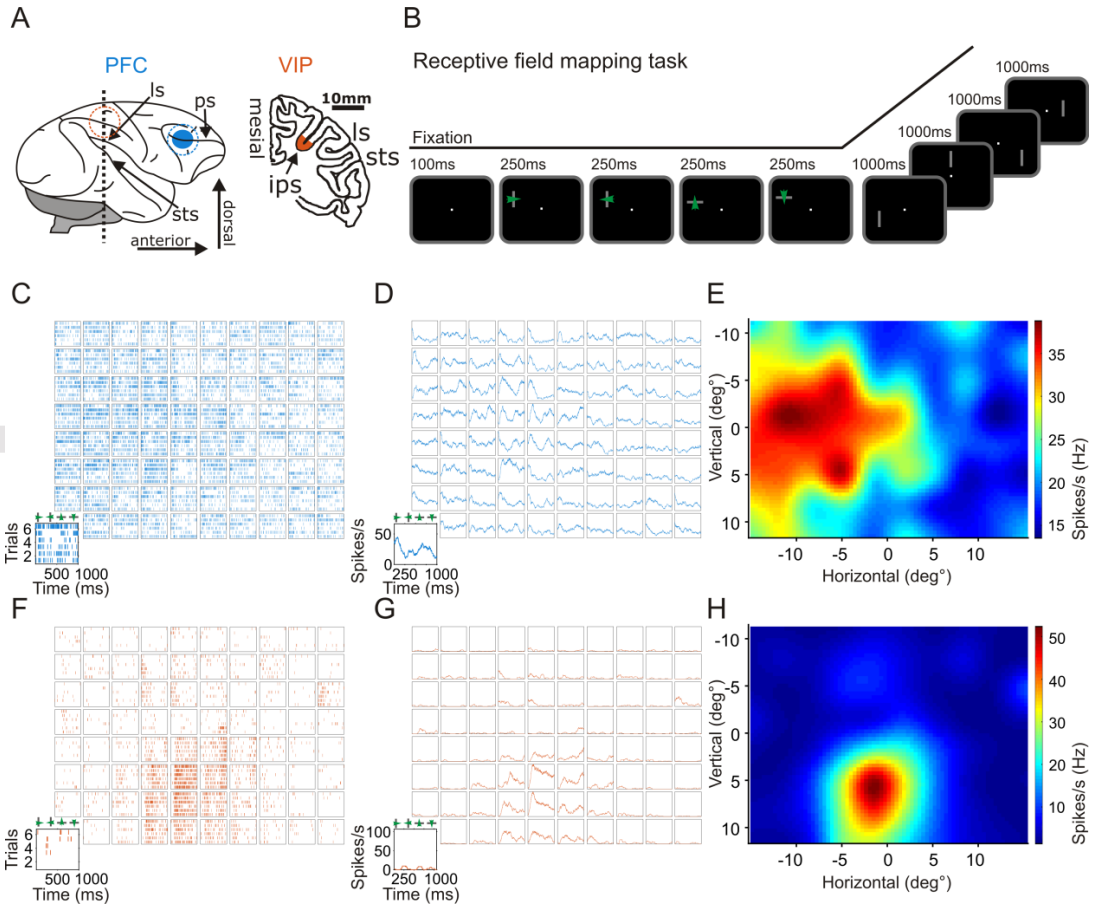

This article is protected by copyright. All rights reserved.

Accepted Article

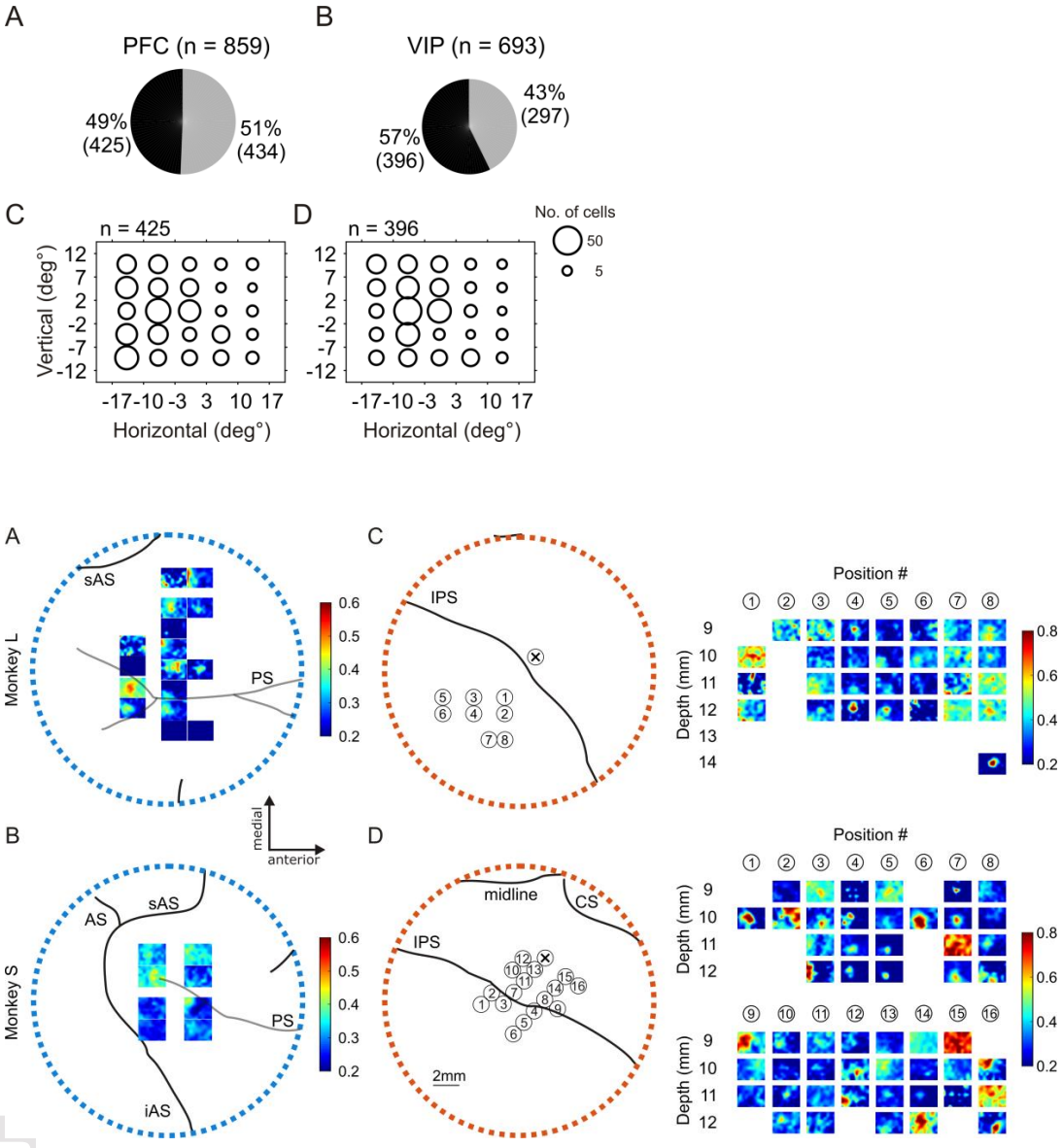

This article is protected by copyright. All rights reserved.

Accepted Article

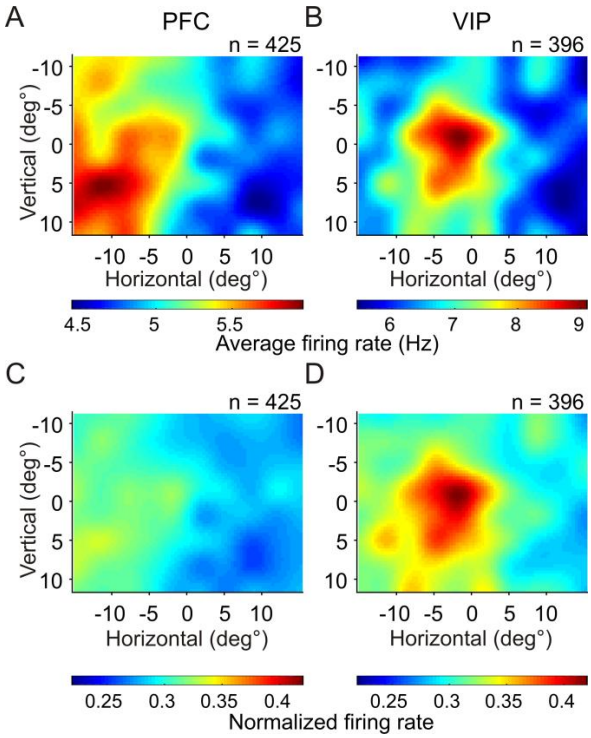

This article is protected by copyright. All rights reserved.

Accepted Article

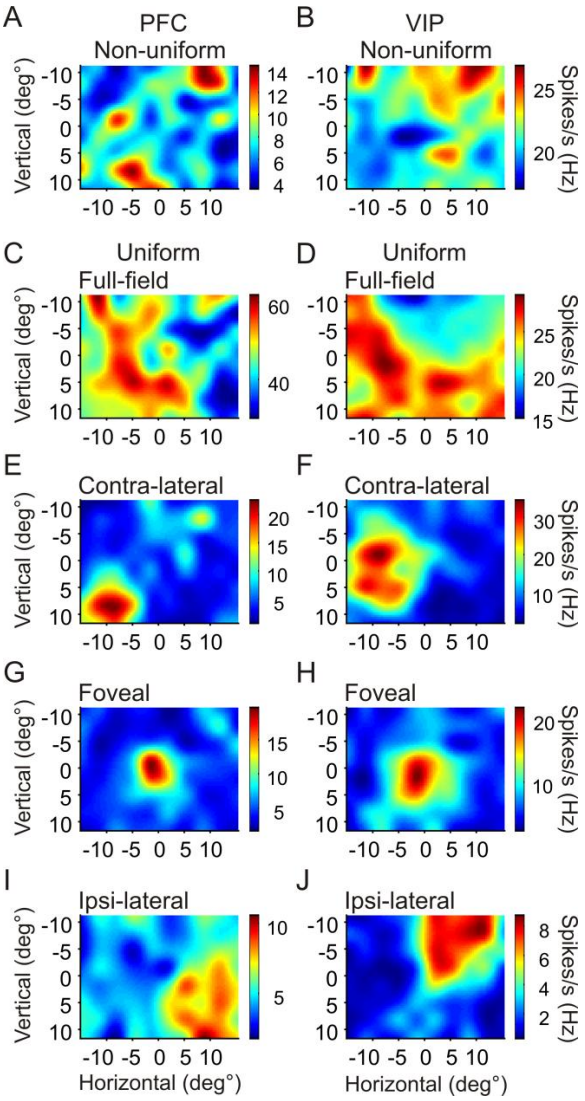

This article is protected by copyright. All rights reserved.

Accepted Article

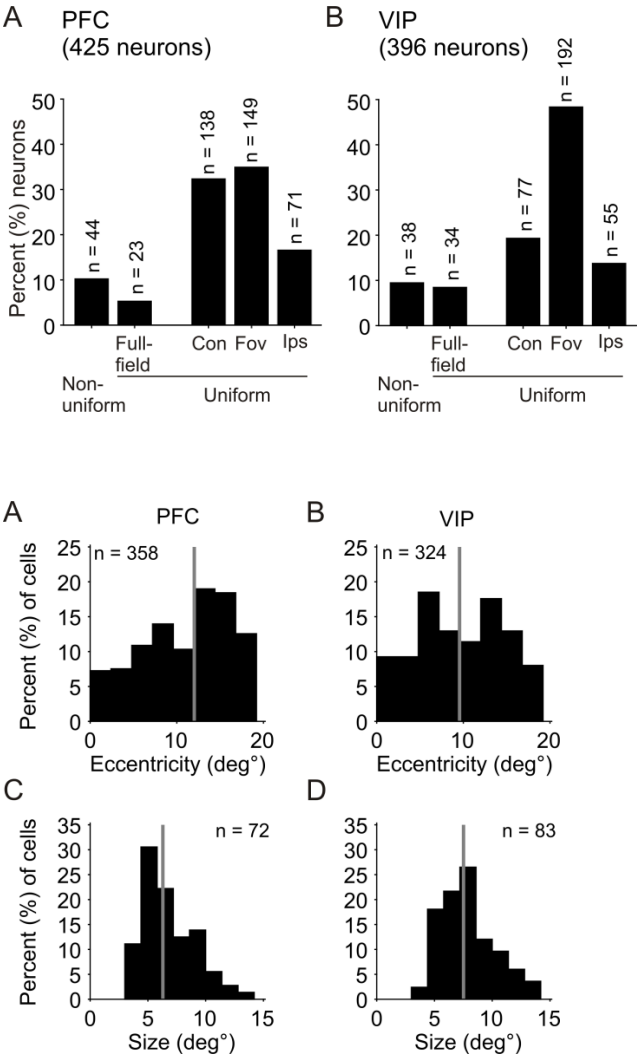

This article is protected by copyright. All rights reserved.

Accepted Article

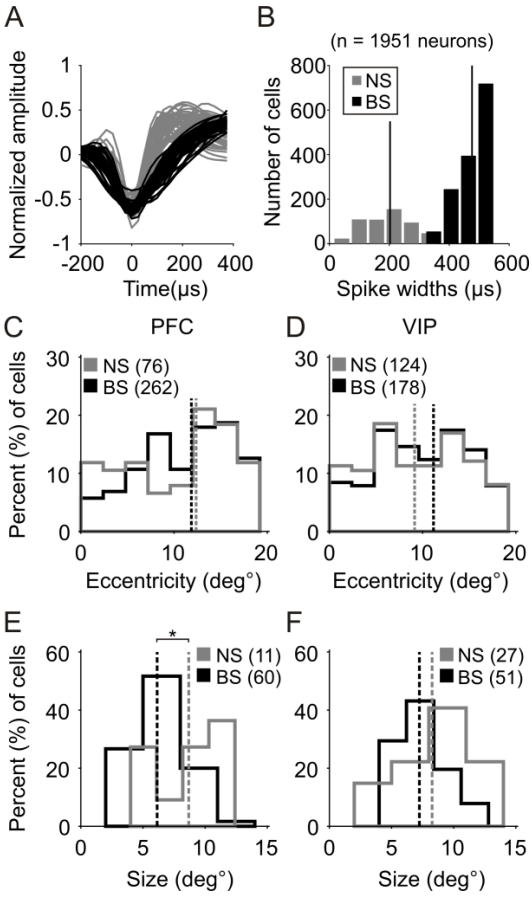

This article is protected by copyright. All rights reserved.

Study 4: Spatiotopy in the fronto-parietal network

Viswanathan, P., Nieder, A. (2017). Visual receptive field heterogeneity and functional connectivity of adjacent neurons in primate fronto-parietal association cortices. *J Neurosci.* **37**(37):8919–8928.

Systems/Circuits

Visual Receptive Field Heterogeneity and Functional Connectivity of Adjacent Neurons in Primate Frontoparietal Association Cortices

Pooja Viswanathan and Andreas Nieder
Animal Physiology, Institute of Neurobiology, University of Tübingen, 72076 Tübingen, Germany

The basic organization principles of the primary visual cortex (V1) are commonly assumed to also hold in the association cortex such that neurons within a cortical column share functional connectivity patterns and represent the same region of the visual field. We mapped the visual receptive fields (RFs) of neurons recorded at the same electrode in the ventral intraparietal area (VIP) and the lateral prefrontal cortex (PFC) of rhesus monkeys. We report that the spatial characteristics of visual RFs between adjacent neurons differed considerably, with increasing heterogeneity from VIP to PFC. In addition to RF incongruences, we found differential functional connectivity between putative inhibitory interneurons and pyramidal cells in PFC and VIP. These findings suggest that local RF topography vanishes with hierarchical distance from visual cortical input and argue for increasingly modified functional microcircuits in noncanonical association cortices that contrast V1.

Key words: functional connectivity; prefrontal cortex; single-unit recordings; ventral intraparietal

Significance Statement

Our visual field is thought to be represented faithfully by the early visual brain areas; all the information from a certain region of the visual field is conveyed to neurons situated close together within a functionally defined cortical column. We examined this principle in the association areas, PFC, and ventral intraparietal area of rhesus monkeys and found that adjacent neurons represent markedly different areas of the visual field. This is the first demonstration of such noncanonical organization of these brain areas.

Introduction

The receptive field (RF) of a neuron, the region of visual space from which its response can be modulated, is one of the basic concepts in vision research (Hubel and Wiesel, 1962). In the primary visual cortex (V1), a visuotopic map for points in the visual field arises from the ordered spatial arrangement of thalamic afferent axons in the cortex (Kremkow et al., 2016). Therefore, adjacent neurons within functional units lying perpendicular to the cortical surface (modules, microcolumns) show nearly identical RF locations (DeAngelis et al., 1999). This organization principle is commonly assumed to be realized even in the high-level association cortices of the frontal, parietal, and temporal lobes so that all neurons within a given microcolumn share the representation of a region of visual field (Suzuki and Azuma, 1983; Wilson et al., 1994; Rosa, 1997).

Received March 27, 2017; revised June 6, 2017; accepted July 13, 2017.
Author contributions: P.V. and A.N. designed research; P.V. performed research; P.V. analyzed data; P.V. and A.N. wrote the paper.
This work was supported by Deutsche Forschungsgemeinschaft Grant NI 618/2-1 to A.N.
The authors declare no competing financial interests.
Correspondence should be addressed to Dr. Andreas Nieder, Animal Physiology, Institute of Neurobiology, Auf der Morgenstelle 28, University of Tübingen, 72076 Tübingen, Germany. E-mail: andreas.nieder@uni-tuebingen.de.
DOI:10.1523/JNEUROSCI.0829-17.2017
Copyright © 2017 the authors 0270-6474/17/378919-10$15.00/0

We tested this prediction and investigated visual RF characteristics of adjacent neurons recorded at the same electrode tip in two association brain areas, the ventral intraparietal area (VIP) in the posterior parietal cortex, and the lateral PFC. The posterior parietal cortex is the termination zone of the dorsal, occipitoparietal visual stream that conveys motion and spatial information from V1 via MT/MST to VIP (Mishkin et al., 1983; Kravitz et al., 2011), which, in turn, is reciprocally connected with the PFC at the apex of the cortical hierarchy (Lewis and Van Essen, 2000). In agreement with such strong visual inputs, neuronal responses to visual parameters of stimuli are readily found in both the VIP (Colby et al., 1993; Duhamel et al., 1998; Chen et al., 2014) and the PFC (Goldman-Rakic, 1995; O'Scalaidhe et al., 1997; Zaksas and Pasternak, 2006), in addition to multimodal and executive function-related signals (Fuster, 2000; Miller and Cohen, 2001; Avillac et al., 2005, 2007; Schlack et al., 2005; Sugihara et al., 2006; Nieder, 2012; Guipponi et al., 2013). Moreover, the VIP and PFC are key nodes of the parietofrontal network processing numerical information (Nieder, 2016; Ramirez-Cardenas et al., 2016). Physiological parameters, such as selectivity latencies to quantity stimuli and categorical robustness, suggest that number information is processed hierarchically between both areas (Viswanathan and Nieder, 2013; Jacob and Nieder, 2014). Whereas VIP seems to be the first cortical hub extracting quantitative information,

the PFC is a putative recipient of information about numerosity. Insights into the visual RF characteristics and wiring patterns of adjacent neurons in the VIP and PFC could elucidate their different roles in numerical processing. Indeed, we find considerable incongruencies in the spatial layout and position of RFs of adjacent neurons, suggesting RF organization that differs not only from that of early visual cortex, but also between these areas of the frontal and parietal association cortex.

Differences in the spatial tuning properties of adjacent neurons suggest distinct neuronal connectivity patterns in association cortices compared with V1. The microcircuitry of V1, formed by dedicated excitatory and inhibitory neurons, is considered canonical and is thought to generalize to other neocortical regions (Douglas and Martin, 2004). For instance, inhibitory interneurons in local microcircuits play a major role in shaping and often, sharpening neuronal response properties of excitatory pyramidal projection neurons (Markram et al., 2004). However, whether brain areas that are higher up the visual hierarchy and display noncanonical circuit properties enabling parallel and reentrant processing required for cognition (Goldman-Rakic, 1988), exhibit the same basic principles remains unknown. We therefore characterized the functional connectivity between adjacent neurons and compared it with the observed RF heterogeneity in VIP and PFC. To identify putative inhibitory interneurons and pyramidal cells in extracellular recordings, we exploited established action potential waveform differences found in PFC between pyramidal cells that tend to exhibit broad action potential waveforms and interneurons that display narrow action potential waveforms (Wilson et al., 1994; Rao et al., 1999; Johnston et al., 2009; Merchant et al., 2012). By comparing the functional connectivity patterns between these two classes of neurons that constitute members of local microcircuits, we identified differential functional interactions that correlated with RF incongruences in VIP and PFC.

Materials and Methods

Experimental setup. Recordings were made in two male rhesus monkeys (Macaca mulatta) weighing between 5.5 and 6.3 kg. The monkeys sat in primate chairs positioned 57 cm from a 15 inch flat-screen monitor within chambers. The monitor had a resolution of 1024 × 768 pixels and a refresh rate of 75 Hz. We used the National Institute of Mental Health Cortex program to present the stimuli, monitor the behavior, and collect behavioral data. An infrared tracking system (ISCAN) was used to monitor the monkeys' eye movements. All data analysis was performed using the MATLAB computational environment (The MathWorks) using custom-written scripts. All experimental procedures were in accordance with the guidelines for animal experimentation approved by the national authority, the Regierungspräsidium Tübingen, Germany.

Behavioral task. Monkeys performed a passive fixation task during the RF measurements. While monkeys fixated a central white square (0.10° × 0.10° of visual angle or dva) and maintained their gaze within 1.75 dva of the fixation point, a light gray moving bar (3° × 0.20°) appeared on the screen at a pseudo-randomly chosen position from a 10 × 8 matrix of positions (see Fig. 1*A*). Each position was sampled for 1000 ms first with the bar oriented vertically moving left to right (0° for 250 ms), then right to left (180° for 250 ms), oriented horizontally moving up (90° for 250 ms), and moving down (270° for 250 ms). Then the bar was displayed at another location in the grid and three other locations after that, thus scanning 5 locations in every trial. The matrix of locations thus covered an area 30.5° × 23° of central vision, centered on the fovea. The monkeys fixated the central fixation spot for the entire period of the trial and were rewarded for successful fixation. Each RF block consisted of 3 trials per position. The RF blocks were interspersed with blocks of a delayed match-to-sample task during which numerosities were presented in the center of the screen (Viswanathan and Nieder, 2013, 2015). We collected up to 4 blocks of RF trials per recording session.

Surgery and neuronal recordings. Both monkeys were first implanted with a head bolt with which we fixated the head to allow eye movements to be monitored during the task. We then implanted recording chambers over the right dorsolateral PFC, centered on the principal sulcus, and the right intraparietal sulcus guided by anatomical MRI of individual monkeys and stereotaxic measurements (see Fig. 1*B*). The surgeries were performed under sterile conditions while the monkeys were under general anesthesia. They received antibiotics and analgesics after the procedure.

We recorded neuronal signals from the 2 monkeys using arrays of eight glass-coated tungsten microelectrodes (Alpha Omega) for each area attached to screw microdrives in a grid with 1 mm spacing. Once the microelectrodes were lowered into the recording position, they were allowed to rest in the position for 30–60 min before recording began. The microelectrodes were not moved further during the recording session. VIP recordings were made exclusively at depths of 9–13 mm below the cortical surface. As has been reported previously, we observed visual and somatosensory responses on VIP electrodes. However, the neurons recorded were not preselected online for any sensory, spatial, or task-related parameter. The electrophysiological signals were amplified and filtered, and waveforms of the actions potentials sampled at 40 kHz from each electrode were stored (Plexon Systems). Sorting of single units was performed offline based on waveform characteristics (Offline Sorter, Plexon Systems). Timestamps of trial events and action potentials were extracted for analysis.

Analysis of spatial selectivity (RF mapping). We analyzed the neuronal activity during the presentation of the moving bar stimulus to test selectivity of single neurons. To account for the well-known differences in response latencies in these two areas (Nieder and Miller, 2004; Viswanathan and Nieder, 2013), we delayed the onset of the 1000 ms analysis window for VIP neurons by 50 ms, and for PFC neurons by 100 ms. The selectivity of single neurons was tested using a three-way ANOVA ($p < 0.05$) (Rainer et al., 1998; Romero and Janssen, 2016) on firing rates calculated in 250 ms analysis windows (corresponding to the duration of a single bar sweep) with position, movement direction, and orientation of the bar as factors. The movement direction was a nested variable of orientation as the direction of movement depended on the orientation of the bar in that position. We downsampled the screen into five zones (top left, top right, bottom left, bottom right, and center) to reduce the number of false-positives from testing each of the 80 positions individually. Repeating the ANOVA with the zones defined in different ways yielded qualitatively and quantitatively similar results. We tested every neuron with a minimum of 10 trials per zone (859 PFC neurons and 693 VIP neurons).

We created raw RF maps for single neurons by averaging the responses over the entire 1000 ms period of visual stimulation at each position and then over all the trials at that position. As the moving bar covered an area of ~3° × 3° in the two different orientations, we linearly interpolated this 10 × 8 map by threefold interpolation in both spatial dimensions (Rainer et al., 1998) to visualize the responses at a resolution of 0.4 dva. We smoothed these with a 2D Gaussian kernel of 2 dva. These steps were taken to create smooth high-resolution RF maps that could be compared with those reported in other studies using large or sparse stimuli, with minimal assumption about the size or shape of the observed RF.

For neurons selective to the factor position in the ANOVA, we conducted a further cross-validation to confirm robust spatial selectivity. To that aim, we created two separate RF maps for each neuron: one from the first half of RF trials and another from the second half of RF trials. We calculated a 2D cross-correlation between the two maps created for each neuron and compared this against a distribution of 2D cross-correlations calculated from 1000 shuffles of each half map as follows:

$$r = \frac{\sum_h \sum_v (Half1 - \overline{Half1})(Half2 - \overline{Half2})}{\sqrt{\left(\sum_h \sum_v (Half1 - \overline{Half1})^2\right)\left(\sum_h \sum_v (Half2 - \overline{Half2})^2\right)}}$$

where *Half*1 is the map created from the first half of trials and *Half*2 is the map created from the second half of trials. The means of the maps are subtracted before summing them over the horizontal (h) and vertical (v) dimensions. Only if the true correlation across halves of trials lay above

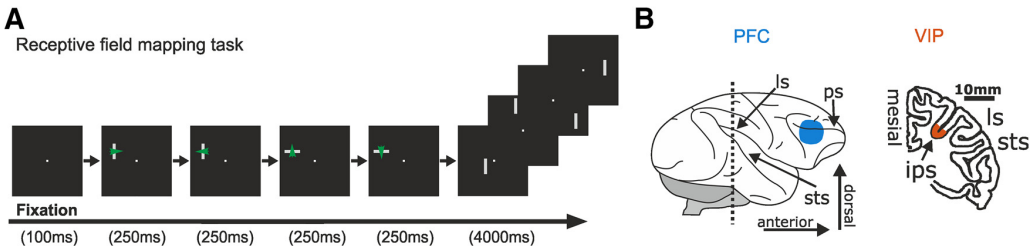

Figure 1. RF mapping in PFC and VIP. ***A***, Passive fixation task. Monkeys fixated a central fixation target while a bar (3° × 0.20°) moving in four directions appeared in five successive locations on the screen. The visual field on the screen was divided into a grid of 80 locations (10 × 8) sampled over 16 trials/cycle. ***B***, Lateral view (left) of a macaque monkey brain and a sagittal section (right) of the intraparietal sulcus at the position indicated by the dotted line. Positions of recording sites in the dorsolateral PFC (cyan) and the VIP (orange) in the depth of the sulcus are shown. ps, Principal sulcus; ls, lateral sulcus; ips, intraparietal sulcus; sts, superior temporal sulcus.

the 95th percentile of the distribution of surrogate correlations (one-tailed, $p < 0.05$), we accepted the neuron and its RF map into further analysis.

Analysis of neuronal pairs. We identified spatially selective neurons that were recorded from the same electrode with some temporal overlap and, thus, at the same location ("adjacent neurons"). To quantify the spatial similarity of their RFs, we calculated a 2D cross-correlation between their raw RF maps (DeAngelis et al., 1999). We did this to have a similarity index comparable across neuron pairs without assuming the shape or size of the RFs and have a measure that is sensitive to shifts of RFs from neuron to neuron in both dimensions as follows:

$$r = \frac{\sum_h \sum_v (Neuron1 - \overline{Neuron1})(Neuron2 - \overline{Neuron2})}{\sqrt{\left(\sum_h \sum_v (Neuron1 - \overline{Neuron1})^2\right) \times \left(\sum_h \sum_v (Neuron2 - \overline{Neuron2})^2\right)}}$$

where *Neuron*1 is the RF map of one of the neurons in the pair and *Neuron*2 is the RF map of the second neuron in the pair. The means of the maps are subtracted before summing them over the horizontal (h) and vertical (v) dimensions. We additionally examined the contributions of the horizontal and vertical dimensions separately to the similarity between neuronal pairs.

We compared the derived true correlation coefficient value of the pair against the distribution of 1000 surrogates obtained from shuffling their maps. If the true coefficient lay above the 97.5th percentile of the shuffled distribution, we judged the neuronal pair to be congruent (two-tailed, $p < 0.05$). If it lay below the 2.5th percentile of the shuffled distribution and <0 (negative), we judged these maps to be inverted. If the true correlation lay within the shuffled distribution (2.5th and 97.5th percentiles), we judged these maps to be incongruent (see Fig. 3).

Classification of cell types using waveforms. We classified all the recorded single units into narrow-spiking (NS) and broad-spiking (BS) neurons based on their waveforms (Diester and Nieder, 2008; Viswanathan and Nieder, 2015; Jacob et al., 2016). We saved the template waveforms for each single unit, sampled at a frequency of 40 kHz (one entry every 25 μs), and only included the waveforms with a trough followed by a crest after reaching the threshold voltage (1951 of 2130 neurons). The troughs of the waveforms were expected to occur within 200–400 μs of crossing the threshold voltage and the crests only after 300 μs of reaching threshold. To maximize the strength of our clustering procedure, we used all the neurons recorded across both areas. We normalized each waveform to the difference between the maximum amplitude and the minimum amplitude and aligned them to their troughs. We then entered the waveforms through a linear classifier (k means; $k = 2$, squared Euclidian distance) to cluster the cells into two categories: NS and BS such that, on average, the units with smaller widths constituted the NS cluster (537 neurons) and those with the larger widths constituted the BS cluster (1414 neurons) (see Fig. 4*A*,*B*).

Cross-correlation between spike trains of neuron pairs. We computed a cross-correlogram by accumulating spike occurrence times in one neuron relative to the spikes of the paired neuron to identify functionally coupled neurons (Aertsen et al., 1989; de Oliveira et al., 1997; Diester and Nieder, 2008) among each pair of neurons that were recorded simultaneously with significant temporal overlap. To increase the number of action potentials, we included trials of the delayed match-to-sample task for this calculation. In addition, we repeated this analysis for a subset of neuronal pairs with sufficiently high firing rate using only trials from RF mapping to confirm that connectivity was independent from task demands. For each pair, one unit was assigned the trigger (in the case of NS-BS pairs, always the NS neuron) and for each spike recorded from this unit, the time delays to each of the spikes of the other unit were plotted in a histogram of ±50 ms delay and a bin width of 1 ms. Repeating this procedure for all spikes and all trials yielded the raw cross-correlogram. We normalized the raw cross-correlogram by calculating a z score (i.e., subtracting the mean and dividing by the SD), rendering it independent from the firing rates of the two units (de Oliveira et al., 1997). To avoid false-positives from short fluctuations, we smoothed the z score with a 3-point boxcar (3 ms). z scores within ±25 ms of the 0th bin that crossed ±2.5 were considered significant to reject the null hypothesis that the correlogram at that point arose from two independent random Poisson processes. We also calculated a shifted predictor by correlating the trigger spike with the other neuron's response in the subsequent trial and the last trial with the first. We calculated the z score of the shifted predictor as well to compare against the true correlogram and ensure significant deflections in the true correlogram were not influenced by other repetitive features, such as the stimulus onset, but truly reflected functional connectivity. Only those pairs with at least 1000 entries (i.e., action potentials or trials) for the correlogram were evaluated. When we included trials from the delayed match to sample task, these were 128 of 276 pairs total. Using only RF mapping trials, we could evaluate the correlograms of 61 pairs.

Results

Visual RFs in PFC and VIP

We mapped the RFs of a total of 859 neurons in PFC (361 from Monkey L and 498 from Monkey S) and 693 neurons in VIP (273 from Monkey L and 420 from Monkey S) with bars moving in different directions that were presented in systematically arranged locations on a screen (Fig. 1*A*,*B*). Many neurons showed spatially selective responses to the stimuli at confined locations of the visual field. The activity of an example neuron from PFC is shown in Figure 2*A*–*C*, and an example neuron from VIP is shown in Figure 2*D*–*F*. The detailed discharges to the different bar locations in the grid are depicted as dot-raster histograms (Fig. 2*A*,*D*) and averaged as spike-density histograms (Fig. 2*B*,*E*). To statistically verify neuronal selectivity, the firing rates elicited by the visual stimuli were tested using a three-way ANOVA (with position, direction, and orientation of the stimulus as factors; $p <$ 0.05). Only spatially selective neurons with a main effect for position were considered for further analyses. In PFC, 64% (545 of 859) of the neurons showed a stimulus position effect, whereas

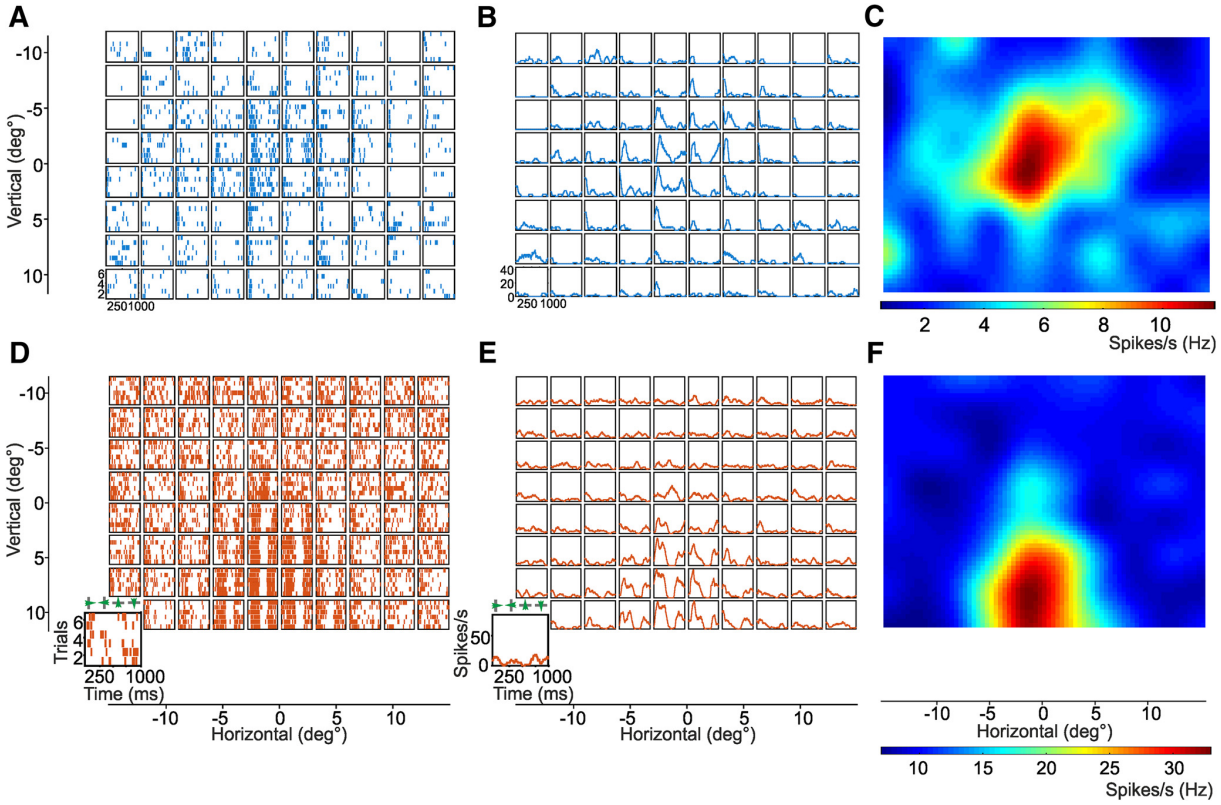

Figure 2. Example neurons with RFs. ***A***, Raster plot of an example spatially selective PFC neuron recorded in Monkey S. Each of the 80 locations is represented by a subplot, within which the dots along each line indicate the action potentials elicited for each trial. ***B***, Peristimulus time histogram for the same neuron as in ***A***. Each location is again represented by a subplot where the colored line indicates the trial-averaged response of the neuron in time. ***C***, Averaged and smoothed high-resolution RF map ("heat map") for the neuron. Colors represent the firing rates across the measured visual field. ***D–F***, The same plots as ***A–C*** for an example neuron recorded in VIP from Monkey L. Enlarged bottom left squares represent the scale of each subplot of ***A***, ***B***, ***D***, and ***E***. The moving bar moved in four different directions within each position of the grid.

69% (480 of 693) of the VIP neurons were found to be spatially tuned (see Materials and Methods).

From these spatially arranged discharges, we created averaged and smoothed RF maps (activity "heat maps" Fig. 2*C*,*F*) for each spatially tuned neuron. To further verify robust and reliable spatial tuning of single cells, we cross-validated the RFs of all ANOVA-selective neurons. For each neuron, two separate RF maps for the discharges to the first and second half of the trials were created. A 2D correlation analysis was applied to the two maps from a given neuron, and the resulting true correlation coefficient was compared with a distribution of coefficients obtained from shuffled surrogates. If the true correlation coefficient was significantly higher than the shuffled coefficients (one-tailed, $p < 0.05$), the neuron was classified as spatially tuned and further analyzed. In the PFC, 50% (425 of 859) of all recorded neurons were spatially selective according to both ANOVA and cross-validation analyses. An even higher proportion of 57% spatially selective neurons (396 of 693) was found in the VIP. This difference in the proportion of spatially tuned neurons between PFC and VIP was significant ($\chi^2 = 9.05$, $p < 0.01$). Some of the neurons displayed complex RFs, but many showed local, uniform RFs centered on the fovea or more contralaterally located, matching the early reports of visual or memory fields in PFC (Mikami et al., 1982; Rainer et al., 1998) and the reports of eye-centered RFs in VIP (Chen et al., 2014).

Heterogeneous spatial RFs despite anatomical proximity

Anatomically nearby neurons in early visual cortex show spatially congruent RFs (DeAngelis et al., 1999), pointing toward an orderly local topographic arrangement of visual space. However, when we inspected RFs from adjacent neurons in PFC and VIP, unexpected RF incongruencies surfaced. We therefore analyzed spatial tuning of adjacent neurons in PFC and VIP. To ensure that neurons were anatomically adjacent, we analyzed neuron pairs that were recorded simultaneously or with some temporal overlap at a given electrode tip and separated based on differential waveform characteristics (off-line spike sorting). Because such neuron pairs were recorded at the same electrode tip, they were at the closest possible anatomical location. We found 127 such adjacent-neuron pairs in PFC (41 from Monkey L and 86 from Monkey S) and 149 pairs in VIP (24 from Monkey L and 125 from Monkey S) consisting of 131 unique neurons in PFC and 148 neurons in VIP. As can be seen in Figure 3, RF congruency was variable between neuron pairs, ranging from almost identical RFs with excitatory hotspots at corresponding visual field locations (Fig. 3*A*,*B*), to clearly dissimilar locations of excitation (Fig. 3*C*,*D*) and, finally, RFs in which excitatory and inhibitory subfields seemed opposite in one neuron of a pair relative to the other (Fig. 3*E*,*F*).

To quantify the similarity or dissimilarity between the RFs of neuron pairs in an unbiased way that accounted for the different

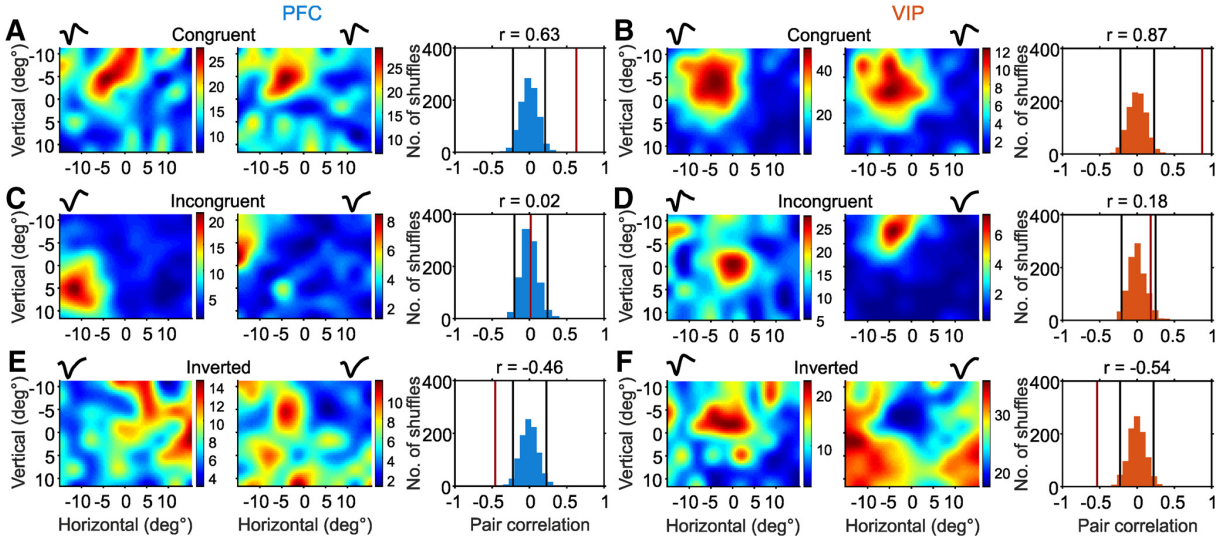

Figure 3. RFs of neuron pairs recorded on the same electrode. Left, PFC neuron pairs. Right, VIP neuron pairs. ***A***, Example of PFC neuron pair recorded in Monkey L whose RF maps (left) were classified as congruent based on their 2D correlation coefficient, *r* (right). The normalized averaged waveforms of these neurons are in miniature above the RF maps. Histogram of correlation coefficients obtained from shuffling the raw RF maps 1000 times and calculating the 2D correlation coefficient 1000 times. Black vertical lines indicate the 2.5th and 97.5th percentiles of the shuffled distribution. Red line indicates the true correlation coefficient obtained from the true RF maps, also stated above the histogram. As the true correlation coefficient is >97.5th percentile of the data (two-tailed, $p < 0.05$), the neuron pair was judged to have congruent RFs. ***B***, Example congruent pair from VIP. ***C***, ***D***, Example of an incongruent pair from each area with their corresponding correlation coefficient. Here, the true correlation coefficient lay within 2.5th and 97.5th percentiles of the shuffled distribution. ***E***, ***F***, Example of an inverted pair from each area. Here, the true correlations were <2.5th percentile of the surrogate distribution and were negative. ***B–F***, The neuron pairs were recorded from Monkey S.

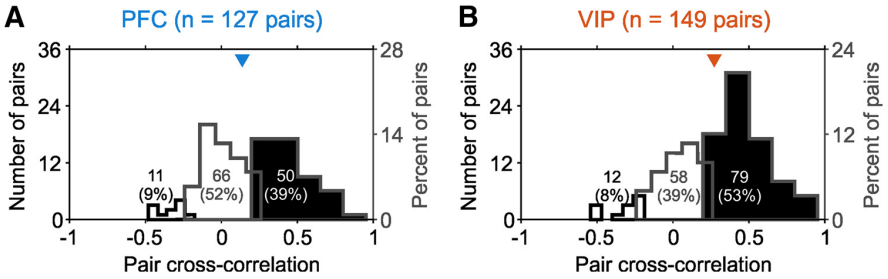

Figure 4. Heterogeneity of RFs of adjacent neurons. ***A***, Frequency distributions of inverted (white histograms with black outline), incongruent (white histograms with gray outline), and congruent neuron pairs (black histograms) from PFC. Overlaid numbers indicate the total number and percentage of pairs contained in the histograms. Colored triangles represent the medians of all the correlation coefficients. ***B***, Frequency distribution of the similarity for VIP neuron pairs. The population of recorded neuron pairs in VIP had a higher correlation coefficient than PFC (Mann–Whitney *U* test, $p < 0.05$). PFC had a significantly higher frequency of incongruent pairs than congruent pairs ($\chi^2 = 5.33$, $p < 0.05$) compared with VIP.

kinds of RFs, we calculated a 2D correlation analysis that considered the entire raw RF map (DeAngelis et al., 1999). The true correlation coefficient for each neuron pair was then compared with a distribution of correlation coefficients derived from 1000 shuffled RF surrogates for the same neuron pair. True correlation coefficients that were significantly larger than the shuffled distribution ($p < 0.05$; positive correlation coefficient) indicated that the RFs of both neurons in the pair were congruent (Fig. 3*A*,*B*, right panels). True correlations that were indistinguishable from the randomly shuffled distribution indicated incongruent RFs of adjacent neurons (Fig. 3*C*,*D*, right panels). Finally, a proportion of RF pairs were significantly negatively correlated with each other ($p < 0.05$; negative correlation coefficient), and these had true correlations smaller than the shuffled distribution (Fig. 3*E*,*F*, right panels). We characterized this last class as inverted RF pairs. A comparison of the frequencies of 2D correlation coefficients across brain areas revealed that 53% of the RFs of adjacent neurons were congruent in VIP, in contrast to only 39% congruent RFs in PFC (Fig. 4*A*,*B*). Comparison of congruent and other RFs showed a significantly higher proportion of congruent RFs in VIP (PFC: 50 of 127, VIP: 79 of 149; $\chi^2 = 5.13$, $p < 0.05$). In particular, the proportion of congruent and incongruent RFs differed significantly between the two areas (PFC: 50 of 116 congruent against 66 of 116 incongruent, VIP: 79 of 137 congruent and 58 of 137 incongruent; $\chi^2 = 5.33$, $p < 0.05$). All categories are taken together; VIP neuron pairs displayed higher correlation coefficients than PFC (median r_{2D} for PFC neuron pairs = 0.14; median r_{2D} for VIP neuron pairs = 0.27; Mann–Whitney *U* test, $z = -2.38$, $p < 0.05$). VIP neuron pairs, on average, were more similar than PFC neuron pairs.

We also calculated the map correlation separately for the horizontal and vertical dimensions. Along the vertical dimension, correlations between neuronal pairs in the VIP did not differ significantly from PFC pairs (median $r_{vertical}$ PFC = 0.12, median $r_{vertical}$ VIP = 0.20; Mann–Whitney *U* test, $z = -1.65$, $p > 0.05$). Along the horizontal dimension, however, correlations for VIP

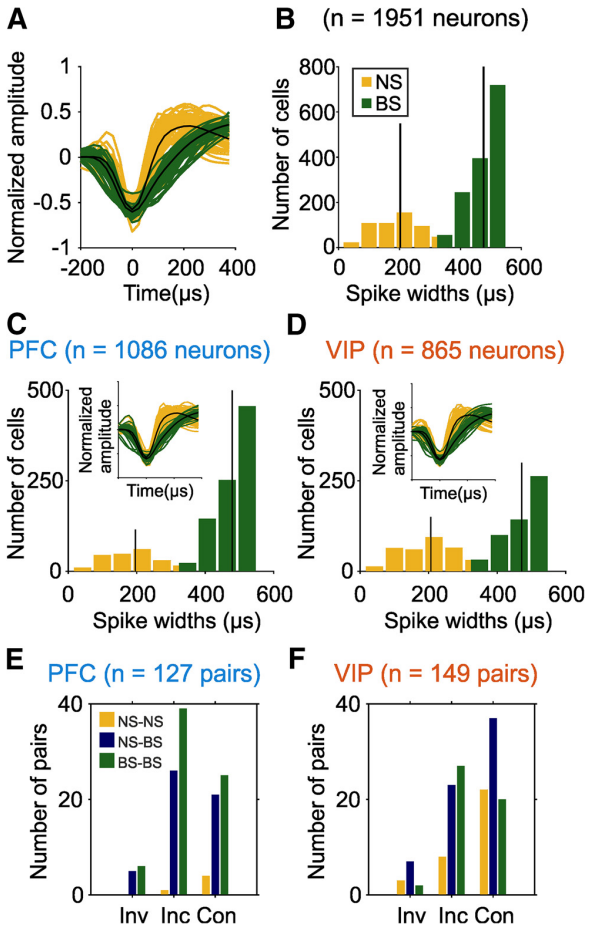

Figure 5. Classification of neuron types according to spike waveform characteristics. ***A***, Spike waveforms of 50 randomly chosen NS neurons (yellow) and BS neurons (green), aligned to their troughs. The mean waveforms of all NS and BS neurons are plotted in black. ***B***, Distribution of spike widths for all NS and BS neurons. Black vertical lines indicate the widths of the average waveforms in each class. ***C***, Histogram of 1086 PFC spike widths colored according to the classification into NS and BS classes with 50 randomly selected PFC waveforms of each class in the inset. The means of all PFC NS and BS neurons are plotted in black. Scale is the same as in ***A***. ***D***, Histogram of 865 VIP spike widths colored by class with 50 randomly chosen VIP waveforms of each class in the inset as in ***C***. ***E***, Distribution of RF similarity. Three classes of neuron pairs in PFC: Inv, Inverted; Inc, incongruent; Con, congruent. Yellow represents NS-NS pairs. Blue represents NS-BS pairs. Green represents BS-BS. ***F***, Same distribution as ***E*** for neuron pairs recorded in VIP.

pairs were again higher than PFC pairs (median $r_{horizontal}$ PFC = 0.04, median $r_{horizontal}$ VIP = 0.19; Mann–Whitney U test, $z = -2.85$, $p < 0.01$).

Comparing RF similarity in pairs of different cell classes

We hypothesized that the observed heterogeneity of adjacent neurons is related to differences in the microcircuitry in association cortex. Therefore, we first classified neurons into putative inhibitory interneurons (NS) and pyramidal projection neurons (BS) based on the waveforms characteristics of their extracellular action potentials (Fig. 5*A*) (Swadlow and Weyand, 1987; Constantinidis and Goldman-Rakic, 2002; Johnston et al., 2009). The spike widths of all the recorded neurons so classified were well separated into two distributions (Fig. 5*B*). As expected based on the abundance of interneurons and projection neurons in the neocortex (Markram et al., 2004; Shepherd, 2004), we found 81% (876 of 1086) of BS and 19% (210 of 1086) of NS neurons in PFC (Fig. 5*C*). In VIP, 62% (538 of 865) of BS and 38% (327 of 865) of NS neurons were detected (Fig. 5*D*). All neuron pairs were thus assigned to BS-BS, NS-BS, or NS-NS pairs. With the exception of NS-NS pairs that were almost absent in PFC, BS-BS (PFC = 70; VIP = 49) and NS-BS (PFC = 52; VIP = 67) pairs were abundant in both association cortices and distributed to the congruent, incongruent, and inverted RF-pair classes according to the proportions of those RF pairs (Fig. 5*E*,*F*). We compared the proportions of congruent versus incongruent pairs in the BS-BS pairs and NS-BS pairs and found a larger proportion of NS-BS pairs in VIP to be congruent ($\chi^2 = 3.87$, $p < 0.05$).

Functional connectivity of adjacent cell classes

If adjacent NS and BS cells constitute elements of microcircuits operating with inhibition and excitation, their connectivity pattern might provide insights concerning the observed differences and heterogeneity in spatial tuning in association cortices. However, even juxtaposed neurons simultaneously recorded at the same electrode tip are not necessarily functionally connected and part of a local circuit. If two neurons are functionally connected, the firing of one cell systematically coincides with, or is influenced by, the activity of the other cell on a millisecond time scale. We therefore tested for functional connectivity of cell pairs based on their temporally correlated discharge patterns by applying a cross-correlation analysis to spike trains. It measures the frequency at which one cell called "target" fires relative to the firing time of a spike in another cell known as "reference" (Salinas and Sejnowski, 2001). Therefore, if two cells are functionally coupled and one cell provides inhibitory input to the other, synchronous spiking should be suppressed resulting in a negative correlation in the cross correlogram at 0 time lag. If, however, one cell provides excitatory input to the other, spiking should coincide, resulting in a positive correlation in the cross correlogram. Alternatively, cells may receive common excitatory or inhibitory input that cause broad positive or negative correlation peaks, respectively.

Although correlations between single neurons in the association cortex are typically rare (Constantinidis et al., 2001; Constantinidis and Goldman-Rakic, 2002), we found a total of 14 pairs of BS-BS and NS-BS pairs in PFC, and 15 such pairs in VIP to be significantly coupled. Functional coupling was constant across RF trials and delayed-match-to-sample trials. In the cell pairs that could be compared, 4 PFC and 4 VIP pairs remained significantly coupled and in the same directions (excitatory or inhibitory) for both trial types. Representative examples of these functionally connected neuron pairs are depicted in Figure 6 (for BS-BS pairs) and Figure 7 (for NS-BS pairs). Overall, we observed more inhibitory connections in PFC and more excitatory connections in VIP (only 3 of 14 excitatory connections in PFC compared with 13 of 15 excitatory connections in VIP, $\chi^2 = 12.46$, $p < 0.001$). In addition, the average widths of the cross correlograms were significantly broader in VIP compared with PFC (Mann–Whitney U test, $p < 0.05$).

Among BS-BS neuron pairs, we observed that 4 of 6 PFC pairs and 5 of 7 VIP were congruent (Fig. 6*A*,*B*). These pairs were connected in opposite ways in the two brain areas. Whereas the PFC pairs' correlogram showed a negative peak indicating forward inhibition (Fig. 6*C*), the VIP pairs showed a sharp positive peak suggesting excitatory connection (Fig. 6*D*). The remaining pairs were incongruent or inverted (Fig. 6*E–H*). Whereas all 6 BS-BS pairs in PFC shared sharp inhibitory connections (Fig. 6*I*), only 1 of 7 VIP BS-BS pairs shared such a connection (Fig. 6*J*).

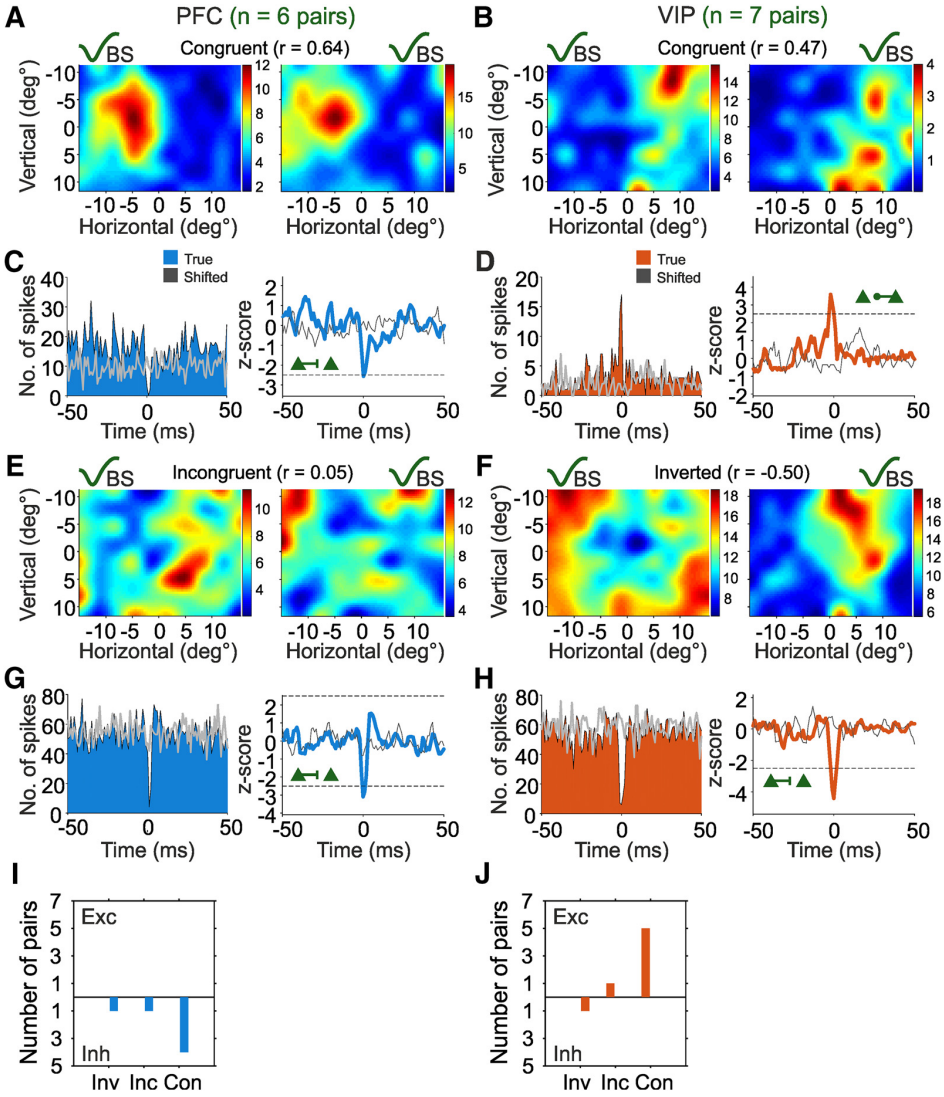

Figure 6. Distinct connectivity of BS-BS pairs in PFC and VIP. ***A***, Example of a BS-BS pair with congruent RFs recorded from the same electrode in PFC. Top, Example waveforms illustrate the cell classes. The neuron used as the trigger to produce the cross-correlogram is presented on the left of each panel. ***B***, An example BS-BS pair from the VIP with congruent RFs. ***C***, Left, Raw cross-correlogram of the neuron pair in color. Gray represents the shifted cross-correlogram. The cross-correlogram shows the distribution of spike times measured in neuron from ***A*** (right) to each spike in ***A*** (left). The shifted cross-correlogram shows the distribution of spike times measured in the subsequent trial. Right, *z* scores obtained from the raw and shifted correlograms, smoothed with a 3 ms boxcar. Dashed line indicates the significance threshold. Here, the BS neuron in ***A*** (left, top) inhibits the other BS neuron (right, top) as denoted by the green triangles linked by an inhibitory connection from left to right. ***D***, Cross-correlogram for the neuron pair presented in ***B***. Here, the BS neuron on the right is exciting the BS neuron on the left as the peak has a negative lag. ***E***, An example of an incongruent BS-BS pair from PFC. ***F***, Example pair from VIP with inverted RFs. ***G***, Cross-correlograms of pair depicted in ***E***. ***H***, Cross-correlogram of pair in ***F***. Example pair ***A*** is from Monkey L and the rest from Monkey S. Putative connection diagrams are shown on each correlogram. ***I***, Summary plot of excitatory (Exc) and inhibitory (Inh) connections and the similarity index of the resultant RFs in PFC. Inv, Inverted; Inc, incongruent; Con, congruent. ***J***, Corresponding plot for RFs in VIP.

Together, a preponderance of inhibitory connections between adjacent putative pyramidal cells in PFC contrasts with mostly excitatory connections between such cell types in VIP. Among NS-NS pairs, 12 of which we found to be functionally connected in VIP show exclusively excitatory connections, which correlated with similar RFs across those pairs (7 of 12 pairs were congruent). We did not find any functionally connected NS-NS pairs in PFC to compare against VIP.

For NS-BS neuron pairs, we observed 8 pairs with significant functional interaction in each area (Fig. 7). Six of these pairs were incongruent or inverted in PFC (Fig. 7*A*,*E*,*I*), whereas 6 of them were congruent in VIP (Fig. 7*B*,*F*,*J*). This difference in RF similarity of adjacent NS-BS pairs between PFC and VIP was statistically significant ($\chi^2 = 4$, $p < 0.05$). In NS-BS pairs of the PFC, we observed mostly sharp inhibitory (5 of 8 pairs) interactions ~0 time lag (Fig. 7*C*,*G*,*K*), indicating forward inhibition of NS on BS cells. In contrast, mostly excitatory (7 of 8 pairs) interactions were observed for NS-BS pairs in VIP (Fig. 7*D*,*H*,*L*). The temporally less precise excitatory interactions in VIP with lags between −10 and 10 ms suggest common excitatory input. Inhibitory interactions between NS-BS neurons resulted in predominantly incongruent or inverted RFs (4 of 5 PFC pairs and 1 VIP pair), whereas excitatory interactions resulted in predominantly congruent RFs (1 of 3 PFC pairs and 6 of 7 VIP pairs) and never in inverted RFs.

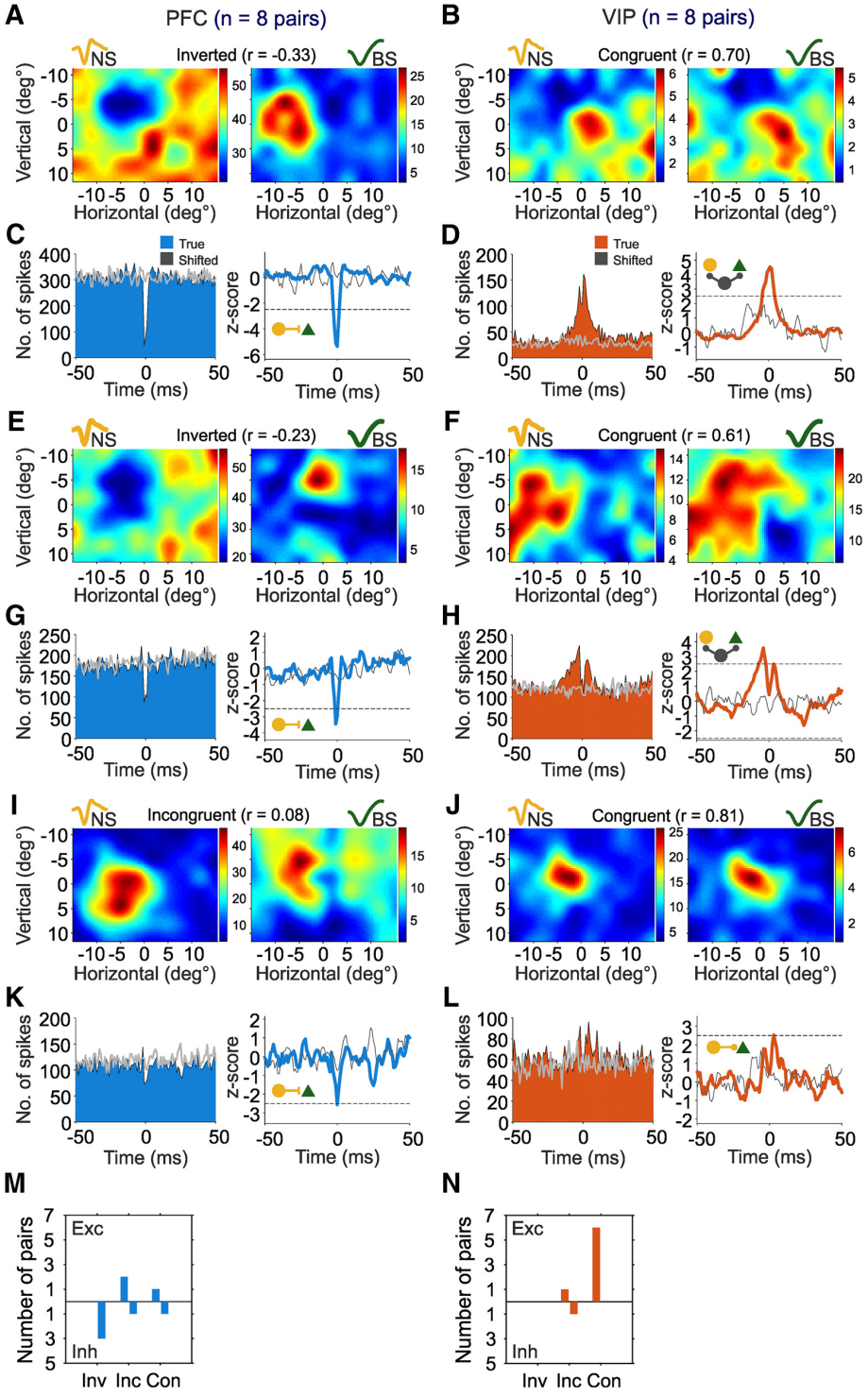

Figure 7. Distinct connectivity of NS-BS pairs in PFC and VIP. ***A***, Example of an NS-BS pair with inverted RFs recorded from the same electrode in PFC. Same layout as in Figure 5 *A*, *B*. ***B***, An example NS-BS pair with congruent RFs from the VIP. ***C***, Raw cross-correlogram of the neuron pair from ***A*** (left) and *z* scores obtained from the correlogram in color. Gray represents the shifted correlogram. Same layout as in Figure 5*C*, *D*. Here, the NS neuron in ***A*** (left, above) depicted with a yellow circle inhibits the BS neuron (right, above) shown as a green triangle. ***D***, Raw cross-correlogram (left) and *z* scores of the neuron pair from ***B***. Here, the NS neuron and BS neuron show a broad peak ~0 ms, indicating the presence of common excitatory input. ***E***, Example NS-BS pair with inverted RFs from PFC. ***F***, Example pair from VIP with congruent RFs. ***G***, Raw cross-correlogram (left) and *z* scores of the neuron pair from ***E***. ***H***, Raw cross-correlogram (left) and *z* scores of the neuron pair from ***F***. ***I***, Example PFC pair with incongruent RFs. ***J***, Example VIP pair with congruent RFs. ***K***, ***L***, Raw cross-correlogram and *z* scores of the neuron pairs from ***I*** and ***J***. Example pairs ***A***, ***B***, ***E***, and ***J*** are from Monkey L; and example pairs ***F*** and ***I*** are from Monkey S. Putative connection diagrams are shown on each correlogram. ***M***, ***N***, Summary plot of excitatory (Exc) and inhibitory (Inh) connections and RF similarity in PFC and VIP, respectively. Inv, Inverted; Inc, incongruent; Con, congruent.

Discussion

We were able to demonstrate functional connectivity between adjacent neurons of extracellularly identified putative inhibitory interneurons (NS) and pyramidal cells (BS). Temporal correlations indicative of functional connectivity between adjacent single neurons in the association cortex are typically rare; only ~5%-10% of simultaneously recorded cell pairs turn out to be functionally connected (Constantinidis et al., 2001; Constantinidis and Goldman-Rakic, 2002; Diester and Nieder, 2008). This is consistent with our findings of ~10% of connected neuron pairs. Despite our large sample of simultaneously recorded cell pairs in both the PFC and the VIP, the number of connected pairs, particularly when segregated into different cell classes, remained relatively small. Despite this limitation, the differences in functional connectivity between putative inhibitory interneurons and pyramidal cells in PFC and VIP are statistically robust.

In the PFC, we found more inhibitory and also more temporally precise functional connections between adjacent neurons than in VIP. Both BS-BS and NS-BS pairs in PFC were characterized by primarily negative and sharp connections. This inhibitory connection pattern in PFC correlated with a higher frequency of incongruent or inverted RFs. Both findings are suggestive of primarily inhibitory effects of adjacent neurons in PFC. Such temporally precise inhibitory effects suggest lateral feedforward inhibition between neurons representing different visual field locations that may modulate neuronal responsiveness, especially to stimulation of the borders of RFs, effectively resulting in smaller excitatory areas. The real world does not, however, consist of single stimuli presented at a time (as in our experiment); virtually all retinal locations are affected simultaneously. This multitude of competing activations at different locations may cause strong inhibitory interactions between neurons located at different points of the visuotopic map and perhaps a substantial shrinkage of excitatory RFs toward their functional center. Lateral inhibition may contribute to the production of such sharp peaks of neural activity as a function of location in the visual field.

The functional connectivity of cell types with respect to the properties of spatial RFs has not been investigated in PFC (or VIP) before. However, it has been shown that neighboring NS and BS cells in the primate PFC can exhibit opposite tuning characteristics. When comparing the responses of NS and BS neurons that were recorded within 400 mm of each other, Wilson et al. (1994) observed opposite spatial location selectivity of NS and BS cells (but see also Rao et al., 1999 for similar spatial preferences of adjacent NS and BS neurons). Moreover, inhibitory connections were predominant in PFC cell pairs with dissimilar spatial tuning profiles (Constantinidis and Goldman-Rakic, 2002). Beyond sculpting the processing of spatial information, inhibitory input by putative interneurons has also been implicated in shaping the tuning to numerosities of putative PFC pyramidal cells (Diester and Nieder, 2008; Nieder, 2016) and tuning to objects of nearby neurons in the IT cortex (Wang et al., 2000, 2002; Tamura et al., 2004). Because different cortical cell types also show distinct sensitivity to dopaminergic influence (Jacob et al., 2013, 2016; Ott et al., 2014), the shaping of RFs may also be modulated by neuromodulators, in addition to GABAergic inhibition.

The functional connectivity patterns in relation to cell types differed markedly in parietal area, VIP. We found more excitatory and temporally less precise connections in VIP relative to PFC. Both BS-BS and NS-BS neuron pairs showed excitatory connections. However, whereas BS-BS pairs exhibited sharp positive correlation peaks indicative of excitatory feedforward excitation, NS-BS pairs mostly showed broad excitatory peaks suggesting common input. This is reminiscent of V1, where fast-spiking interneurons and neighboring pyramidal neurons have been found to share excitatory input (Yoshimura and Callaway, 2005; Yoshimura et al., 2005). Consistent with the idea of common input is the finding of mostly congruent RFs of NS-BS pairs. This points to a V1-like response pooling within a certain local population (Swadlow and Gusev, 2002). These remarkable differences in the functional connectivity of adjacent cortical cell types between PFC and VIP argue for substantial differences in the wiring of posterior parietal cortex that shares patterns with early visual areas, and prefrontal local circuits that seem to have developed differently.

The observed incongruencies in spatial RF characteristics and functional connectivity argue for differences in microcolumn organization between neocortical areas that subserve different functions. The reciprocally connected association areas of the parietal and frontal cortices are particularly well suited to maintain information across time and to exert cognitive control (Miller and Cohen, 2001). In contrast to early visual cortices, the areas of the posterior parietal and prefrontal cortices are connected not only to each other (Lewis and Van Essen, 2000), but also up to over a dozen other widely distributed cortical areas, all interconnected by common thalamic input from the medial pulvinar nucleus (Selemon and Goldman-Rakic, 1988). In addition, the areas in this network display noncanonical circuit properties (Goldman-Rakic, 1988); in contrast to canonical circuits of the sensory and motor cortices, many connections within this network lack a clear sensory-motor hierarchical polarity with consistent feedforward and feedback laminar termination patterns. Instead, the noncanonical network seems to be designed for parallel and reentrant processing. Such recurrent loops of the noncanonical association cortex give rise to persistent (or sustained) neuronal activity that enables neurons to actively buffer and process information during working memory periods (Merten and Nieder, 2012). Because high-level cognitive functioning would be impossible without persistent activity, microcircuits and their excitatory and inhibitory neuronal connections might be geared toward reentrant loops and, therefore, inevitably differ from sensory neocortex.

References

Aertsen AM, Gerstein GL, Habib MK, Palm G (1989) Dynamics of neuronal firing correlation: modulation of "effective connectivity." J Neurophysiol 61:900–917.

Avillac M, Denève S, Olivier E, Pouget A, Duhamel JR (2005) Reference frames for representing visual and tactile locations in parietal cortex. Nat Neurosci 8:941–949. CrossRef Medline

Avillac M, Ben Hamed S, Duhamel JR (2007) Multisensory integration in the ventral intraparietal area of the macaque monkey. J Neurosci 27: 1922–1932. CrossRef Medline

Chen X, DeAngelis GC, Angelaki DE (2014) Eye-centered visual receptive fields in the ventral intraparietal area. J Neurophysiol 112:353–361. CrossRef Medline

Colby CL, Duhamel JR, Goldberg ME (1993) Ventral intraparietal area of the macaque: anatomic location and visual response properties. J Neurophysiol 69:902–914. Medline

Constantinidis C, Goldman-Rakic PS (2002) Correlated discharges among putative pyramidal neurons and interneurons in the primate prefrontal cortex. J Neurophysiol 88:3487–3497. CrossRef Medline

Constantinidis C, Franowicz MN, Goldman-Rakic PS (2001) Coding specificity in cortical microcircuits: a multiple-electrode analysis of primate prefrontal cortex. J Neurosci 21:3646–3655. Medline

DeAngelis GC, Ghose GM, Ohzawa I, Freeman RD (1999) Functional micro-organization of primary visual cortex: receptive field analysis of nearby neurons. J Neurosci 19:4046–4064. Medline

de Oliveira SC, Thiele A, Hoffmann KP (1997) Synchronization of neuronal activity during stimulus expectation in a direction discrimination task. J Neurosci 17:9248–9260. Medline
Diester I, Nieder A (2008) Complementary contributions of prefrontal neuron classes in abstract numerical categorization. J Neurosci 28:7737–7747. CrossRef Medline
Douglas RJ, Martin KA (2004) Neuronal circuits of the neocortex. Annu Rev Neurosci 27:419–451. CrossRef Medline
Duhamel JR, Colby CL, Goldberg ME (1998) Ventral intraparietal area of the macaque: congruent visual and somatic response properties. J Neurophysiol 79:126–136. Medline
Fuster JM (2000) Executive frontal functions. Exp Brain Res 133:66–70. CrossRef Medline
Goldman-Rakic PS (1988) Topography of cognition: parallel distributed networks in primate association cortex. Annu Rev Neurosci 11:137–156. CrossRef Medline
Goldman-Rakic PS (1995) Cellular basis of working memory. Neuron 14:477–485. CrossRef Medline
Guipponi O, Wardak C, Ibarrola D, Comte JC, Sappey-Marinier D, Pinède S, Ben Hamed S (2013) Multimodal convergence within the intraparietal sulcus of the macaque monkey. J Neurosci 33:4128–4139. CrossRef Medline
Hubel DH, Wiesel TN (1962) Receptive fields, binocular interaction and functional architecture in the cat's visual cortex. J Physiol 160:106–154. CrossRef Medline
Jacob SN, Nieder A (2014) Complementary roles for primate frontal and parietal cortex in guarding working memory from distractor stimuli. Neuron 83:226–237. CrossRef Medline
Jacob SN, Ott T, Nieder A (2013) Dopamine regulates two classes of primate prefrontal neurons that represent sensory signals. J Neurosci 33:13724–13734. CrossRef Medline
Jacob SN, Stalter M, Nieder A (2016) Cell-type-specific modulation of targets and distractors by dopamine D1 receptors in primate prefrontal cortex. Nat Commun 7:13218. CrossRef Medline
Johnston K, DeSouza JF, Everling S (2009) Monkey prefrontal cortical pyramidal and putative interneurons exhibit differential patterns of activity between prosaccade and antisaccade tasks. J Neurosci 29:5516–5524. CrossRef Medline
Kravitz DJ, Saleem KS, Baker CI, Mishkin M (2011) A new neural framework for visuospatial processing. Nat Rev Neurosci 12:217–230. CrossRef Medline
Kremkow J, Jin J, Wang Y, Alonso JM (2016) Principles underlying sensory map topography in primary visual cortex. Nature 533:52–57. CrossRef Medline
Lewis JW, Van Essen DC (2000) Corticocortical connections of visual, sensorimotor, and multimodal processing areas in the parietal lobe of the macaque monkey. J Comp Neurol 428:112–137. CrossRef Medline
Markram H, Toledo-Rodriguez M, Wang Y, Gupta A, Silberberg G, Wu C (2004) Interneurons of the neocortical inhibitory system. Nat Rev Neurosci 5:793–807. CrossRef Medline
Merchant H, de Lafuente V, Peña-Ortega F, Larriva-Sahd J (2012) Functional impact of interneuronal inhibition in the cerebral cortex of behaving animals. Prog Neurobiol 99:163–178. CrossRef Medline
Merten K, Nieder A (2012) Active encoding of decisions about stimulus absence in primate prefrontal cortex neurons. Proc Natl Acad Sci U S A 109:6289–6294. CrossRef Medline
Mikami A, Ito S, Kubota K (1982) Visual response properties of dorsolateral prefrontal neurons during visual fixation task. J Neurophysiol 47:593–605. Medline
Miller EK, Cohen JD (2001) An integrative theory of prefrontal cortex function. Annu Rev Neurosci 24:167–202. CrossRef Medline
Mishkin M, Ungerleider LG, Macko KA (1983) Object vision and spatial vision: two cortical pathways. Trends Neurosci 6:414–417. CrossRef
Nieder A (2012) Supramodal numerosity selectivity of neurons in primate prefrontal and posterior parietal cortices. Proc Natl Acad Sci U S A 109:11860–11865. CrossRef Medline
Nieder A (2016) The neuronal code for number. Nat Rev Neurosci 17:366–382. CrossRef Medline
Nieder A, Miller EK (2004) A parieto-frontal network for visual numerical information in the monkey. Proc Natl Acad Sci U S A 101:7457–7462. CrossRef Medline
O'Scalaidhe SP, Wilson FA, Goldman-Rakic PS (1997) Areal segregation of face-processing neurons in prefrontal cortex. Science 278:1135–1138. CrossRef Medline
Ott T, Jacob SN, Nieder A (2014) Dopamine receptors differentially enhance rule coding in primate prefrontal cortex neurons. Neuron 84:1317–1328. CrossRef Medline
Rainer G, Asaad WF, Miller EK (1998) Memory fields of neurons in the primate prefrontal cortex. Proc Natl Acad Sci U S A 95:15008–15013. CrossRef Medline
Ramirez-Cardenas A, Moskaleva M, Nieder A (2016) Neuronal representation of numerosity zero in the primate parieto-frontal number network. Curr Biol 26:1285–1294. CrossRef Medline
Rao SG, Williams GV, Goldman-Rakic PS (1999) Isodirectional tuning of adjacent interneurons and pyramidal cells during working memory: evidence for microcolumnar organization in PFC. J Neurophysiol 81:1903–1916. Medline
Romero MC, Janssen P (2016) Receptive field properties of neurons in the macaque anterior intraparietal area. J Neurophysiol 115:1542–1555. CrossRef Medline
Rosa MG (1997) Cerebral cortex, Vol 12: Extrastriate cortex in primates (Rockland KS, Kaas JH, Peters A, eds). New York: Plenum.
Salinas E, Sejnowski TJ (2001) Correlated neuronal activity and the flow of neural information. Nat Rev Neurosci 2:539–550. CrossRef Medline
Schlack A, Sterbing-D'Angelo SJ, Hartung K, Hoffmann KP, Bremmer F (2005) Multisensory space representations in the macaque ventral intraparietal area. J Neurosci 25:4616–4625. CrossRef Medline
Selemon LD, Goldman-Rakic PS (1988) Common cortical and subcortical targets of the dorsolateral prefrontal and posterior parietal cortices in the rhesus monkey: evidence for a distributed neural network subserving spatially guided behavior. J Neurosci 8:4049–4068. Medline
Shepherd GM (2004) The synaptic organization of the brain, Ed 5. New York: Oxford UP.
Sugihara T, Diltz MD, Averbeck BB, Romanski LM (2006) Integration of auditory and visual communication information in the primate ventrolateral prefrontal cortex. J Neurosci 26:11138–11147. CrossRef Medline
Suzuki H, Azuma M (1983) Topographic studies on visual neurons in the dorsolateral prefrontal cortex of the monkey. Exp Brain Res 53:47–58. Medline
Swadlow HA, Gusev AG (2002) Receptive-field construction in cortical inhibitory interneurons. Nat Neurosci 5:403–404. CrossRef Medline
Swadlow HA, Weyand TG (1987) Corticogeniculate neurons, corticotectal neurons, and suspected interneurons in visual cortex of awake rabbits: receptive-field properties, axonal properties, and effects of EEG arousal. J Neurophysiol 57:977–1001. Medline
Tamura H, Kaneko H, Kawasaki K, Fujita I (2004) Presumed inhibitory neurons in the macaque inferior temporal cortex: visual response properties and functional interactions with adjacent neurons. J Neurophysiol 91:2782–2796. CrossRef Medline
Viswanathan P, Nieder A (2013) Neuronal correlates of a visual "sense of number" in primate parietal and prefrontal cortices. Proc Natl Acad Sci U S A 110:11187–11192. CrossRef Medline
Viswanathan P, Nieder A (2015) Differential impact of behavioral relevance on quantity coding in primate frontal and parietal neurons. Curr Biol 25:1259–1269. CrossRef Medline
Wang Y, Fujita I, Murayama Y (2000) Neuronal mechanisms of selectivity for object features revealed by blocking inhibition in inferotemporal cortex. Nat Neurosci 3:807–813. CrossRef Medline
Wang Y, Fujita I, Tamura H, Murayama Y (2002) Contribution of GABAergic inhibition to receptive field structures of monkey inferior temporal neurons. Cereb Cortex 12:62–74. CrossRef Medline
Wilson FA, O'Scalaidhe SP, Goldman-Rakic PS (1994) Functional synergism between putative gamma-aminobutyrate-containing neurons and pyramidal neurons in prefrontal cortex. Proc Natl Acad Sci U S A 91:4009–4013. CrossRef Medline
Yoshimura Y, Callaway EM (2005) Fine-scale specificity of cortical networks depends on inhibitory cell type and connectivity. Nat Neurosci 8:1552–1559. CrossRef Medline
Yoshimura Y, Dantzker JL, Callaway EM (2005) Excitatory cortical neurons form fine-scale functional networks. Nature 433:868–873. CrossRef Medline
Zaksas D, Pasternak T (2006) Directional signals in the prefrontal cortex and in area MT during a working memory for visual motion task. J Neurosci 26:11726–11742. CrossRef Medline

Study 5: Number within and without the receptive field

Viswanathan, P., Nieder, A. (in preparation). Category tuning for stimuli within and outside receptive fields by primate prefrontal and parietal neurons

Category tuning for stimuli within and outside receptive fields by primate prefrontal and parietal neurons

Pooja Viswanathan & Andreas Nieder*

Animal Physiology, Institute of Neurobiology, Auf der Morgenstelle 28, University of Tübingen, 72076 Tübingen, Germany

Number of figures: 9
Number of words: Abstract – 229, Main text – 6378

Keywords: receptive field, numerosity, prefrontal cortex, posterior parietal cortex

* To whom correspondence should be addressed:
E-mail: andreas.nieder@uni-tuebingen.de

ABSTRACT

The primate fronto-parietal network is interdependent and synergistically involved in a variety of functions. During tasks presenting discriminative stimuli in different parts of space, single neurons in the network encode spatial as well as non-spatial variables of the task such as motion direction, speed or abstract categories. Recent studies have shown that these variables are processed in interconnected areas of the network in a distributed and parallel fashion. It is not known to what extent and how the location of stimuli dictates responses to other essential features like numerosity. To truly dissociate these factors from each other, we mapped the receptive fields of single neurons in prefrontal cortex (PFC) and the ventral intraparietal area (VIP) as monkeys passively fixated the centre of the screen. We then recorded these neurons during two kinds of discrimination tasks (colour or number) where the stimuli were always displayed in the centre of the screen. We found that the location of PFC receptive fields at the centre of the screen strongly predicted the recruitment of those neurons in encoding the number of dots in the discrimination task, but not the colour of those dots. VIP neurons, on the other hand, were strongly feature-selective if they were spatially-selective, regardless of the location of their receptive field. Further, the presence of spatial selectivity or the location thereof did not affect the strength of number discriminability in the selective neurons in either area.

INTRODUCTION

The fronto-parietal network comprising numerous areas of frontal and parietal cortices, are highly interconnected (Lewis & Van Essen, 2000) and jointly implicated in visuospatial processing. In particular, these areas have been studied together in tasks testing spatial working memory or the processing of spatial cues. Damage or inactivation of either node changes the nature of spatial tuning in the other and produces deficits in the associated behaviours (Quintana *et al.*, 1989; Chafee & Goldman-Rakic, 2000; Wardak *et al.*, 2011; Suzuki & Gottlieb, 2013). However, many areas in the fronto-parietal network are also thought to play a central role in many non-spatial cognitive functions, like decision-making (Merten & Nieder, 2012), rule-guided behaviour (Bongard & Nieder, 2010; Eiselt & Nieder, 2013) as well as estimation of magnitudes like number (Nieder, 2012; Ramirez-Cardenas *et al.*, 2016), proportions (Tudusciuc & Nieder, 2009; Vallentin & Nieder, 2010) as well as perceptual categories (Freedman & Assad, 2006; Swaminathan & Freedman, 2012).

Whether the spatial location of stimuli and the non-spatial discriminative features of stimuli co-exist in the same neuronal populations in not clearly understood. Some lines of evidence indicate that they might because higher order association areas are uniquely poised to have neurons that engage in both aspects. Ventral intraparietal area in the posterior parietal cortex receives multi-modal input and single neurons respond to bi-modal or multi-modal stimuli in relation to a common spatial reference frame (Avillac *et al.*, 2005, 2007). For instance, certain neurons respond selectively to visual stimuli in the fovea and tactile stimuli on the muzzle of the monkey (Duhamel *et al.*, 1998). Some multi-modal neurons respond selectively to a specific number of items presented in simultaneous visual or sequential auditory form (Nieder, 2012). Similarly, neurons in the prefrontal cortex respond to multi-modal stimuli or various phases of a task: sensory, mnemonic or response-related (Fuster & Alexander, 1971; Suzuki, 1985; Mochizuki & Funahashi, 2016). Other neurons are responsive to internal states

such as covert attention, reward expectation or arousal (Leon & Shadlen, 1999; Roesch & Olson, 2004; Asaad & Eskandar, 2011; Tremblay *et al.*, 2015). Thus, the responses of single neurons are shaped by factors that may be spatial or non-spatial in nature.

An important respect in which space can dictate a neuron's response is through its receptive field (RF). In higher order areas, stimuli within a neuron's RF can drive its response faster than stimuli outside the RF (Mountcastle *et al.*, 1975; Wimmer *et al.*, 2016). Stimuli within the RF can elicit a greater mnemonic response than the same stimuli presented outside of the RF (Funahashi & Bruce, 1989; Rainer *et al.*, 1998). Spatial positions of stimuli also drive the choice-related signals such that upcoming movements into the preferred spatial field are predicted better than those into the opposite spatial field (Hasegawa *et al.*, 2000; Shadlen & Newsome, 2001). Therefore, it is necessary to dissociate the spatial and non-spatial aspects of a task to determine how they interplay since RFs are not static and can change during a task as a result of spatial attention even in lower order areas like V4 and MT.

We addressed this problem by comparing the locations of visual receptive fields (RF) and stimulus-selective responses of single neurons to the varying colour and number of dots recorded in prefrontal cortex and the ventral intraparietal area. Interleaved blocks allowed us to create detailed RF maps of many neurons from trials of passive fixation as well as observe the same neurons during discrimination tasks without a spatial component. We used two kinds of delayed match-to-sample tasks, the first was a colour discrimination task and the second a number discrimination task. This gave us the unique opportunity to contrast two different stimulus features across two different areas and specifically contrast how the spatial and non-spatial aspects of stimulus processing interact.

MATERIALS AND METHODS

Experimental animals

Two adult male rhesus monkeys (Macaca mulatta), monkey L and monkey S served as subjects for this experiment. They weighed 5.5 to 6.3kg in the duration of this study. They were socially housed in groups of two to four monkeys of the same sex. During experiments, the monkeys sat in primate chairs within darkened experimental chambers. The primate chairs were positions 57cm from a flat-screen monitor (15″, 1024x768 display resolution at 75Hz) which was used for stimulus presentation. They received fluid rewards upon successful completion of trials. All experimental procedures have been reported previously (Viswanathan & Nieder, 2013, 2015, 2017) and were in accordance with the guidelines for animal experimentation approved by the national authority, the Regierungspräsidium, Tübingen, Germany.

Behavioural tasks

We trained both monkeys using the NIMH Cortex programme to present the stimuli, monitor their behaviour and collect their responses. We used an infrared eye-tracking system (ISCAN, Cambridge, MA). The monkeys performed a delayed match-to-sample task (see **Figure 1A**) with two kinds of discriminative stimuli, colours and numbers (see **Figure 1B**). Each trial began when the monkeys fixated within 1.75° of a central fixation spot for 500ms, a sample display then came on for 800ms and disappeared thereafter giving way to a delay period of 1000ms. Following this, a test display was shown for 1200ms. During the colour discrimination task, the monkeys were trained to respond to test stimulus if it matched the colour of the sample stimulus that appeared at the beginning of the trial. The monkeys were then trained to discriminate the stimuli based on the number of coloured dots and respond to

the test stimulus if it matched the sample stimulus in the number of items. If a non-match test display was shown, the monkeys had to withhold their response until a match stimulus appeared. We presented the 5 colours (Purple, Yellow, Green, Blue and Red) in all 5 numbers (one to five dots) for the colour discrimination task. For the number discrimination task, we presented one to five dots in black colour. New stimulus images were created for every session with the dots placed at randomised positions and of randomised sizes. To ensure that the lower visual features, like coloured area and the density of display that co-vary with increasing number of dots in randomly generated 'standard' images did not influence the monkeys' behaviour, we created a set of 'control' stimuli that equated these values across numbers within the 6° grey background circle. The various factors, colour in the first task, number, stimulus protocol ('standard' or 'control' type of stimuli), type of trials (match or non-match) were balanced across trials. The various conditions could be sampled over a minimum of 200 trials.

We used a passive fixation task to map the receptive fields of single neurons. The blocks of passive fixation task were interleaved with blocks of the delayed match-to-sample task. For each trial, monkeys fixated a central fixation spot as a moving bar appeared at five successful locations. The moving bar was grey in colour, had the dimensions of 3° of visual angle (or dva) in length and 0.20° in breadth. The bar appeared at each position in two orientations moving at a constant speed of 8°/sec in four directions, first oriented vertically moving left and right, then oriented horizontally moving up and down. Each position was explored for 1000ms and five positions were tested in each trial (see **Figure 1C**) such that the whole screen (30.5°x23°, 80 positions) could be sampled over 16 such trials (see **Figure 1D**).

Electrophysiological recordings

We implanted the monkeys with a head bolt in the early stages of behavioural training. The head bolt enabled us to immobilize the head during training and recording sessions and monitor their eye movements. After their behavioural performance reached an average of 80% correct discrimination of stimuli, we implanted recording chambers over the dorsolateral prefrontal cortex, centred on the principal sulcus and area VIP in depths of the intraparietal sulcus guided by anatomical MRI and stereotaxic measurements (see **Figure 2** and **3**). Both chambers were implanted in the right hemisphere of both monkeys. The surgical procedures were performed under sterile conditions while the monkeys were under general anaesthesia and received post-surgical care. The electrophysiological signals were amplified, filtered and waveforms of the action potentials sampled at 40kHz were stored (Plexon Systems, USA) so that they could be sorted offline. We recorded 1186 PFC (507 from monkey L, 679 from monkey S) and 944 VIP (388 from monkey L, 556 from monkey S) neurons from 52 sessions of colour discrimination (23 with monkey L, 29 with monkey S) and 60 sessions of number discrimination (33 with monkey L, 27 with monkey S), both combined with RF measurements.

Neuronal data analysis

All data analysis was performed using custom-written scripts in the MATLAB computational environment (Mathworks). We analysed all the neurons that were recorded for at least 2 trials per position during the passive fixation blocks and 30 trials per sample number during the delayed match-to-sample blocks. An additional criteria of a minimum firing rate of 0.5Hz during the DMS trials, in the period from fixation to delay was imposed on the neurons. We used a default latency of 50ms for VIP neurons and 100ms for PFC neurons to place our analysis windows. The default latency values were based on well-established response latencies in these two areas (Nieder & Miller, 2004a; Viswanathan & Nieder, 2013). For the

current study, we analysed responses in 389 PFC neurons and 338 VIP neurons that passed the criteria for both blocks.

Visual receptive fields

We have described the procedure of creating receptive field maps in detail before (Viswanathan & Nieder, 2017). Briefly, we selected visually responsive neurons on the basis of a 3-factor ANOVA with the factors position, direction and orientation on firing rates collected in 250ms windows. For the neurons with a main effect of position ($p < 0.05$), we created RF maps by averaging the responses at each position, interpolating the responses and smoothing the responses in two dimensions with a Gaussian function. We then checked that these RF maps were consistent across trials by creating two maps for each neuron with half the trials. We compared the correlation between the first and second maps against a shuffled distribution of correlations obtained from shuffled first and second maps ($p < 0.05$). After this test was passed, we obtained RF maps for 65% (252/389) PFC neurons and 62% (210/338) VIP neurons that pass our criteria for both blocks. We normalised each map to its maximum across all positions. The RF of each cell was defined as the area where the neuron exhibited more than half-max activity (Rainer *et al.*, 1998; Romero & Janssen, 2016). Average maps across groups of neurons were created by averaging these normalised maps.

Single neuron responses to task variables

We have described the procedure for testing the neurons for stimulus-selective responses in detail before (Viswanathan & Nieder, 2015). For the colour discrimination task, we tested neurons for colour-selective, number-selective and stimulus protocol-selective responses with a 3-factor ANOVA. For the number discrimination task, we tested neurons with a 2-factor ANOVA for the stimulus features of number and protocol. We did this for the sample phase with firing rates collected in 800ms windows with the area-appropriate offsets. We also did this for the delay phase with firing rates collected in the last 800ms of the delay period. We

evaluated all these tests with an alpha of 0.01. The neurons that showed a main effect of colour or a main effect of number were thus termed colour-selective or number-selective neurons. Their tuning functions were created by averaging their responses to the corresponding sample type across all trials (for instance, towards all red-coloured samples, or towards all samples with 3 dots) in the specified analysis window. During the colour discrimination task, we found 10% (22/215) PFC neurons and 14% (25/184) VIP neurons showed colour selectivity and 16% (34/215) PFC neurons and 14% (26/184) VIP neurons were number-selective. Overall, 18% (69/389) of PFC neurons and 13% (45/338) of VIP neurons showed number selectivity across both DMS tasks. For the number-selective neurons, we created average tuning curves by centring individual tuning curves at the preferred number and expressing responses to the other numbers as the numerical distance from the preferred number. The response to the preferred number was considered as 100% and to the least preferred number as 0%. All other values were normalised to this scale.

Analysis of stimulus selectivity by RF type

To compare the stimulus-selective responses across the different kinds of RFs, we classified the neurons into 3 classes: neurons that do not show a significant RF (nRF), neurons whose RFs do not overlap with the centre where the DMS task stimuli were always shown (RF-out) and neurons whose RFs overlap with the centre of the screen/DMS stimuli (RF-in). The stimuli in the DMS task were always displayed centrally, around the fixation target. Stimulus overlap was present if the RF covered the area occupied by the grey circle or if the RF maxima occurred inside the grey circle. We compared the proportions of the three classes of neurons in our recorded population and those that are selective for the various task variables using the chi-square test of independence, evaluated with an alpha of 0.05. We examined the population activity across time in the 3 classes by normalising the firing rates to the baseline collected during the middle 350ms of the fixation period and dividing by standard deviation

of baseline across trials. We used a sliding window Kruskal-Wallis test to test class-wise differences in this activity and consider differences significant if they are consistent across 50 or more consecutive windows (>50ms). We calculated a receiver operating characteristic (ROC) curve to evaluate how well the task features are discriminated by the selective neurons. We considered the response towards the most preferred stimulus (colour/number) as the true positive rate and the response towards the least preferred stimulus as the false positive rate. Using these, an ROC curve was generated for each neuron, from which the area under the ROC curve was an indicator of how well the neuron discriminated between its preferred and least preferred stimulus. A value of 0.5 indicated chance level discrimination and a value of 1 indicated ideal discrimination. We also calculated AUROC values in a sliding window of 50ms moved in steps of 1ms to have a time-resolved test of stimulus discriminability between the 3 neuronal classes.

RESULTS

We studied the activity of single neurons in PFC and VIP during a delayed match-to-sample task where the visual stimuli were dots within a grey circle presented centrally (**Figure 1A**). Two monkeys were trained to perform a colour discrimination task and subsequently, after a period of further training, a number discrimination task. The monkeys fixated a central fixation spot and held the response bar for 500ms of fixation, following which a sample stimulus was displayed for 800ms. The sample dots then disappeared for 1s delay and were followed by a test display. The monkeys were trained to respond if the test stimuli matched the sample stimuli in the relevant feature and withhold response if it did not until a matching stimulus appeared. The task structure remained identical for both tasks. The stimuli during the colour discrimination task varied in colour (5 colours) and number (1-5) of coloured dots (**Figure 1B**) within the grey circle while the number discrimination task had stimuli with uniformly coloured black dots. To ensure that the monkeys' behaviour and the neuronal activity were independent of co-varying visual features, we used two set of stimuli. The 'standard' dots were randomly sized and spaced while the 'control' dots summed to the same area and had the same average spacing such that the total coloured area and density stayed constant with increasing number of dots. Both monkeys performed much better than chance at the discrimination tasks (Viswanathan & Nieder, 2013, 2015).

We further characterised the receptive fields of PFC and VIP neurons using a moving bar presented at various locations of the screen as the monkeys passively fixated the central fixation spot (**Figure 1C**). Five positions were sampled in each trial such that the entire screen (80 positions) could be mapped over 16 trials (**Figure 1D**) embedded within a block. This allowed us to obtain detailed RF maps of neurons that showed spatial selectivity (Viswanathan & Nieder, 2017)(Viswanathan & Nieder, *in press*). PFC neurons displayed more contra-lateral RFs than VIP, which had predominantly foveal RFs.

As the blocks of the active discrimination task and the passive fixation task were interleaved during the recording sessions, we obtained information about task-related activity and spatial selectivity from 389 PFC neurons and 338 VIP neurons. We traced the recording sites to the anatomical locations based on the MR images and stereotaxic measurements (**Figures 2** and **3**). PFC recordings were made around the principal sulcus in monkey L (**Figure 2B,** *left*) and monkey S (**Figure 2B,** *right*). VIP recordings were made in the depths of the intraparietal sulcus in monkey L (**Figure 2C** and **D,** *left*) and monkey S (**Figure 2C** and **D,** *right*). The proportions of colour-selective neurons (**Figure 2**) and number-selective neurons (**Figure 3**) at the various sites are indicated by their colour in both figures. The RFs at the various locations did not show a strong site-wise distribution (Viswanathan & Nieder, *in press*).

Next, we examined the RFs of neurons exhibiting stimulus selectivity. The colour discrimination task involved simple category membership as we used primary colours and did not vary hue in a continuous fashion. Both the monkeys excelled at the task and performed with greater than 97% accuracy. However, selective responses to colour were not common in PFC or VIP. 10% (22/215) PFC neurons responded selectively to the colour of the stimuli and 14% (25/184) VIP neurons were colour-selective. Notably, the DMS stimuli were always shown centrally, around the fixation target whereas the recorded neurons had a range of visual RFs all over the screen. We observed that some colour-selective PFC and VIP neurons had RFs that overlapped with the location of the colour stimuli (**Figures 4A** and **B**, respectively). But some neurons were selective for colour despite having RFs that did not overlap with the location where the colour stimuli were shown (**Figures 4C** and **D**). Despite the monkeys being engaged in a colour discrimination task, neurons in both areas responded selectively to the varying number of dots in the sample stimuli. In fact, a larger proportion of PFC neurons were selective for number than colour (chi-square = 4.59, $p < 0.05$). Over both tasks, 18% (69/389) PFC neurons were selective for the number of dots and 13% (45/338)

VIP neurons were number-selective. We also found neurons exhibiting classical tuning curves for the number of dots. Some of these neurons in PFC and VIP had receptive fields that overlapped with the location of the discriminative stimuli (**Figures 5A** and **B**). Many neurons were selective for number stimuli even when they were presented outside their RFs (**Figures 5C** and **D**).

In order to quantify the relationship between category selectivity and spatial selectivity, we classified the recorded neurons into 3 types based on their spatial selectivity; neurons that were not significantly spatially-selective (**Figure 6A** and **B**), neurons that had RFs away from the centre (**Figure 6C** and **D**) and neurons that had RFs overlapping with the task stimulus location (**Figure 6E** and **F**). The average maps in **Figure 6** depict the responses of such RFs, each map normalised and then those belonging to a class averaged for each area. In PFC, we found 35% (137/389) of the neurons belonging to the no-RF-class, 48% (186/389) belonging to the stimulus outside RF class, and 17% (66/389) belonging to the central-RF class, respectively. In VIP, we found a higher proportion of neurons with central RFs where the stimuli were presented. The distribution of neurons by RF class was more equitable than in PFC, 38% (128/338), 38% (130/338) and 24% (80/338), respectively. The proportions were significantly different across area (chi-square = 8.034, $p < 0.05$). This difference in relative proportions was even stronger when we only considered the neurons recorded during colour discrimination exclusively (chi-square = 11.262, $p < 0.01$). PFC neurons were distributed as 27% (57/215) with no RFs, 57% (123/215) with stimulus outside RFs and 16% (35/215) with stimulus in RFs across the 3 classes while VIP neurons were distributed as 34% (62/184), 41% (75/184) and 26% (47/184), respectively.

Of these classes, we calculated the probability of exhibiting colour selectivity given the RF location (**Figure 7**). During the colour discrimination task, we found that PFC neurons were not differentially selective to the task features of colour based on RF type (chi-

square = 1.042, p = 0.5939). While 7% (4/57) of neurons without a significant RF were selective for colour, 11% (13/123) with stimulus out of RF and 14% (5/35) with stimulus in RF were also selective for the colour of discriminative stimuli. Similarly, colour selectivity was distributed equitably across the 3 RF classes in VIP with 8% (5/62) colour-selectivity in the nRF class, 17% (13/75) in stimulus out of RF and 15% (7/47) in those with stimulus in their RFs (chi-square = 2, p = 0.3679).

Notably, when we considered selectivity for number across the colour and number discrimination tasks, the probability of exhibiting number selectivity differed across RF classes (**Figure 8**). In PFC, only 10% (14/137) of neurons without RFs were selective, 18% (33/186) of neurons with stimulus outside RFs were selective and as many as 33% (22/66) of neurons with stimulus in RFs were selective for the number of dots in the sample phase (chi-square = 10.749, p = 0.0046). This bias was also present when we considered number-selective populations in the two tasks separately. We saw an overrepresentation of stimulus-selective responses in neurons with RFs overlapping with the stimulus location despite these being the smallest proportions of PFC RFs. Only 17% of our PFC neurons have such RFs and as reported earlier, PFC neurons have a large proportion of contra-lateral fields (Mikami *et al.*, 1982; Suzuki, 1985)(Viswanathan & Nieder, *in press*). In VIP, we saw a similar, albeit weaker effect. When we considered number-selectivity over all recording sessions, we found a slight over-representation of stimulus selectivity in neurons that are spatially-selective. While only 6% (8/128) of spatially non-selective neurons show stimulus-selectivity, as many 17% (22/130) and 19% (15/80) spatially-selective neurons with stimulus outside of RF and stimulus in RF show stimulus selectivity (chi-square = 7.098, p = 0.0288). This difference was not seen for number-selective neurons recorded during the colour discrimination task (chi-square = 3.971, p = 0.137).

While RF classes played a part in the recruitment of neurons in number discrimination, we

tested whether they determine the strength of modulation by number (**Figure 9**) by comparing number discriminability in number-selective neurons across the three RF classes. We calculated numerosity tuning curves for the 3 classes of number-selective neurons (**Figure 9A** and **B**). The tuning sharpness and width were remarkably similar across classes. In PFC, number neurons had median AUROC values of 0.71, 0.69 and 0.70 (Kruskal-Wallis, chi-square = 1.76, p = 0.4145). VIP receptive field classes have median AUROC values of 0.70, 0.70 and 0.72 (Kruskal-Wallis, chi-square = 3.4, p = 0.1824). The stimuli were well discriminated by the selective populations irrespective of their spatial selectivity during passive fixation.

DISCUSSION

We recorded neurons in PFC and VIP as monkeys performed a discrimination task and a passive fixation task in interleaved blocks. We used the passive fixation task to map the visual receptive fields of many neurons. By mapping the RFs of the neurons independently from a discrimination task, we were able to compare the nature of their spatial responses to the non-spatial responses towards features of discriminative stimuli. We divided neuronal responses during passive fixation to three classes: no significant RF, RFs that did not overlap with the centre where the stimuli of the discrimination task were shown (stimulus outside RF) and RFs that overlapped with the centre (stimulus in RF). We found the selectivity to colour and number categories to be largely independent of the RFs. While colour selectivity was equitably distributed across RF classes, number selectivity recruited specifically the 'stimulus in RF' class in PFC and the spatially-selective neurons in VIP. Although the RF class did bias the recruitment of neurons in number selectivity in both areas, their RF membership did not reflect the strength of selectivity.

Differences in RF classes across areas

The distribution of RF classes in PFC and VIP were significantly different with PFC showing far less neurons for which the stimulus was displayed within their RF. This is in agreement with the strong contralateral bias reported in PFC visual responses (Mikami *et al.*, 1982; Rainer *et al.*, 1998) (Viswanathan & Nieder, *in press*) and the frequently foveal responses reported in VIP neurons (Viswanathan & Nieder, *in press*). Interestingly, bimodal neurons in VIP tend to have contralateral (15-30°) visual fields (Duhamel *et al.*, 1998) but visual responses have a median eccentricity of 10-12° from the fovea (Duhamel *et al.*, 1997) (Viswanathan & Nieder, *in press*). This indicates that the mapping of additional modalities occurs differentially for different visual RF locations. A direct comparison of the modulation

of firing rates by their RFs across PFC and VIP neurons has showed that VIP RFs show higher responses within their RFs than without. Additionally, a higher proportion of VIP neurons show spatial selectivity. With this in mind, we hypothesized that VIP neurons would be differentially recruited by non-spatial task variables based on their RFs whereas PFC task responses would be more independent of the location of their RFs.

RF locations and task recruitment

Our study provided us a unique opportunity to examine selective recruitment of neurons. Other studies examining the interplay of spatial and non-spatial variables rely on within-neuron comparisons of representations of non-spatial features by presenting stimuli either within a neuron's RF or outside it (Freedman & Assad, 2009; Wimmer *et al.*, 2016). Many others involve behavioural responses that are spatial in nature like eye movements toward or away from RF thus making it difficult to dissociate the non-spatial influences of the stimuli and the spatial influences of choice (Constantinidis *et al.*, 2001). By mapping the RFs of neurons separately and by using a delayed match-to-sample task without a spatial component, we were able to compare stimulus selectivity across RF classes.

Neurons in both areas were weakly but correspondingly recruited by the colour stimuli by RF class. Thus, regardless of whether the neurons were spatially selective or where their RFs were located, they showed colour-selective responses. PFC colour-selective neurons were between 7 to 14% of the different RF classes and VIP neurons were between 8 to 17% of the different RF classes. The weak colour-selectivity in our population is typical of PFC neurons (Lara & Wallis, 2014). Colour responses are known to be quite dynamic in fronto-parietal areas such that information about colour stimuli arises early in selective populations and varies over the course of the trial (Astrand *et al.*, 2015). Fronto-parietal neurons are also strongly driven by task difficulty and arousal while our monkeys performed this colour

discrimination task with 97% accuracy, which might further explain a lower recruitment by colour in our data.

The recruitment of neurons for number selectivity tells a different story. Both areas consist of neurons strongly selective for number despite having no significant RFs or having their RFs elsewhere. A much larger fraction of PFC neurons responds selectively to number when the stimulus is shown within their RFs while spatially-selective VIP neurons are number-selective in a larger fraction regardless of stimulus location. Within the rarer population of foveal RFs in PFC, we see a two to three-fold increase in number-selective responses than the other RF classes. One explanation for this over-representation is that spatial attention to the stimulus location selectively recruits neurons with RFs at that location. Specifically as stimulus comparisons, such as those during a discrimination task, require PFC neurons providing stimulus-related signals (Wimmer *et al.*, 2016), neurons responsive to the stimulus location are most informative. Some of these neurons might be neurons receiving information from foveal VIP neurons. Within the magnitude system, PFC is placed downstream to VIP. Parietal cortex has been shown to precede PFC in extracting magnitudes from stimuli (Nieder & Miller, 2004b; Viswanathan & Nieder, 2013). Many areas of the posterior parietal cortex are reciprocally connected with PFC and it is not known whether inputs to PFC from areas like LIP, VIP are spatially organised (Lewis & Van Essen, 2000). It is possible that VIP neurons containing information about magnitude specifically project to PFC neurons representing the foveal visual field. Such a hierarchy would put PFC in a position to exert top-down influence on VIP number representations across the visual field (Chafee & Goldman-Rakic, 2000; Crowe *et al.*, 2013). Colour information, on the other hand, might arrive in PFC from a different system and thus, dependent on the spatial organisation of upstream visual areas.

Stimulus discriminability

To test if stimulus discriminability was truly independent of the RFs in association areas, we examined the strength of number-selectivity. Across RF classes, despite differences in recruitment of neurons towards number discrimination, we did not see differences in the strength of discrimination in the selective neurons in either area. Directional stimuli presented in either visual hemifields were strongly represented by lateral PFC neurons during a motion discrimination task. As the direction signals were 40ms earlier from the contralateral hemifield than the ipsilateral hemifield, it has been speculated that the source of information differs across space such that direct inputs from upstream MT drives the contralateral responses and those from the opposite PFC drive the ipsilateral responses (Wimmer *et al.*, 2016). Neurons in lateral intraparietal area exhibited lower firing rates to motion stimuli presented outside their RFs but nevertheless strongly encoded the arbitrary learned category membership of those stimuli (Freedman & Assad, 2009). The position of the stimuli (within RF or out) was strongly encoded at the beginning of the stimulus period but the category encoding which started later remained strong for either position. PFC and VIP neurons in our study are strongly selective for the number of dots in the visual stimuli regardless of their RFs, similar to those found in area MT selective for direction (Zaksas & Pasternak, 2006a). Further time-resolved analysis will examine whether number encoding is subject to similar temporal differences based on the neurons' RFs. However, abstract categories are often encoded at different, short time periods of a trial whereas object locations are encoded throughout the trial (Stoet & Snyder, 2004; Zaksas & Pasternak, 2006b). This suggests that abstract categories might be encoded independently of location within single neurons in the association areas, especially in areas that generate location independent top-down modulation like the PFC.

FIGURE LEGENDS

Figure 1. Behavioural tasks. (**A**) We used two kinds of discriminative stimuli within a delayed match-to-sample task (DMS). During the colour discrimination task, monkeys were trained to match the colour of a multi-dot display and for the number discrimination task, the number of dots within the display. Each trial began with a fixation period during which the monkeys fixated on a central fixation spot and held a response bar. As they continued to fixate and hold the bar, a sample display was shown which had to be remembered through a delay period to be matched to following test displays. If the test display matched the sample display in the colour (top panel) or number (bottom panel) of dots, the monkeys responded by releasing the bar. If it did not, they withheld their response until a matching stimulus appeared. Every successful trial was rewarded. (**B**) The colour stimuli spanned 5 colours, red, blue, green, yellow and purple presented in all numbers. The number stimuli ranged from one to 5 dots. Note that the displays could not be matched based on other visual features like appearance, size of dots and density. The 'standard' set of stimuli consisted of randomly sized and spaced dots. The 'control' set of stimuli equalised the summed area of dots across number and the average spacing between the dots. (**C**) A passive fixation task helped us map the neuronal receptive fields. As the monkeys fixated the central fixation spot, a grey moving bar appeared at 5 successive positions for 1000 ms each. At each position, the bar moved at constant speed right to left, left to right, then oriented horizontally moving up, moving down. The directions of motion are indicated by the green arrow. Successful fixation throughout the trial resulted in a fluid reward. (**D**) The screen was divided into a 10x8 grid of 80 positions which were sampled over 16 trials. The blocks of passive fixation were interleaved with blocks of DMS tasks in the recording session, each session beginning with a DMS block.

Figure 2. Recording sites in the right dlPFC and VIP during the colour discrimination task. (**A**) Lateral view of the rhesus monkey brain (*left*) with the approximate location of the recording chambers over the right hemisphere. The filled area within the recording chamber indicates the location of recording sites. Various sulci are marked and labelled: PS – principal sulcus, CS – central sulcus, LS – lateral sulcus, STS – superior temporal sulcus. The coronal section at the level of the IPS (*right*) indicates the location of our VIP recording sites. (**B**) Recording sites within PFC in monkey L (*left*) and monkey S (*right*) around the anatomical features, sAS – superior arcuate sulcus, iAS – inferior arcuate sulcus, AS – arcuate sulcus. For each recording site, we calculate the percentage of colour-selective neurons. The size of circles indicates the number of neurons recorded at each site. The colour of the circles indicates the percentage of neurons that exhibited colour selectivity. (**C**) VIP recording sites mapped on the surface of cortex in monkey L (*left*) and monkey S (*right*), CS – central sulcus. (**D**) However, VIP recordings were made in the depth of IPS and the scatter plot depicts individual sites in depth.

Figure 3. Number-selective neurons in the right dlPFC and VIP. Same layout as **Figure 2**. (**A**) PFC recording chambers and individual recording sites in monkey L (left) and monkey S (right). (**B**) VIP recording chambers and recording sites mapped onto the surface of cortex. (**C**) Individual recording sites in the depth of IPS.

Figure 4. Example neurons: receptive fields and colour selectivity. (**A**) Example PFC neuron with the RF overlapping stimulus location as indicated by the warmer colours around the grey circle marking the stimulus location (left panel). The map is normalised to the maximum firing rate across locations, stated above the map. The same neuron responds during the DMS task to stimuli shown within the grey circle and the response for each colour is averaged

(right panel), error bars are the standard error of the mean (ANOVA, $p < 0.01$). It is significantly selective for the red coloured dots. (**B**) Example VIP neuron; foveal RF (left panel) and selectivity for purple coloured dots in the sample (right panel). This neuron also has an RF that overlaps with the stimulus location. (**C**) An example PFC neuron that responds selectively to the yellow samples despite having a non-foveal RF. (**D**) A VIP colour-selective neuron and its non-foveal RF.

Figure 5. Example neurons: receptive fields and number selectivity. (**A**) A PFC neuron exhibiting selectivity for the number of dots in the sample display which overlaps with its RF (left panel) and its number tuning curve (right panel). (**B**) VIP neuron with a foveal RF and selectivity for 4 dots. (**C**) PFC neuron with a selective response for 5 dots with an eccentric RF. (**D**) VIP number-selective neuron with a large para-foveal RF.

Figure 6. Three classes of RFs involved in discrimination tasks. (**A**) Neurons showing no spatial selectivity during the RF mapping in PFC. Their activity is normalised and averaged and display no hotspots. (**B**) The same population of neurons in VIP show heightened activity but without hotspots. (**C**) Neurons in PFC that have RFs in areas other than where the DMS stimuli are shown. Here, we see a hotspot in lower, left side which is contra-lateral to all the neurons. (**D**) Neurons in VIP with RFs non-overlapping with stimuli. (**E**) PFC neurons that have RFs overlapping with stimulus location. (**F**) same as **E** for VIP neurons. The number of neurons comprising each class are indicated above each map. The maps are all normalised to the same scale to highlight the overlap of RFs.

Figure 7. Probability of colour-selective responses by RF class (*top panel*). Relative proportions of RF classes in PFC (*middle panel*) and VIP (*bottom panel*) from **Figure 5** are

indicated by the size of the Pacman-style pie charts. (**A**) The proportion of colour-selective neurons in the non-spatially selective class of neurons is depicted by the open-ness of the Pacman-style pie and the coloured area. The percentage is indicated next to the shapes. (**B**) The proportion of colour-selective neurons when the stimulus was outside the RF. (**C**) The proportion of colour-selective neurons when the stimulus was inside the RF. (**D-F**) The same as **A-C** for neurons in VIP. Neither area shows a significant deviation of colour-selective neurons in any RF class.

Figure 8. Probability of number-selective responses by RF class. Same layout as **Figure 6**. (**A**) The proportion of number-selective neurons with no RFs. (**B**) Number-selective neurons with RFs away from the stimulus location. (**C**) PFC neurons with RFs overlapping the stimulus location show the highest proportion of number-selective neurons. (**D-F**) The same as **A-C** for neurons in VIP. VIP number neurons are proportionally distributed in the stimulus outside RF and inside RF classes, more than those without RFs.

Figure 9. Strength of number discriminability by RF class. (**A**) Averaged tuning curves for number-selective PFC neurons for each RF class, error bars are the standard error of the mean. Responses were centred on the preferred number and normalised such that responses towards the preferred number was considered 100% and responses towards the least preferred number were 0%. All other responses were expressed as response to a numerical distance from the preferred number. (**B**) Tuning curves for VIP number-selective neurons. (**C**) AUROC values calculated from the sample phase in PFC neurons by RF class. Each data point (circle) is the AUROC value of a number-selective neuron and the black horizontal lines are the median values for each RF class. (**D**) AUROC values for VIP neurons. There was no significant difference in stimulus discriminability across RF classes for either area.

ACKNOWLEDGMENTS:

This work was supported by DFG grant NI 618/2-1 to A.N.

The authors declare no competing financial interests.

AUTHOR CONTRIBUTIONS:

P.V. and A.N. designed research; P.V. performed research; P.V. analysed data; P.V. and A.N. wrote the paper.

REFERENCES:

Asaad, W.F. & Eskandar, E.N. (2011) Encoding of both positive and negative reward prediction errors by neurons of the primate lateral prefrontal cortex and caudate nucleus. *J. Neurosci.*, **31**, 17772–17787.

Astrand, E., Ibos, G., Duhamel, J.-R., & Ben Hamed, S. (2015) Differential dynamics of spatial attention, position, and color coding within the parietofrontal network. *J. Neurosci.*, **35**, 3174–3189.

Avillac, M., Ben Hamed, S., & Duhamel, J.-R. (2007) Multisensory Integration in the Ventral Intraparietal Area of the Macaque Monkey. *J. Neurosci.*, **27**, 1922–1932.

Avillac, M., Denève, S., Olivier, E., Pouget, A., & Duhamel, J.-R. (2005) Reference frames for representing visual and tactile locations in parietal cortex. *Nat. Neurosci.*, **8**, 941–949.

Bongard, S. & Nieder, A. (2010) Basic mathematical rules are encoded by primate prefrontal cortex neurons. *Proc. Natl. Acad. Sci. U. S. A.*, **107**, 2277–2282.

Chafee, M. V & Goldman-Rakic, P.S. (2000) Inactivation of parietal and prefrontal cortex reveals interdependence of neural activity during memory-guided saccades. *J. Neurophysiol.*, **83**, 1550–1566.

Constantinidis, C., Franowicz, M.N., & Goldman-Rakic, P.S. (2001) The sensory nature of mnemonic representation in the primate prefrontal cortex. *Nat. Neurosci.*, **4**, 311–316.

Crowe, D.A., Goodwin, S.J., Blackman, R.K., Sakellaridi, S., Sponheim, S.R., MacDonald, A.W., & Chafee, M. V (2013) Prefrontal neurons transmit signals to parietal neurons that reflect executive control of cognition. *Nat. Neurosci.*, **16**, 1484–1491.

Duhamel, J.-R.R., Bremmer, F., Ben Hamed, S., & Graf, W. (1997) Spatial invariance of visual receptive fields in parietal cortex neurons. *Nature*, **389**, 845–848.

Duhamel, J.R., Colby, C.L., & Goldberg, M.E. (1998) Ventral intraparietal area of the macaque: congruent visual and somatic response properties. *J. Neurophysiol.*, **79**, 126–136.

Eiselt, A.-K. & Nieder, A. (2013) Representation of abstract quantitative rules applied to spatial and numerical magnitudes in primate prefrontal cortex. *J. Neurosci.*, **33**, 7526–7534.

Freedman, D.J. & Assad, J.A. (2006) Experience-dependent representation of visual categories in parietal cortex. *Nature*, **443**, 85–88.

Freedman, D.J. & Assad, J.A. (2009) Distinct encoding of spatial and nonspatial visual information in parietal cortex. *J. Neurosci.*, **29**, 5671–5680.

Funahashi, S. & Bruce, C.J. (1989) Mnemonic coding of visual space in the monkey ' s dorsolateral prefrontal

cortex. *J. Neurophysiol.*, **61**, 331–349.

Fuster, J.M. & Alexander, G.E. (1971) Neuron activity related to short-term memory. *Science*, **173**, 652–654.

Hasegawa, R.P., Matsumoto, M., & Mikami, A. (2000) Search target selection in monkey prefrontal cortex. *J Neurophysiol*, **84**, 1692–1696.

Lara, A.H. & Wallis, J.D. (2014) Executive control processes underlying multi-item working memory. *Nat. Neurosci.*, **17**, 876–883.

Leon, M.I. & Shadlen, M.N. (1999) Effect of expected reward magnitude on the response of neurons in the dorsolateral prefrontal cortex of the macaque. *Neuron*, **24**, 415–425.

Lewis, J.W. & Van Essen, D.C. (2000) Corticocortical connections of visual, sensorimotor, and multimodal processing areas in the parietal lobe of the macaque monkey. *J. Comp. Neurol.*, **428**, 112–137.

Merten, K. & Nieder, A. (2012) Active encoding of decisions about stimulus absence in primate prefrontal cortex neurons. *Proc. Natl. Acad. Sci.*, **109**, 6289–6294.

Mikami, A., Ito, S., & Kubota, K. (1982) Visual response properties of dorsolateral prefrontal neurons during visual fixation task. *J. Neurophysiol.*, **47**, 593–605.

Mochizuki, K. & Funahashi, S. (2016) Prefrontal spatial working memory network predicts animal's decision making in a free choice saccade task. *J. Neurophysiol.*, **115**, 127–142.

Mountcastle, V.B., Lynch, J.C., Georgopoulos, A., Sakata, H., & Acuna, C. (1975) Posterior parietal association cortex of the monkey: command functions for operations within extrapersonal space. *J. Neurophysiol.*, **38**, 871–908.

Nieder, A. (2012) Supramodal numerosity selectivity of neurons in primate prefrontal and posterior parietal cortices. *Proc. Natl. Acad. Sci. U. S. A.*, **109**, 11860–11865.

Nieder, A. & Miller, E.K. (2004a) A parieto-frontal network for visual numerical information in the monkey. *Proc. Natl. Acad. Sci. U. S. A.*, **101**, 7457–7462.

Nieder, A. & Miller, E.K. (2004b) Analog numerical representations in rhesus monkeys: evidence for parallel processing. *J. Cogn. Neurosci.*, **16**, 889–901.

Quintana, J., Fuster, J.M., & Yajeya, J. (1989) Effects of cooling parietal cortex on prefrontal units in delay tasks. *Brain Res.*, **503**, 100–110.

Rainer, G., Asaad, W.F., & Miller, E.K. (1998) Memory fields of neurons in the primate prefrontal cortex. *Proc. Natl. Acad. Sci. U. S. A.*, **95**, 15008–15013.

Ramirez-Cardenas, A., Moskaleva, M., & Nieder, A. (2016) Neuronal Representation of Numerosity Zero in the

Primate Parieto-Frontal Number Network. *Curr. Biol.*, **26**, 1285–1294.

Roesch, M.R. & Olson, C.R. (2004) Neuronal activity related to reward value and motivation in primate frontal cortex. *Science*, **304**, 307–310.

Romero, M.C. & Janssen, P. (2016) Receptive field properties of neurons in the macaque anterior intraparietal area. *J. Neurophysiol.*, **115**, 1542–1555.

Shadlen, M.N. & Newsome, W.T. (2001) Neural basis of a perceptual decision in the parietal cortex (area LIP) of the rhesus monkey. *J. Neurophysiol.*, **86**, 1916–1936.

Stoet, G. & Snyder, L.H. (2004) Single neurons in posterior parietal cortex of monkeys encode cognitive set. *Neuron*, **42**, 1003–1012.

Suzuki, H. (1985) Distribution and organization of visual and auditory neurons in the monkey prefrontal cortex. *Vision Res.*, **25**, 465–469.

Suzuki, M. & Gottlieb, J. (2013) Distinct neural mechanisms of distractor suppression in the frontal and parietal lobe. *Nat. Neurosci.*, **16**, 98–104.

Swaminathan, S.K. & Freedman, D.J. (2012) Preferential encoding of visual categories in parietal cortex compared with prefrontal cortex. *Nat. Neurosci.*, **15**, 315–320.

Tremblay, S., Pieper, F., Sachs, A., & Martinez-Trujillo, J. (2015) Attentional filtering of visual information by neuronal ensembles in the primate lateral prefrontal cortex. *Neuron*, **85**, 202–215.

Tudusciuc, O. & Nieder, A. (2009) Contributions of primate prefrontal and posterior parietal cortices to length and numerosity representation. *J. Neurophysiol.*, **101**, 2984–2994.

Vallentin, D. & Nieder, A. (2010) Representations of visual proportions in the primate posterior parietal and prefrontal cortices. *Eur. J. Neurosci.*, **32**, 1380–1387.

Viswanathan, P. & Nieder, A. (2013) Neuronal correlates of a visual "sense of number" in primate parietal and prefrontal cortices. *Proc. Natl. Acad. Sci. U. S. A.*, **110**, 11187–11192.

Viswanathan, P. & Nieder, A. (2015) Differential impact of behavioral relevance on quantity coding in primate frontal and parietal neurons. *Curr. Biol.*, **25**, 1259–1269.

Viswanathan, P. & Nieder, A. (2017) Visual receptive field heterogeneity and functional connectivity of adjacent neurons in primate fronto-parietal association cortices. *J. Neurosci.*, **37**, 8919–8928.

Viswanathan, P. & Nieder, A. (*in press*) Comparison of visual receptive fields in the dorsolateral prefrontal cortex (dlPFC) and ventral intraparietal area (VIP) in macaques. *Eur. J. Neurosci.*

Wardak, C., Olivier, E., & Duhamel, J.-R. (2011) The relationship between spatial attention and saccades in the

frontoparietal network of the monkey. *Eur. J. Neurosci.*, **33**, 1973–1981.

Wimmer, K., Spinelli, P., & Pasternak, T. (2016) Prefrontal Neurons Represent Motion Signals from Across the Visual Field But for Memory-Guided Comparisons Depend on Neurons Providing These Signals. *J. Neurosci.*, **36**, 9351–9364.

Zaksas, D. & Pasternak, T. (2006a) Area MT Neurons Respond to Visual Motion Distant From Their Receptive Fields Area MT Neurons Respond to Visual Motion Distant From Their Receptive Fields. *J. Neurophysiol.*, 4156–4167.

Zaksas, D. & Pasternak, T. (2006b) Directional signals in the prefrontal cortex and in area MT during a working memory for visual motion task. *J. Neurosci.*, **26**, 11726–11742.

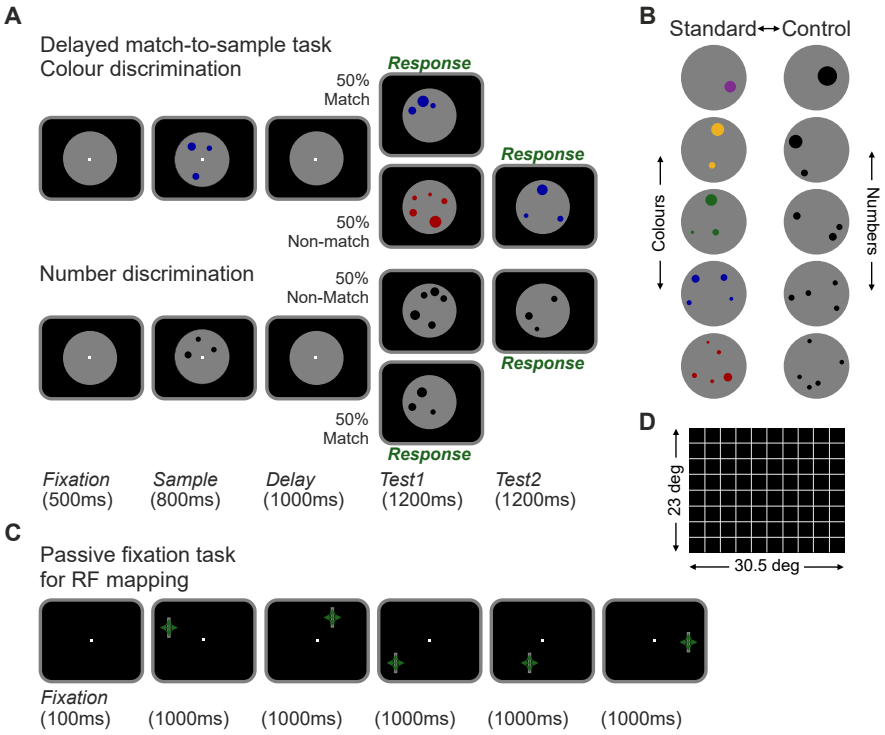

Figure 1 (Viswanathan & Nieder)

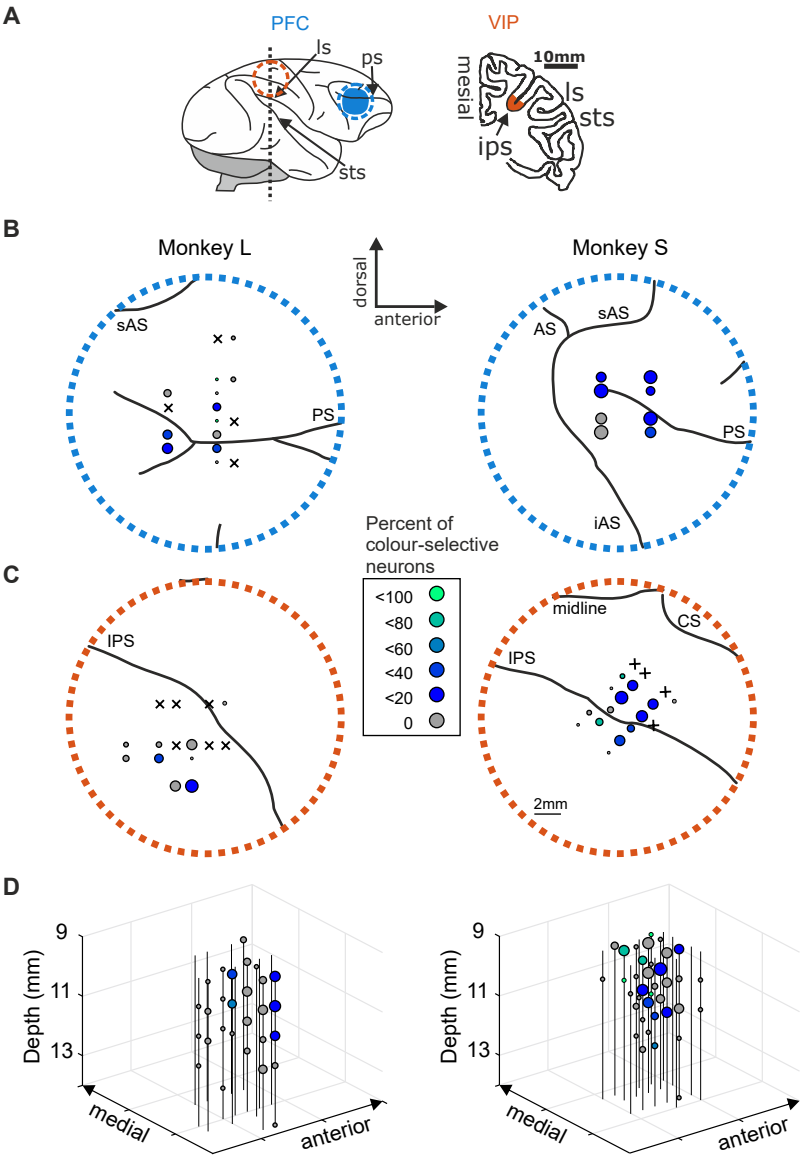

Figure 2 (Viswanathan & Nieder)

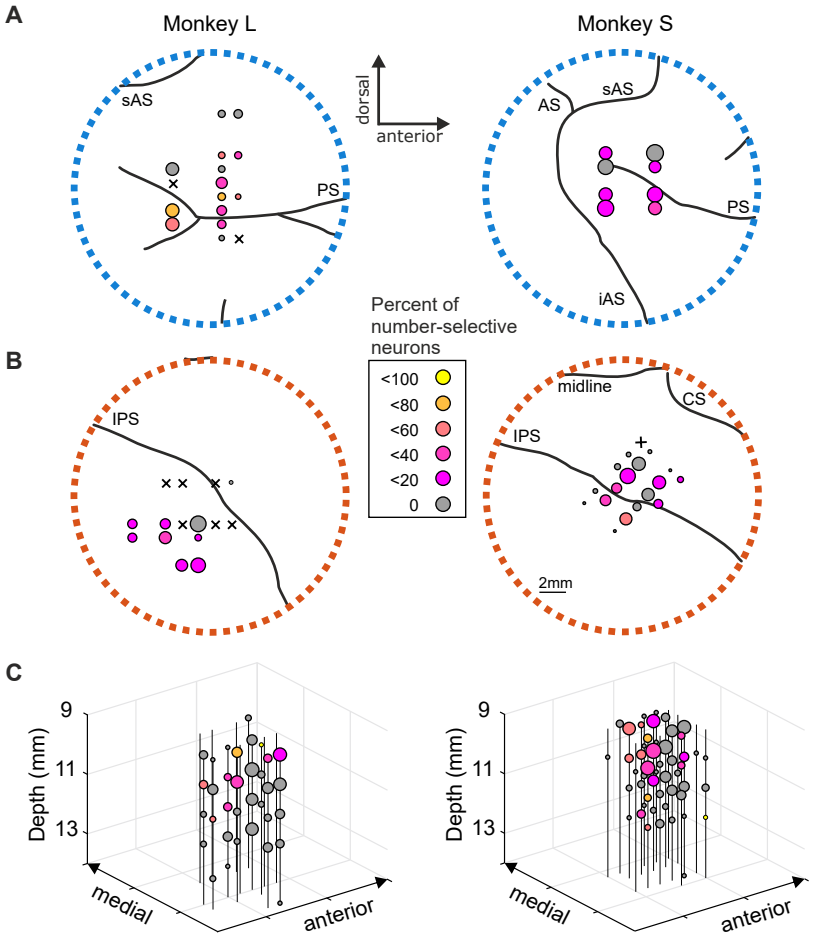

Figure 3 (Viswanathan & Nieder)

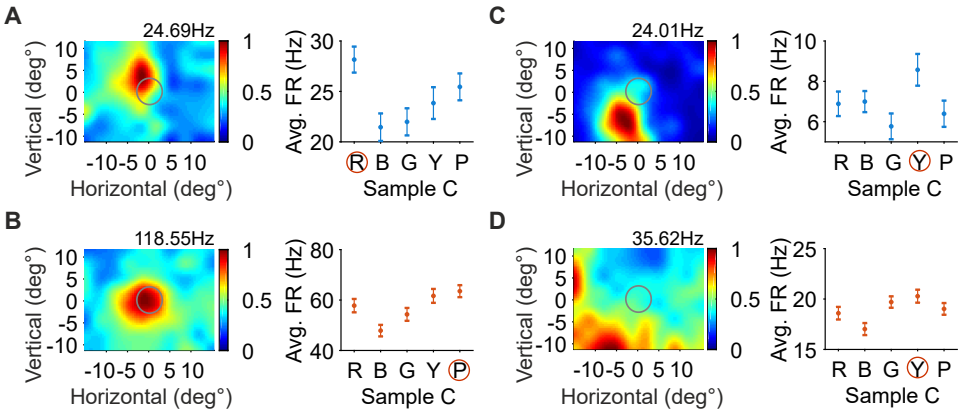

Figure 4 (Viswanathan & Nieder)

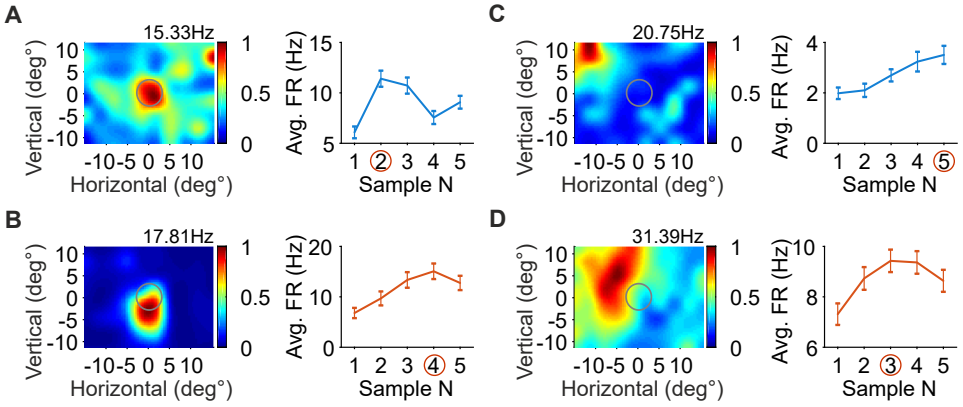

Figure 5 (Viswanathan & Nieder)

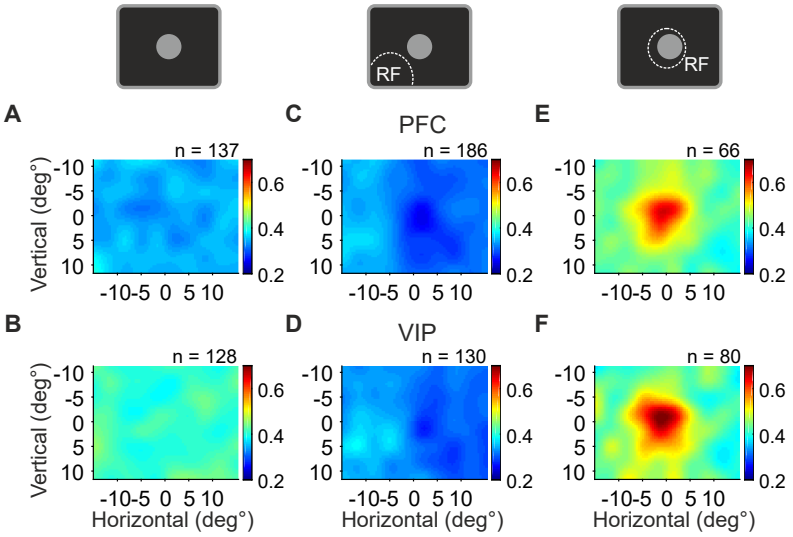

Figure 6 (Viswanathan & Nieder)

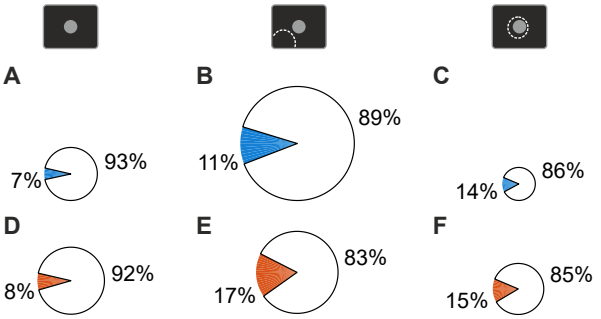

Figure 7 (Viswanathan & Nieder)

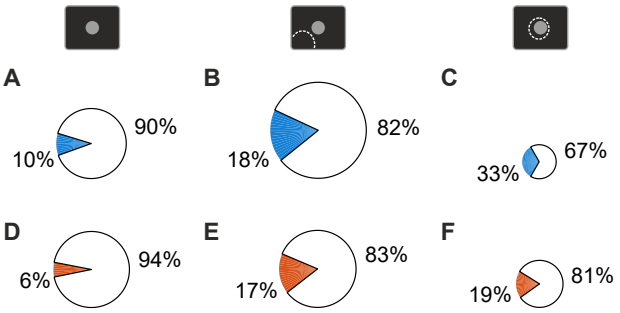

Figure 8 (Viswanathan & Nieder)

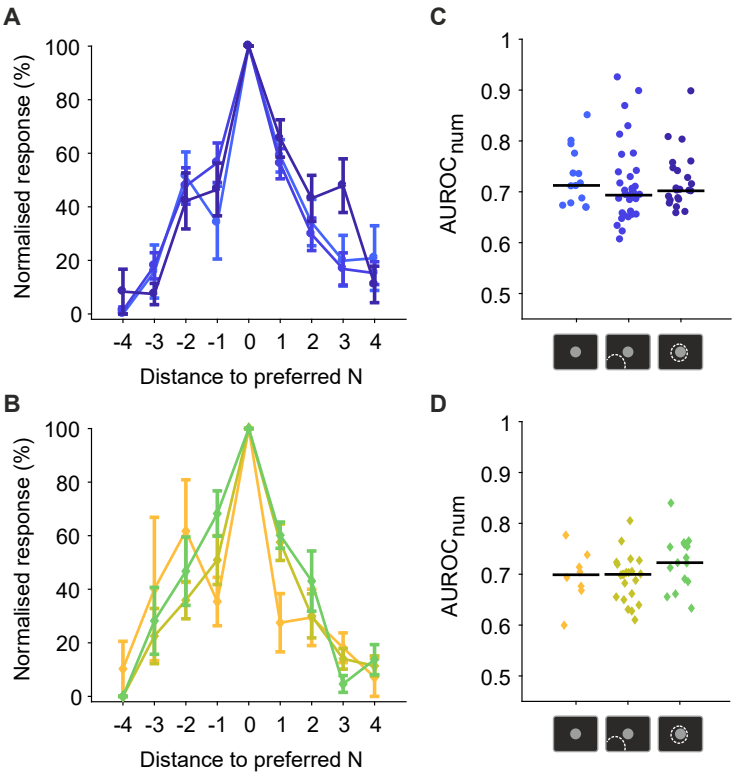

Figure 9 (Viswanathan & Nieder)